

University of Nottingham
UK | CHINA | MALAYSIA

THE ROLE OF THE CALPAIN SYSTEM IN BREAST CANCER PROGRESSION AND TREATMENT RESPONSE

Richa Vasan

(MSI, MRes)

Thesis submitted to the University of Nottingham for the degree of Doctor of Philosophy

June 2022

Abstract

The calpain system is a system of cysteine proteases that are involved in several cellular functions including cell migration, survival and death. Unregulated expression of the calpain system is implicated in breast cancer. However, the functioning of its individual components in regulating breast cancer disease progression and clinical outcomes remains largely unknown. The present study aimed to assess the role of the calpain system in breast cancer progression and treatment response. This aim was achieved by inhibiting intracellular calpain activity using three different strategies.

The first strategy to inhibit intracellular calpain activity was by molecular overexpression of different calpastatin isoforms. T47D and MDA-MB-231 cells overexpressing calpastatin types I, II and III were established and types I and II were successfully overexpressed in both the cells lines. Calpastatin types I and III had a general diffused cytoplasmic while calpastatin type II had a distinct perinuclear subcellular distribution in both the cell lines. RNA-sequencing data analyses revealed that in T47D cells (luminal subtype) calpastatin types I and II, and in MDA-MB-231 cells (Triple Negative Breast Cancer (TNBC) subtype) calpastatin types II and III may have a joint role in a high number of cellular functions, owing to the number of overlapping DEGs. Overexpression of different calpastatin types in T47D and MDA-MB-231 cells significantly affected several pathways that predicted activation or inhibition of genes. These included genes like, Prion protein (PRNP), Farnesyltransferase subunit beta (FNTB), Phospholipase c gamma 1 (PLCG1) in T47D cells; and Chromatin Licensing and DNA Replication Factor 1 (CDT1), PIH1 Domain Containing 1 (PIH1D1), Microtubule associated scaffold protein 2 (MTUS2) in MDA-MB-231 cells. Although these genes have shown to have some association with breast cancer, there have been no studies reporting their association with the calpain system.

The second strategy to inhibit calpain activity was by using novel small molecule calpain inhibitors. A novel FRET based bioassay was developed to assess intracellular calpain activity in live breast cancer cells. Intracellular calpains were activated using calcium ionophore A23187 at an optimised dose of 10 μM for 2 hours ($P<0.0001$). PD150606 was used to inhibit calpain

activity and as a comparator for novel inhibitors. The novel compounds 1, 9 and 10 showed significant inhibition of calpain activity at lower doses ($P<0.01$) compared to PD150606, therefore were concluded to be more potent inhibitors of calpain activity. The novel compounds did not influence breast cancer cell proliferation however, they reduced the cell survival significantly by 60%-80% in MDA-MB-231 cells, suggesting that these compounds may have anticancer properties by causing direct cell lethality. The third strategy was using calpain 1, 2 and 4 CRISPR/Cas9 KO MDA-MB-231 cells. Knocking out calpain 1 and 2 did not influence cell proliferation rate and doubling times compared to the WT cells, while Capns1 KO cells had a significantly reduced cell growth rate and a higher doubling time of ($P=0.0001$). Both Capn2 and Capns1 KO cells had significantly reduced plating efficiencies ($P=0.001$ and $P<0.01$) attributing to low cellular attachment and proliferation rates, respectively. While no effect was seen on doxorubicin cell proliferation, knocking out calpains 2 ($P<0.001$, $P<0.0001$ and $P=0.01$) and 4 ($P<0.001$ and $P<0.001$) induced marginally significant sensitisation to doxorubicin treatment in terms of clonogenic cell survival, in normoxic conditions (21% O2). Presence of hypoxia (1% O2) reduced cell proliferation in WT, Capn1 KO and Capn2 KO cells and plating efficiency in WT, Capn2 KO and Capns1 KO cells. Hypoxia (1% O2) also induced resistance to doxorubicin in all the cell lines in terms of cell proliferation and survival. Whilst knocking out calpains 2 and 4 made breast cancer cells more resistant to radiation treatment in normoxia (21% O2), presence of hypoxia (1% O2 for 24 hours) made Capn1 KO (SF8- 1E-05) and Capn2 KO (SF8- 4.57E-06) cell lines significantly sensitive to radiation treatment compared to the WT cells (SF8- 1.6E-04).

Bioinformatic analyses on CAPN1, CAPN2, CAPNS1 and CAST genes revealed that the cell cycle, DNA replication, tight junction were some of the pathways altered significantly by the calpain system genes. The differentially expressed genes, Protein phosphatase 1 catalytic subunit alpha (PPP1CA), Protein kinase AMP-activated non-catalytic subunit beta 2 (PRKAB2), DNA polymerase epsilon 2, accessory subunit (POLE2), Retinoblastoma binding protein 4 (RBBP4) and Proteasome 20S subunit beta 5 (PSMB5) were seen to be significantly associated with overall and breast cancer specific survival, and RBBP4 protein was expressed in Luminal

and TNBC cells and had a predominantly nuclear localisation in breast cancer tissues.

In conclusion, the current study reports that different calpastatin isoforms have differential localisation, suggesting they may have different intracellular functions. The project also reports, a novel FRET based assay to assess intracellular calpain activity in live cells, and that the novel compounds are potent calpain inhibitors. In addition, although further work is required, the current study shows that genetic aberration of calpains 2 and 4 may have a sensitising effect on doxorubicin response in normoxia (21% O2) and genetic aberration of calpains 1 and 2 leads to significant radiosensitisation in the presence of hypoxia (1% O2).

Presentations and grants

Presentations

- Oral presentation "Calpains/calpastatin in Breast Cancer". Annual NBCRC Research Day 2020, October 6-8, Nottingham, UK.
- Oral presentation "The role of calpains and calpastatin in breast cancer progression and treatment response". Sue Watson Oral presentation event 2019, October 29, Nottingham, UK.
- Poster presentation "The role of calpains and calpastatin in breast cancer progression and treatment response". Cancer research Nottingham 2019, September 16, Nottingham, UK.
- Poster presentation "The role of calpains and calpastatin in breast cancer progression and treatment response". Annual NBCRC Research Day 2019, May 14, Nottingham, UK.

Grants

- Foundation main grant 2020, Funds for Women Graduates
- NBCRC Pilot Grant 2020, NBCRC.

Acknowledgements

I would like to express my sincerest gratitude to my supervisors Professor Stewart Martin and Dr. Sarah Storr for their invaluable guidance and support throughout term of my study. I am grateful for their generous supervision which inspired and motivated me to learn and become better every day.

I express my gratitude to the University of Nottingham for granting me the Vice Chancellor's Scholarship for research excellence (International) award, towards my studies. I am grateful to the NBCRC for the Pilot grant that funded the RNA sequencing part of the project. I would also like to thank the Funds for Women Graduates, for awarding me the Foundation main grant towards my living expenses during the final year of my PhD.

I thank our collaborators Professor. T. Parr for providing us with calpastatin isoform constructs, Professor R. Allemann for providing us the novel calpain inhibitors, Professor P.L. Davies for providing us with the FRET plasmid and Professor. P. Greer for providing us the CRISPR/Cas9 calpain knock out cell lines.

I would like to specially thank my colleagues, Dr. Abdullah, Dr. Yao, Dr. Sukkarn, Dr. Aiyappa, Behnaz Saidy and Muazzez Yilmaz for their support and creating a positive and constructive work environment in the lab.

A special thanks to my parents, Mr. Sunil Vasan and Mrs. Priti Vasan, and my brother, Mr. Ribhu Vasan for their unlimited care and support, and for inspiring me to keep going during the tough times. A huge thank you to my husband, Mr. Callum McCue for his patience, constant support and encouragement throughout the term of my studies.

Abbreviations

°C	degree Celsius
2D	2-dimensional
IMRT	intensity modulated radiotherapy
3D	3-dimensional
AC	doxorubicin and cyclophosphamide
ADCC	antibody dependent cell-mediated cytotoxicity
ADP	adenosine diphosphate
AI	aromatase inhibitor
AJCC	American Joint Committee on Cancer
ALL	acute lymphoblastic leukaemia
ALND	axillary lymph node dissection
AML	acute myeloid leukaemia
AMOT	angiomotin
AMOTL1	angiomotin Like 1
APBI	accelerated partial breast irradiation
ASIR	age standardised increase rates
ATCC	American type culture collection
ATG5	autophagy-related 5
BAX	BCL2 associated X
BCS	breast conserving surgery
BCT	breast conserving therapy
B-H	Benjamini-Hochberg
BID	BH3 interacting domain death agonist
BMI	body mass index
BT	brachytherapy
C/T	chemotherapy
Ca2+	calcium ions
CA9	carbonic anhydrase 9
CACNA2D4	calcium voltage-gated channel auxiliary subunit alpha2delta2
Capn1	calpain 1
Capn1 KO	calpain 1 knock out
Capn2	calpain 2
Capn2 KO	calpain 2 knock out
Capn4	calpain 4
Capn4 KO	calpain 4 knock out
CAST	calpastatin
CAST I	calpastatin type I
CAST II	calpastatin type II
CAST III	calpastatin type III
CCNB1	cyclin B1
CCNB2	cyclin B2
CDC25A	cell division cycle 25A
CDC25C	cell division cycle 25C

CDH1	cadherin 1
CDK5	cyclin dependent kinase 5
cDNA	complementary DNA
CDT1	Chromatin Licensing And DNA Replication Factor 1
cells/ml	cells per mili litre
CFP	cyan fluorescent protein
CFRT	conventional multi-fractionated radiotherapy
CHEK2	checkpoint kinase 2
cm2	centimetre square
CO2	carbon dioxide
CAN	copy number aberration
CREB	CREB binding protein
CysPc	cysteine protease core
DAPI	4',6-diamidino-2-phenylindole
DCIS	ductal carcinoma in situ
DDT	dichlorodiphenyltrichloroethane
DEG	differentially expressed genes
DFI	disease free interval
DFS	disease free survival
DMEM	Dulbecco's modified eagle's medium
DMSO	dimethyl sulfoxide
DNA	deoxyribonucleic acid
DT	doubling time
EBC	early stage invasive breast cancer
EBRT	external beam radiotherapy
EDTA	ethylenediaminetetraacetic acid
EGF	epidermal growth factor
EGFR	epidermal growth factor receptor
EJC	exon junction complex
EMR	electromagnetic radiations
EMT	epithelial-mesenchymal transition
ER	oestrogen receptor
ERK	Extracellular signal-regulated kinase
FAK	focal adhesion kinase
FDA	food and drug administration
FDR	false discovery rate
FITC	fluorescein isothiocynate
FLNA	filamin A
FNTB	Farnesyltransferase subunit beta
FOXA1	forkhead box A1
FRET	forster resonance energy transfer
g	gram
GAS2	growth arrest specific 2
GDC	genomic data commons data portal
GFP	green fluorescent protein
GLOBOCAN	global cancer statistics

GPCR	G-protein coupled receptors
GRB7	growth factor receptor bound protein 7
Gy	gray
Gy/minutes	gray/minutes
h	hour
H2O	water
H2O2	hydrogen peroxide
H3O	hydronium
HA-tag	haemagglutinin tag
HDAC1	histone deacetylase 1
HDI	human development index
HER1	human epidermal growth factor receptor-1
HER2	human epidermal growth factor receptor-2
HER3	human epidermal growth factor receptor-3
HER4	human epidermal growth factor receptor-4
HFRT	hypofractionated radiotherapy
HIF	hypoxia inducible factor
HIF1α	hypoxia inducible factor-1α
HIF2α	hypoxia inducible factor-2α
HPRT	Hypoxanthine-guanine phosphoribosyltransferase
HR	hormone receptor
HRT	hormone replacement therapy
HRP	horseradish peroxidase
HSP90	heat shock protein 90
HUVEC	human umbilical vein endothelial cells
IBC	inflammatory breast cancer
IC50	half maximal inhibitory concentration
IDC	invasive ductal carcinoma
IF	Immunofluorescence
IGF-1	insulin like growth factor 1
IGF-1R	insulin like growth factor 1 receptor
IHC	immunohistochemistry
ILC	invasive lobular carcinoma
ILK	integrin linked kinase
IMRT-SIB	IMRT-simultaneous integrated boost
IPA	ingenuity pathway analysis
IR	ionising radiation
kDa	kilo Dalton
KEGG	kyoto encyclopedia of genes and genomes
keV/μm	kiloectronvolt/ micrometer
KO	knock out
kV	kilo volt
LABC	locally advanced primary breast cancer
LB	lysogeny broth
LCIS	lobular carcinoma in situ
LET	Linear energy transfer

LGMD2A	limb girdle muscular dystrophy type 2A
LHRH	luteinizing hormone-releasing hormone
LINC00958	Long intergenic non-protein coding RNA 958
LINC02582	Long intergenic non-protein coding RNA 2582
LQM	linear quadratic model
LVI	lymphovascular invasion
mAb	monoclonal antibody
MAGEA10	MAGE family member A10
MAGEB2	MAGE family member B2
MAGEC1	MAGE family member C1
MAGEC2	MAGE family member C2
MAGOH	mago homolog
MBC	metastatic breast cancer
m-calpain	milli-calpain
MEM	minimum essential medium
METABRIC	Molecular taxonomy of Breast Cancer International Consortium
Mg2+	magnesium
MIR	mortality-to-incidence ratio
mM	milli molar
mm	milli meter
mmHg	millimeter of mercury
MMP	matrix metallopeptidase
mRNA	messenger RNA
MTEC	Mammary tumour epithelial cells
mTOR	mechanistic target of rapamycin kinase
MTUS2	microtubule associated scaffold protein 2
MYC	MYC-proto oncogene
N2	nitrogen
NCIC	National Cancer Institute of Canada
NF-Kb	nuclear factor-kappa B
NGS	Nottingham Grading System
NHS	National Health Services
nM	nano molar
nm	nano metre
NPI	Nottingham Prognostic Index
NPI+	Nottingham Prognostic Index Plus
NSAIDS	non-steroidal anti-inflammatory drugs
NST	no specific type
NTC	no template controls
O2	oxygen
OCLN	Occludin
OER	oxygen enhancement ratio
OFH	oxygen fixation hypothesis
OH°	hydroxyl radical
OS	overall survival

PAEC	pulmonary artery endothelial cell
PAH	polycyclic aromatic hydrocarbons
PARP	poly (ADP-ribose) polymerase
PBS	phosphate buffered saline
PBST	phosphate buffered saline tween
PCNA	Proliferating Cell Nuclear Antigen
PCOS	polycystic ovary syndrome
pCR	pathological complete response
PE	plating efficiency
PFA	Paraformaldehyde
PGM5	Phosphoglucomutase 5
PHD	prolyl hydroxylases
PIH1D1	PIH1 Domain Containing 1
PIP	Prolactin Induced Protein
PKA	Protein kinase A
PKC	Protein kinase C
PLAUR	plasminogen activator, urokinase receptor
PLCG1	phospholipase c gamma 1
POLE2	DNA polymerase epsilon 2, accessory subunit
PPP1CA	protein phosphatase 1 catalytic subunit alpha
PR	Progesterone receptor
PRKAB2	protein kinase AMP-activated non-catalytic subunit beta 2
PRNP	Prion protein
PSMA7	proteasome 20S subunit alpha 7
PSMB5	proteasome 20S subunit beta 5
PTEN	phosphatase and tensin homolog
PTGS2	prostaglandin endoperoxide synthase 2
qRT-PCR	quantitative reverse transcriptase- polymerase chain reaction
RBBP4	retinoblastoma binding protein 4
RCT	randomised control trial
RFS	relapse free survival
RNA	ribonucleic acid
rpm	revolutions per minute
S100A8	S100 calcium binding protein A8
SABR	stereotactive ablative radiotherapy
SBR	Scarff-Bloom-Richardson
SD	standard deviation
SDA-PAGE	sodium dodecyl sulphate polyacrylamide gel electrophoresis
SERD	selective ER down-regulators
SERM	selective ER modulators
SF	surviving fraction
SH3BGRL	SH3 domain binding glutamate rich protein like
SLNB	sentinel lymph node biopsy
SMAD2	SMAD family member 2

SNP	single nucleotide polymorphism
SPF	S -phase fraction
SRS	stereotactic radiosurgery
STK11	serine/threonine kinase 11
STR	short tandem repeat
TBI	traumatic brain injury
TCGA	the cancer genome atlas
TKI	tyrosine kinase inhibitor
TMA	Tissue microarray
TNBC	triple negative breast cancer
TNF	tumour necrosis factor
TP53	tumour protein 53
TREM1	Triggering Receptor Expressed On Myeloid Cells 1
TSP1	Thrombospondin 1
UK	United Kingdom
UNS	unspecified group
V	volts
VEGF	Vascular Endothelial Growth Factor
WBI	whole breast irradiation
WEBGESTALT	WEB-based GEne SeT AnaLysis Toolkit
WHO	world health organisation
WT	wild type
YFP	yellow fluorescent protein
µ-calpain	micro-calpain
µg	microgram
µg/ml	microgram per millilitre
µg/µl	microgram per microliter
µM	micromolar

Table of contents

Abstract ..... **i**
Presentations and grants ..... **iv**
Acknowledgements ..... **v**
Abbreviations ..... **vi**
Table of contents ..... **xii**
List of tables ..... **xvi**
List of figures ..... **xviii**
Chapter 1-Introduction **1**
1.1 Introduction to Breast cancer 2
1.1.1 Breast cancer epidemiology 2
1.1.2 Risk factors 3
1.1.3 Breast cancer classification 7
1.1.4 Predictive and prognostic factors 12
1.1.5 Breast cancer treatment 21
1.2 The calpain system 31
1.2.1 Structure 31
1.2.2 Calpain classification and nomenclature 32
1.2.3 Activation and regulation 34
1.2.4 Calpain function 35
1.2.5 Calpain system and disease 39
1.3 Calpain system and breast cancer 40
1.4 Overall study hypothesis, aims and objectives 41
Chapter 2- Molecular overexpression of calpastatin isoforms **44**
2.1 Abstract 45
2.2 Introduction 46
2.2.1 Calpastatin structure 47
2.2.2 Calpastatin isoforms 48
2.2.3 Subcellular Calpastatin distribution 50
2.2.4 Calpastatin and cancer 51
2.2.5 Hypothesis and aims 52
2.3 Materials and Methods 53
2.3.1 Breast cancer cell lines and reagents 53
2.3.2 Subculture 54
2.3.3 Cell storage and recovery 54
2.3.4 Cell growth curves by proliferation assay 55
2.3.5 Plating efficiency 55
2.3.6 Stable transfection of CAST isoforms 56

2.3.7 Western Blotting 57
2.3.8 Measurement of mRNA expression 58
2.3.9 Cell immunofluorescence 60
2.3.10 RNA sequencing sample preparation and data analysis 60
2.3.11 Statistical analysis 62
2.4 Results 62
2.4.1 HA tagged calpastatin isoforms expression in cells 62
2.4.2 mRNA expression of calpastatin isoforms 64
2.4.3 Intracellular localisation of calpastatin isoforms 67
2.4.4 RNA sequencing data analysis 69
2.5 Discussion 77
Chapter 3- Small molecule novel calpain inhibitors 92
3.1 Abstract 93
3.2 Introduction 94
3.2.1 Activation of calpains 94
3.2.2 Calpain inhibitors 96
3.2.3 Allosteric inhibition of calpains 97
3.2.4 Novel small molecule calpain inhibitors 98
3.2.5 Measurement of calpain activity 99
3.2.6 Hypothesis and aims 101
3.3 Materials and Methods 102
3.3.1 Cell lines, growth media and cell culture 102
3.3.2 t-BOC calpain activity assay 102
3.3.3 Development of the FRET bioassay system 103
3.3.4 Preparation of drugs 105
3.3.5 Cell proliferation and clonogenic assays 106
3.3.6 Statistical analysis 107
3.4 Results 107
3.4.1 Inhibition of calpain activity using the t-BOC assay 107
3.4.2 Development of the FRET bio assay 110
3.4.3 Induction of calpain activity using the FRET bio assay 111
3.4.4 Inhibition of calpain activity using the FRET bio assay 112
3.4.5 Effect of novel compounds on cell proliferation and survival 115
3.4.6 Specificity of the novel compounds 1, 9 and 10 116
3.5 Discussion 117
Chapter 4- Use of CRISPR/Cas9 calpain knock out cell lines 124
4.1 Abstract 125
4.2 Introduction and aims 127

4.2.1 Calpains and cancer 127
4.2.2 Conventional treatments for breast cancer 128
4.2.3 Hypoxia and cancer and the calpain system 132
4.2.4 Hypothesis and aims 134
4.3 Material and methods 135
4.3.1 Cell lines, reagents, and subculture 135
4.3.2 Cell storage, recovery and mycoplasma checks 136
4.3.3 Western blotting 136
4.3.4 Cell growth curves and plating efficiency 137
4.3.5 Doxorubicin treatment proliferation and clonogenic response 138
4.3.6 Cell growth curves and plating efficiency in hypoxia 138
4.3.7 Doxorubicin treatment proliferation and survival response in hypoxia 139
4.3.8 Cell radiation response in hypoxia vs normoxia 139
4.3.9 Statistical analysis 140
4.4 Results 140
4.4.1 Effect of knocking out calpains 1, 2 and 4 on cell proliferation and plating efficiency 140
4.4.2 Effect of knocking out calpains on doxorubicin response 143
4.4.3 Cell proliferation and plating efficiency in hypoxic growth conditions 146
4.4.4 Effect of knocking out calpains on doxorubicin response in hypoxia.. 149
4.4.5 Effect of hypoxia and normoxia on radiation response in calpain knock out cells 152
4.5 Discussion 156
Chapter 5- Bioinformatic analyses 167
5.1 Abstract 168
5.2 Introduction 169
5.2.1 Bioinformatics analyses 169
5.2.2 Cancer datasets 169
5.2.3 Pathway analysis 170
5.2.4 RBBP4 171
5.2.5 Hypothesis and aims 172
5.3 Materials and methods 173
5.3.1 Differentially expressed genes 173
5.3.2 Pathway enrichment analysis 173
5.3.3 Survival analysis on TCGA data 174
5.3.4 Patient cohorts 174
5.3.5 Tissue microarray 175
5.3.6 Antibody specification and optimisation 175

5.3.6 Immunohistochemistry 176
5.4 Results 177
5.4.1 Differentially expressed genes 177
5.4.2 Pathway enrichment analysis 177
5.4.3 Pathway commonalities in datasets 179
5.4.4 Survival analysis on TCGA 180
5.4.5 Analysis with the METABRIC dataset 186
5.4.6 RBBP4 protein expression 197
5.5 Discussion 198
Chapter 6- General Discussion, limitations and suggestions for future work 206
6.1 General discussion 207
6.2 Limitations and suggestions for future work 224
6.3 Conclusions 229
References 231
Appendix A: Supplementary information for Chapter 2 262
Appendix B: Supplementary information for Chapter 3 278
Appendix C: Supplementary information for Chapter 4 285
Appendix D: Supplementary information for chapter 5 292
Appendix E: Permission for republish or display content 295

List of tables

Table 1. 1 Risk of Developing Breast Cancer 4
Table 1. 2 TNM system in breast cancer staging. 16
Table 1. 3 Summary of NPI scores and their associations with prognosis and 10-year survival..... 17
Table 1. 4 Molecular subtypes characteristics and recommended systemic therapy 19
Table 1. 5 Calpain types and their expression in different tissue types. 33
Table 2. 1 Summary of different calpastatin transcripts..... 49
Table 2. 2 Primer sequences for HPRT, CAST I and CAST II 64
Table 2. 3 Linear equations of standard curves and amplification efficiencies of PCR reactions for HPRT, CAST I and CAST II genes 65
Table 2. 4 Number of DEGs 70
Table 2. 5 Top 30 DEGs associated with the overexpression of CAST I, CAST II and CAST III in T47D cells..... 71
Table 2. 6 Top 30 DEGs associated with the overexpression of CAST I, CAST II and CAST III in MDA-MB-231 cells 72
Table 2. 7 Number of pathways enriched by DEGs associated with CAST I, CAST II and CAST III expression in T47D and MDA-MB-231 cells..... 75
Table 2. 8 Genes significantly affected by the expression of CAST I in T47D cells 76
Table 2. 9 Genes significantly affected by the expression of CAST II in T47D cells 76
Table 2. 10 Genes significantly affected by the expression of CAST III in T47D cells 76
Table 2. 11 Genes significantly affected by the expression of CAST I in MDA-MB-231 cells 76
Table 2. 12 Genes significantly affected by the expression of CAST II in MDA-MB-231 cells 76
Table 2. 13 Genes significantly affected by the expression of CAST III in MDA-MB-231 cells 77
Table 4. 1 List of antibodies and dilutions..... 137
Table 4. 2 Table summarising the DT and PE for WT and calpain KO cells..... 143
Table 4. 3 Summary of doubling times and plating efficiencies hypoxia (1%O2) vs normoxia (21% O2) 148
Table 4. 4 Normoxic (21% O2) vs hypoxic (1% O2) proliferation IC_{50} values. . 150
Table 4. 5 PEs and radiobiological parameters for WT and Capn1 KO cells 153
Table 4. 6 PEs and radiobiological parameters for WT and Capn2 KO cells 154
Table 4. 7 PEs and radiobiological parameters for WT and Capns1 KO cells..... 155
Table 4. 8 MDA-MB-231 WT and Calpain KO OER and SF8 values in normoxia and hypoxia..... 155
Table 4. 9 MDA-MB-231 WT and Calpain KO radio enhancement values at 1% survival in normoxia and hypoxia 156
Table 5. 1 List of antibodies and dilutions. 176
Table 5. 2 Number of DEGs obtained from METABRIC and TCGA 177
Table 5. 3 Pathways enriched by altered CAPN1 expression 178
Table 5. 4 Pathways enriched by altered CAPN2 expression 178
Table 5. 5 Pathways enriched by altered CAPNS1 expression 178
Table 5. 6 Pathways enriched by altered CAST expression 179
Table 5. 7 Common DEGs between datasets for CAPN1 179
Table 5. 8 Common DEGs between datasets for CAPN2 179
Table 5. 9 Common DEGs between datasets for CAPNS1 180

Table 5. 10 Common DEGs between datasets for CAST 180
Table 5. 11 List of calpain system associated genes..... 186
Table 5. 12 Associations between the expression of RBBP4 probes 1 and 2 and the breast cancer clinicopathological variables. 196

List of figures

Figure 1. 1 Schematic structure of the calpain molecules 32
Figure 1. 2 Schematic representation of the involvement of the calpain genes in cell migration and invasion. 36
Figure 1. 3 Calpains and their associations with survival related pathways.. 37
Figure 1. 4 Calpains and their associations with cell death related pathways. 38
Figure 2. 1 Schematic representation of gDNA, cDNA and protein Calpastatin ... 48
Figure 2. 2 Expression of HA-tagged calpastatin type I, II and III in T47D and MDA-MB-231 cells 63
Figure 2. 3 Calpastatin isoform specific primer binding sites 64
Figure 2. 4 Melt curves for HPRT, CAST 1 and CAST 2 65
Figure 2. 5 Overexpression of CAST I and CAST II in T47D and MDA-MB-231 cells. 66
Figure 2. 6 Intracellular localisation of calpastatin type I, II and III in T47D and MDA-MB-231 cells 68
Figure 2. 7 CAST II intracellular localisation 69
Figure 2. 8 Overlapping and unique DEGs 73
Figure 2. 9 Overlapping and unique DEGs between T47D and MDA-MB-231 cells overexpressing 74
Figure 3. 1 Activation of calpain by calcium 96
Figure 3. 2 Novel calpain inhibitor structures 98
Figure 3. 3 Binding domains of different calpain inhibitors 99
Figure 3. 4 Design of the FRET based biosensor to assess calpain activity in live cells 101
Figure 3. 5 Calpain activity inhibition by calpeptin using t-BOC assay 108
Figure 3. 6 Inhibition of calpain activity by the novel compounds using the tBOC assay and fluorescence 109
Figure 3. 7 FRET vector transfection efficiency 110
Figure 3. 8 Activation of calpains 111
Figure 3. 9 Inhibition of calpains by PD150606 113
Figure 3. 10 Inhibition of calpains using novel compounds 114
Figure 3. 11 Effect of novel compounds on cell proliferation and survival 116
Figure 3. 12 Inhibition of calpain activity by novel compounds on calpain 1 KO cells 117
Figure 4. 1 Cell line characterisation of the MDA-MB-231 WT and calpain KO cell lines 141
Figure 4. 2 Plating efficiencies for the MDA-MB-231 WT and calpain KO cell lines 142
Figure 4. 3 Effect of knocking out calpains on doxorubicin response on cell proliferation 144
Figure 4. 4 Effect of knocking out calpains on doxorubicin response on cell survival 145
Figure 4. 5 Cell growth curves, doubling times and Plating efficiencies of the MDA-MB-231 WT and calpain KO cell lines in the presence of normoxia (21% O2) and hypoxia (1% O2) 147
Figure 4. 6 Effect of knocking out calpains on doxorubicin response on cell proliferation in hypoxia (1% O2) 149
Figure 4. 7 Effect of knocking out calpains on doxorubicin response on clonogenic cell survival in hypoxia (1% O2) 151
Figure 4. 8 MDA-MB-231 WT and calpain 1 KO cell lines response to radiotherapy 152

Figure 4. 9 MDA-MB-231 WT and calpain 2 KO cell lines response to radiotherapy 154
Figure 4. 10 MDA-MB-231 WT and calpain 4 KO cell lines response to radiotherapy 155
Figure 5. 1 Survival analysis for PPP1CA gene 181
Figure 5. 2 Survival analysis for AMOT gene 182
Figure 5. 3 Survival analysis for PRKAB2 gene 182
Figure 5. 4 Survival analysis for AMOTL1 gene 182
Figure 5. 5 Survival analysis for RAB13 gene 183
Figure 5. 6 Survival analysis for MAGOH gene 183
Figure 5. 7 Survival analysis for POLE2 gene. 184
Figure 5. 8 Survival analysis for YWHAG gene. 184
Figure 5. 9 Survival analysis for HDAC1 gene 185
Figure 5. 10 Survival analysis for RBBP4 gene 185
Figure 5. 11 Survival analysis for PSMB5 gene 185
Figure 5. 12 Correlation between the calpain system and associated DEGs. 187
Figure 5. 13 Survival analysis of Calpain 1 and associated DEG probes 190
Figure 5. 14 Survival analysis of Calpain 2 and associated DEG probes 191
Figure 5. 15 Survival analysis of Calpain 4 probes and associated DEG probes 192
Figure 5. 16 Survival analysis of CAST probes and associated DEG probes 194
Figure 5. 17 RBBP4 expression in breast cancer cells and tissue. 197

Chapter 1-Introduction

1.1 Introduction to Breast cancer

1.1.1 Breast cancer epidemiology

Breast cancer is one of the most commonly diagnosed cancer types. In the year 2020 an estimated 2.3 million new cases were reported according to the Global Cancer Statistics (GLOBOCAN) data. It remains the 5th cause of cancer-related deaths worldwide (Sung *et al.*, 2021). In the United Kingdom alone, about 55,900 new cases of breast cancer are diagnosed, and counts for 15% new cancer cases every year (CRUK, 2021b). Breast cancer age standardised incidence rates (ASIR) are positively and significantly associated with the Human development Index (HDI), according to the GLOBOCAN data 2018 (Sharma, 2021). The 2020 data shows that ASIR was highest (75.6 for every 100,000) in very high HDI countries and was much lower (27.8 for every 100,000) in medium to low HDI countries (Ferlay *et al.*, 2020a).

Breast cancer is the leading cause of cancer related deaths in the women worldwide. While incidence rates were high in developed nations, countries in Asia and Africa had a total of 63% of total death in 2020 (Ferlay *et al.*, 2020a). The mortality-to-incidence ratio (MIR), a representative indicator of 5-year survival rates, was 0.30 globally in 2020 (Ferlay *et al.*, 2020a). The latest CRUK report shows that there were about 11,500 deaths, making it the 4th most common cause of cancer (2nd in females) related deaths in the United Kingdom. These deaths account for 7% of all cancer related deaths in the UK. The mortality rates are the highest in people more than 90 years of age and 48% of all breast cancer deaths are reported in people aged 75 years and over (CRUK, 2021b). The mortality rates have decreased by around 39% in the UK since 1970s. This is because of increased public awareness, better screening and improved treatments (Youlden *et al.*, 2012).

The 5-year survival rates in countries with developed healthcare were 89.6% for localised cancer and 75.4% for regional cancer. While in nations with less developed healthcare, the survival rates were 76.3% to 47.4% in local and invasive breast cancer, respectively (Sankaranarayanan *et al.*, 2010). In the UK, the 1-year survival for patients diagnosed with breast

cancer is around 95.8% and the 5-year survival is around 85% (CRUK, 2021b).

In the UK, the breast cancer mortality rates have been projected to decrease by 26% by the year 2035, while the incidences and deaths would have increased worldwide. Current projections indicate that the number of new cases detected annually would reach 2.7 million, while the number of deaths would be 0.87 million, globally (CRUK, 2021b; Ferlay *et al.*, 2020b).

1.1.2 Risk factors

1.1.2.1 Gender

One of major factors that is associated with a high risk of development of breast cancer is gender. Females have enhanced hormonal stimulation, unlike males where the levels of female hormones are significantly low. Consequently, females are more vulnerable to disturbances in hormone balances which can be associated with an increased risk of disorders including cancer (Key *et al.*, 2013). Males account for less than 1% of the population affected by breast cancer. Breast cancer in males is a rare disease and accounts for less than 1% of all breast cancer. The risk factors for breast cancer in males include, older age, genetic mutations, a family history of breast cancer, higher oestrogen levels, klinefelter syndrome and exposure to radiation (Giordano, 2018).

1.1.2.2 Age

Age plays a crucial role in the development of both female and male breast cancer. The risk of breast cancer development grows with advanced age, mentioned in table 1.1 (Siegel *et al.*, 2021). In the United Kingdom, 48% of all breast cancers diagnosed are in women of age 50 or more, and the incidence of breast cancer are highest in women above 90 (CRUK, 2021b). Interestingly, it was observed, that when breast cancer is diagnosed in groups under 40 years of age, they have a more aggressive form. The breast cancer subtype (described in section 1.1.3) most commonly diagnosed in premenopausal women is the resistant triple negative type, while women over 70 years of age are more commonly diagnosed with the luminal subtype (Collaborative Group on Hormonal Factors in Breast Cancer

(CGHFBC, 2001)). Age along with several other factors such as accumulation of cellular alterations and exposure to potential carcinogens can lead to an increased risk of development of cancer with time.

Table 1. 1 Risk of Developing Breast Cancer. Adapted from (Siegel *et al.*, 2021). The risk of developing invasive breast cancer in selected age intervals in females (United States of America), assessed between 2015- 2017.

Age interval (years)	Probability (%) of developing invasive breast cancer.
Birth–49	2.1 or 1 in 49
50–59	2.4 or 1 in 42
60–69	3.5 or 1 in 28
70 and older	7.0 or 1 in 14
From birth to death	12.9 or 1 in 8

1.1.2.3 Genetic mutations and family history

Presence of certain genetic mutations is associated with a high risk of development of breast cancer. These include mutations in two major genes, BRCA1 and BRCA2 located on chromosome 17 and 13 respectively, which are highly associated with breast cancer development (Shiovitz *et al.*, 2015). Mutations in the BRCA genes are dominant and are commonly inherited. However, the presence of several sporadic mutations in genes such as CDH1, PTEN, TP53 and STK11 have also been reported to have a high association to breast cancer development. Other genes, that have shown to be involved in the repair of DNA and interact with the BRCA genes including- BRIP1, PALB2, CHEK2, and ATM have moderate associations with the risk of breast cancer (reviewed in (Łukasiewicz *et al.*, 2021)).

A history of breast cancer in the immediate family is associated with a greater risk of breast cancer (Hartmann *et al.*, 2005). In addition, a history of any non-cancerous modifications in the breast like- atypical hyperplasia, carcinoma in-situ and several other proliferative or non-proliferative lesions can increase the risk significantly (reviewed in (Łukasiewicz *et al.*, 2021)).

1.1.2.4 Reproductive history

The association between exposure to endogenous hormones, oestrogen and progesterone in particular, and the high risk of breast cancer has been well established. First menstruation, pregnancy, breastfeeding, menopause and the simultaneous occurrence of hormonal imbalance are all crucial events that can lead to a possible stimulation of breast cancer development. Early age menarche is a risk factor for breast cancer and is also associated with engagement of lymph node and tumour grade (Orgéas *et al.*, 2008). Additionally it was shown that an early age at the time of menarche can lead to poor prognosis overall. However, early menopause can reduce the risk of breast cancer (Titus-Ernstoff *et al.*, 1998).

Incidence of pregnancy provides certain security against the potential of breast cancer. However, this protection was observed only after a term of 33 week since the start of pregnancy (Husby *et al.*, 2018). An early age full term first pregnancy followed by more births are linked to a reduced risk of breast carcinogenesis (Albrektsen *et al.*, 2005; Bernstein, 2002). In addition, occurrence of preeclampsia during pregnancy has been reported to lower the risk of breast cancer in women. The imbalance of hormones like decreased oestrogen and insulin-like growth factor 1 levels, and increased progesterone, cortisol, insulin, androgens, corticotropin-releasing factor, human chorionic gonadotropin, IGF-1 binding protein levels, during preeclampsia have shown to reduce the risk of breast cancer (Innes *et al.*, 1999). Moreover, it was also shown that a longer duration of breastfeeding can reduce the risk of developing oestrogen receptor/progesterone receptor (ER/PR) positive and negative breast tumours (Ursin *et al.*, 2005).

1.1.2.5 Breast tissue density

In clinical practice, several categories including high density, low density and fatty breasts have been established. The breast tissue density remains inconsistent throughout the lifetime. Females with lower Body Mass Index (BMI) and who are of young age, pregnant or lactating or on hormone replacement therapy have a greater breast tissue density (Checka *et al.*, 2012). It is seen generally that greater breast tissue density correlates to

a greater risk of breast cancer development in both premenopausal and postmenopausal women (Kim *et al.*, 2020).

1.1.2.6 Exogenous drugs

Females receiving Hormone replacement therapy (HRT) are at a risk of developing breast cancer and the risk increases with the duration of therapy. In a group of 16,608 women receiving a combination of oestrogen and progesterone, the risk of breast cancer development after a 5 year follow-up was 26% higher than the placebo group (Chlebowski *et al.*, 2009). Use of combination of oestrogen and progestin HRT has shown to have a higher risk of breast cancer compared to oestrogen alone form of treatment. It was also shown that the combination HRT is commonly associated with more aggressive forms of cancer that are node positive (Chlebowski *et al.*, 2010; Prentice *et al.*, 2008). Prentice and colleagues also showed that women who start the treatment soon after their menopause and continue for many years may be particularly at a higher risk (Prentice *et al.*, 2008). However, the risk of breast cancer reduces within 2 years of termination of treatment (Chlebowski *et al.*, 2009).

1.1.2.7 Other factors

Other factors like physical activity, body mass index (BMI), alcohol intake, smoking, and exposure to chemicals and other drugs and ionising radiation can have an effect on breast cancer development (Łukasiewicz *et al.*, 2021). Regular physical activity is considered a protective factor against breast cancer development. There are several explanations to it which include, physical activity reduces exposure to the endogenous sex hormones, alters insulin-like growth factor-1 levels, or changing immune system responses (Łukasiewicz *et al.*, 2021). BMI is another risk factor for breast cancer. Wang and colleagues showed that women over 50 years of age and a higher BMI have a greater risk of cancer development than women with a lower BMI (Wang *et al.*, 2019c). It was also shown that a greater BMI is associated with more aggressive forms of tumour like a greater tumour size and a high lymph node metastasis. Greater BMI is also associated with higher mortality rates and probability of cancer relapse in premenopausal women (Sun *et al.*, 2018). Smoking and alcohol intake are another major risk factors for

breast cancer. It is the content of alcoholic consumption that effects the risk of cancer development. Possible explanations include alcohol intake induces an increase in oestrogen levels which leads to a hormonal imbalance which can increase the risk of carcinogenesis in the female organs (Erol *et al.*, 2019). In addition the carcinogens in tobacco absorbed by the breast tissue can increase the risk of mutations in tumour suppressor (p53) and oncogenes. Therefore, both active and passive smoking can significantly promote carcinogenesis induction (Terry *et al.*, 2002).

Chemicals like dichlorodiphenyltrichloroethane (DDT) and polychlorinated biphenyl (PCB) are the most investigated in terms of breast cancer as early exposure can disrupt development of mammary glands. Exposure to such chemicals can induce mammary carcinogenesis. Polycyclic aromatic hydrocarbons (PAH), synthetic fibres, organic solvents, oil mist and insecticides have all been potentially linked with breast cancer. Other drugs that can potentially be a risk factor for breast cancer include antibiotics, antidepressants, and Non-Steroidal Anti-Inflammatory Drugs (NSAIDS) (reviewed in (Łukasiewicz *et al.*, 2021)) .

In addition, previous exposure to radiation therapy is a risk of development of breast cancer. The risk of developing secondary malignancies after radiation therapy treatment may be an individual factor and may depend on the patient's individual characteristics despite it being a quite frequent phenomenon and causes much clinical concern. Malignancies caused by radiation exposure is associated with an individual's age. Patients who receive radiation treatment before 30 years of age are at a higher risk of developing breast cancer (Ng *et al.*, 2015). In addition, a family history of breast cancer patients who receive radiotherapy may increase the risk of occurrence of cancer (Łukasiewicz *et al.*, 2021).

1.1.3 Breast cancer classification

1.1.3.1 Histological subtypes

Breast cancer is a heterogeneous disease. It is comprised of many distinct forms that have different morphology, clinical presentation and response to treatment (Weigelt *et al.*, 2010b; Weigelt *et al.*, 2009).

The growth pattern of a tumour can be described by its histology. Pathologists have identified several specific morphological and cytological patterns that have been consistently associated with distinctive clinical presentation or outcomes which are called histological types. Breast cancer is broadly classified into ductal or lobular; cancers arising from the ducts of the breast are called ductal and cancers arising from the lobules of the breast are called lobular carcinomas. These can be further classified as carcinoma in situ or invasive (infiltrative) carcinomas (Malhotra *et al.*, 2010). Carcinomas in situ can be either ductal carcinoma in situ (DCIS) or lobular carcinoma in situ (LCIS). Carcinoma in situ tends to be confined to the ducts or lobules; DCIS is a heterogeneous group of non-malignant tumours and accounts for more (20-30%) than LCIS (2%) of breast cancer types (Malhotra *et al.*, 2010; Weigelt *et al.*, 2010b). Based on the tumour architecture, DCIS is further subclassified into- Comedo, Cribiform, Micropapillary, Papillary and Solid while LCIS has low histological variation (Malhotra *et al.*, 2010).

Fully malignant, invasive or infiltrative carcinomas are also a heterogeneous group of tumours that can invade the surrounding tissue and metastasise to different sites in the body. These include infiltrating ductal (IDC), invasive lobular (ILC), mucinous, tubular, medullary, and papillary carcinomas. IDC is the most common subtype of all and accounts for 70-80% and ILC accounts for 10% of all invasive carcinomas (Li *et al.*, 2005). Based on the degree of nuclear pleomorphism, tubule formation and mitotic index IDC can be either well-differentiated (grade 1), moderately differentiated (grade 2) or poorly differentiated (grade 3) (Lester *et al.*, 2009).

Clinically, breast cancers can be categorised into early stage invasive breast cancer (EBC), locally advanced primary breast cancer (LABC) or metastatic breast cancer (MBC) based on tumour type, histological grade, tumour size, nodal involvement and lymphovascular invasion (LVI) (Edge *et al.*, 2010). Generally, early stage invasive cancers are at stage I and II that can spread beyond the breast ducts and lobes and invade the surrounding tissues. The five year survival rates are 98% for local and 83.6% for regional types of EBC. LABC refers to all stage III cancers and are characterised by the presence of tumours >5 cm in diameter; tumours spread into the skin or

chest muscles; positive lymph node status. LABC is generally spread within the breast or ipsilateral nodal areas. The five year survival rate is generally 55% for this type of cancer (Maughan *et al.*, 2010). Stage III or IV may also include Inflammatory breast cancer (IBC).

Inflammatory breast cancer is a relatively rare and a rapidly progressing form of LABC, associated with a more aggressive phenotype. It is characterised by the presence of diffuse erythema and oedema, no palpable mass, higher nuclear grade and negative hormone receptor status (Li *et al.*, 2005; Maughan *et al.*, 2010). It accounts for 2.5% of all invasive breast cancer types (Li *et al.*, 2005; Robertson *et al.*, 2010). IBC is generally diagnosed as a node positive disease with tumours that are high grade and have poor survival outcome (Li *et al.*, 2005; Maughan *et al.*, 2010)

Stage IV refers to the Metastatic Breast Cancer (MBC) where the disease has spread to distant sites in the body through the blood and/or lymphatic system. These lesions invade vital organs and develop multiple foci that decline the patient's health (Jin *et al.*, 2015). These distant lesions become challenging to surgically remove and develop resistance to forms of therapy available currently. In addition to distant lymph nodes, common target sites for MBC include lung, bone, brain and liver (Jin *et al.*, 2015; Maughan *et al.*, 2010) . The five year survival rate in patient with MBC is only about 23.3% (Maughan *et al.*, 2010).

1.1.3.2 Molecular subtypes

In a genomic study by Perou and colleagues, breast cancer was categorised into 4 main subtypes including luminal A, luminal B, human epidermal growth factor-2 (HER2) enriched, and triple negative breast cancers (TNBC) (Perou *et al.*, 2000a; Sørlie *et al.*, 2001). The above mentioned classification categorises breast cancer into ER positive (luminal), or ER negative tumours. ER positive tumours are divided into luminal A and luminal B. ER negative tumours are classed as- HER2 enriched and ER/PR/HER2 negative, triple negative breast cancer (TNBC) (Perou *et al.*, 2000a).

Luminal cancers are ER positive tumours and account for 70% of all breast cancer cases in the Western population (Howlader *et al.*, 2014). Luminal

cancers most commonly present as IBC of no specific type (NST) but can rarely differentiate into invasive lobular, invasive cribriform, tubular, mucinous, and invasive micropapillary carcinomas (Makki, 2015; Weigelt *et al.*, 2010b). Proliferation and luminal regulated pathways distinguish luminal tumours into Luminal A and B subtypes that have different clinical outcome. Luminal A tumours account for 50-60% of all breast cancer types and are characterised by the expression of ER and/or PR, negative expression of HER2 and low Ki67 index (the cell proliferation nuclear marker), by immunohistochemistry (Carey *et al.*, 2006; Yersal *et al.*, 2014). The ER transcription factors activate genes like ERα, GATA binding protein 3, X-box binding protein 1, hepatocyte nuclear factor 3 α, and oestrogen-regulated LIV-1 that are characteristic for the luminal epithelium lining of the mammary glands (Sørlie *et al.*, 2001; Weigelt *et al.*, 2010a). While luminal B tumours account for 15-20% of all breast tumours and are ER positive, may be PR negative and/or HER2 positive and a higher Ki67 index compared to the luminal A subtype. This has a lower expression of genes typical for the luminal epithelium like PR and FOXA1 (Prat *et al.*, 2013; Sørlie *et al.*, 2001; Xu *et al.*, 2015a). However, the expression of ER does not vary between luminal A and luminal B and can be used to distinguish ER positive from ER negative disease (Sørlie *et al.*, 2001; Weigelt *et al.*, 2010a). Another subgroup of luminal type, luminal C was identified that differs from luminal A and luminal B by the high expression of certain novel genes whose function is not known yet (Sørlie *et al.*, 2001). Luminal A tumours have low expression of proliferation genes, are usually of low grade histologically and have the best prognosis. While Luminal B tumours have a more aggressive phenotype, higher rate of proliferation, higher histological grade and a significantly worse prognosis compared to the luminal A disease (Perou *et al.*, 2000a; Sørlie *et al.*, 2001; Weigelt *et al.*, 2010a).

The HER2 enriched tumours are characterised by the high expression of HER2 and absence of ER and PR expression. It accounts for 10-15% of breast cancers. The gene expression pattern for this subtype includes high expression of genes in ERBB2 amplicon including ERBB2/HER2 and GRB7 and low expression of ER and basal gene clusters (Łukasiewicz *et al.*, 2021;

Sørlie *et al.*, 2001). The HER2 enriched tumours exhibit a more aggressive clinical behaviour. They have a higher rate of proliferation, high histological and nuclear grade and an intermediate to poor clinical outcome compared to the luminal subtypes (Sørlie *et al.*, 2001; Weigelt *et al.*, 2010a).

The triple negative breast cancer (TNBC) is a heterogeneous collection of breast cancers that are characterised by the absence of ER, PR and HER2. It one of the most aggressive forms of breast cancer with the worst clinical outcome (Sørlie *et al.*, 2001). It accounts for approximately 20% of all breast cancers and is more common in women under 40 years of age (Plasilova *et al.*, 2016). About 80% of breast cancers arising in BRCA1 germline mutations tend to be TNBC. They usually have a high histological and nuclear grade, central necrotic zones, high mitotic index, pushing borders and a conspicuous lymphocytic infiltrate (Fulford *et al.*, 2006; Livasy *et al.*, 2006; Reis-Filho *et al.*, 2006). The gene expression profiling of TNBC revealed six subtypes including basal like (BL1 and BL2), mesenchymal (M), mesenchymal stem-like (MSL), immunomodulatory (IM), and luminal androgen receptor (LAR), and an unspecified group (UNS) (Lehmann *et al.*, 2011; D. Wang *et al.*, 2019b). Another subtype, basal-like, was also identified by the study by Perou and colleagues. It is characterised by the absence of hormone receptor expression and overexpression of keratin 5 and 17, laminin, and fatty acid binding protein 7 (Sørlie *et al.*, 2001). The terms basal-like and triple-negative breast cancer have been used interchangeably, however not all TNBC are of basal type (Santonja *et al.*, 2018).

Sorlie and colleagues showed that there was a significant difference in the TP53 mutation status among the different molecular subtypes of breast cancer. It was shown that only 13% (low) of luminal tumours exhibited TP53 mutated status; while 71% (intermediate to high) of HER2 enriched and 82% (high) of triple negative exhibited the TP53 mutated status (Sørlie *et al.*, 2001). There also is a significant difference in terms of clinical outcome, among the different breast cancer types. The HER2 and the TNBC were associated with the short overall and relapse free survival with TNBC having the shortest survival. Overexpression of the HER2 oncoprotein is a known prognostic factor that is associated with poor survival in breast

cancer. However, with the development of anti-HER2 therapies (Trastuzumab) this patient group has an improved disease-free survival (DFS) and overall survival (OS) (Pinto *et al.*, 2013). The ER positive tumours however, have better clinical outcome than the ER negative tumours. The luminal A tumour subtype has the best overall and relapse free survival, while luminal B and C have a shorter overall and relapse free survival compared to the luminal A subtype (Sørlie *et al.*, 2001).

In addition to the above mentioned classification, to study the impact of genomic aberrations on the transcriptome, 2000 breast tumours of the METABRIC (Molecular Taxonomy of Breast Cancer International Consortium) (Curtis *et al.*, 2012) were used to perform integrated analysis of both genomic and transcriptomic data (Dawson *et al.*, 2013). The germline variations including CNVs (Copy Number Variants) and SNPs (Single Nucleotide Polymorphisms), and the somatic aberrations including CNAs (Copy Number Aberrations) were included in the analysis. These were found to be associated with gene expression alterations out of which the effects of cis-acting CNAs dominated. Joint copy number and gene expression clustering analysis classified breast cancer into 10 novel molecular subgroups. These 10 integrative clusters were shown to be associated with distinct CNAs and gene expression alterations, which demonstrated the tumour heterogeneity in ER, PR and HER2 positive tumours. In addition these 10 groups were shown to be associated with distinct clinical presentation and outcomes (Dawson *et al.*, 2013).

1.1.4 Predictive and prognostic factors

A prognostic factor is any parameter that provides information on the clinical outcome of the patient at the time of diagnosis, while a predictive factor is a parameter that is associated with the response to an administered form of therapy. These predictive and prognostic factors are used in a clinical setting to determine correlations between the clinicopathological factors and the clinical outcome (Cianfrocca *et al.*, 2004).

1.1.4.1 Ethnicity and age

Studies have shown that African American and Hispanic women have a decreased survival with breast cancer. This could likely be due to issues like lack of access to care leading to diagnosis at a higher stage. It may also be interesting to note that survival in African American women may be poor even at lower stage (Daly *et al.*, 1985; Elledge *et al.*, 1994; Pierce *et al.*, 1992).

Age is a prognostic factor for breast cancer with two studies demonstrating that patients below 35 years of age have a worse prognosis (Albain *et al.*, 1994; Nixon *et al.*, 1994). In addition, patients who are below 35 years of age, have worse histopathological features than the patients above 35 years of age. They also demonstrated that five year overall and relapse-free survival rates were 65% and 40%, respectively in patients under 35 years; and 98% and 80% respectively, for patients over 35 years of age (Yildirim *et al.*, 2000).

1.1.4.2 Tumour size

Tumour size is linked with axillary lymph node involvement but is also an independent prognostic factor. A large tumour size increases the probability of recurrence. In a study by Carter and colleagues, patients with tumours size <1cm had a 5 year overall survival (OS) of about 99%, tumours between 1 cm and 3 cm had a 5 year OS of 89% , and tumours between 3 cm and 5 cm had a 5 year OS of about 86% (Carter *et al.*, 1989). Rosen and colleagues showed a significant association between the tumour size and 20-year recurrence free survival. They found that tumours <1 cm had a 20-year relapse free survival (RFS) of 88%, tumours between 1.1 cm to 3 cm had a 20-year RFS of 72%, and tumours between 3.1 cm to 5 cm had a 20-year RFS of 59% (Rosen *et al.*, 1993).

The median time to developing into metastatic disease reduces with the increase in tumour size. Tumour size is an influential prognostic factor used to make treatment decisions for node negative patients (Carter *et al.*, 1989; Fisher *et al.*, 1969; Koscielny *et al.*, 1984; Rosen *et al.*, 1993).

1.1.4.3 Axillary lymph node status

Axillary lymph node status is the most significant prognostic factor for patients with early stage disease. There is a direct relationship between nodal involvement and distant metastasis and recurrence (Nemoto *et al.*, 1983; Saez *et al.*, 1989). Lymph node positive status is significantly associated with the risk of recurrence (Saez *et al.*, 1989).

The 5-year survival for patients with node negative disease was shown to be 82.8%, for 1-3 positive nodes was 73%, for 4-12 positive nodes was 45.7%, and for >13 positive nodes was 28.4% (Fisher *et al.*, 1983).

1.1.4.4 Tumour grade

Grading of tumours has prognostic significance. Certain histologic subtypes like tubular, mucinous, and medullary have a better prognosis than unspecified breast cancer (Carstens *et al.*, 1985; Clayton, 1986; Ridolfi *et al.*, 1977). Multiple grading systems have been proposed but the most widely accepted one is the Scarff-Bloom-Richardson (SBR) classification (Bloom *et al.*, 1957). According to this system, differentiation, pleomorphism, and mitotic index are scored from 1 to 3 and each category are added. Grade 1 tumours are considered to be well differentiated and have a score of 3 to 5 (good prognosis), grade 2 are moderately differentiated tumours and refer have a score of 6 to 7 (intermediate prognosis), and grade 3 are poorly differentiated tumours that have a score of 8 to 9 (poor prognosis) (Bloom *et al.*, 1957; Le Doussal *et al.*, 1989).

The SBR classification was modified by Elston and Ellis and is known as the Nottingham Grading System (NGS) (Elston *et al.*, 1991). It is the most widely used system today and has been recommended by many international committees such as the World Health Organisation (WHO), American Joint Committee on Cancer (AJCC), European Union (EU), and the UK Royal College of Pathologists (UK RCPath) (Rakha *et al.*, 2010).

1.1.4.5 Breast cancer staging

The American Joint Committee on Cancer (AJCC) categorises breast cancer into 5 stages based on the size of the primary tumour (T), presence and extent of involvement of the lymph nodes (N), and presence or absence of

metastasis (M) (Edge *et al.*, 2010). Stage 0 is referred to carcinoma in situ that is characterised by disease with the absence of invasion of cancer cells into breast tissue basement membrane. Stage I and II are denoted to early stage breast cancer. Stage I is characterised by a small invasive tumour without the involvement of nodes and stage II is characterised by the involvement of axillary lymph node. Stage III is referred to as locally advanced disease which is diagnosed by the presence of a large tumour with extensive lymph node involvement and Stage IV is advanced or metastatic disease. This is described as the migration of cancer cells beyond the primary site(s) into distant organs (Edge *et al.*, 2010; Wells *et al.*, 2013). The 5-year survival for stage 0 patients is 100%, for stage I-II is 90%, stage III is about 72% and stage IV is 26% according to Office for National statistics, England 2019 (CRUK, 2021a). Table 1.2 summarises the TNM system.

Table 1. 2 TNM system in breast cancer staging. Adapted from (CRUK, 2020)

Stage	Tumour size	Lymph nodes	Metastasis
0	DCIS or LCIS	Absent	None
I Ia	Invasive carcinoma ▪ <= 2cm	▪ No lymph nodes	None
Ib	▪ <= 2 cm		None
II IIa	Invasive carcinoma ▪ <= 2 cm; OR ▪ > 2 cm <5 cm	▪ 1 to 3; OR ▪ No lymph nodes	None
IIb	▪ 2cm < 5 cm; OR ▪ > 2cm < 5 cm	▪ Small areas of cancer cells in the lymph nodes; OR ▪ 1 to 3 (armpit or near breastbone)	None
III IIIa	Invasive carcinoma ▪ Any size; OR ▪ > 5cm	▪ 4 to 9 (armpit or near breastbone) ▪ Clusters of cancer cells in lymph nodes	None
IIIb	▪ Tumour spread to the skin of the breast or chest wall; OR ▪ Inflammatory breast cancer	▪ Negative or up to 9 lymph nodes	None
IIIc	Tumour of any size	10 or more (in the armpit, or above or below the collar bone, near the breast bone)	None
IV	Invasive carcinoma of any size	Negative or positive lymph nodes	Present

Abbreviations: DCIS, Ductal carcinoma *in situ*; LCIS, Lobular carcinoma *in situ.*

1.1.4.6 Nottingham prognostic Index

The Nottingham Prognostic Index (NPI) is a reliable, sensitive and a widely used clinicopathological prognostic tool to evaluate the clinical outcome of a patient and help clinicians determine the course of treatment. It combines tumour size, lymph node status and the histological grade of the tumour. It

has been validated by additional studies in Nottingham and several studies in many other countries (Lee *et al.*, 2008). The above three factors were combined to create the formula-

NPI= Lymph node stage (1-3) + Histological grade (1-3) + Tumour size X 0.2

Where, tumour size is in cm; lymph node stage: 0 nodes score 1, 1-3 nodes score 2, and >3 nodes score 3; and histological grade 1 score 1, grade 2 score 2, and grade 3 score 3 (Lee *et al.*, 2008). The NPI scores divide breast cancer patients into six prognostic groups summarised in the table (Lee *et al.*, 2008).

Table 1. 3 Summary of NPI scores and their associations with prognosis and 10-year survival. Adapted from (Lee *et al.*, 2008)

NPI score	Prognosis	10-year survival
2.02-2.4	Excellent	96%
2.41-3.4	Good	93%
3.41-4.4	Moderate 1	81%
4.41-5.4	Moderate 2	74%
5.41-6.4	Poor	55%
6.41-6.8	Very poor	38%

Abbreviations: NPI, Nottingham Prognostic Index.

Nottingham Prognostic Index plus (NPI+) is an updated form of NPI prognostic tool that combines more variables to give an improved breast cancer patient outcome stratification (Green *et al.*, 2016).

1.1.4.7 Lymphovascular Invasion (LVI)

Peritumoural LVI is when the cancer cells enter the lymphatic and blood vessels. It has demonstrated to have prognostic significance and is associated with local and distant recurrence. Presence of LVI has shown to be correlated to the risk of recurrence and death. Patients with LVI-positive stage I disease had a recurrence rate of 38%, while that of LVI-negative stage I disease patients was 22% (Rosen *et al.*, 1989). A study by the International Breast Cancer Study Group, demonstrated that the presence of LVI was associated with an increased (15%) risk of 5-year recurrence, in a randomised group of 1275 patients with node-negative disease. Therefore

LVI can be applied to make treatment decisions especially for patients with node negative disease (Neville *et al.*, 1992).

Our group at Nottingham demonstrated that presence of LVI was significantly associated with adverse disease free interval (DFI) and poor overall survival in breast cancer patients. The group also showed that in early stage breast cancer, vascular invasion (VI) is predominantly lymphatic invasion (LI) and is an independent prognostic factor (Mohammed *et al.*, 2011).

1.1.4.8 Hormone receptor status

The presence of ER and PR in breast cancer has both predictive and prognostic significance. In a trial of patients with early stage breast cancer, it was reported that women with ER positive tumours had a 5 year disease free survival (DFS) of 74% and an OS of 92%. While those women with ER negative tumours had a DFS of 66% and OS of 82%. As will be discussed later (section 1.1.5) a variety of treatment options exist for breast cancer patients (including surgery, radiotherapy, chemotherapy, molecularly targeted- and anti-hormonal therapies) with the optimum one, or combination, being chosen based upon clinical presentation and breast cancer phenotype. The presence of ER and PR can aid in determining the response to adjuvant hormonal therapy (Fisher *et al.*, 1988). Studies have shown that overexpression of HER2 also has a significant predictive role to determine chemotherapy and endocrine therapy response. Cooke et al. showed breast cancer patients with high levels of HER2 had a poor clinical outcome (Cooke *et al.*, 2001). An analysis of 47 studies showed that overexpression of HER2 was an independent predictive tool. (Ross *et al.*, 1998). Table 1.4 summarises the characteristics, prognosis, and recommended treatment for each molecular subtype of breast cancer.

Table 1. 4 Molecular subtypes characteristics and recommended systemic therapy. Adapted from (Waks *et al.*, 2019).

Molecular subtype	Characteristics	Prognosis	Recommended systemic therapy
Luminal A	ER+ PR+/- HER2- Ki-67 low	Good	Endocrine therapy +/- HER2 targeted therapy
Luminal B	ER+ PR+/- HER2+/- Ki-67 high	Good	Endocrine therapy +/- HER2 targeted therapy +/- cytotoxic chemotherapy
HER-2 enriched	HER-2 amplified/ overexpressed ER/PR- Ki-67 any	Intermediate to poor	HER2 targeted therapy+ cytotoxic chemotherapy
Basal-like	ER- PR- HER2- (triple negative)	Poor	Cytotoxic chemotherapy

Abbreviations: ER, oestrogen receptor; PR, progesterone receptor; HER2, human epidermal growth factor receptor-2.

1.1.4.9 Markers of proliferation

Tumour proliferation rates have been correlated with prognosis. The recognised markers of proliferation include S-phase fraction (SPF), thymidine labelling index, mitotic index, and proliferation antigens such as Ki-67 and proliferating cell nuclear antigen (PCNA) (Amadori *et al.*, 1998; Brown *et al.*, 1996; Thor *et al.*, 1999). A study by the San Antonio Breast Cancer Database reported that high SPF was associated with adverse survival (Wenger *et al.*, 1998). Similarly, in the NSABP B-14 trial where patients with ER-positive, node-negative tumours were randomised to be given tamoxifen or placebo, patients with high SPF tumours had an increased risk of both recurrence and death compared to those with low SPF tumours (Bryant *et al.*, 1998).

1.1.4.10 Genome profiling assays and other tools

Genome profiling assays assess several biomarkers of prognostic importance to aid prediction of clinical outcome. These include tools like Oncotype Dx and Mammaprint. Oncotype Dx measures the gene expression of 16 tumour related genes and 5 reference genes using quantitative real-time polymerase chain reaction (qRT-PCR) to determine the risk of tumour relapse within 10 years. This technique is applicable for ER positive tumours and classes risk into low, intermediate or high risk categories (Paik *et al.*, 2004). Mammaprint is a 70 gene signature assay that is used for both ER positive and ER negative early stage cancers and classes them into high risk and low risk groups. This gene assessment tool determines the genes involved in carcinogenesis like invasion and metastasis (Cardoso *et al.*, 2016).

Other predictive and prognostic tools include Adjuvant! Online and NHS PREDICT. These are web based tools that use mathematical and computational algorithms that help determine the course of therapy for patients. Adjuvant! Predicts breast cancer outcomes for 10 years with or without adjuvant systemic therapy (Olivotto *et al.*, 2005). While PREDICT is a prognostication model to determine overall and breast cancer specific survival for patients treated for early breast cancer in the UK (Wishart *et al.*, 2010).

The Prosigna, (formerly known as Prediction Analysis of Microarray 50 PAM50) is a signature assay evaluating the activity of 58 genes. The gene activity is analysed and fed into an algorithm that includes tumour hormonal expression and clinicopathological assessment based on its size and proliferative potential. The results are assigned an ROR (risk of relapse) score scaled between 0-100 where 0-40 is low, 41-60 is intermediate, or 61-100 is high risk node-negative cancers. The PAM50 gene signature can be used by a physician alongside clinicopathological parameters for patients with breast cancer to select an adjuvant therapy (Zubair *et al.*, 2020).

In a study Bartlett and colleagues described the first prospective direct comparison of commercially available multiparameter test in a randomised trial of early breast cancer patients in the OPTIMA (Optimal Personalised

Treatment of early breast cancer using Multiparameter Analysis) (Bartlett *et al.*, 2016; Stein *et al.*, 2016). The samples were tested using Oncotype DX recurrence score in addition with five other multiparameter tests including the Mammaprint and PAM50. A comparison of intrinsically classifying tests revealed modest agreement between the tests with a discordance in results seen in 40.7% of patients. When comparing all the prognostic tests classifying low or intermediate vs high risk showed a modest agreement, with only 30.8% of patients classed as low or intermediate risk and only 8.6% consistently classed as high risk. No consensus was seen in 60.6% of patients across all the tests. Therefore, no test was seen to be superior in terms of consistency in agreement with another test (Bartlett *et al.*, 2016).

A study by Sammut et al, reported a multi-omics machine based model that combines pre-therapy features, such as tumour mutational and copy number landscapes, immune infiltration, T-cell dysfunction, exclusion, and tumour proliferation. This approach was seen to predict a pathological complete response (pCR) in a validation cohort of 75 patients that received neo-adjuvant therapy (Sammut *et al.*, 2022).

1.1.5 Breast cancer treatment

Treatment strategies for breast cancer depend on the clinical presentation and the molecular subtype of the disease. It is generally given as multimodal therapy and involves a combination of surgery with radiotherapy, chemotherapy, hormonal and/or targeted therapy. Treatment is given in two main strategies including local therapy and systemic therapy (Waks *et al.*, 2019).

1.1.5.1 Local therapy

Local therapy aims to remove the primary tumour. It includes surgery with or without radiotherapy and is generally administered to patients with early stage breast cancer including stages I and II (Waks *et al.*, 2019).

Surgery

Surgery is generally the first treatment option for operable breast tumours and is performed for complete resection of the breast tumour. The main

target is to completely excise the primary tumour with local lymph nodes to minimize recurrence. Modes of surgery include: lumpectomy, or breast conserving surgery (BCS), which involves excision of breast tumour tissue with margin of healthy breast tissue, and mastectomy which refers to the excision of the whole breast with the nearby breast tissue, the skin and the nipple (ABS, 2009). Breast conserving therapy (BCT) includes BCS with inclusion of adjuvant radiotherapy given to reduce the risk of recurrence. Patients who underwent BCS with radiation treatment had a reduced mortality hazard ratio of 0.728 whilst patients who were given BCS without radiotherapy had a higher mortality hazard ratio of 1.105, when compared to total mastectomy (Vinh-Hung *et al.*, 2004). The involved lymph nodes are assessed by sentinel lymph node biopsy (SLNB) or an axillary lymph node dissection (ALND). This helps in removing cancer cells spread to the lymph nodes which prevents future recurrence (Morrow *et al.*, 2001).

Radiotherapy

To limit the risk of local/distant recurrence radiotherapy is often given as adjuvant treatment following surgery. In the UK it is given as hypofractionated radiotherapy (HFRT) to patients with early invasive breast cancer. The delivery of radiation doses higher than 2 Gy in a fewer fractions over a shorter period of time is called hypofractionation. Unlike conventional multi-fractionated radiotherapy (CFRT) used internationally, which is a total dose of 50 Gy administered in 25 fractions of 2 Gy over a 5 week period, radiation therapy in the UK is administered in higher doses per fraction in shorter overall treatment time i.e. 40 Gy in 15 fractions over a 3-week period (NICE, 2018). A study by Haviland et al. has demonstrated that hypofractionated radiotherapy results in fewer complications such as breast shrinkage, telangiectasia, and breast oedema (Haviland *et al.*, 2013). In early stage disease, BCS is followed by radiotherapy to restrict the tumour growth and improve breast cancer specific and overall survival (NICE, 2018). Radiotherapy after mastectomy is only recommended in patients who have a high risk of recurrence including tumour size > 5 cm, > 4 axillary lymph node involvement and positive LVI margins (Cardoso *et al.*, 2019). A study by the EBCTCG reported that post BCS radiotherapy can have significant clinical benefits. The risk of developing regional or distant

recurrence was reduced by 16% overall, and the risk of breast cancer related death was reduced by 4% (Darby *et al.*, 2011). It was reported in a study that administration of radiotherapy before surgery can enhance the accessibility of the tumour resulting in better tumour resection, in patients with LABC (van der Leij *et al.*, 2015). During the Covid-19 pandemic, the breast cancer radiotherapy regimen was revised and the administration of radiation was reduced to a fewer fractions. This had several benefits including reduction of the risk of nosocomial virus transmission and improvement of the machine capacity during reduced staff levels due to redeployment or sickness. One of the regimens included the FAST-Forward RCT which includes administration of 26 Gy of radiation in five fractions over a period of one week, and showed to be safe for normal tissue effects up to a period of 5 years (Coles *et al.*, 2020; Murray Brunt *et al.*, 2020).

MBC patients with bone and brain metastasis may be given radiotherapy to relieve tumour related symptoms (Cardoso *et al.*, 2014). Recently, short courses of highly focussed and extremely high-dose radiotherapies have been considered as alternative treatment to surgery for oligometastasis. These include stereotactic radiosurgery (SRS) and stereotactic ablative body radiotherapy (SABR). Both have been accepted widely for the treatment of extracranial metastasis because of their high efficacy and minimum invasive nature (Otake *et al.*, 2019).

Targeted Intraoperative Radiotherapy (TARGIT) has been gaining interest as a potential form of radiation therapy. TARGIT uses a mobile irradiation system to distribute a single large dose of 20 Gy, of low-energy X-rays, over ~30 minutes during surgery, directly into the area of the resected tumour before the closure of the incision (Vaidya *et al.*, 2010). It was recently reported that patients with early breast cancer treated with (TARGIT-IORT) had a comparable long term breast cancer efficacy and significantly lower non-breast cancer related mortality, compared with external beam radiotherapy (EBRT) (Vaidya *et al.*, 2020). In the IMRT-MC2 study (NCT01322854) it was reported that intensity modulated radiation therapy with simultaneous integrated boost (IMRT-SIB) can shorten the adjuvant radiation therapy duration without hindering the clinical outcomes (Hörner-Rieber *et al.*, 2021).

Other forms of radiotherapy includes brachytherapy (BT) and accelerated partial breast irradiation (APBI). APBI uses an accelerated delivery of radiation dose to the lumpectomy bed with a margin of 1-2 cm (Skowronek *et al.*, 2012). Brachytherapy uses iridium-192 as is radiation source which is sealed and placed at the tumour site of surgery. Both of the aforementioned forms of radiotherapy shorten the time of therapy and does not require whole breast irradiation (WBI) (Skowronek *et al.*, 2014).

1.1.5.2 Systemic therapy

Systemic therapy is given to patients with locally advanced or metastatic disease with the type of treatment dependent upon the tumour subtype. It is also an adjuvant to treat early invasive breast cancer. Neoadjuvant systemic therapy is given with the aim to reduce the tumour size and minimise surgery for patients with locally advanced disease. For metastatic disease, it is given to reduce disease burden and related symptoms, and to improve the quality of life. Systemic therapy for breast cancer includes chemotherapy, hormonal therapy and targeted therapy (Gemignani *et al.*, 2014).

Chemotherapy (C/T)

Conventional cytotoxic agents include- anthracyclines, platinum compounds, and alkylating agents (Lind, 2011). C/T is administered for the treatment of both early stage and advanced breast cancer. Cytotoxic chemotherapy is usually administered as a polychemotherapeutic regimen. The first combination of chemotherapy regimen tested included cyclophosphamide, methotrexate and 5- fluorouracil (5-FU), the CMF regimen. The trial patients were administered 12 cycles of CMF after radical mastectomy. Patients showed an improved DFS and OS for CMF compared to the control group (Bonadonna *et al.*, 1976). Chemotherapy combinations including doxorubicin have since been assessed in clinical trials. The NSABP B-15 evaluated melphalan and 5-fluorouracil with or without doxorubicin. It was shown that patients with doxorubicin administration had an improved 5 year DFS and a trend for improved OS (Fisher *et al.*, 1989). Other drug combinations include- 5-FU, Adriamycin (doxorubicin) and cyclophosphamide (FAC) (Hortobagyi *et al.*, 1983); 5-FU 500 mg/m^2,

epirubicin 50 mg/m^2, cyclophosphamide 500 mg/m^2 (FEC50) (FESG, 1988); 5-FU 500 mg/m^2,epirubicin 100 mg/m^2, cyclophosphamide 500 mg/m^2 (FEC100) (FASG, 2001). Taxanes are an important class of cytotoxic compounds used commonly in chemotherapeutic combinations for breast cancer. A combination of docetaxel and doxorubicin (AT) is effective in patients with LABC and MBC. A study comparing the efficacy and response of AT and AC (doxorubicin and cyclophosphamide) showed that AT significantly improved the time to disease progression and overall response rate compared to patients given AC. There was, however, no difference in OS (Nabholtz *et al.*, 2003). The National Cancer Institute of Canada (NCIC) Clinical Trial Group tested the combination of docetaxel and epirubicin to determine the optimal dosing regimens for docetaxel and epirubicin combination therapy in patients with LABC. The epirubicin/docetaxel combination induced strong reductions in tumour RNA integrity in some patients. The investigators concluded that this combination can be administered in LABC patients with acceptable toxicity (Trudeau *et al.*, 2015).

Platinum based agents are conventionally used against ovarian cancer. However, some studies have demonstrated their efficacy in certain breast cancer types, such as cancers harbouring BRCA1/2 mutations associated with basal and triple negative breast cancer. They have also been assessed in polychemotherapeutic regimens. Cisplatin has been tested in combination with Adriamycin (doxorubicin) and cyclophosphamide (Creagan *et al.*, 1984); with 5-FU and etoposide (Saphner *et al.*, 1991). Other agents including vinblastine (Trump *et al.*, 1981), epirubicin (Martoni *et al.*, 1984), methotrexate, cyclophosphamide, mitomycin C and vincristine (Smith *et al.*, 1992) have also been evaluated in combination with cisplatin. In a study by Telli et al. patients received gemcitabine and carboplatin in combination with iniparib. The patients with BRCA mutations and triple negative breast cancer displayed a higher overall response compared to patients with wild type BRCA (Telli *et al.*, 2015).

Other chemotherapy regimens include- docetaxel (Taxotere), doxorubicin (Adriamycin) and cyclophosphamide (TAC); epirubicin, followed by CMF (E-CMF). The standard regimen for early stage TNBC disease is adjuvant

anthracyclins and taxanes (NICE, 2018). The EBCTCG reported that the 10 year breast cancer mortality was reduced by one third in patients who underwent a polychemotherapy regimen of anthracyline, taxane and alkylator when compared to patients who did not receive chemotherapy (Peto *et al.*, 2012). Chemotherapy can also be administered in combination with targeted therapy (Hassan *et al.*, 2010).

The treatment for LABC include chemotherapy, surgery and radiotherapy in combination with hormonal or targeted therapies. Neoadjuvant chemotherapy with an anthracycline/taxane regimen of a maximum of six cycles is administered to shrink larger inoperable tumours. Which is generally followed by segmental or modified radical mastectomy (NICE, 2018). A similar form of treatment regimen is administered to LABC patients with triple negative disease. A sequential neoadjuvant regimen of anthracyclin and paclitaxel is given to shrink the tumour size to make them operable (Witherby *et al.*, 2016). Patients with triple negative MBC receive chemotherapy given sequentially until disease progression, as the standard first line treatment. A combined regimen of anthracycline or taxanes, like taxane-fluorouracil-doxorubicin-cyclophosphamide (T-FAC) or doxorubicin-cyclophosphamide-taxane have shown to be effective in a small group of patients (Hudis *et al.*, 2011).

The concept of synthetic lethality is a new approach to target tumour cells. It relies upon the fact that mutations in a single DNA repair gene allows cell viability to be maintained but mutations in genes of two complimentary DNA repair pathways (i.e. single strand and double strand DNA repair pathways) cause cell death (Kaelin, 2005). An excellent example for this is the use of Olaparib which is a poly ADP-ribose polymerase (PARP) inhibitor. It is used against BRCA-mutated tumours, which are involved in double strand break repair. PARP1 is an enzyme involved in single strand break repair, which is consequently inhibited by Olaparib (Lord *et al.*, 2015). Thus, leading to cell death in cancer cells without affecting normal cells that are BRCA competent. According to the OlympiAD trial, patients treated with olaparib had a 42% reduced risk of disease progression or death and the median PFS was 2.8 months longer compared to standard therapy. The use of

olaparib for treatment of metastatic triple negative breast cancer has been approved (Robson *et al.*, 2017; Robson *et al.*, 2019).

Endocrine/hormonal therapy

Breast tumours that express oestrogen and progesterone receptors can respond to hormone therapy which involves using agents to interfere with oestrogen levels and/or response (Puhalla *et al.*, 2012). The treatment strategy is dependent on the menopausal status of the patient. Endocrine therapy can be categorised in to- selective ER modulators (SERM) such as tamoxifen and raloxifene, selective ER down-regulators (SERD) such as fulvestrant, aromatase inhibitors (AI) such as letrozole, and anastrozole, and luteinizing hormone-releasing hormone (LHRH) analogues (Gombos, 2019; Lewis *et al.*, 2005; Puhalla *et al.*, 2012; Tan *et al.*, 2007a).

Tamoxifen acts as an oestrogen antagonist that blocks the oestrogen receptors in tumour cells (Lewis *et al.*, 2005). Hence, it is given to premenopausal patients. AIs are recommended to postmenopausal patients. These inhibit the transformation of other hormones into oestrogen by inhibiting the aromatase enzyme (Puhalla *et al.*, 2012).

Early stage breast cancer patients with HR positive disease are given endocrine therapy to inhibit the binding of oestrogen with ER (Chang *et al.*, 2013). The standard care for patients with HR positive disease is tamoxifen or aromatase inhibitors for pre and post-menopausal women for 5 years. However, certain studies have shown that a 10 year adjuvant treatment with endocrine therapy can improve DFS and OS (Davies *et al.*, 2013; Gray *et al.*, 2013). Patients with HR positive LABC with operable or inoperable tumours are administered endocrine therapy (tamoxifen or AI) depending on their menopausal status (Witherby *et al.*, 2016). Hormone therapy has been used as a neoadjuvant therapy for patients with ER positive tumours which are inoperable with the aim of improving the probability of conducting a surgery (Smith *et al.*, 2005).

The first line of treatment for MBC patients with ER positive disease is endocrine therapy using tamoxifen for premenopausal women; AI, fulvestrant, or combination of fulvestrant and AI or the combination of an AI with palbociclib (cyclin dependent kinase (CDK) 4/6 inhibitor) (Witherby

et al., 2016). Studies report the use of bisphosphonates for post-menopausal women with a high risk of recurrence have significant reduction in distant recurrence, bone recurrence, and breast cancer mortality after treatment (EBCTCG, 2015).

Targeted therapy

Targeted therapy is recommended against specific molecular targets in breast cancer. Several targeting agents have been established that include drugs against HER family receptors, Insulin growth factor 1 receptor (IGF-1R), signalling pathways PI3K/AKT/mTOR, vascular endothelial growth factor (VEGF) and heat shock protein HSP90. Targeting the EGFR family has been very efficient against breast tumours with HER2 overexpression (Mohamed *et al.*, 2013).

HER2 is a member of the human epidermal growth factor receptor (EGFR) family which has three homologous receptors: HER1, HER3, and HER4. These receptors are activated by ligand binding followed by homo or heterodimerisation with the other members of the family. Thus, activating the receptors aiding in phosphorylation cascades to activate the downstream pathways (Rimawi *et al.*, 2015).

Trastuzumab was the first targeted therapy agent against HER2+ metastatic breast cancer (Romond *et al.*, 2005). It is the standard adjuvant form of therapy for HER2 positive early stage breast cancers (Slamon *et al.*, 2011). There are a variety of possible mechanisms of action, these include: (a) inhibiting the cleavage of the extracellular domain of HER2 leading to blocking of p95- mediated signal transduction, (b) binding of trastuzumab to HER2 leads to disruption in homo- or heterodimerisation, (c) recruiting immune effectors and initiation of antibody dependent cell-mediated cytotoxicity (ADCC), and (d) induced degradation via endocytosis (Hudis, 2007).

Studies show that trastuzumab administration every 3 weeks for 12 months can improve DFS and OS in early stage breast cancer patients (Piccart-Gebhart *et al.*, 2005; Smith *et al.*, 2007). In patients with the tumour size >3 cm, neoadjuvant chemotherapy with docetaxel and carboplatin is recommended followed administration of adjuvant trastuzumab for a year

(Witherby *et al.*, 2016). For early stage high risk patients treated with neoadjuvant taxane and trastuzumab, trastuzumab-emtansine (T-DMI) is advised post-surgery (Verma *et al.*, 2012). Despite its efficacy in improving HER2+ breast cancer patient outcome, some patients show resistance (Bonifazi *et al.*, 2014).

A combination of chemotherapy consisting of docetaxel and carboplatin followed by surgery is administered to patients with HER-2 enriched LABC. This may be followed by a trastuzumab therapy regimen of one year to reduce the risk of recurrence (Cardoso *et al.*, 2014). The first line therapy for HER2 enriched MBC is a combination of pertuzumab, trastuzumab and docetaxel according to the Cleopatra trial (Swain *et al.*, 2015). The use of trastuzumab emtansine (T-DMI) conjugate resulted in better disease control and overall survival (Diéras *et al.*, 2017). This is now the second line of treatment for HER2 enriched MBC patients (Lewis Phillips *et al.*, 2008).

Pertuzumab is another monoclonal antibody that has recently been developed to overcome trastuzumab resistance. The mechanism of action includes binding to the extracellular domain of HER2 as with trastuzumab, but to an epitope of domain II unlike trastuzumab which binds to domain IV. This prevents the receptor from homo or heterodimerising hence preventing the activation of the downstream signalling pathway (Franklin *et al.*, 2004).

Lapatinib is a dual tyrosine kinase inhibitor (TKI) that binds to HER1 and HER2. It binds to their intracellular domains to inhibit phosphorylation of receptor and block the activation of downstream signalling. A clinical study demonstrated the efficacy of the combination of lapatinib with capecitabine in HER2 metastatic breast cancer after adjuvant trastuzumab treatment (Geyer *et al.*, 2006). This led to FDA approval of lapatinib for metastatic breast cancer with HER2 overexpression.

Other targeted therapies include, Neratinib (Chan *et al.*, 2015) and Afatinib (Lin *et al.*, 2012)which are small molecule tyrosine kinase inhibitors against HER2 family receptors. Additionally, novel agents targeted against EGFR

family, mTOR, HSP90 etc. are under development (Lu *et al.*, 2012; O'Sullivan *et al.*, 2014).

One of these agents include CDK4/6 inhibitors. Currently approved CDK4/6 inhibitors include palbociclib, ribocicib, and abemaciclib. The combination of Palbociclib and letrozole was shown to significantly improve PFS in patients with advanced hormone receptor positive breast cancer (Finn *et al.*, 2015). In combination with trastuzumab, Palbociclib showed safety and better survival outcomes in patients with pretreated HER2+ disease (Ciruelos *et al.*, 2020). The second FDA approved CDK4/6 inhibitor, Ribociclib demonstrated improved PFS in combination with letrozole in hormone receptor positive metastatic breast cancer patients (Hortobagyi *et al.*, 2018). In combination with trastuzumab, it was shown to be safe in HER2+ breast cancer (Goel *et al.*, 2019). Abemaciclib, in combination with AIs, have also shown to significantly improve PFS in hormone receptor positive metastatic breast cancer patients (Goetz *et al.*, 2017), while in a combination with trastuzumab and fulvestrant, it demonstrated significantly improved PFS in HER2+ breast cancer patients (Tolaney *et al.*, 2020).

The immune system is known to play a crucial role in the development of breast cancer. The tumour cells escape the immune system by regulation of T-cell activity causing suppression of immune response (Pardoll, 2012). The immune checkpoint, PD-1 and its receptor, PDL-1 have been used to target the immune suppression in breast cancer. An anti-PDL-1 antibody, Atezolizumab has shown to prolong PFS and OS in combination with nab-paclitaxel for patients with locally advanced or metastatic TNBC (Schmid *et al.*, 2020b). Another anti-PDL1 antibody, Durvalumab was shown to increase pCR rate when given in combination with an anthracycline taxane based neoadjuvant therapy for early TNBC (Loibl *et al.*, 2019). The anti-PD-1 antibody, Pembrolizumab has shown to have efficacy in patients with advanced TNBC. In combination with chemotherapy, in pretreated patients with locally recurrent or metastatic TNBC, Pembrolizumab demonstrated significantly and clinically improved PFS compared to chemotherapy plus placebo (Cortes *et al.*, 2020). In early TNBC patients the combination of Pembrolizumab with chemotherapy was shown to have significantly improved pCR rate (Schmid *et al.*, 2020a).

As indicated above targeted therapy is a very effective therapeutic strategy but not all patients respond with resistance often encountered – there is, as a result, interest in predictive biomarkers. One protein biomarker that has yielded encouraging results is the expression of calpain. Data from our group has shown that Calpain 1 expression is associated with adverse relapse free survival in HER2 positive breast cancer patients treated with trastuzumab following adjuvant therapy (Pu *et al.*, 2016b). In addition to playing a role in response to trastuzumab our group has also shown a role in breast cancer disease progression, overall survival across various cancer types and also resistance to other anticancer treatments (Storr *et al.*, 2013; Storr *et al.*, 2012; Storr *et al.*, 2015).

1.2 The calpain system

The calpain system is involved in a number of important cellular processes in relation to cancer progression and treatment response (Storr *et al.*, 2011a).

1.2.1 Structure

Calpains are a conserved family of intracellular cysteine proteases expressed in a range of cells and tissues. They were first described in 1964 by Guroff, as a neutral proteinase extracted from rat brain (Guroff, 1964). Ishiura et al. later extracted calpain from chicken skeletal muscle and named it calcium-activated neutral protease (CANP) (Ishiura *et al.*, 1978). Some members of the calpain family rely on calcium ions and a neutral pH for their proteolytic activity. The μ-calpains and the m-calpains were named on the basis of the calcium ion concentration required for their activation. Both μ-calpains and m-calpains are heterodimers consisting of a catalytic subunit (80 kDa) and a regulatory subunit (28 kDa). The catalytic subunits differ between the two types as they are formed by calpain 1 (encoded by CAPN1) or calpain 2 (encoded by CAPN2) respectively. The regulatory subunit is common to both the isoforms and is encoded by CAPNS1 (Storr *et al.*, 2011a).

The catalytic subunit has four domains- DI to DIV and the regulatory subunit has two DV to DVI. DI is autolysed when calpains are activated by calcium. DII is a conserved protease domain which is divided in to IIa and

IIb that on binding with calcium forms a single domain (II) that has the catalytic cleft (Storr *et al.*, 2011a). The DIII domain is involved in structural changes when binding with calpastatin and has the characteristic C2 domains (Croall *et al.*, 1991; Sorimachi *et al.*, 2010). The DIV and DVI are carboxy terminal domains and contain five EF hands. The fifth EF hand is involved in dimerization of the subunits (Imajoh *et al.*, 1987; Minami *et al.*, 1987). Despite the DII protease subunit being conserved, there exists a divergence in these subunits within the isoforms as a result, not all calpains are activated by calcium or require the regulatory subunit (Blanchard *et al.*, 1997). Figure 1.1 shows the structure of μ-calpain and different domains of the calpain family members.

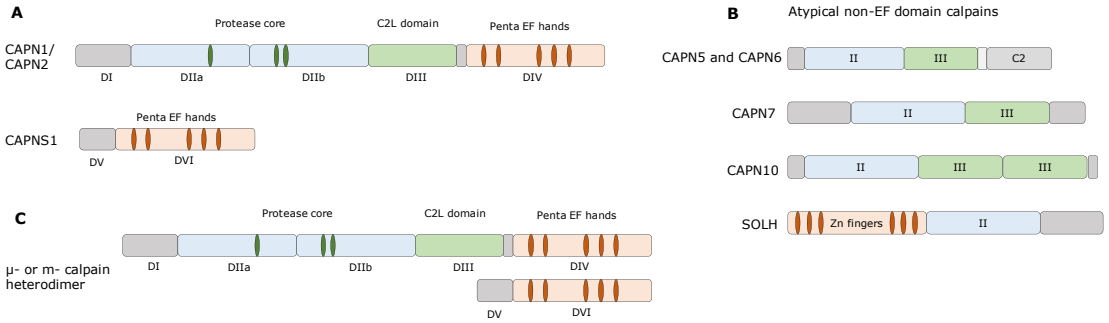

Figure 1. 1 Schematic structure of the calpain molecules. (A) CAPN1/2 (large subunits) containing the protease domains, DIIa and DIIb; the C2L domain, DIII; and the DIV domain with PEF hands (shown by orange ovals). The small subunit CAPNS1 also contains the PEF hands that aid in dimerization and formation of the heterodimers. **(B)** Atypical, non-EF hands containing members of the calpain family. **(C)** μ- calpain or m-calpain heterodimer formed of CAPN1/CAPN2 (large subunits) and CAPNS1 (small subunit). Adapted from (Storr *et al.*, 2011a). Copyright© 2011 by Springer Nature with permission conveyed through Copyright Clearance Centre Inc.

1.2.2 Calpain classification and nomenclature

Calpains can be classified as typical or classical calpains and atypical or non-classical calpains, based on their structural characteristics. Classical or typical calpains are characterised by the presence of DII, DIII and DIV domains. Out of fifteen identified calpains nine are classical calpains. These include- calpain-1 to -3,-8,-9 and calpain-11 to calpain-14. The non-classical or the atypical calpain types are characterised by the presence of irregular C2L domain and missing EF-hand sequences in DIV that have mechanisms necessary for typical forms of calpains. These include calpain-

5 to -7 and -10 and small optilobe-homology (SOLH) and PalB subfamilies (Goll *et al.*, 2003; Sorimachi *et al.*, 2010).

Calpains are also grouped depending on their tissue expression. Table 1.5 shows calpains that are expressed ubiquitously or that have tissue specific expression.

Table 1. 5 Calpain types and their expression in different tissue types. Adapted from (Sorimachi *et al.*, 2010).

Calpain type	Tissue expression
Calpain 3	Skeletal muscle
Calpain 6	Placenta and embryonic muscle
Calpain- 8 and -9	Gastrointestinal system
Calpain 11	Testis
Calpain 12	Hair follicles
Remaining calpain types	Ubiquitous expression

Although the above mentioned calpains have tissue specific expression, these can also be expressed in other tissues but at lower levels.

Calpain cDNA studies by Ohno et al. revealed the complete structure of the catalytic subunit of calpain. Whilst discussed below (section 1.2.3) it consists of two important domains DII and DIV (Ohno *et al.*, 1984). Several subsequent cDNA studies led to the identification of additional calpain related molecules, including its endogenous inhibitor, calpastatin. Calpains are named according to their corresponding gene products, for eg. CAPN1, CAPN2 and CAPNS1 (Goll *et al.*, 2003). Another form of naming calpains includes a numerical nomenclature- calpain-1 which is the large subunit encoded by, CAPN1; calpain-2, the large subunit encoded by, CAPN2; calpain-4, the small subunit encoded by, CAPNS1 etc. The conventional heterodimer of calpain-1 and the small subunit calpain-4 is denoted by μ-calpain and the conventional heterodimer of calpain-2 and the small subunit calpain-4 is denoted by m-calpain (Storr *et al.*, 2011a).

Fifteen different isoforms of calpain have been identified by the presence of protease domains two of which are ubiquitously expressed and have been extensively studied. These include micro-calpains (μ-calpains) and milli

calpains (m-calpains). μ-calpains and m-calpains are sometimes also referred to as, conventional calpains while the others are known as unconventional calpains (Goll *et al.*, 2003).

1.2.3 Activation and regulation

Some calpains are activated in the presence of calcium ions and extracellular signal-regulated kinase (ERK) through growth factor signalling (Glading *et al.*, 2001). Activation of calpains causes structural and conformational changes that are discussed in chapter 3. Calpain activity is regulated by autolytic cleavage, phosphorylation, phospholipid interaction and through its endogenous inhibitor, calpastatin (Storr *et al.*, 2011a).

Calpastatin (CAST) is the endogenous inhibitor of μ-calpain and m-calpain and is expressed ubiquitously. It consists of an L domain that contains an N terminal XL region, and four inhibitory domains (I-IV) (Wendt *et al.*, 2004) that can reversibly inhibit up to four calpain heterodimers. Structural changes in calpain allow inhibition by each inhibitory domain of the calpastatin molecule (Hanna *et al.*, 2008). These are liberated from intracellular storage aggregates into the cytosol as a result of calcium influx for calpain interaction (Averna *et al.*, 2003). Unlike the calpains, CAST is a single gene with several promoters that generate distinct calpastatin isoforms with variation at their N terminals. Type I and Type II calpastatin have the L domain but differ in N terminal sequences. Type III calpastatin is a product of a promoter that is associated with the untranslated region 1u. Type IV calpastatin is a testis specific isoform which is a product of a promoter between exons 14 and 15 (Cong *et al.*, 1998; Sensky *et al.*, 2006). In addition to use of alternative promoters transcripts are alternatively spliced at the L-domain, resulting in the generation of several polypeptides from a single gene. A small region at the calpastatin L domain has been shown to partially reprime L-type calcium channels after voltage gated activation. The inhibitory specificity, efficacy and cellular location of calpastatin is effected by the post-translational phosphorylation by PKA (Averna *et al.*, 2001).

1.2.4 Calpain function

1.2.4.1 Cell migration

An important characteristic of tumour cells is their ability to invade surrounding tissue and metastasise to different sites. The calpain system targets multiple proteins including E-cadherin, a member of the transmembrane glycoproteins family that has an important role in cell to cell adhesion, and maintaining adherence junctions. Calpains have been shown to cleave E-cadherin into a truncated form in breast cancer (Rios-Doria *et al.*, 2003). Calpains have also been shown to proteolyse β-catenin that can disrupt its stable structure and cause nuclear accumulation of protein fragments leading to tumorigenesis in breast and prostate cancers (Rios-Doria *et al.*, 2004). Focal adhesion protein, involved in integrin-mediated adhesion, can be directly cleaved by calpains to regulate adhesion complex disassembly at the rear of cells during migration (Franco *et al.*, 2004). Ezrin is another important membrane/cytoskeleton linking protein that can regulate integrin-based focal adhesion and invadopodia formation. In breast cancer cells, calpain 1 has been shown to interact with ezrin. Downregulation of ezrin leads to reduced cleavage of other calpain substrates including talin, focal adhesion kinase (FAK) and contractin which is associated with focal adhesion and disassembly of invadopodia (Hoskin *et al.*, 2015).

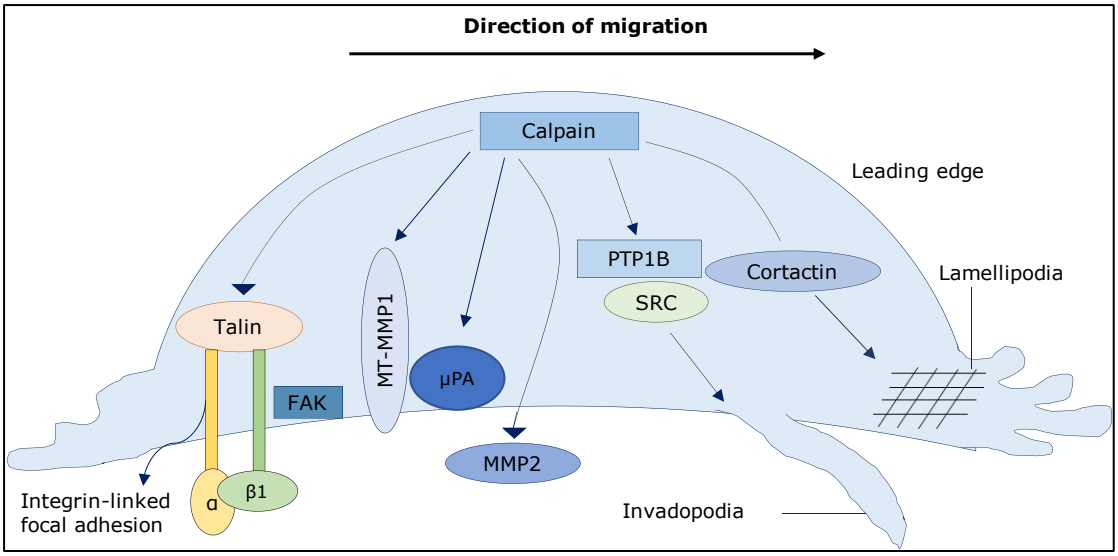

Figure 1. 2 Schematic representation of the involvement of the calpain genes in cell migration and invasion. Calpains regulate cell migration and interactions with integrins and focal adhesion kinase (FAK); membrane-type matrix metalloproteinase 1 (MT-MMP1); urokinase plasminogen-type activators (uPAs) and matrix metalloproteinase 2 (MMP2). Calpains are also involved Invadopodia formation via protein tyrosine phosphatase 1B (PTP1B)-SRC; actin reorganisation via cortactin. Calpains are also involved in laemellipodia and pseudopod stabilisation at the leading edge. Reproduced from (Storr *et al.*, 2011a). Copyright© 2011 by Springer Nature with permission conveyed through Copyright Clearance Centre Inc.

SiRNA silencing of calpains can inhibit matrix metalloproteinases (MMPs) secretion and reduce cell adhesion and invasion ability in osteosarcoma cells (Fan *et al.*, 2009). The small subunit calpain 4 upregulates MMP2 by activating the nuclear factor (NF-κB) or FAK-Src signalling pathways to promote cell invasion and metastasis (Dai *et al.*, 2014; Storr *et al.*, 2015). There is also evidence of crosstalk between calpain 2 and haematopoietic PBX-interacting protein that can regulate cell migration and adhesion in breast cancer cells (Bugide *et al.*, 2015). In summary, the calpains are important regulators of tumour cell migration and invasion that leads to metastasis and disease progression.

1.2.4.2 Cell survival and death

Calpain activity promotes cellular pro-survival functions via p53 and nuclear factor-kB (NF-κB). Calpains cleave wild type p53 affecting protein stability and inhibiting p53 mediated apoptosis (Gonen *et al.*, 1997; Kubbutat *et al.*, 1997). The growth arrest specific protein 2 (GAS2) has been shown to associate with calpain and prevent cleavage of p53 leading to enhanced p53

stability (Benetti *et al.*, 2001). Additionally, calpains can promote survival through the activation of NF-κB by the proteolysis of its inhibitor IκBα. Activation of epidermal growth factor receptor (EGFR) and tumour necrosis factor (TNF) in breast cancer cells regulates cleavage of IκBα (Han *et al.*, 1999; Pianetti *et al.*, 2001). Proteolysis of IκBα is mediated by μ-calpain (Shumway *et al.*, 1999), m-calpain (Han *et al.*, 1999), and calpain-3 (Baghdiguian *et al.*, 1999) and can be disrupted by overexpression of calpastatin (Chen *et al.*, 2000a). Calpains are also responsible for proteolysis of several other substrates that promote apoptosis, such as the transcription factor MYC. MYC has shown to reduce expression of calpastatin leading to increased calpain activity (Conacci-Sorrell *et al.*, 2010; Small *et al.*, 2002). Figure 1.3 shows associations of calpains with survival related pathways.

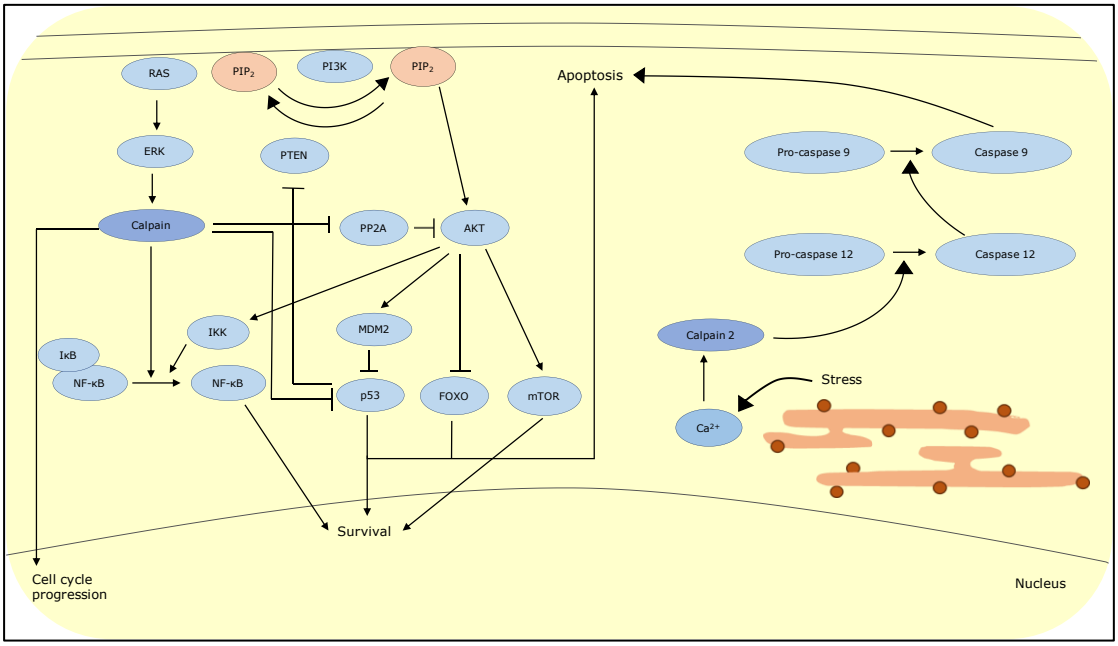

Figure 1. 3 Calpains and their associations with survival related pathways. Calpain is implicated with the activation of nuclear factor-κβ (NF-κβ) by degrading Iκβ and stabilisation of p53. Calpains are also involved in modulating forkhead box O (FOXO) transcription factor activity through protein phosphatase 2A (PP2A). Calpains are also involved in the cleavage of caspase 12 during endoplasmic reticulum stress, leading to apoptosis. Reproduced from (Storr *et al.*, 2011a). Copyright© 2011 by Springer Nature with permission conveyed through Copyright Clearance Centre Inc.

Calpains have also been shown to associate with caspase cysteine protease machinery such as- caspase 7, caspase 9, caspase 10, and caspase 12 during the induction of apoptosis. Caspase 7 and caspase 10 are activated

by calpain cleavage while caspase 9 is inactivated by calpain cleavage (Chua *et al.*, 2000; Gafni *et al.*, 2009). Calpain can activate caspase 12 during endoplasmic reticulum stress causing apoptosis (Martinez *et al.*, 2010; Tan *et al.*, 2006). Calpains also cleave members of the apoptosis regulating BCL-2 family, thus promoting apoptosis. These include BAX and BID-mediated cytochrome-c release, and cleavage of BCL-2 (Gao *et al.*, 2000; Gil-Parrado *et al.*, 2002; Mandic *et al.*, 2002; Wood *et al.*, 1998). Figure 1.4 shows the associations of calpains with cell death related pathways.

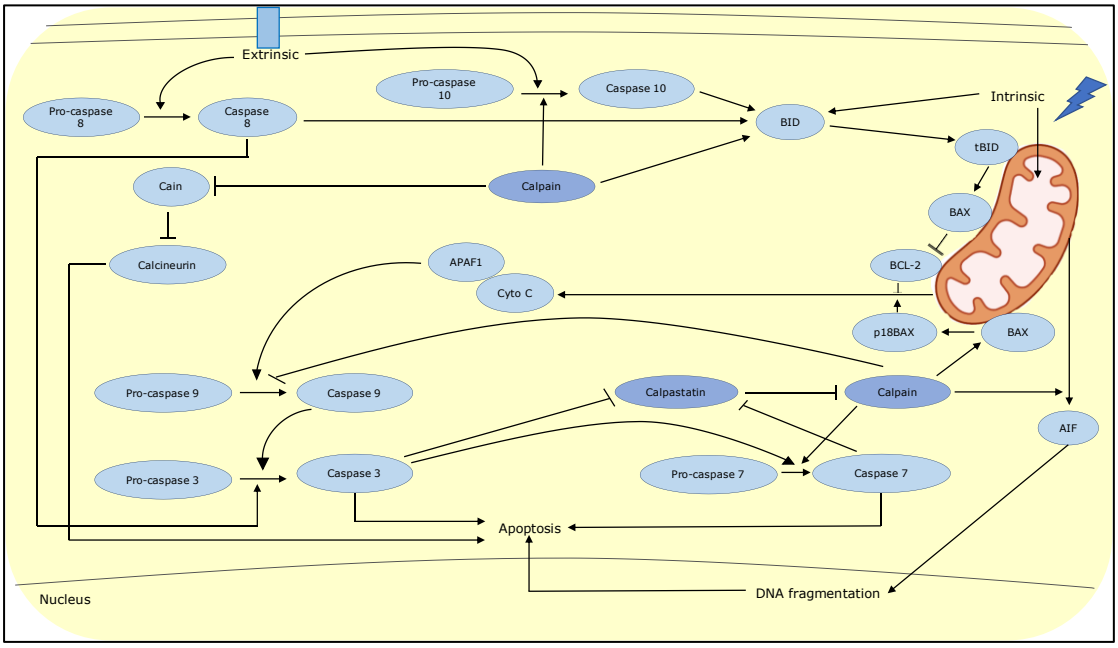

Figure 1. 4 Calpains and their associations with cell death related pathways. Calpain activity can influence both extrinsic and intrinsic apoptotic pathways. Calpains are implicated in the cleavage of caspase 10 and caspase 7 leading to their activation, although cleavage of certain caspase family members by calpains can lead to their inactivation. Calpains also cleave BCL-2 family members, including BAX, to promote apoptosis. Apoptosis-inducing factor (AIF); cytochrome c (Cyt c); Iκβ kinase (IKK); phosphatidylinositol-3, 4, 5-triphosphate (PIP_3).Reproduced from (Storr *et al.*, 2011a). Copyright© 2011 by Springer Nature with permission conveyed through Copyright Clearance Centre Inc.

The prosurvival or proapototic activity of calpains is very context, and cell type dependent. Abnormal calpain activity can cause or accelerate disease progression. Some of these include: neurodegenerative disease, cataract formation, myocardial infarction and limb-girdle muscular dystrophy type 2A (LGMD2A) (Storr *et al.*, 2011a).

1.2.4.3 Calpains and autophagy

The role of calpains in the process of autophagy is controversial. Calpains cleave autophagy-related 5 (ATG5) which is involved in the formation of autophagosomes that can enclose proteins or organelles to undergo lysosomal degradation. The truncated ATG5 is then translocated to mitochondria where it interacts with BCL-X_L that results in the release of cytochrome c (Yousefi *et al.*, 2006).

Calpains also cleave the α-subunit of heterotrimeric G proteins resulting in their activation and leading to an increase in intracellular levels of cyclic AMP that negatively regulates autophagy (Williams *et al.*, 2008). However, some studies have reported that in response to serum deprivation, ceramide and etoposde decreased expression of calpain in murine fibroblast cells, resulting in apoptosis rather than autophagy (Demarchi *et al.*, 2006). In addition, Cheng and colleagues have shown that small molecule inhibition of calpains leads to increased oridonin-induced apoptosis and decreased autophagy in fibrosarcoma cells (Cheng *et al.*, 2008).

1.2.5 Calpain system and disease

Mutations in members of the calpain family or disruption in calpain activity can result in several pathological disorders, including cancer. Dysregulation of calcium homeostasis can cause disruption in calpain activity resulting in neurodegenerative diseases such as Parkinson's disease, Alzheimer's disease, and Huntington disease (reviewed in (Vosler *et al.*, 2008). Mutations in calpain 3 (CAPN3, also known as p94) have been reported to cause a skeletal muscle disorder, limb-girdle muscular dystrophy 2A (LGDM2A) which is the most extensively studied calpainopathies (Ono *et al.*, 2016).

Increased cleavage of alpha-spectrin by calpains produces breakdown products that have been found in the cerebrospinal fluid of traumatic brain injury (TBI) patients when compared to patients with other disorders related to the central nervous system (Farkas *et al.*, 2005). Disrupted calpain activity has been implicated with a wide number of additional diseases including, cataracts, pulmonary hypertension, polycystic ovary

syndrome (PCOS), cardiac disease, multiple sclerosis and ageing (reviewed in (Chakraborti *et al.*, 2012).

Several studies have shown involvement of the calpain system in cancer. In one study upregulated μ-calpain activity via differential CAST gene expression was associated with high risk childhood acute lymphoblastic leukaemia (ALL) at blast stage (Mikosik *et al.*, 2015). Niapour and colleagues reported a significant negative association between calpain activity and levels of calpastatin in acute myeloid leukaemia (AML) at blast stage. (Niapour *et al.*, 2012). Upregulated mRNA levels of calpain 1 was observed in renal cell carcinoma, and has been associated with advanced lymph node status in patients (Braun *et al.*, 1999). High expression of m-calpain has been demonstrated in colorectal adenocarcinoma (Lakshmikuttyamma *et al.*, 2004). Disrupted expression of calpains also dysregulates calpastatin expression. Salehin et al. showed that high levels of calpastatin protein was observed in endometrial tumour samples (Salehin *et al.*, 2010).

1.3 Calpain system and breast cancer

A transcriptomic study investigating regulators of metastasis, by Storr et al. 2011, analysed gene expression in 91 breast cancer patient tumour samples. 89 transcripts were associated significantly with the presence of Lymphovascular Invasion (LVI). Calpastatin was reported to have the second lowest selection error (the first being an uncharacterised gene/expressed sequence tag). On further analysis of breast cancer specimens by real-time PCR and immunohistochemistry (IHC), it was found that both low expression of calpastatin mRNA and protein levels were significantly associated with the presence of LVI. Such results suggest that calpastatin plays an important role in the regulation of breast cancer metastasis (Storr *et al.*, 2011b). High calpain levels have been associated with the migrating ability of breast cancer cells. In another IHC study by Storr et al. 2011, 93 tumour samples of patients with primary breast cancer treated with surgery and adjuvant chemotherapy followed by trastuzumab treatment, demonstrated that calpain 1 expression was associated with relapse free survival in breast cancer patients treated with trastuzumab after adjuvant chemotherapy (Storr *et*

al., 2011c). In a confirmatory study, in an expanded breast cancer patient cohort treated with trastuzumab from Nottingham (n=194), including 72 of the previously reported cohort and an independent cohort of 87 patients from Newcastle, it was shown that expression of calpain 1 was associated with relapse-free survival in both the cohorts, with high expression associated with adverse relapse-free survival. In the combined cohort, calpain 1 expression was also associated with poor relapse-free survival (Pu *et al.*, 2016b). In a cohort of early-stage invasive breast cancer patients (n=1371), it was seen that high calpain-2 expression in basal-like or triple-negative disease was significantly associated with adverse breast cancer-specific survival. This was also verified in an independent cohort of 387 patients (Storr *et al.*, 2012a). In a study by Storr et al., on large but operable inflammatory and non-inflammatory primary breast cancer tumours with neoadjuvant chemotherapy, it was demonstrated that high calpastatin and low calpain 2 expression was significantly associated with adverse breast cancer-specific survival, in non-inflammatory breast cancer patients. They also showed that low calpastatin and calpain 1 expression was associated with adverse survival of the inflammatory breast cancer patients (Storr *et al.*, 2016). The above studies support that calpain expression is important in cancer progression and is also associated with response to various treatments that affect overall survival in patients. The precise way, and mechanisms, that the calpain system operates to influence progression and therapeutic response remains unclear. It is, therefore, important to examine how the calpain system affects response to treatment in breast cancer cell lines, with a view to understanding mechanisms and, potentially, novel treatment strategies.

1.4 Overall study hypothesis, aims and objectives

Hypothesis

The current project hypothesises that-

Altering calpain activity will alter breast cancer cellular behaviour and response to conventional therapies, i.e. inhibition of calpain activity will

alter breast cancer cellular behaviour and render them sensitive to conventional forms of therapy

Aims

1. To assess the role of calpain system in regulating breast cancer cell behaviour and response to therapy.

2. To assess and categorise genes altered by the differential expression of calpain system genes using the publically available datasets, validating importance of identified targets in breast cancer cell lines and patient tumour tissue.

Objectives

To assess the role of calpains in regulating cell behaviour and breast cancer treatment response, calpain activity was inhibited in breast cancer cell lines using 3 different strategies:

1. Molecular overexpression of Calpastatin isoforms. The objectives in this strategy included:

- To generate cell lines overexpressing Calpastatin isoforms I, II, and III by performing transfections and single cell cloning.
- To identify intracellular localisation of each isoform.
- To assess cell characteristics and chemotherapeutic drug and radiation treatment response in calpastatin isoforms overexpressing breast cancer cell lines.
- To conduct RNA sequencing to examine differential expression/localisation of each isoform and to identify potential targets interacting with different isoforms of calpastatin.

2. Use of novel small molecule calpain inhibitors- the objectives for this strategy included:

- To assess calpain activity inhibition by the commercially available inhibitor, calpeptin, using the conventional tBOC assay.
- To develop a novel FRET based assay to assess calpain activity in live breast cancer cells.

- To demonstrate activation and inhibition of calpains using the novel FRET based assay in breast cancer cell.
- To assess the specificity of novel calpain inhibitors using the FRET based assay.
- To assess the effect of novel calpain inhibitors on breast cancer cell behaviour and chemotherapeutic and radiation response.

3. Using calpain CRISPR/Cas9 calpain knock out cell lines. The objectives for this strategy included:

- To assess the effect of knocking out calpains 1, 2 and 4 on cell proliferation and clonogenic plating efficiency.
- To assess the effect of knocking out calpains 1, 2 and 4 on normoxic doxorubicin and radiation response.
- To assess the effect of knocking out calpains 1, 2 and 4 on cell proliferation and survival under hypoxic growth.
- To assess the effect of knocking out calpains 1, 2 and 4 on doxorubicin and radiation response under hypoxic growth conditions.

To examine the differentially expressed genes (DEGs) altered by the calpain system in the regulation of breast cancer progression and treatment response, bioinformatics analyses were done using publicly available breast cancer datasets. The objectives include-

- To assess the significant DEGs associated with differential expression of Calpain 1, Calpain 2, Calpain 4 and Calpastatin genes using the METABRIC and TCGA datasets.
- To assess the pathways enriched and perform survival analyses on the DEGs associated with the calpain system genes.
- To assess correlations between the calpain system genes and the associated DEGs.
- To validate the protein expression of the shortlisted gene from above in breast cancer patient samples and to determine its associations with survival.

Chapter 2- Molecular overexpression of calpastatin isoforms

2.1 Abstract

Background: The calpain system has shown to be involved in progression of breast cancer therapy response and clinical outcomes in different subtypes of breast cancer, by the current group. The endogenous calpain inhibitor, Calpastatin (CAST) is the single gene with multiple promoters which generates distinct calpastatin isoforms. The differential intracellular localisation and roles of different variants is unknown. Therefore, this study aimed to generate breast cancer cells stably expressing calpastatin type I, II and III to assess their differential localisation and effect on breast cancer cellular behaviour and treatment response.

Methods: T47D and MDA-MB-231 breast cancer cells were used in this study. HA-tagged constructs of calpastatin isoforms I, II and III were stably transfected in T47D and MDA-MB-231 using Geneticin G418 as a selection marker. A monoclonal population expressing each calpastatin subtype was generated by single cell cloning. The HA-tagged calpastatin protein expression was assessed by Western blotting, the fold change in each calpastatin isoform was determine by RT-qPCR and their localisation was assessed by cell immunofluorescence. T47D and MDA-MB-231 cells were sent for RNA sequencing and several bioinformatic analyses were performed on the DEGs obtained by the overexpression of different calpastatin isoforms using the Qiagen IPA package.

Results- T47D and MDA-MB-231 cells overexpressing calpastatin isoforms I, II and III were generated. A single band was seen for calpastatin type I, a duplet band was seen for calpastatin type II and multiple bands were seen for calpastatin type III by Western blot analysis. CAST I cells had a 2.6-fold and 6.22-fold increase in calpastatin type I expression compared to the WT and mock-transfected control cells ($P<0.01$ and $P<0.01$, respectively) in MDA-MB-231 cells and ($P<0.0001$) in T47D cells. Calpastatin type II expression was 5.8 fold higher in MDA-MB-231 cells and 3.1 fold higher in T47D cells compared to the WT and mock-transfected control cells ($P=0.01$ and $P<0.05$; and $P<0.05$ and $P=0.001$, respectively). Calpastatin types I and III were seen to have a diffused cytoplasmic while calpastatin type II had a distinct perinuclear localisation in both the cell lines.

T47D calpastatin types I, II and III had 9525, 8886 and 4684 DEGs, respectively, while MDA-MB-231 cells overexpressing calpastatin type I, II and III had 2433, 3700 and 10395 DEGs, respectively. The DEGs overlapping between the expressions of calpastatin types I/II, II/III and I/III were 2977, 711 and 907, respectively and the number of DEGs unique to the expression of calpastatin type I, II and III were 3165, 2723 and 593 respectively, in T47D cells. In MDA-MB-231 cells DEGs overlapping between the expressions of calpastatin types I/II, II/III and I/III were 351, 1561 and 617, respectively and the number of uniquely expressed DEGs associated with the expression of calpastatin types I, II and III were 594, 916 and 7341, respectively.

Calpastatin types I, II and III associated DEGs in T47D cells enriched pathways including, RHOGDI signalling, Wound healing signalling, PI3K/AKT signalling, tumour microenvironment pathway, cyclins and cell cycle regulation. While in MDA-MB-231 cells DEGs enriched integrin signalling, endoplasmic reticulum stress pathway, wound healing, pyroptosis pathways. These pathways were mapped for their association of different calpastatin types with the 'target' and 'node' genes that were listed to be taken for further analysis to establish associations with survival and breast cancer clinical outcomes.

Conclusions- Calpastatin types I, II and III were successfully transfected and monoclonal populations overexpressing different calpastatin isoforms were generated. Fold change in calpastatin isoforms I and II were determined in both the cell lines and were seen to be significantly overexpressed. Different calpastatin isoforms had differential localisation. RNA sequencing of cells overexpressing different calpastatin isoforms revealed that calpastatin types I, II and III may have different number of associations intracellularly. RNA sequencing data also identified the significantly activated and inhibited pathways enriched by the DEGs associated with the expression of each calpastatin isoform.

2.2 Introduction

The protein inhibitor of calpains, Calpastatin, was named in 1979 by Takashi Murachi (Murachi, 1989). It was purified in 1982 from human erythrocytes as a 70 kDa polypeptide that inhibited both μ- and m-calpains (Takano *et*

al., 1982). It is present only in vertebrate tissues with its genomic sequence lacking in Drosophila, C. elegans, and Saccharomyces cerevisiae (Goll *et al.*, 2003).

2.2.1 Calpastatin structure

Cloning and sequencing studies identified that calpastatin has four repeating, roughly homologous, inhibitory domains having 140 amino acids each (Figure 2.1). Domains I, II, III and IV are the inhibitory domains. However, the N terminal domain, and L domain, did not have inhibitory activity (Wendt *et al.*, 2004). Each inhibitory domain can inhibit one calpain molecule, suggesting one molecule of calpastatin can inhibit multiple calpain molecules (Emori *et al.*, 1988; Imajoh *et al.*, 1987). Further examinations of calpastatin sequences identified three subdomains A, B and C within each inhibitory domain (Maki *et al.*, 1988; Uemori *et al.*, 1990). Sequencing data showed that each of the subdomains, A, B and C, were encoded by a single exon. In addition to these three subdomains a fourth exon encodes the region from subdomain C to the end of the domain (Maki *et al.*, 1989).

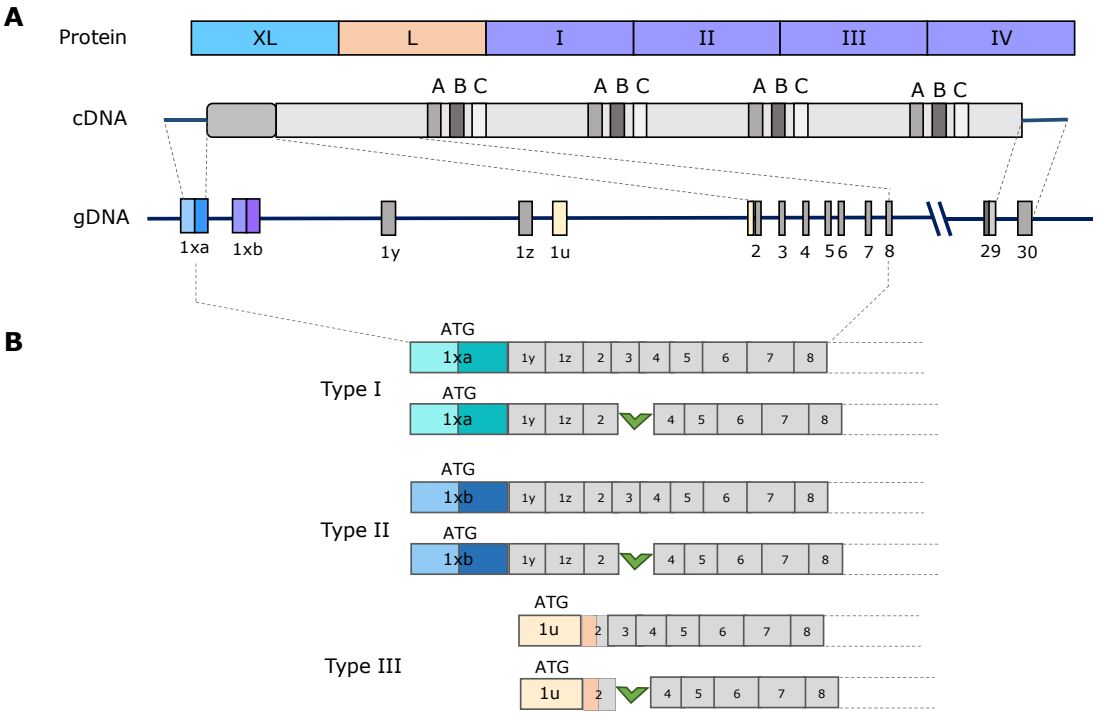

Figure 2. 1 Schematic representation of gDNA, cDNA and protein Calpastatin. (A) The cDNA encoding Calpastatin is represented in terms of L domain protein, containing the XL region and the inhibitory domains (I-IV). Each inhibitory domain containing subdomains A, B and C. The gDNA shows the 5' (L-domain) and 3' exons of the Calpastatin gene. Transcription from putative promoters located immediately after 5' to exons 1xa, 1xb and 1u result in formation of different transcripts from one gene. (B) gDNA for the 5' ends of the resulting transcripts that result in multiple protein types. Reproduced form (Storr *et al.*, 2011a), Nature Reviews Cancer. Copyright© 2011 by Springer Nature with permission conveyed through Copyright Clearance Centre Inc.

As mentioned in chapter 1, CAST is a single gene with several promoters and with alternative splicing mechanisms in the L domain that generates distinct calpastatin isoforms, with variation at the N terminal. (Lee *et al.*, 1992b; Takano *et al.*, 1999). Some conservation of the calpastatin gene structure, and the multiple transcripts generated from it, has been shown in human, mouse (Takano *et al.*, 2000) and porcine (Parr *et al.*, 2001) gene structures with mRNAs encoding for longer L and XL domains.

2.2.2 Calpastatin isoforms

The single CAST gene, encodes the multiple calpastatin isoforms, is located on chromosome 5q15 (Storr *et al.*, 2015). Calpastatin types I, II, III and IV are the most widely studied isoform types, their characteristics are summarised in Table 2.1.

Calpastatin type I and II contain L domain with differences in N-terminal sequences are generated from different exons 1xa and 1xb. A promoter associated with the untranslated exon 1u results in the generation of calpastatin type III that lacks the XL region from the L domain and calpastatin type IV is a testis specific isoform that lacks L domain and the inhibitory domain I due to its promoter region lying between exon 14 and 15 (Storr *et al.*, 2011a; Takano *et al.*, 2000).

Table 2. 1 Summary of different calpastatin transcripts. Adapted from (Goll *et al.*, 2003).

Transcript characteristics	Protein characteristics
Type I- contains exon 1xa, 1y, 1z, exons for L and all four inhibitory domains. Predicts an 85- kDa polypeptide	Rate of migration in SDS-PAGE and tissue expression are unknown
Type II- contains exons 1xb, 1y, 1z, exons for L and all four inhibitory domains. Predicts a 84 kDa polypeptide	Migrates as a 145-kDA polypeptide in SDS-PAGE; contains XL domain that has three protein kinase A sites in some species; present in cardiac tissue.
Type III- prototypal; contains exons for all four inhibitory domains; predicts a 77-78 kDa polypeptide	Migrates as a 135-kDa polypeptide in SDS-PAGE; present in mammalian skeletal muscle and many other tissues
Deletion of exon 3 in L domain; contains all four inhibitory domains; predicts a 74-75 kDa polypeptide	Migrates as a 125-kDa polypeptide in SDA-PAGE; present in skeletal muscle and other tissues
Deletion of exons 3 and 6 in L domain; contains all four inhibitory domains; predicts a 72-73 kDa polypeptide	Rate of migration in SDA-PAGE and tissue expression unknown
Lacks the L and I domains; predicts a 46-kDa polypeptide	Migrates as a 70-kDa polypeptide in SDS-PAGE; in human and rabbit erythrocytes; possibly also in other cells where it may have been identified as a degradation product
Type IV-lacks the L and I and a part of domain II; molecular weight unknown	Rate of migration in SDS-PAGE is unknown, transcript found only in testis
Lacks domains L, I and II; predicts a 35-kDa polypeptide	Rate of migration in SDS-PAGE approx. 55 kDa; found in human testis
Lacks domains L, I, II and III; predicts a 18.7-kDa polypeptide	Rate of migration in SDS-PAGE unknown; found in human testis

Alternative splicing occurs differently in different species and generates different calpastatin isoforms. It was seen that deletion of the region that

corresponds to exon 3 occurs partially in human calpastatin cDNA clones (Lee *et al.*, 1992a; Lee *et al.*, 1992b) and has been seen in all cDNA clones in rats (Ishida *et al.*, 1991; Lee *et al.*, 1992a). Rat calpastatin isoforms have exons 4 and/or exon 6 deletion while exon 5 deleted isoforms are found in human calpastatin (Takano *et al.*, 1999). Exon deletion has also been observed in inhibitory domain I, with exon 11 deleted isoforms in humans and exon 12 deleted isoforms in mouse (Lee *et al.*, 1992b; Takano *et al.*, 1999). Exon 11 deleted isoforms are expressed in the brain tissues and neuroblastoma cell lines and are not detected in heart or liver tissues in humans (Lee *et al.*, 1992b).

The effects of expression of different calpastatin splice variants has not been widely studied. De Tullio et al. showed that absence of exon 6 promotes intracellular storage aggregate formation (De Tullio *et al.*, 2009) and absence of exon 3 results in deletion of amino acid stretch KKRHKK form the L domain, which has shown to been involved in calpastatin binding to biomembranes (Goll *et al.*, 2003). Additionally, an exon 3 containing calpastatin transcript has shown to have a crucial role in the regulation of lymphovascular invasion in breast cancer. In a previous study, Storr et al. showed that downregulation of an exon 3 containing variant and low levels of calpastatin was significantly associated with the presence of lymphatic invasion (LI) in breast cancer (Storr *et al.*, 2011b).

2.2.3 Subcellular Calpastatin distribution

The members of the calpain system, calpains and calpastatin, are principally co-localised in the cytoplasm with a slight assembly around the nuclear region (Gil-Parrado *et al.*, 2003). During the influx of calcium, calpains are dissociated from calpastatin, crucial for calpain activation, followed by re-localisation of calpains to the plasma membrane. The calpains at the plasma membrane regulate downstream targets such as those affecting cell migration or adhesion modulators. Calpastatin remains in the cytoplasm during such calpain activation (Gil-Parrado *et al.*, 2003; Stifanese *et al.*, 2010).

Calpastatin has also been reported to have a perinuclear localisation. This might be a consequence of aggregation of calpastatin after its dissociation

from the calpain bound complex. It has been predicted that this localisation might result in an increased cell migration and reduced nuclear calpain-mediated pro-survival effects (Averna *et al.*, 2003). Similarly, nuclear accumulation of calpastatin may promote cell death by suppressing the pro-survival functions of nuclear calpain (Vo *et al.*, 2019).

Calpastatin has shown to be distributed predominantly in the cytoplasm with some granularity and heterogeneity between adjacent tumour cells, in breast cancer tissues. Calpastatin has been also detected in the nucleus, albeit rarely (Storr *et al.*, 2012c; Storr *et al.*, 2016).

2.2.4 Calpastatin and cancer

Several cancer types have shown aberrant calpastatin expression. Low expression of calpastatin has been reported in gastric cancer ($P<0.0001$, n=51) (Liu *et al.*, 2017), ovarian cancer (Salehin *et al.*, 2011) and colorectal adenocarcinoma ($P<0.05$, n=50) (Lakshmikuttyamma *et al.*, 2004). Low expression of calpastatin has been clinically correlated with cancer progression and worse outcome in operable inflammatory breast cancer and patients with bile duct and ampullary carcinomas (Storr *et al.*, 2012c; Storr *et al.*, 2016). While, high expression of calpastatin was reported in endometrial cancer ($P=0.037$, n=29) (Salehin *et al.*, 2010).

Several calpastatin studies have been previously done by the current group in breast cancer. In 2011, Storr et al. had shown that downregulation of calpastatin protein ($P=0.025$, n=53) and the exon 3 containing variant ($P=0.014$, n=56) was associated significantly with the presence of LI (Storr *et al.*, 2011b). This was later confirmed in a larger cohort (n=1266), with data showing that high expression of calpastatin was associated with absence of intra-tumoural LI $P=0.0014$ (Storr *et al.*, 2012a) suggesting that calpastatin may play an important role in the regulation of initial metastatic steps by regulating LVI. This negative association was also seen between calpastatin expression and various clinicopathological characteristics in breast cancer. The same study showed that calpain-1 was significantly associated with several clinicopathological variables such as tumour grade and ER expression. It was also demonstrated that high expression of calpain-2 in basal-like or triple-negative disease was significantly associated

with poor breast cancer-specific survival, suggesting that the calpains and calpastatin work together as a system in regulating breast cancer characteristics. Low expression of the exon 3 containing calpastatin transcript was significantly associated with higher NPI (P=0.012), larger tumour size (> 2 cm, P=0.003), and a negative HER status (P=0.042). Low expression of calpastatin protein was associated with ER and PR negative status (P=0.010 and 0.022, respectively) and basal phenotype P=0.0008 (Storr *et al.*, 2011b). While high calpastatin expression was significantly associated with low risk clinicopathological parameters such as small tumour size (< 2 cm, P=0.022), low NPI (P=0.001), low grade (P=0.002), older patients (≥40 years, P=0.002), ER and PR positive (P=0.001 and P<0.001, respectively) and non-basal phenotype of breast cancer P=0.003 (Storr *et al.*, 2012a). In a separate study, calpastatin was found to be correlated with lymph node status (P=0.007), NPI (P=0.003), HER2 expression level (r=0.350, P=0.001), and HER2 gene amplification (r=0.258, P=0.027) in patients with HER2-positive disease treated with trastuzumab after adjuvant chemotherapy. It was also established that calpain 1 expression was significantly associated with relapse-free survival in the same cohort (Storr *et al.*, 2011c).

In a cohort of large but operable primary breast tumours treated with neoadjuvant chemotherapy, low expression of calpastatin was significantly associated with adverse breast cancer specific survival in inflammatory breast cancers P=0.020, n=43. While high expression of calpastatin was significantly associated with adverse disease-specific survival in patients with non-inflammatory breast cancer P=0.035, n=94 (Storr *et al.*, 2016). In summary, high expression of calpastatin was associated with improved disease-specific survival in inflammatory breast cancer disease while, low expression of calpastatin was associated with improved breast cancer-specific survival in large but operable non-inflammatory primary breast cancer treated with neoadjuvant chemotherapy.

2.2.5 Hypothesis and aims

The above findings, with some minor exceptions, suggest that downregulated expression of calpastatin is associated with breast cancer progression and response to therapy. Although calpastatin isoforms I, II

and III originate from one gene, their individual roles in regulating calpain activity, cell behaviour and treatment response remain largely unknown.

Hypothesis

Therefore, in this chapter we hypothesise, in line with the project's overall hypothesis, inhibiting calpain activity by molecular overexpression of calpastatin isoforms I, II and III will alter breast cancer cell behaviour and make them more sensitive to conventional forms of therapy.

Aims

1. Establish monoclonal populations of stably transfected breast cancer cell models overexpressing calpastatin isoform type I, type II, or type III in two different subtypes of breast cancer cells (T47D and MDA-MB-231 cell lines).
2. Quantify the levels of overexpression of calpastatin isoform type I, type II and type III in T47D and MDA-MB-231 cell lines.
3. Examine the subcellular distribution of calpastatin isoform type I, type II and type III in both cell line models.
4. Assess the effect of overexpression of calpastatin isoform type I, type II and type III on breast cancer cell proliferation and plating efficiency.
5. Assess the effect of overexpression of calpastatin isoform type I, type II and type III on chemotherapeutic drug and radiation response in T47D and MDA-MB-231 cell lines.
6. Conduct RNA-seq analysis on T47D and MDA-MB-231 overexpressing calpastatin isoform type I, type II and type III cell lines to examine differential expression linked to each isoform, assess effects on signalling pathways and to identify potential targets interacting with different isoforms of calpastatin.

2.3 Materials and Methods

2.3.1 Breast cancer cell lines and reagents

MDA-MB-231 and T47D breast cancer cell lines were cultured in Minimal Essential Medium (MEM) and Dulbecco's Modified Eagle Medium (DMEM)-high glucose (Sigma, UK) respectively. The cell lines were originally

obtained from American Type Culture Collection (ATCC). MDA-MB-231 cell media was supplemented with 1% non-essential amino acids solution (Sigma, UK), 2mM L-glutamine (Sigma, UK), 1% penicillin/ streptomycin (Sigma) and 10% Iron supplemented donor bovine serum (Gibco) while T47D medium was supplemented with 10% donor bovine serum and 1% penicillin/streptomycin. Cell cultures were maintained in a humidified incubator with 5% CO_2 at 37°C. Subculturing was limited to a maximum of 15 passage window. The serum was heat activated at 56°C for 30 minutes before use and was batch tested approximately every 18 months to ensure the batch to batch consistency was maintained. The cells were authenticated every six months using multiplex short tandem repeat (STR) DNA profiling analysis (Powerplex 16, Promega). Cells in culture were also regularly checked for mycoplasma contamination on a monthly basis.

2.3.2 Subculture

Cells were sub-cultured and grown in normal growth media until reaching 70-80% confluency in T-25 cm^2, T-75 cm^2, or T-175 cm^2 tissue culture flasks according to the experimental requirements. To passage confluent flasks, media was aspirated and cells were washed with phosphate buffered saline (PBS) (Ca^{2+} and Mg^{2+} free) (Sigma), and detached using 0.05% trypsin-EDTA (Sigma) to cover the monolayer of cells for 2-5 minutes, with incubation at 37°C. Following incubation flasks were observed under the microscope and trypsin-EDTA was inactivated using complete culture medium. The cells were split in the ratio 1:10 or 1:5 by adding appropriate volume of fresh complete media to the trypsinised cells and transferring them into a new tissue culture flask. The new flask was maintained at 37°C with 5% CO_2 until the next passage was required.

2.3.3 Cell storage and recovery

Cells were frozen in liquid nitrogen for preservation and long term storage. Cells cultured to 70-80% confluency were trypsinised and counted using a haemocytometer. They were centrifuged at 1000 rpm for 5 minutes, and a suspension of $2x10^6$ cells/ml was prepared in freezing medium containing 10% dimethyl sulfoxide (DMSO). 500 µl of cell suspension was aliquoted into bar coded cryovials and stored overnight in a -80ºC freezer using a 'Mr

frosty' system. The cryovials were then transferred into liquid nitrogen for long term storage.

Cells were recovered from liquid nitrogen by rapid thawing in a 37°C water bath. The thawed cell suspension was transferred into 9 ml complete medium. The cell suspension was centrifuged at 1000 rpm for 5 minutes and the supernatant was discarded. The resulting cell pellet was resuspended in 1 ml of fresh medium and transferred into a T-25 cm^2 flask containing 4 ml of fresh medium. The flask was then placed into a humidified incubator at 37°C. The medium was replaced the following day to remove any residual DMSO.

2.3.4 Cell growth curves by proliferation assay

Cell growth curves were produced from cell proliferation experiments and used to calculate cell doubling times, to ensure cells were growing as expected. $1x10^5$cells/well were seeded in 6- well plates, in triplicate, and placed in a humidified incubator at 37ºC, 5% CO_2 for attachment. They were allowed to grow over a period of 0-96 hours. At every 24h time point, appropriate wells were washed with 1 ml PBS followed by cell detachment using 500 µl of trypsin-EDTA. Cells were checked under the microscope for detachment and trypsinsation stopped using 500 µl of complete medium. Cells were counted using the haemocytometer. The cell counts were used to calculate the average number of cells for each time point. Cell growth curves were generated by plotting the average cell number on the y-axis against time point on the x-axis to determine the doubling time of each cell line (Figure A1.1A, Table A1.1 in Appendix A). The data in this chapter represent the average number of cells ± SD of three independent experiments.

2.3.5 Plating efficiency

The plating efficiency of a cell line describes the cell's inherent ability to divide. Plating efficiency experiments were conducted in parallel to cell proliferation experiments. After counting cells for the 24 hour time point from the cell growth experiment, cells were serially diluted to the required lower seeding density, seeded into T-25cm^2 flasks and allowed to grow in a humidified incubator at 37°C with 5% CO2. The flasks were left undisturbed

for a period of 14 or 21 days for MDA-MB-231 and T47D cells respectively, to form colonies. Flasks were washed with PBS, and colonies fixed with 50% methanol for 15 minutes followed by 100% methanol for another 15 minutes. After fixation, colonies were stained using 0.5% crystal violet. After staining flasks were gently washed with tap water and allowed to dry completely before counting. Colonies having more than 50 cells were counted as surviving colonies (Figure A1.1B). The plating efficiency was calculated using the following formula-

$$PE\ (\%) = \frac{\text{Number of colonies formed}}{\text{Number of cells plated}} \times 100$$

The data in this chapter represent the average number of cells ± SD of three independent experiments.

2.3.6 Stable transfection of CAST isoforms

MDA-MB-231 and T47D cells were chosen to perform the transfection of different calpastatin isoforms. The cDNA constructs of calpastatin type I, type II and type III linked with an HA tag on the plasmid construct (pZS-green1-N1) was designed and provided by Professor T. Parr's group, School of Biosciences, University of Nottingham. The nucleotide sequence of the cDNA constructs and the HA tagged plasmid maps are mentioned in Appendix A (Section A1.2). Clonal populations of stably transfected calpastatin type I and type III in T47D cells and calpastatin type I and type II in MDA-MB-231 cells was previously generated in the lab by Dr. B.Sukkarn.

For the transfection of calpastatin type III into MDA-MB-231 cells, Lipofectamine 3000(Invitrogen) was used as the transfecting reagent and the manufacturer's protocol was followed. $3.6x10^5$ cells were seeded in 6-well tissue culture plates the day before transfection and allowed to grow to 70-80% confluency. Media was replaced with antibiotic free Opti-MEM reduced serum media (Thermo Fisher Scientific) the next day. Lipofectamine 3000 and the plasmid containing calpastatin type III were diluted in Opti-MEM Reduced Serum Media. Diluted plasmid and diluted Lipofectamine mixtures were prepared in different ratios (1.5-3 µL Lipofectamine 3000 per 1 µg of DNA). The complex was incubated for 10-

15 minutes at room temperature and added dropwise to the cells according to the manufacturer's protocol. The transfection media was removed and the selection media containing 750 µg/mL Geneticin (Gibco), optimised previously by Dr. Sukkarn, was applied to the cells after 2-4 days post transfection. Cells were then grown and expanded in the presence of selection antibiotic (Geneticin) to obtain a total multipopulation of transfected cells.

Single clonal populations were obtained from total multipopulations of transfected MDA-MB-231 and T47D cells using the limiting dilution method. Upon trypsinisation, a cell suspension of 10 cells/ml was prepared. 100 µl of this suspension was aliquoted into each well of a 96-well plates (Corning) to obtain and average of 1 cell/well. Plates were incubated for 14 or 21 days for MDA-MB-231 and T47D cells respectively, for single cells to grow into colonies. After incubation, the wells with single colonies were marked and transferred into 48 well plates. Once confluent, these cells were expanded to obtain confluent T-175cm^2 monoclonal cultures. Cell lysates were prepared and Western blotting conducted to examine CAST isoform expression via the HA tag. Tables A1.2 and A1.3 in Appendix A shows the number of clones obtained and analysed for T47D and MDA-MB-231 cells.

2.3.7 Western Blotting

Clonal populations of transfected MDA-MB-231 and T47D cells were harvested and washed twice with PBS to remove trypsin. Cells were counted and spun down. The pellet was resuspended in RIPA Buffer (Sigma) containing 10% protease and phosphatase inhibitor cocktail (Thermo-Scientific) and 0.5 M EDTA solution (Thermo-Scientific). The suspension was incubated on ice for 20 minutes and the resulting lysates centrifuged at 13,000 rpm for 10 minutes to remove cell debris. The supernatant was carefully transferred to a new eppendorf and stored at -20 ℃.

Protein samples were prepared and loaded onto precast polyacrylamide Bolt™ 4-12% Bis-Tris Plus Gels (Novex Life Technology). The gel was placed inside the MiniGel tank (Life technologies). The MOPS-SDS running buffer (ThermoFisher Scientific) was filled in the tank to completely immerse the gel. 20 µL of prepared sample and 9 µL of pre-stained molecular weight

protein marker (SeeBlue Plus2, Invitrogen) was loaded per well. The gel was run at 200V for 26 minutes. Separated proteins were transferred on to a 0.45 µm nitrocellulose membrane (Whatman GE Healthcare) by electroblotting. The gel and the membrane were sealed tightly in a cassette and the transfer was performed using the BOLT (Invitrogen) at 10V for 90 minutes.

The membranes were blocked using the blocking buffer (3% non-fat milk dissolved in 0.05% PBS Tween) for one hour at room temperature. After blocking, the membranes were incubated overnight at 4˚C with primary antibodies for HA Tag (Abcam, dilution 1:1000) and for β-actin (Abcam, dilution 1:1000), which was used as a loading control. After overnight incubation, the membranes were washed thrice with PBST for 5 minutes followed by secondary antibodies (IRDye donkey anti-rabbit, dilution 1:10000 and IRDye donkey anti-mouse, dilution 1:10000, LI-COR) binding for 1 hour at room temperature. The membranes were viewed using the Odyssey infrared imaging technology (LI-COR Biosciences) with the Image Studio software (V4.1) The protein expression was quantified and normalised against β-actin protein expression. Figures A1.2 and A1.3 in Appendix A shows the blots of surviving clones of T47D and MDA-MB-231 cell lines.

2.3.8 Measurement of mRNA expression

2.3.8.1 Total RNA extraction and cDNA synthesis

Stably calpastatin type II transfected, mock transfected, and WT MDA-MB-231 and T47D cells were used to isolate total RNA. Samples were independently collected in triplicates from subconfluent cultured cells using the RNAprotect Cell Reagent (76526, Qiagen, Netherlands) and RNeasy Plus Mini Kit (74134, Qiagen, Netherlands). To isolate total RNA, RNase-free materials were used including RNase-free pipette tips and collection tubes. The working area including the micropipettes and microcentrifuge was cleaned for RNase using the RNaseZap™ (Sigma-Aldrich, Germany) reagent.

Cells were seeded T-25cm^2 flasks a day before, allowed to adhere and become subconfluent. The flasks were placed in a humidified incubator at

37°C overnight. To extract the total RNA, the media was removed from the flasks and the cells washed with 3 ml PBS three times. To detach the cells, 500 µl of RNAprotect cell reagent was added to the cells and pipetted up and down to aid detachment. The cell and the RNAprotect cell reagent mixture was transferred in 1.5 ml Eppendorf tubes and stored at -80°C.

The total RNA was extracted from the mixture of cells and RNAprotect reagent using the RNeasy Protect Mini Kit according to the manufacturer's instructions. The amount and the purity of the eluted RNA was measured using a NANODROP 2000c Spectrophotometer (Thermo Scientific, USA). The eluted RNA was stored at -80°C until further use. cDNA was synthesised from the RNA extracted using an RT^2 First Strand Kit (330404, Qiagen, Netherlands) according to the manufacturer's instructions. The reaction tubes containing the synthesised cDNA were stored at -20°C for long term storage.

2.3.8.1 Real-time quantitative Polymerase Chain Reaction analysis (RT-qPCR)

To measure the fold change in CAST II expression, standards were prepared from the MDA-MB-231 and T47D cDNA samples. HPRT and CAST II standards were prepared using 1 in 2 dilutions to generate standard curves. A total reaction volume of 10 µl was prepared using 1 µl cDNA, 1 µl each forward and reverse primers, 5 µl SYBR Green ROX qPCR MAstermix (2x) (330253, Qiagen, Netherlands), and 2 µl RNase-free water (AM9935, Invitrogen, USA). HPRT and CAST II primers were used as 100 nM and 10 nM dilutions respectively. The standards, samples and no template controls (NTCs) were run in triplicates in an optical 96-well PCR plate (Thermo Fisher, USA). The PCR reactions were performed using the Viia7™ Real-Time PCR system (Applied Biosystems). The software Quant Studio™ Real-Time PCR was programmed to run for 40 cycles of 95°C for 15 seconds to denature the DNA, and 60°C for 1 minute for annealing and extension. After 40 cycles the same software was used for analysis. Expression of CAST II in both the cell lines was calculated relative to their HPRT expression. CAST II expression in both the cell lines was calculated and presented as average gene expression to the respective control ± SD of three independent experiments, each performed in triplicate.

2.3.9 Cell immunofluorescence

To identify the sub-cellular localisation of different HA tagged CAST isoforms in the MDA-MB-231 and T47D transfected cells, immunofluorescence (IF) was carried out. IF microscopy is the most commonly used technique to study the intracellular localisation of proteins of interest. Cells were seeded at a density of $1x10^5$ onto coated sterile coverslips (Corning) in 6-well plates. After attachment, cells were washed with PBS twice for 5 minutes followed by fixing with 4% paraformaldehyde (PFA) in PBS for 20 minutes. The fixed cells were then blocked using blocking buffer (10% goat serum (Sigma-Aldrich, Germany) and 0.3% Triton X-100 (Sigma-Aldrich, Germany) in PBS) for 60 minutes. After blocking cells were incubated with primary antibody for HA Tag (HA tag (6E2) Ms mAb (Alexa 488 conjugated), diluted 1:800, Cell Signaling Technologies) in antibody dilution buffer (1% bovine serum albumin (Sigma-Aldrich, Germany) and 0.3% Triton™ X-100 in PBS) and incubated overnight at 4˚C in the dark. This was followed by staining for F-actin (Alexa Flour 635 Phalloidin, Thermo Fisher Scientific) in 1:40 dilution in PBS for 1 hour in the dark at room temperature. After incubation, the cells were washed with 0.1% PBS-Tween-20 five minutes for three times. Coverslips were mounted on the slide using mounting media with DAPI (Vectashield, Vector Laboratories Inc., Burlingame, USA) and stored at 4°C. Images were viewed using Leica TCS-NT confocal laser scanning microscope (Leica microsystems) using different levels of magnification.

2.3.10 RNA sequencing sample preparation and data analysis

Breast cancer cells overexpressing calpastatin isoforms and their respective mock transfected control cell lines were induced to activate the calpain system before the cell pellets were sent for RNA sequencing. T47D and MDA-MB-231 cells lines overexpressing calpastatin type I, type II, type III and controls, each of three independent passages were seeded in T-175 cm^2 flasks and allowed to grow until confluent. The cells were treated with 10µM of Calcium Ionophore A23187 (Sigma-Aldrich) for 2 hours (concentration and time determined previously) to activate the calpain system (optimised in section 3.4.4). After treatment, cells were immediately washed, counted to a cell suspension of $5x10^6$ cells, frozen as

cell pellets and stored in 1.5 ml Eppendorf tubes at -80°C. A total of 24 samples were then packed and sent on dry ice to Novogene (UK) Company Ltd, Cambridge for RNA sequencing.

Samples were run for RNA sequencing with 50 million reads. Post sequencing analysis including genome alignment, and normalisation of transcripts differential expression was included in the package agreed with the company. The workflow of RNA-sequencing included, library construction of total RNA, followed by sequencing which was followed by bioinformatics analysis. The bioinformatic analyses work flow included, Quality control of the raw data, followed by mapping to the reference genome (Homo sapiens GRch38/hg38), and followed by gene expression quantification which was followed by correlation and differential expression analysis. The differential gene expression analysis was conducted using the DESeq2 R package by the company.

A differentially expressed gene (DEG) list was obtained for each CAST isoform overexpressing cell line compared to the mock transfected controls. The Ingenuity Pathway analysis (IPA) tool was used to further analyse the DEG lists for each sample. Each DEG list was uploaded onto the IPA package and core analysis was performed. The core analysis of each CAST isoform resulted in canonical pathways enriched by each DEG list.

The pathways enriched by the DEG list of each isoform type were referred to as canonical pathways. To select the significantly enriched pathways the Fisher's Exact Test *P*-value was set to a –log of 1.3. To shortlist the number of significantly enriched pathways further, the Benjamini-Hochberg (B-H) Multiple testing correction *P*-value was applied. The z-score is an IPA tool that predicts the degree of activation or inhibition of a pathway. The pathways were arranged according to their z-score. A positive z-score correlates to activation of a pathway and a negative z-score correlates to inhibition of a pathway. Based on this feature the top 10 activated and inhibited pathways were shortlisted.

The top 10 lists of activated and inhibited pathways were further tested for a double criteria. A z-score of ≥2 or ≤-2 was considered as significantly activated or significantly inhibited pathway. The p-value was used to measure how significantly a pathway was enriched. Pathways that were

significantly enriched and had a z-score ≥2 or ≤-2 qualified the double criteria and were taken forward for further analysis.

The qualified pathways from the above two criteria were further tested for their associations with CAST isoforms. The 'Build' tool, followed by the 'Path Explorer' tool, was used to find associations of CAST with each pathway. The CAST gene was added to each pathway and associations were made using the 'Path Explorer' tool to the genes in the pathway using the DEG list for the respective CAST type. Associations were then mapped from CAST to several genes on the pathway using evidence from published literature and the IPA knowledge database. The genes interacting directly with calpastatin were mapped as 'target' genes, and the ones acting as an intermediate molecule between CAST and the 'target' gene were mapped as an indirect association and were called the 'node' gene. The 'target' and 'node' genes were selected using the DEG list for each calpastatin type.

2.3.11 Statistical analysis

All graphs were constructed using GraphPad Prism 9 software. Data are presented as the mean values ± Standard Deviation (SD) of at least two independent experiments, each performed in duplicate or triplicate (or six replicates for clonogenic assay). Student's *t*-test was performed for comparing two groups and one-way ANOVA was performed to compare more than 2 groups, and a *P*-value< 0.05 was considered to be statistically significant.

2.4 Results

2.4.1 HA tagged calpastatin isoforms expression in cells

Following transfections and generation of clonal populations calpastatin types I, II and III expression was detected, as no antibodies can detect separate isoforms, using Western blotting to detect the HA tag (Figure 2.2A and 2.2C). HA-tagged calpastatin type I, type II and type III protein expression were first normalised against β-actin expression and were presented as relative expression to their respective mock transfected controls (Figure 2.2B and 2.2D).

Single bands were observed for HA-tagged calpastatin type I, and a duplet bands observed for HA-tagged calpastatin type II in T47D and MDA-MB-231

cell lines. Multiple bands were observed for calpastatin type III in both cell lines however, these bands were more prominent in MDA-MB-231 cells. HA-tagged calpastatin type I was significantly expressed in CAST I transfected T47D and MDA-MB-231 cells compared to their respective mock-transfected controls (*P*-values <0.001 and <0.01 respectively). HA-tagged calpastatin type II was significantly expressed in CAST II transfected T47D and MDA-MB-231 cells compared to their respective mock-transfected controls (*P*-values =0.001 and <0.01 respectively). HA-tagged calpastatin type III was significantly expressed in CAST III transfected T47D and MDA-MB-231 cells compared to their respective mock-transfected controls (*P*-values <0.05 and <0.05 respectively). HA-tagged calpastatin type III showed similar levels of expression in both the cell lines T47D and MDA-MB-231 cells. Whilst it would have been useful to conduct some mass spectroscopy the reason for, and identity of, the multiple bands of HA-tagged calpastatin type III could not be investigated further due to time constraints.

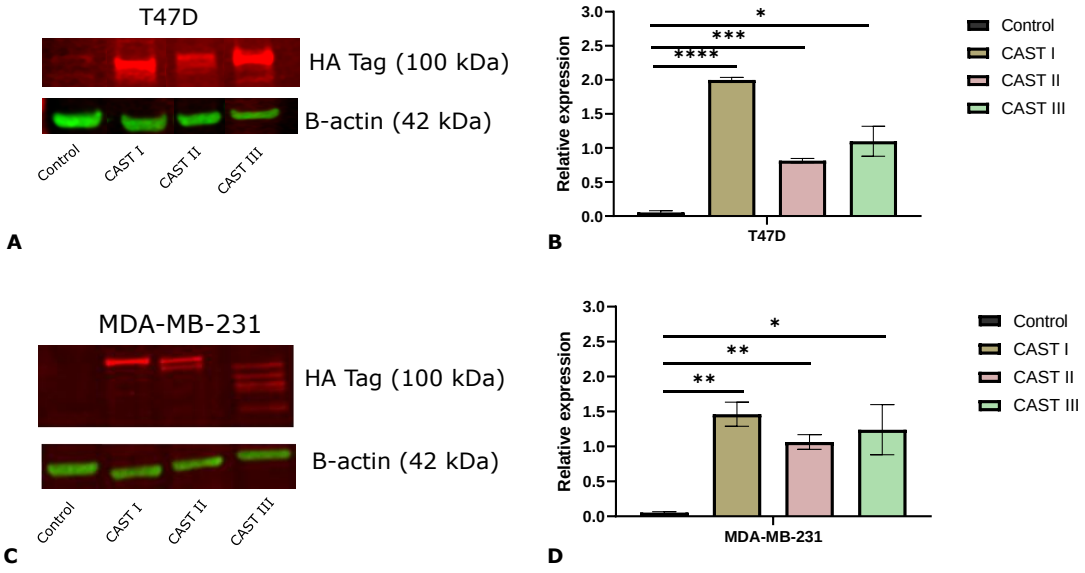

Figure 2. 2 Expression of HA-tagged calpastatin type I, II and III in T47D and MDA-MB-231 cells. Representative blots showing HA-tagged calpastatin types I, II and III (red bands, ~100 kDa) and β-actin, used as sample loading control (green bands, 42 kDa) in T47D (A) and MDA-MB-231 (C) cells. Quantitative analysis of each calpastatin isoform expression presented as ratio to β-actin expression in T47D (B) and MDA-MB-231 (D) cells. The data is presented as relative expression to their respective mock transfected controls. Data represents mean values ± SD of three independent experiments. Statistical analysis is represented by *(*P*<0.05), ** (*P*<0.01), *** (*P*<0.001).

Fold change in total calpastatin type I, II and III protein expression could not be determined due to unavailability of calpastatin isoform specific antibodies. To determine the fold change in isoform specific expression, calpastatin type I and II specific primers were designed and the overexpression was measured by RT-qPCR.

2.4.2 mRNA expression of calpastatin isoforms

To assess the level of overexpression of calpastatin type I, II and III RT-qPCR was performed. Primers specific to calpastatin types I and II were designed, using the BLAST package, complimentary to the exons 1xa and 1xb in the XL domains, respectively (Figure 2.3). Calpastatin type III specific primers could not be generated as exon 1u sequence was not included on the vector. However, protein translation experiments conducted in the lab by Dr. T. Parr demonstrated that calpastatin type III protein was produced using the constructs with translation starting at an ATG site within exon 2. Table 2.2 shows the primer sequences for HPRT, CAST I and CAST II genes.

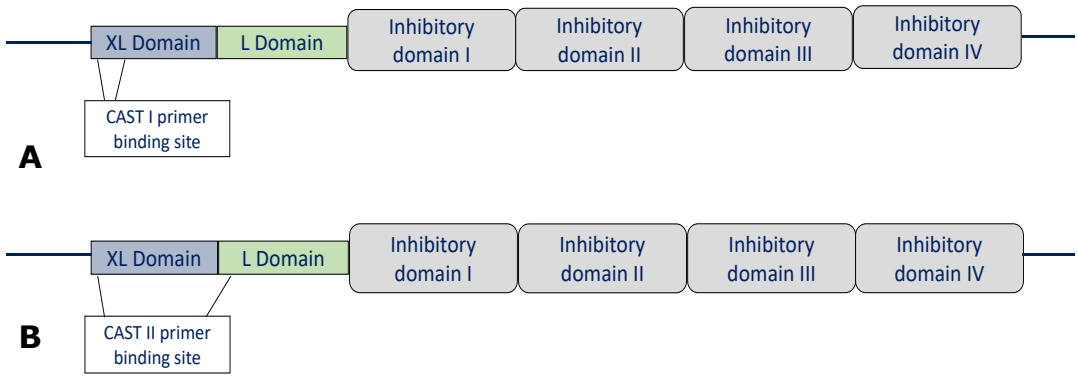

Figure 2. 3 Calpastatin isoform specific primer binding sites. Calpastatin type I (A) specific primer binds in the XL domain of the sequence. Calpastatin type II (B) specific primer binds to the XL and a part of L domain of the sequence.

Table 2. 2 Primer sequences for HPRT, CAST I and CAST II

Genes	Primer sequence
HPRT	Forward- 5'-AAATTCTTTGCTGACCTGCTG-3'
	Reverse- 5'- TCCCCTGTTGACTGGTCATT-3'
CAST I	Forward- 5'-CCGCCGCACCCA-3'
	Reverse- 5'-CCTTTCTTTTCTCCTGGTTTGGA-3'
CAST II	Forward- 5'-GCTGGTGGTACAAGACGCAT-3'
	Reverse- 5'-CCATCTGTTGGCTGACTGGA-3'

Overexpression of calpastatin type I and type II mRNA was measured by determining the fold change in expression levels of these genes relative to their respective mock transfected controls and wild type cells using RT-qPCR technique (section 2.3.8).

Calpastatin type I and type II mRNA expression levels were quantified using the relative standard curve method. Expression of calpastatin type I was previously determined by Dr. Sukkarn (Sukkarn, 2020). Expression of calpastatin type II was assessed in this section. MDA-MB-231 calpastatin type II cDNA was used as standards. Six standards were prepared using a 2 fold serial dilution. RT-qPCR was run for 40 cycles and the standard curves were generated. HPRT and CAST II had amplification efficiencies of, E= 97.58% and E= 79.94%, respectively. The standard curves for HPRT and CAST II had a linearity (R^2 value) of 0.9876 and 0.9685. Melt curves (Figure 2.4) of HPRT, CAST I (from Dr. Sukkarn's thesis, (Sukkarn, 2020)) and CAST II showed one peak which suggests the PCR product was amplified in each reaction without the presence of primer dimers or contamination from gDNA. Presence of only one peak also indicated the specificity of primers. Linear equations of standard curves with amplification efficiencies of HPRT, CAST I (Sukkarn, 2020) and CAST II expression are presented in Table 2.3.

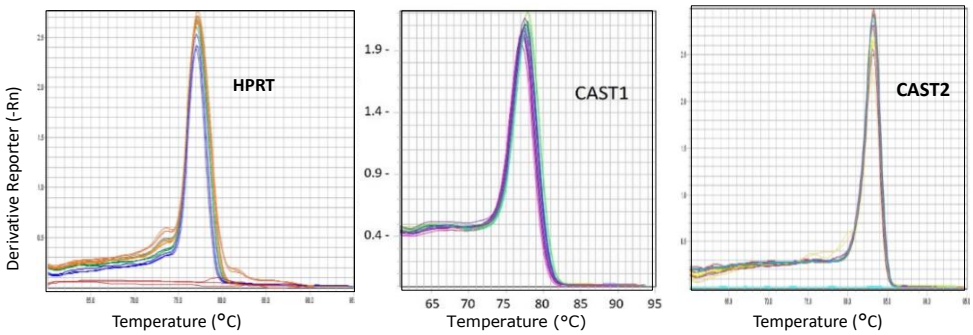

Figure 2. 4 Melt curves for HPRT, CAST 1 and CAST 2. Standard serial dilutions were prepared for HPRT, CAST1 and CAST2 with NTC. All the standards were amplified for their respective gene product.

Table 2. 3 Linear equations of standard curves and amplification efficiencies of PCR reactions for HPRT, CAST I and CAST II genes

Gene	Standard curve linear equation	R^2	Amplification efficiency (%)
HPRT	y=-3.3812x + 27.821	0.9876	97.58
CAST I	y=-3.9647x + 34.071	0.9851	78.74
CAST II	y=-3.9194x + 33.599	0.9685	79.94

HPRT, calpastatin type I and type II standard curves showed linearity as seen by their R^2 values. Standard curves were used to derive respective HPRT and calpastatin type II quantities in sample cells. Calpastatin type II expression was calculated relative to HPRT expression in T47D and MDA-MB-231 WT, mock transfected control and CAST II cells. Calpastatin type II expression relative to HPRT expression was then normalised against WT and mock transfected cells to calculate the fold change in calpastatin type II expression (Figure 2.5B). Data for calpastatin type I (Figure 2.5A) is mentioned in Dr. Sukkarn's thesis (Sukkarn, 2020).

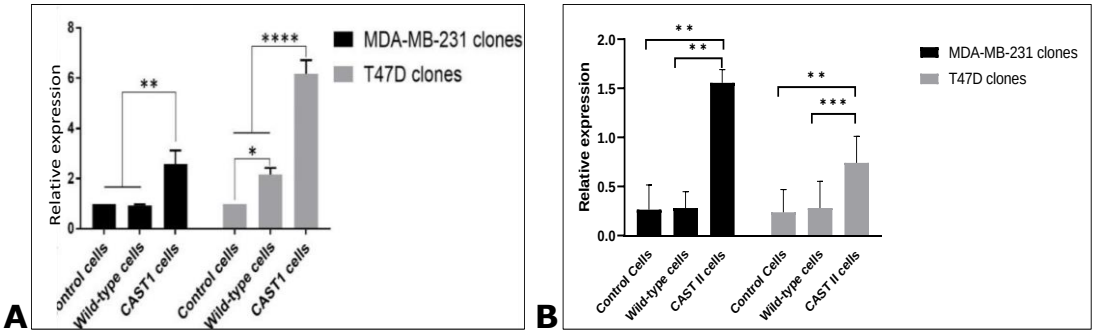

Figure 2. 5 Overexpression of CAST I and CAST II in T47D and MDA-MB-231 cells. Samples were prepared from separate passage numbers of WT cells, mock transfected control cells and CAST II transfected cells. Expression of HPRT and CAST II were extrapolated from standard curves. CAST II expression (B) in CAST II cells relative to expression in mock-transfected control and wild-type cells was normalised to HPRT expression. Overexpression of CAST I (A) was calculated by Dr. Sukkarn. Data represents mean values ± SD of three independent experiments conducted in triplicate. Statistical analysis was carried out using the Student's *t*-test *(*P*<0.05), ** (*P*<0.01), *** (*P*<0.001).

Calpastatin type I expression in MDA-MB-231 WT and mock-transfected control cells were comparable while CAST I transfected MDA-MB-231 cells had a significantly higher (2.60 fold increase) CAST I expression compared to its mock-transfected controls and WT cells (*P*<0.01 and *P*<0.01, respectively). In T47D, the WT cells had a significantly higher expression (~ 2 fold, *P*=0.0155) of calpastatin type I compared to its mock-transfected controls suggesting plasmid transfection or the presence of Geneticin had an effect on calpastatin type I expression. As expected, calpastatin type I expression in CAST I transfected T47D cells was significantly higher (6.22 fold increase, *P*<0.0001) compared to its WT and mock-transfected cells.

Calpastatin type II expression in MDA-MB-231 WT, T47D WT and their respective mock-transfected control cells were comparable (*P*=0.960 and

P=0.912, respectively). In MDA-MB-231 CAST II cells, expression of calpastatin type II was significantly higher (5.8 fold increase) compared to its WT and mock-transfected control cells (*P*=0.01 and *P*<0.01, respectively). In T47D CAST II cells, calpastatin type II expression was significantly higher (3.1 fold increase) compared to its WT and mock-transfected control cells (*P*=0.01 and *P*=0.001, respectively).

In summary, calpastatin isoform types I and II were overexpressed in T47D and MDA-MB-231 cells as shown by the HA-tagged protein expression, and mRNA expression in comparison with their respective WT and mock-transfected control cells. Fold change in calpastatin type III expression in T47D and MDA-MB-231 cells could not be determined as primers specific to calpastatin type III could not be designed. Calpastatin isoforms I, II and III were successfully overexpressed in T47D and MDA-MB-231 cells and therefore were regarded as valid models to assess changes in phenotypic behaviour in the respective cell lines. Overexpression of calpastatin type III however could not be measured by RT-qPCR but were shown to be translated into calpastatin type III protein in translation experiments.

2.4.3 Intracellular localisation of calpastatin isoforms

Calpastatin type I, II and III overexpressing T47D and MDA-MB-231 cells and their mock-transfected control cells were assessed for cellular distribution of calpastatin isoforms. HA-tagged calpastatin type I, II and III were detected using the Alexa 488 conjugated HA-tag antibody. The nucleus and F-actin fibres were stained with DAPI and Alexa Flour 635 Phalloidin, respectively. Figure 2.6 shows representative images of T47D and MDA-MB-231 cells overexpressing calpastatin types I, II and III at 40x magnification.

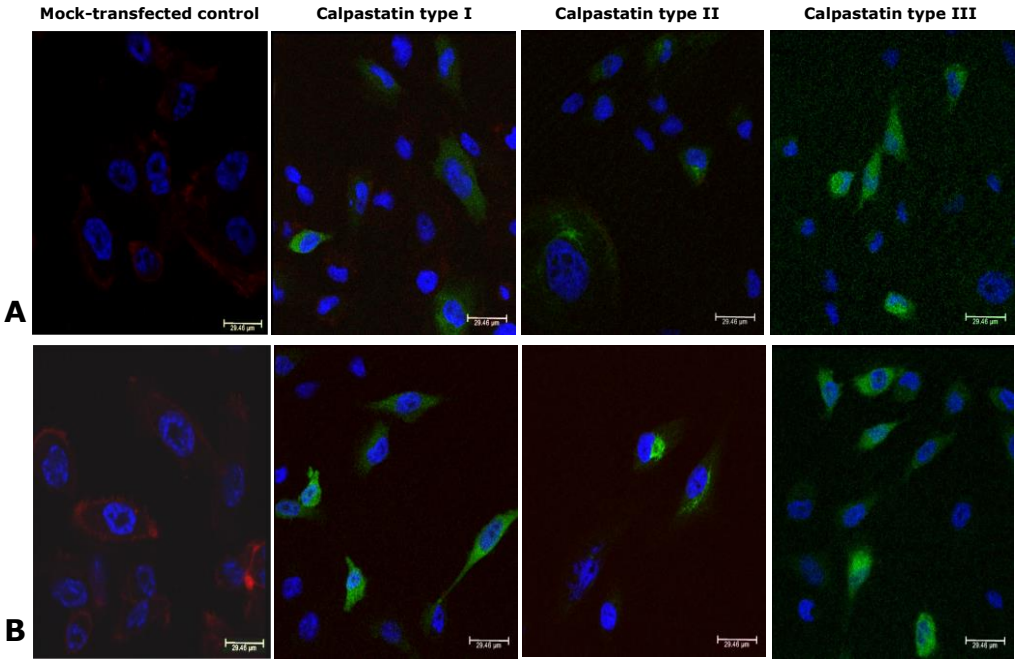

Figure 2. 6 Intracellular localisation of calpastatin type I, II and III in T47D and MDA-MB-231 cells. The left panel represents the mock transfected T47D and MDA-MB-231 cells. The next panel shows the localisation of HA-tagged CAST I (green), the next panel represents the intracellular localisation of HA-tagged CAST II (green) and the panel on the right shows the localisation of HA-tagged CAST III (green) in (A) T47D and (B) MDA-MB-231 cells under 40x magnification.

Mock-transfected T47D and MDA-MB-231 cells showed cell cytoskeleton with F-actin (red) and nucleus (blue) with no presence of HA-tagged proteins. CAST I transfected T47D and MDA-MB-231 cells showed that HA-tagged calpastatin type I (green) was diffused throughout the cytoplasm. HA-tagged calpastatin type II showed a unique localisation. It was seen to have a punctate and predominantly perinuclear form of distribution in T47D and MDA-MB-231 cell lines. A general diffused cytoplasmic localisation was seen in T47D and MDA-MB-231 cell transfected with calpastatin type III. A very faint signal was observed for F-actin (red) in calpastatin transfected cells. This could be due to technical error or use of old Alexa Flour 635 Phalloidin reagent. Calpastatin type II was seen to have a unique intracellular distribution at 20x, 40x and 63x (oil immersion) magnifications in both cell types (Figure 2.7).

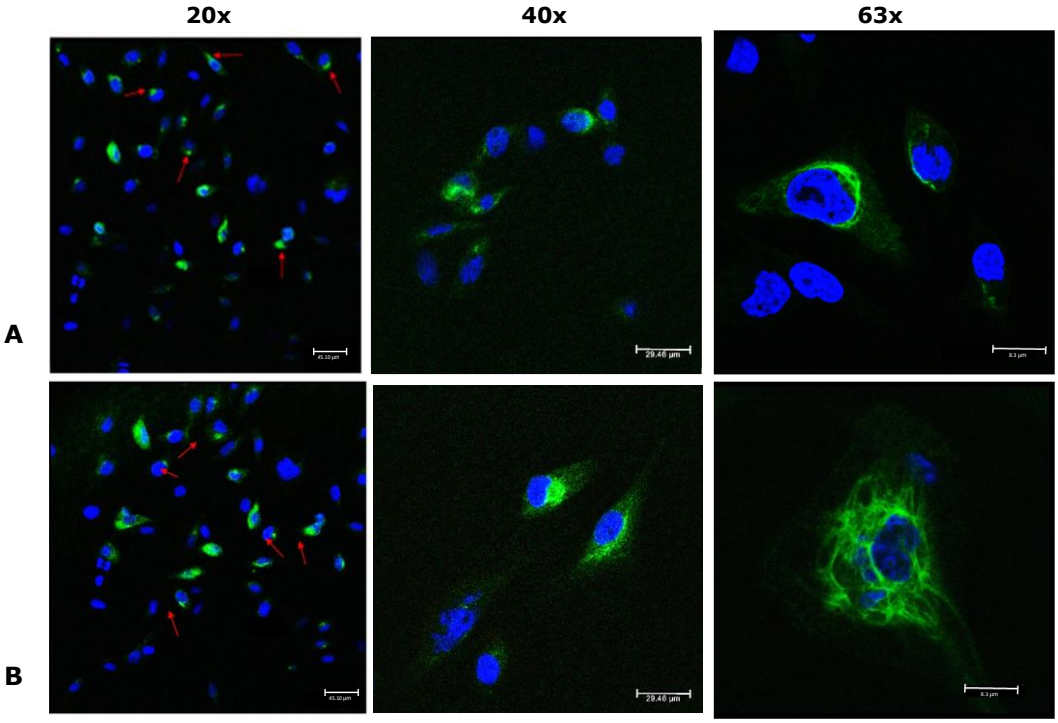

Figure 2. 7 CAST II intracellular localisation. Representative images of calpastatin type II intracellular localisation in (A) T47D and (B) MDA-MB-231 cells under 20x, 40x and 63x magnifications.

Localisation of calpastatin type II in the cells was more distinct when observed at 63x magnification. The calpastatin type II seemed to be present in a 'basket-like' structure around the nucleus. It is unclear why calpastatin type II has such distribution intracellularly. Had time allowed additional steps would have been used to conduct additional IF experiments to understand the interaction between calpastatin type II and other cellular proteins expressed in and around the nucleus. However, due to time constraints this could not be investigated further.

Differential localisation of calpastatin type I, II and III suggests that they may have differential roles intracellularly. To investigate this further, T47D and MDA-MB-231 cells overexpressing calpastatin type I, II and III were sent for RNA sequencing to Novogene UK to understand the interaction pattern and associated genes and pathways with each calpastatin isoform.

2.4.4 RNA sequencing data analysis

2.4.4.1 Calpastatin isoforms differentially expressed genes (DEGs)

After RNA sequencing, a gene was declared to be differential expressed if the change observed in expression index or read counts between calpastatin

type I, II and III overexpressing and mock-transfected T47D and MDA-MB-231 cells was statistically significant. The DEG lists for calpastatin type I, II and III in T47D and MDA-MB-231 cells were obtained from Novogene UK Table 2.4 represents the number of DEGs associated with the overexpression of CAST I, CAST II and CAST III in T47D and MDA-MB-231 cells.

Table 2. 4 Number of DEGs

Calpastatin isoform type	Number of DEGs	Calpastatin isoform type	Number of DEGs
T47D CAST I	9525	MDA-MB-231 CAST I	2433
T47D CAST II	8886	MDA-MB-231 CAST II	3700
T47D CAST III	4684	MDA-MB-231 CAST II	10395

Overexpression of calpastatin type I and II in T47D cells had similar number of DEGs while overexpression of calpastatin type III had a much lower number of DEGs. It was seen that calpastatin type I and II overexpression in MDA-MB-231 cells had a similar number of DEGs while the overexpression of calpastatin type III in MDA-MB-231 cells had a much higher number of DEGs. This data suggests that calpastatin type III may have different roles in different breast cancer cell types. As presented in table 2.4 the number of differentially expressed genes for each calpastatin type in both the cell lines is vast. The complete list of DEGs for each calpastatin isoform can be accessed on the website https://github.com/RichaVasan/CAST-DEGs.git. Tables 2.5 and 2.6 enlist the top 30 significantly differentially expressed genes with calpastatin type I, II and III in T47D and MDA-MB-231 cell lines, arranged in decreasing order of their level of significance of differential expression with the overexpression of calpastatin type I, II or III. Several genes have previously been shown to be associated with breast cancer including clinical outcomes. These genes are discussed in detail in section 2.5.

Table 2. 5 Top 30 DEGs associated with the overexpression of CAST I, CAST II and CAST III in T47D cells

T47D					
CAST I	**p-value**	**CAST II**	**p-value**	**CAST III**	**p-value**
PTGS2	5.62E-302	FAM133A	1.08E-302	MAGEA10	7.12E-232
PLAUR	9.38E-302	EPHA3	8.15E-285	SH3BGRL	3.06E-176
S100A8	4.71E-283	SH3BGRL	9.67E-281	LINC00958	2.56E-168
CXCL2	5.03E-275	EREG	9.14E-277	CPED1	3.30E-140
MAGEA11	1.50E-270	ALDH1A3	4.84E-275	TAGLN	5.11E-127
AL365181.3	4.93E-265	C3	5.27E-262	MAP7D3	1.34E-110
NGFR	6.71E-261	LAMB4	7.22E-259	CNN1	5.09E-108
MAP7D3	5.52E-256	PEG10	1.27E-251	SLIT2	2.31E-101
OR51B5	5.08E-250	MAGEA11	6.17E-248	EYA2	5.63E-101
SH3BGRL	6.16E-247	EGLN3	1.19E-245	ZBTB18	2.40E-98
PDP1	6.42E-241	FKBP10	8.55E-243	NRP1	1.66E-96
EMP1	2.11E-239	LINC01419	1.22E-231	MAGEA11	8.22E-96
RARRES1	1.23E-229	ADAMTS19	2.65E-227	LINC01419	3.80E-95
SGCE	3.27E-223	ABCA8	2.27E-226	HSPB8	8.45E-94
ALCAM	8.70E-223	CNN1	6.99E-225	GLB1L2	4.86E-91
PLAT	7.33E-217	MAGEC2	3.24E-222	TSPYL5	1.88E-87
TAGLN	3.47E-215	CAST	3.21E-215	C1QTNF6	2.50E-87
SGK1	9.65E-213	GJA5	1.65E-213	BARX2	6.85E-82
CPED1	1.20E-212	HAPLN1	4.52E-208	RNASE7	3.53E-81
ITGA3	1.20E-203	SLC9A7	1.33E-199	CAV1	3.75E-81
LINC01287	3.32E-201	LINC01029	1.18E-194	EPHA3	8.87E-79
TNFSF18	9.80E-201	DLL1	1.27E-193	EHD2	6.47E-76
ELF5	6.17E-200	CAV1	5.84E-192	SYT14	1.59E-74
CYP1B1	8.66E-200	IL17RD	1.12E-188	IFI27	2.86E-73
PEG10	6.20E-195	MAP7D3	1.71E-188	TNC	7.88E-73
IL6	4.60E-186	MAGEA10	9.88E-187	AC108752.1	2.78E-70
EHD2	1.39E-181	RCSD1	3.54E-178	CACNA2D1	1.22E-65
CPQ	2.70E-177	PIP	8.14E-178	CLDN7	5.30E-65
TNC	3.64E-177	PTGER3	1.53E-175	C1RL	8.91E-65
MATN2	1.87E-176	CTSS	5.90E-175	FGFBP1	1.33E-64

Table 2. 6 Top 30 DEGs associated with the overexpression of CAST I, CAST II and CAST III in MDA-MB-231 cells

MDA-MB-231					
CAST I	**p-value**	**CAST II**	**p-value**	**CAST III**	**p-value**
SSX1	4.03E-151	LINC02582	4.87E-84	PGM5	2.03E-85
MAGEC1	2.13E-136	CACNA2D4	4.10E-79	MAGEB2	4.21E-78
MAGEC2	6.47E-122	DCAF12L1	3.41E-75	EFEMP1	1.58E-75
TIE1	7.56E-96	PGM5	1.43E-66	ARHGAP30	5.21E-68
ANXA10	4.84E-85	MAGEC1	1.23E-63	LCP1	1.69E-66
DCAF12L1	3.76E-79	CD33	2.87E-59	HCLS1	8.94E-66
MAGEA3	1.89E-77	TIE1	3.04E-59	CLDN1	2.18E-63
KBTBD8	2.08E-76	TNFSF18	3.43E-57	SCEL	9.58E-63
TSPYL5	1.89E-75	AADAC	1.12E-54	PCSK9	9.00E-61
FAM83A	1.31E-72	AADACP1	2.44E-53	HLA-DPA1	3.59E-58
CACNA2D4	2.29E-72	LINC00839	9.06E-52	CDC42EP5	6.13E-58
ARHGAP30	1.05E-69	TREML2	4.54E-51	PTPRN2	7.41E-58
MAGEA11	2.64E-68	AC093627.4	1.43E-45	IL1B	5.88E-56
LINC02582	3.12E-64	C5orf46	7.00E-45	MUC5AC	8.26E-56
CD33	5.56E-64	DTX3	8.43E-45	COL6A3	1.03E-55
SERPINB2	7.09E-64	PCSK9	2.00E-42	COL5A1	1.14E-55
TREML2	9.55E-61	FST	1.52E-41	ZNF542P	1.27E-54
CACNG7	1.77E-60	MAGEA6	2.77E-41	OBSCN	2.39E-54
TGFBI	8.65E-57	CLCF1	7.40E-41	ARMCX2	2.75E-54
FAM133A	2.98E-56	ARHGAP30	1.36E-40	IL1A	3.12E-54
SAMSN1	4.12E-54	PTPRU	2.14E-39	ATOH8	2.88E-52
NES	9.57E-54	FAM83A	1.38E-38	MAGEC1	2.10E-51
RND1	1.81E-53	EPHB1	1.99E-37	LINC02582	7.43E-51
SPANXD	4.18E-53	NAP1L5	3.64E-37	TENM1	4.33E-46
NRXN1	8.08E-49	GYPC	1.54E-36	TSTD1	3.50E-45
ADARB1	1.34E-48	FKBP9	2.84E-36	NKX2-1	4.23E-44
APCDD1L	1.96E-48	ANXA10	1.01E-35	MCAM	3.55E-43
ADGRE1	1.19E-44	FBXL7	4.37E-35	HLA-DRA	8.54E-42
EPHB1	1.94E-44	AC245041.2	2.04E-34	SEMA6B	9.40E-42
ADGRG1	1.08E-43	PPP4R3C	2.12E-34	C20orf197	1.73E-41

2.4.4.2 Overlapping and unique DEGs

Assessments were done to investigate the overlap and uniqueness of DEGs associated with the overexpression of calpastatin type I, II and III in T47D and MDA-MB-231 cell lines. To assess the overlap of differential gene expression between calpastatin type I, II and III in both the cell lines, Venn diagrams were constructed (Figure 2.8) using the DeepVenn tool accessed at https://www.deepvenn.com/.

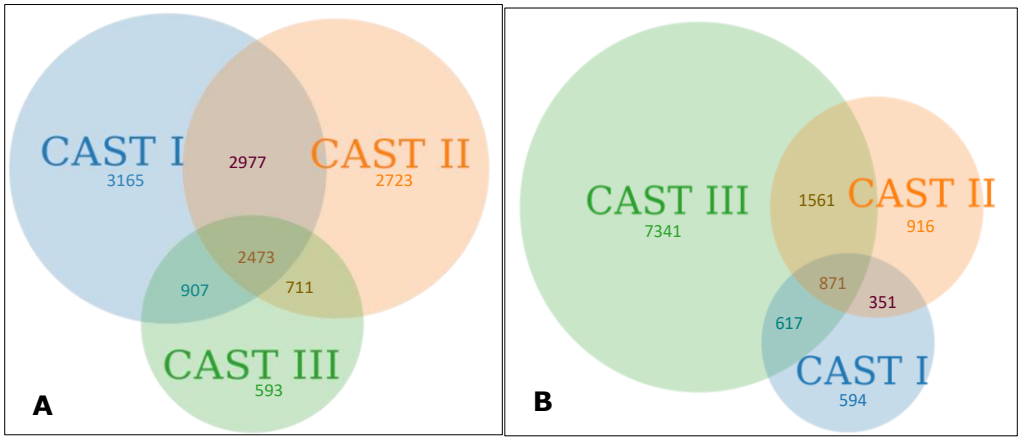

Figure 2. 8 Overlapping and unique DEGs between CAST I, CAST II and CAST III in (A) T47D and (B) MDA-MB-231 cells.

In T47D cells the number of DEGs overlapping between the expressions of calpastatin types I/III and calpastatin types II/III were comparable (907 and 711, respectively), while the number of DEGs overlapping with the expression of calpastatin types I/II was much higher (2977). The number of DEGs unique to the expression of calpastatin type I and calpastatin type II were comparable (3165 and 2723, respectively), while the number of DEGs unique to the expression of calpastatin type III was much lower (593) suggesting that calpastatin type III may have fewer associations compared to calpastatin type I and II in luminal breast cancer cells.

In MDA-MB-231 cells, the number of DEGs overlapping between the expression of calpastatin types I/II and calpastatin types I/III were somewhat comparable (351 and 617, respectively), while the number of DEGs overlapping with the expression of calpastatin types II/III was much higher (1561). The number of uniquely expressed DEGs associated with the expression of calpastatin type I and calpastatin type II were comparable (594 and 916, respectively), while the number of uniquely expressed DEGs associated with the expression of calpastatin type III was much higher (7341). Such data suggests that calpastatin type III may have a higher number of associations compared to calpastatin type I and II in triple negative breast cancer cells.

Assessments were conducted to investigate the overlap and uniqueness of DEGs associated with the overexpression of calpastatin type I, II and III between T47D and MDA-MB-231 cells (Figure 2.9).

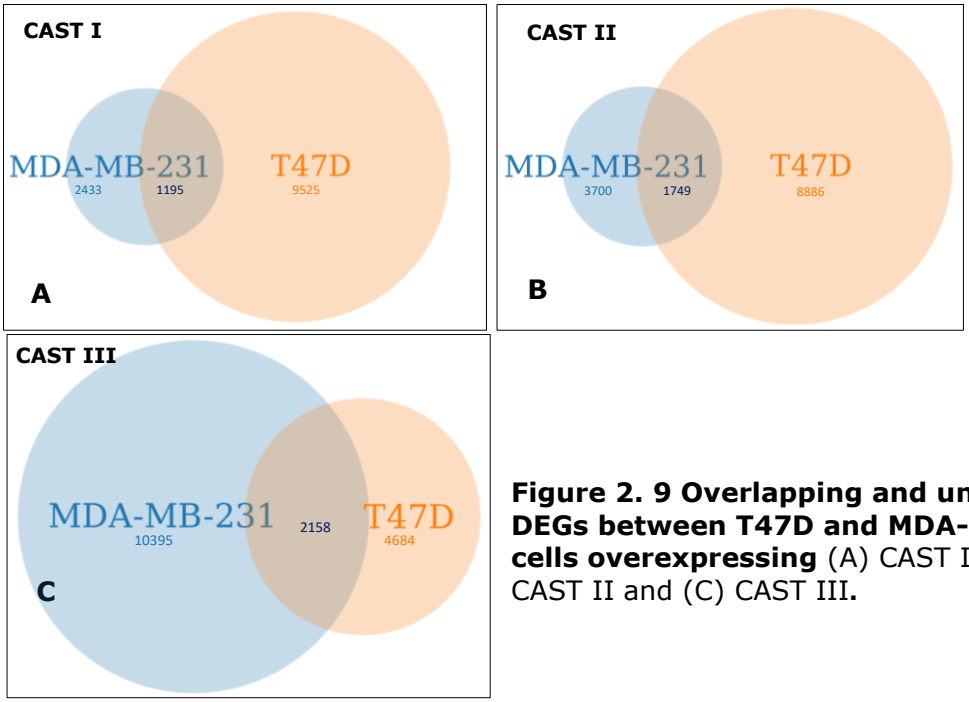

Figure 2. 9 Overlapping and unique DEGs between T47D and MDA-MB-231 cells overexpressing (A) CAST I, (B) CAST II and (C) CAST III**.**

The overlap in the expressions of calpastatin types I, II and III were comparable (1195, 1749 and 2158 genes, respectively) between T47D and MDA-MB-231 cell lines. The number of unique DEGs associated with the expression of calpastatin types I and II were comparable (9525 and 8886, respectively), while the number of unique DEGs with the expression of calpastatin type III was much lower (4684), in the luminal breast cancer, T47D cell line.

The DEGs unique to the expression of calpastatin types I and II were comparable (2433 and 3700, respectively), while the DEGs unique to the expression of calpastatin type III was much higher (10395), in the triple negative breast cancer, MDA-MB-231 cell line.

2.4.4.3 Pathway enrichment and significantly affected pathways

Pathway enrichment analyses were done on the DEGs associated with the overexpression of calpastatin type I, II and III in T47D and MDA-MB-231 cells using the IPA package. The number of significant pathways enriched by the DEGs associated with each calpastatin type are shown in table 2.7.

Table 2. 7 Number of pathways enriched by DEGs associated with CAST I, CAST II and CAST III expression in T47D and MDA-MB-231 cells

		Calpastatin type I	Calpastatin type II	Calpastatin type III
T47D cells	All significantly enriched pathways	652 ↓	664 ↓	648 ↓
	Pathways with BH correction applied	425	426	425
MDA-MB-231 cells	All significantly enriched pathways	567 ↓	610 ↓	620 ↓
	Pathways with BH correction applied	417	418	425

The number of pathways enriched by all the DEG lists were > 400. Using the z-score tool, these pathways were predicted for their activation or inhibition. The tables in section A1.5 (Appendix A) show the top 10 inhibited or activated pathways enriched by the DEGs associated with the overexpression of calpastatin type I, II and III in T47D and MDA-MB-231 cells.

The pathways that were significantly enriched and altered (inhibited or activated) by the DEGs associated with the expression of calpastatin type I, II and III in both the cell lines were taken forward for further analysis to find their associations with calpastatin. Associations were mapped on each pathway enriched and altered significantly by the DEGs associated with calpastatin type I, type II and type III. The associations made were either direct (target gene) or indirect (node gene) using the genes in the DEG list.

Alterations in DEGs resulted from overexpression of calpastatin type I, type II and type III in T47D and MDA-MB-231 cells were mapped against known calpastatin interactions or associations. These mapped interactions/associations can be accessed at https://github.com/RichaVasan/CAST-and-pathway-associations.git.
Tables 2.8-2.13 represent the 'target' and 'node' genes associated directly or indirectly with calpastatin expression in pathways mentioned in section A1.5 (Appendix A). These genes were either significantly upregulated (red arrow) or downregulated (green arrow) in the pathways significantly

affected by the expression of calpastatin types I, II and III in T47D and MDA-MB-231 cells.

Table 2. 8 Genes significantly affected by the expression of CAST I in T47D cells

CDKNB ↓	TP53 ↑	GRB2 ↑	IL17A ↑	TIRAP ↑	STAT3 ↑
CDH2 ↑	NFLBIA ↑	CDK5R2 ↑	STAT6 ↓	SMAD ↑	CXCL8 ↑
DPYSL3 ↑	PIK3R1 ↓	SRC ↑	CD5R1 ↑	SERPTNE ↑	FOS ↑
CDK5R1 ↓	CEBPA ↓	CASP3 ↓	CDKN1B ↑	SMAD4 ↑	RGF2 ↓
PRKCA ↑	VIRMA ↑	AKT ↑	NAPPA ↑	TGFBR1 ↑	MYC ↑
PRNP ↑	PLEKHA4 ↑	CAPN8 ↓	ADRB2 ↑	CEBPB ↑	JUN ↑
CDH4 ↑	CASP1 ↑	PLEKHA ↓	CNR1 ↑	TIMP1 ↑	ITGB3 ↑
CDH1 ↑	ACTA1 ↑	NFKBIA ↑	SOD2 ↑	CCL3 ↑	
TLN1 ↑	FYN ↑	ACTA2 ↑	PTK2 ↑	FOXO ↑	
CRK ↑	MMP9 ↑	BCL2 ↓	COLIA ↑	NLF1 ↓	
CAPN1 ↑	AMPK ↑	GSK3B ↑	TGFB1 ↑	PPARG ↑	

Table 2. 9 Genes significantly affected by the expression of CAST II in T47D cells

PIK3R1 ↓	DPYSL3 ↓	CDK5R1 ↑	PRK3R1 ↓	PIK3R1 ↓	CADH1 ↑
FOS ↓	SLC2A4 ↓	CAPN1 ↓	CDK5 ↑	ABL1 ↑	AKT ↓
PRNP ↑	CASP8 ↓	CAPN2 ↑	GSK3B ↑	CASP7 ↑	PCLG1 ↓
FYN ↑	SRC ↓	PRKD ↑	GRB2 ↓	ACTA ↑	CARK ↑
BDNF ↓	CDKN1B ↑	PCLB2 ↑	MAPT ↑	SLC2A4 ↓	MMP9 ↓
TP53 ↑	CASP7 ↑	ACTBL2 ↑	MTOR ↑	FNTB ↑	
CDH1 ↓	CDKR2 ↑	CASP3 ↓	CDC42 ↓	CDK1B ↑	
CRK ↑	BID ↑	CTNNB1 ↑	MAPK14 ↓	PCLAF ↓	
CEBPA ↓	ACTA1 ↑	RAPGEF1 ↓	VIRMA ↓	PIH1D1 ↑	

Table 2. 10 Genes significantly affected by the expression of CAST III in T47D cells

TP53 ↑	PRNP ↑	PIK3R1 ↑	ACTBL2 ↑	FNTB ↑	CRK ↑
CDK1B ↓	CAPN2 ↑	ACTA2 ↓	PLEKHA4 ↑	MAPT ↑	CASP8 ↑
RBL1 ↓	NCL ↓	PLCG1 ↓	IL17A ↑	CRK ↑	MMP9 ↑
CDH2 ↓	STAT6 ↑	BID ↓	CDKN1B ↑	NCSI ↑	LIX1L ↑
CEBPA ↓	GSK3B ↑	CASP1 ↑	CDK5R1 ↑	CASP3 ↑	GRB2 ↓

Table 2. 11 Genes significantly affected by the expression of CAST I in MDA-MB-231 cells

GSK3B ↑	CDH2 ↓	CAV1 ↑	MAPT ↓	PCLAF ↑	PLEKHA4 ↑
PLCG1 ↑	SRC ↑	VCL ↑	CASP3 ↑	CHEK2 ↑	MMP9 ↓
A-ACTIN ↑	EZR ↓	CTTN ↑	AR ↑	MTUS2 ↓	CDC42 ↑

Table 2. 12 Genes significantly affected by the expression of CAST II in MDA-MB-231 cells

CASP3 ↑	SRC ↑	MAPT ↑	GRB2 ↑	BID ↑	CASP7 ↑
IL1A ↑	CDH2 ↓	GSK3B ↓	CDK5 ↑	CEBPA ↑	HSPA5 ↑

Table 2. 13 Genes significantly affected by the expression of CAST III in MDA-MB-231 cells

PIH1D1 ↓	NFKB1A ↓	AKT ↓	PCLAF ↓	VIM ↑	CAMK4 ↓
PLEKHA4 ↑	MEF2D ↓	SHC1 ↓	CAPN8 ↓	EGFR ↓	CFTR ↑
CDK5 ↑	IL17A ↑	SRC ↓	MTUS2 ↓	MMP1 ↑	CDH1 ↓
HMGN2 ↑	TP53 ↑	MEF2A ↓	CDK5R2 ↓	MAP2K1 ↓	GSK3B ↓
CASP1 ↓	RAS ↓	RAF1 ↓	ACTBL2 ↓	CASP3 ↓	ATF4 ↑
ACTA1 ↑	CAPN1 ↑	CDH2 ↓	CASP8 ↓	ELAV1 ↓	DPYSL3 ↓
IL1A ↓	FYN ↑	MAPT ↓	TLR3 ↓	DYNC1LI2 ↓	PRCKA ↓
MMP9 ↑	PLC ↓	STAT6 ↓	AR ↓	POLA2 ↓	NFKB ↓
CDKN1B ↓	CAPN2 ↓	ACTA2 ↓	FOS ↓	ILA ↓	ENDOG ↓

Due to time constraints, further analysis was halted however a suggestion for future analysis would include performing correlations and survival analysis with the above genes using the METABRIC breast cancer dataset.

2.5 Discussion

Calpastatin is the endogenous inhibitor of calpains. Our group have previously shown its involvement in breast cancer progression through LI. Previous studies have shown that expression of calpastatin is negatively associated with breast cancer progression, lymph node status and presence of LI (Storr *et al.*, 2011b). High expression of calpastatin is associated significantly with low risk clinicopathological features including breast cancer recurrence, older age of patients (≥ 40 years), small tumours (<2 cm), low NPI, low grade, ER and PR positive and non-basal phenotype (Storr *et al.*, 2012a). While, low expression of calpastatin was significantly associated with tumour size, NPI, negative ER and PR status, and basal phenotype (Storr *et al.*, 2011b).

T47D and MDA-MB-231 cells were used in this study to generate breast cancer cell lines stably transfected with calpastatin isoforms. These cell lines were selected as they represent two subtypes of breast cancer, with T47D being a luminal cell line and MDA-MB-231 cell line representing TNBC. An array of cell lines were previously assessed for expression of calpain system proteins by Dr. Sukkarn.

Low levels of calpastatin protein and mRNA expression were observed in T47D and MDA-MB-231 cells. The T47D cell line had medium-to-high

expression of all calpains (Sukkarn, 2020), and had promising characteristics with shortest doubling time amongst other luminal cell lines and a PE of ~20%. The T47D cell line was therefore selected as the luminal cell line for transfection of calpastatin isoforms. The basal-like cell lines all had comparable levels of calpain-1, 2 and 4 expression, however MDA-MB-231 cells had a PE of 69.07±6.74% and the shortest doubling time (~19 hours). Therefore, it was chosen as the basal-like cell type for calpastatin isoform transfection (Sukkarn, 2020).

DNA constructs containing cDNA encoding HA-tagged full-length calpastatin isoforms I, II and III or empty vector were transfected in T47D and MDA-MB-231 WT cells. A monoclonal population of T47D cells expressing HA-tagged calpastatin type I and type III and MDA-MB-231 cells expressing calpastatin type I and type II, and a multiclonal population of T47D cells expressing calpastatin type II were generated by Dr. Sukkarn previously. A monoclonal population of T47D cells expressing calpastatin type II was generated in the current study by, following transfection, single cell cloning under selection antibiotic was performed in 96-well plates. Wells having single colonies were transferred to 48-well plates. The surviving clones were transferred into 24-well through to 6-well plates (Table A1.2). The surviving clones were then transferred to T-25cm^2 flasks and were allowed to grow and expand in selection media. Cell lysates were prepared for 8 surviving clones and were checked for HA-tagged calpastatin type II expression by Western blot (Figure A1.2). Clone 3 was seen to have maximum expression of HA-tagged calpastatin type II and was selected as a valid model for calpastatin type II expression in T47D cells. To overexpress calpastatin type III, DNA constructs for CAST III were transfected in MDA-MB-231 cells using the transfection reagent Lipofectamine 3000. This involved the formation of cationic lipid and the DNA which enters the cell through endocytosis, diffuse through cytoplasm and enter the nucleus for gene expression (Cardarelli *et al.*, 2016)

Different DNA: transfection reagent ratios were used (1:1.5-3) to optimise the maximum transfection efficiency. After which, the cells were allowed to grow in the presence of selection media containing 750 µg/mL Geneticin. A lot of cell death was observed after the addition of the selection media. The media was changed continuously allowing the living cells to grow and expand. Surviving cells from each dilution were seeded in 96-well plates for the generation of a monoclonal population by performing single cell cloning. Wells with single colonies were taken forward and allowed to grow and expand (Table A1.3). Cell lysates were prepared from the surviving clones and HA-tagged calpastatin type III expression was detected by Western blot (Figure A1.3). The lysates prepared form clones transfected with DNA: transfection reagent 1:1.5 did not seem to have any HA-tagged calpastatin type III expression. This was an unexpected observation as the colonies grew and survived in the presence of the selection antibiotic (A1.3A). Cell lysates prepared from clones transfected with the 1:3 ratio expressed HA-tagged calpastatin type III which was observed by the presence of multiple bands (A1.3B). Clone 1 was seen to have the maximum expression of HA-tagged calpastatin type III and was selected as a valid model for calpastatin type III expression in MDA-MB-231 cell line.

The luminal cells T47D and the TNBC cells MDA-MB-231 were assessed for the expression of calpastatin isoforms I, II and III. Cell lysates were prepared and Western blot analysis performed to detect the HA-tagged calpastatin isoform protein expression. HA-tagged calpastatin types I and II were detected as a single band and duplet band, respectively in both the cell lines, while HA-tagged calpastatin type III was detected as multiple bands that were more prominent in MDA-MB-231 cells. There are few explanations for multiple bands reported however, they are frequently observed. It is thought that the presence of multiple bands might represent proteolytic products or observed as a result of protease degradation at the N-terminal of the transcript (Goll *et al.*, 2003). This however could not be investigated further due to time and funding constraints.

The relative expression of HA-tagged calpastatin type I was higher than the relative expression of HA-tagged calpastatin types II and III in both the cell lines. The relative expression levels of HA-tagged calpastatin type II was

marginally higher in MDA-MB-231 cells than T47D cells. While the expression of HA-tagged calpastatin type III were comparable in both T47D and MDA-MB-231 cell lines. Interestingly, the relative expression of HA-tagged calpastatin type I was higher in T47D cells compared to MDA-MB-231 cells, suggesting low expression of calpastatin in TNBC subtype of breast cancer cells.

The overexpression of calpastatin isoforms in T47D and MDA-MB-231 cells was also determined by RT-qPCR. The overexpression of calpastatin type I was determined by Dr. Sukkarn and described in the section 3.4.2 of her thesis (Sukkarn, 2020).Calpastatin type I expression was significantly higher in CAST I transfected cells compared to the mock-transfected control and WT cells in T47D and MDA-MB-231 cell lines. The fold change calculated was 6.22 fold (P<0.0001) and 2.60 fold (P<0.01) in T47D and MDA-MB-231 cells, respectively, compared to their mock-transfected control cells. Expression of calpastatin type I was ~2 fold (P=0.015) higher in WT cells compared to the mock transfected controls in T47D cells suggesting that the plasmid transfection procedure or the presence of Geneticin had an effect on calpastatin type I expression in T47D cells.

Calpastatin type II expression was significantly higher in CAST II transfected cells compared to the mock-transfected control and WT cells in T47D and MDA-MB-231 cell lines. The fold change calculated was 3.1 fold (P<0.05) and 5.8 fold (P=0.01) in T47D and MDA-MB-231 cells, respectively, compared to their mock-transfected control cells.

In summary, calpastatin types I and II were overexpressed in T47D and MDA-MB231 cells compared to their respective mock-transfected controls and WT cells. It was seen that the calpastatin type I mRNA expression was higher in T47D cells compared to MDA-MB-231 cells. This observation is in line with the HA-tagged calpastatin type I protein expression data, suggesting that calpastatin type I has higher levels of expression in luminal subtypes than the basal-like subtype. While the calpastatin type II mRNA expression was marginally higher in MDA-MB-231 cells than in T47D cells. This is in line with the HA-tagged calpastatin type II protein expression data.

In general, calpastatin type I mRNA expression was higher in both the cell lines compared to calpastatin type II mRNA expression. This is also in line with the protein expression data where the expression of HA-tagged calpastatin type I protein expression in both the cell lines was higher than HA-tagged calpastatin type II protein expression.

In summary, calpastatin types I, II and III were successfully overexpressed in two different breast cancer subtype cell lines and are therefore valid models to assess changes in their phenotypic behaviour. Overexpression of calpastatin type III could not be determined using RT-qPCR as specific primers could not be designed due to exon 1u not present on the constructs. However, translation experiments confirmed the production of calpastatin type III protein from the CAST III constructs. This was possible as translation for the protein begins at exon 2 on the sequence.

Subcellular distribution of calpastatin types I, II and III were assessed in both the cell lines. Calpastatin types I and III were localised throughout the cytoplasm in both the cell lines. This data is consistent with the finding that calpastatin was distributed principally in the cytoplasm in breast cancer tissues detected by immunohistochemical staining (Storr *et al.*, 2012a; Storr *et al.*, 2011b; Storr *et al.*, 2015). Gil-Parrado et al, showed that calpastatin has generally a homogenous distribution in the cytoplasm with some around the nuclear region in the large cell lung cancer 103H cell line (Gil-Parrado *et al.*, 2003). Calpastatin type II had a unique punctate and predominantly perinuclear localisation.

A previous study observed that calpastatin was distributed as an aggregate that was confined in two granule-like structures without the presence of membranes, that was nearly absent in the nucleus and the cytosol, in human neuroblastoma LAN-5 cells (De Tullio *et al.*, 1999). Similar localisation was also observed in murine erythroleukemia MEL and pheochromocytoma PC12 cells, and human aortic smooth muscle AoSMC cells (De Tullio *et al.*, 1999). Interestingly, it was seen that these calpastatin aggregates were affected by the increase in intracellular Ca2+ levels leading to a gradual diffusion of calpastatin in the cytosol (De Tullio *et al.*, 1999).

In another study, it was established that during the resting stage of cells, when calcium dependent proteolysis is not required, calpastatin is associated in large aggregates, and is almost completely unavailable for calpain inhibition. When there is an increase in intracellular calcium levels, calpastatin becomes available in cytosol (Averna *et al.*, 2003). The perinuclear localisation of calpastatin type II observed in T47D and MDA-MB-231 cells observed in this study could be a consequence of aggregation of calpastatin before or after stimulation by calcium (Averna *et al.*, 2003). This could also potentially indicate that calpastatin types I and III are the isoforms that get diffused into cytoplasm after calcium stimulation. Time permitting, it would have been interesting to examine how distribution patterns of calpastatin type II might change during calpain activation and inhibition. This could be assessed by treating T47D and MDA-MB-231 cells overexpressing calpastatin type II with calcium ionophore A23187 or a calpain inhibitor. It would also be interesting to observe what effect external factors like hypoxia may have on the distribution of calpastatin type II.

To understand the differential expression and localisation of calpastatin types I, II and III in T47D and MDA-MB-231 cells, sequencing of these transcripts was done. T47D and MDA-MB-231 cells overexpressing calpastatin types I, II and III and were sent for RNA-sequencing to Novogene, UK. Cell lines overexpressing calpastatin types I, II and III, and their respective mock-transfected control cells were treated with 10 μM of calcium ionophore A23187 (concentration optimised previously, shown in chapter 3) to activate the calpain system, and were sent for RNA sequencing to Novogene, UK. After sequencing, DEG lists were obtained by comparing each isoform group to their respective mock-transfected control group. The significantly DEG were taken forward for further analysis.

The number of DEGs associated with the expression of calpastatin type I and type II in T47D cells were comparable, 9525 and 8886 respectively. While the number of DEGs associated with calpastatin type III expression in T47D cells was considerably less, 4684. In MDA-MB-231 cells, the number of DEGs associated with the expression of calpastatin type I and II were comparable, 2433 and 3700 respectively. While the number of DEGs associated with the expression of calpastatin type III was considerably

higher, 10395. Such data may suggest that calpastatin types have different roles in each cell types. Calpastatin types I and II may have fewer intracellular associations in basal like cell type (MDA-MB-231 cell line) than in luminal cell type (T47D cell line). While the reverse may be true for calpastatin type III.

The number of DEGs associated with the expression of calpastatin types I, II and III too extensive to be completely listed in this thesis however the list can be accessed at https://github.com/RichaVasan/CAST-DEGs.git. The top 30 most significant DEGs associated with calpastatin types I, II and III expression in T47D and MDA-MB-231 cells were listed in Tables 2.5 and 2.6. The most significant DEG associated with the expression of calpastatin type I in T47D cells was PTGS2. High expression of PTGS2 has previously shown to be associated with high rates of grade 3, and ER and PR negative tumours. It has also been predicted to have a response to neoadjuvant Celecoxib in HER2 negative breast cancer patients (D. E. Cremoux *et al.*, 2018). In a study, it was previously reported that in the neuroblastoma cell line SH-SY5Y, overexpression of calpastatin averted the expression of the inflammatory agent PTGS2 induced by methamphetamine toxicity (Chetsawang *et al.*, 2018), suggesting an inverse biological relation. The urokinase plasminogen activator receptor (PLAUR) gene has previously been shown to regulate proliferation and migration in triple negative breast cancer (LeBeau *et al.*, 2013). There have been no reports demonstrating a direct association of the PLAUR gene with calpastatin. The PLAUR gene has however, been linked to enhanced invasion potential in breast cancer cells through its interaction with the integrin (Annis *et al.*, 2018). The calpain system has also been associated with the integrin and growth factor mediated signalling leading to increased migration of the cells (Franco *et al.*, 2005), therefore there may be an association between PLAUR and the calpain system that is yet to be explored. The S100A8 is a calcium-binding protein that are upregulated during inflammatory response. This protein has shown to be associated with loss of oestrogen receptor in breast cancer (Bao *et al.*, 2016). The calpastatin type II expression in T47D cells associated DEG, Family with sequence similarity 133 Member A (FAM133A) and has been shown to have a mutated status in breast cancers, there have

been no direct associations reported with breast cancer yet. Upregulation of Ephrin type A Receptor 3 (EPHA3) mediated by high expression of Sam68 plays a role in breast cancer metastasis (Chen *et al.*, 2020). The SH3 domain binding Glutamate Rich Protein like 3 (SH3BGRL) has shown to drive autophagy mediated chemoresistance in breast cancer. It has also shown to be related with breast cancer relapse and poor prognosis (S. Zhang *et al.*, 2021).There have been no direct associations reported between SH3GRL and calpastatin till date. However, SH3BGRL has been shown to bind to HER2 and stabilizes its activation which led to reduced cell sensitivity to HER2 targeted drugs (H. Li *et al.*, 2020a). HER2 has also shown to upregulate calpastatin by regulating Brk/PTK6 stability in breast cancer cells (Ai *et al.*, 2013). Therefore, there may be an association between SH3BGRL and regulation of calpastatin mediated by HER2 that may exist. Melanoma associated antigen 10 (MAGEA10), the most significant DEG associated with expression of calpastatin type III in T47D cells has been shown to have high expression in TNBC. Expression of MAGEA10 was significantly associated with ER negative and HER2 negative tumours (Badovinac Črnjević *et al.*, 2012). SH3BGRL was significantly differentially expressed with calpastatin type I and type III in T47D cells. As mentioned previously, it has shown to be involved in chemoresistance in breast cancer (S. Zhang *et al.*, 2021) and may have an association with calpastatin expression. Long intergenic Non-protein coding RNA 958 (LINC00958) has been shown to be overexpressed in breast cancer cells and it was shown that upregulation of LINC00958 contributed to tumour progression in breast cancer cells (Rong *et al.*, 2021).

The synovial sarcoma X breakpoint 1 (SSX1) gene, the most significantly differentially expressed with the expression of calpastatin type I in MDA-MB-231 cells, has shown to be expressed in breast carcinoma (Mashino *et al.*, 2001), and has been predicted to have a synergistic effect in basal like breast tumour (Laisné *et al.*, 2021). Other DEGs with the expression of calpastatin type I included, Melanoma associated antigen C1 and C2 (MAGEC1 and MAGEC2) that have demonstrated to be associated with high tumour grade and reduce relapse-free survival in breast cancer patient specimens (Hou *et al.*, 2016). Long Intergenic Non-Protein Coding RNA

2582 (LINC02582), the most significant DEG with the expression of calpastatin type II in MDA-MB-231 cells, expression has demonstrated to be associated with radioresistance in breast cancer cells (B. Wang *et al.*, 2019a). Calcium Voltage-Gated Channel Auxiliary Subunit Alpha 2 Delta 4 (CACNA2D4) has shown to be down-regulated in basal subtype of breast cancer compared to Luminal B subtype (Gao *et al.*, 2021). The most significant DEG associated with the expression of calpastatin type III in MDA-MB-231 cells, Phosphoglucomutase 5 (PGM5) has been shown to promote proliferation and migration in breast cancer cells through aerobic glycolysis. It has shown to be significantly downregulated in breast cancer patients and low expression was predicted to be associated with poor prognosis in breast cancer (Ran *et al.*, 2021).Although no direct associations have been reported yet with calpastatin, the miR-1224-3p/PGM5 axis has shown to regulate the expression of cell cycle, apoptosis and EMT related markers and hence, may have associations with the calpain/calpastatin system that are yet to be reported. The Melanoma-associated antigen B2 (MAGEB2) gene has shown to be upregulated in breast cancer tissue and can potentially serve as effective immunotherapeutic targets (Mogushkova *et al.*, 2017). The EGF Containing Fibulin Extracellular Matrix Protein 1 (EFEMP1) gene cascade with HIF2α has shown to mediate hypoxic effects on breast cancer stem cells (Kwak *et al.*, 2016).

Assessments were conducted to identify the number of overlapping and unique DEGs between calpastatin types I, II and III in T47D and MDA-MB-231 cells. In T47D cells, the number of DEGs overlapping with the expression of calpastatin type I and calpastatin type II was considerably higher than the number of overlapping DEGs with the expression of calpastatin type I and type III, and calpastatin type II and type III (2977 vs 907 and 711, respectively). This indicates that calpastatin type I and type II may have considerably higher number of gene associations and therefore, may function together in a higher number of cellular processes compared to calpastatin type III in luminal subtype of breast cancer. While the number of DEGs unique to expression of calpastatin type III was considerably lower than that of calpastatin type I and calpastatin type II

(593 vs 3165 and 2723, respectively), suggesting that calpastatin type III may have a role in considerably less cellular functions compared to calpastatin type I and type II in luminal breast cancer subtype.

While in MDA-MB-231 cells, it was seen that the number of DEGs overlapping with the expression of calpastatin type II and calpastatin type III was considerably higher than the number of overlapping DEGs with the expression of calpastatin type I and type II, and calpastatin type I and type III (1561 vs 351 and 617, respectively). This indicates that calpastatin types II and III may have much higher number of associations and hence may play a role in a higher number of cellular functions together compared to calpastatin type I in TNBC subtype. While the number of DEGs unique to expression of calpastatin type III was considerably higher than that of calpastatin type I and calpastatin type II (7341 vs 594 and 916, respectively), suggesting that calpastatin type III may play a role in a much higher number of cellular functions compared to calpastatin types I and II in the TNBC subtype.

The number of overlapping and unique DEGs between two breast cancer cell types expressing different calpastatin isoforms were also investigated. It was seen that the number of DEGs overlapping with the expression of calpastatin type I, II and III was comparable between T47D and MDA-MB-231 (1195, 1749 and 2158, respectively). The number of DEGs unique to the expression of calpastatin type I was much lower in MDA-MB-231 cells than the number of unique DEGs to the expression of calpastatin type I in T47D cells (2433 and 9525, respectively), suggesting that calpastatin type I may have much higher associations and may play a role in a much higher number of cellular functions in luminal subtype compared to the TNBC subtype. The number of unique DEGs associated with the expression of calpastatin type II in MDA-MB-231 cells was much lower than the DEGs associated with the expression of calpastatin type II in T47D cells (3700 and 8886, respectively) suggesting that calpastatin type II may have higher associations and may play a role in a higher number of cellular functions in luminal subtype compared to the TNBC subtype. The number of DEGs uniquely associated with the expression of calpastatin type III in MDA-MB-231 cells was much higher than the DEGs uniquely associated with the

expression of calpastatin type III in T47D cells (10395 and 4684, respectively) suggesting that calpastatin type III may have higher associations and may have a role in a higher number of cellular functions in TNBC subtype compared to the luminal subtype.

The DEG lists associated with the expression of calpastatin type I, II and III in T47D and MDA-MB-231 cells were uploaded on the IPA package by Qiagen and core analysis was performed to determine pathways enriched by these DEGs. The number of significantly enriched pathways were approximately 600 for each calpastatin type DEG list in T47D and MDA-MB-231 cells. The number of significantly enriched pathways was reduced by applying the Benjamini-Hochberg (B-H) Multiple Testing Correction. The B-H Multiple Testing Correction method is applied to a test to decrease the False Discovery Rate (FDR) by eliminating the number of false positives. After the B-H Multiple Testing Correction was applied, the number of significantly enriched pathways was reduced to ~ 400 for each calpastatin type DEG list in T47D and MDA-MB-231 cells.

Another powerful tool of the IPA package is the z-score. The z-score tool predicts the overall effect on an enriched pathway. An enriched pathway can be predicted to be inhibited or activated. The Rho guanine dissociation inhibitor (RhoGDI) protein signalling was predicted to be the most significantly inhibited pathway enriched by the DEGs associated with the expression of calpastatin type I in T47D cells. Larsen et al, demonstrated that genetic disruption of calpains lead to reduced levels of RhoGDI protein by proteome analysis, indicating there is a regulatory connection between the calpain system and RhoGDI signalling (Larsen *et al.*, 2008). Moreover, Bozza et al, demonstrated that the inhibition of RhoGDI significantly associated with breast cancer progression (Bozza *et al.*, 2015).

The wound healing signalling pathway was predicted to be a significantly activated pathway enriched by the DEGs associated with the expression of calpastatin type I in T47D cells. A study by Yue et al, demonstrated that overexpression of calpastatin increased cell migration in uveal melanoma cells (Yue *et al.*, 2019). Previous data (unpublished) from our group also

demonstrated that calpastatin type I overexpression in T47D cells, increased the cell migration abilities in T47D cells.

Interestingly, several pathways significantly predicted to be activated by calpastatin type I DEGs were associated with other diseases such as the osteoarthritis pathway, pulmonary fibrosis idiopathic signalling pathway, Cardiac hypertrophy signalling and hepatic fibrosis signalling pathway, reinforcing the important role the calpain system plays in health and disease (section 1.2.5).

The DEGs associated with the expression of calpastatin type II in T47D cells significantly enriched and predicted inhibition of neuropathic pain signalling in dorsal horn neurons, GPCR-mediated nutrient sensing in enteroendocrine cells, synaptogenesis signalling pathway, CDK5 signalling, and G beta gamma signalling pathways. Calpastatin has shown to play a crucial role in deregulation of CDK5 in brain tissue (Sato *et al.*, 2011) and low expression of CDK5 expression is associated with poor clinical outcome to breast cancer patients (Saidy *et al.*, 2020). Pathways predicted to be significantly activated by the DEGs associated with calpastatin type II in T47D cells include PD-1, and PD-L1 cancer immunotherapy pathways, Apelin adipocyte signalling pathway, Inhibition of angiogenesis by TSP1, PI3K/AKT signalling and ILK signalling. It has been shown that PD-L1 protein is stabilised by the expression of calpains. An intracellular increase in calcium levels leads to calpain dependent cleavage of Beclin-1 that leads to blocking of autophagic degradation of PD-L1, in cancer cells (Bockel *et al.*, 2021). Targeting the PD-1/PD-L1 system has demonstrated to have a potential response in metastatic breast cancer (Schütz *et al.*, 2017). Pianetti et al, has previously implicated that there is a link between NF-KB activation caused by the calpain system and PI3K/AKT signalling mediated ERBB2 signalling in primary human and rat breast cancer specimens (Pianetti *et al.*, 2001).

The DEGs associated with the expression of calpastatin type III in T47D cells significantly enriched and predicted inhibition of cyclins and the cell cycle regulation pathway. Calpains have been shown to regulate the cell cycle in particular the transition between G1 and S phase (Jánossy *et al.*, 2004; Joy *et al.*, 2006; Mellgren 1997). The cell cycle regulators cyclin D1

and cyclin E are calpain substrates which lead to progression of cell cycle (Choi *et al.*, 1997; Wang *et al.*, 2003) Several pathways are predicted to be activated significantly by the DEGs associated with the expression of calpastatin type III in T47D cells including, hypercytomkenimia/hyperchemokinemia in the pathogenesis of influenza, wound healing signalling pathway, neuroinflammation signalling pathway, interferon signalling and several more. As mentioned previously, there has been evidence suggesting calpastatin overexpression was associated with increased migration (wound healing ability) (Yue *et al.*, 2019) and previous findings from our group.

The above mentioned significantly enriched and affected pathways by the DEGs associated with the expression of calpastatin types I, II and III in T47D and MDA-MB-231 cells were taken forward to determine associations with calpastatin. Using the 'Path explorer' tool from the IPA package, direct interactions and indirect associations were mapped between CAST and the genes in the pathways. Target and node genes were identified and predicted for their up or downregulation. The genes will, in further work, be analysed for their association with survival and clinicopathological parameters using the breast cancer METABRIC database.

There is already some evidence reported showing links between such target or node genes and breast cancer. For instance, PRNP gene has shown to be a driver metastasis in breast cancer (López-Cortés *et al.*, 2020). In a recent study it was reported that FNTB promoter polymorphisms are independent predictors of prognostic biomarkers in early TNBC patients (Bachmann *et al.*, 2022). The PLCG1 gene was seen to be expressed abnormally in breast cancer and seen to have an interplay with HER2/HER3/PI3K signalling in mediating migration in HER2 expressing breast cancer cells (Balz *et al.*, 2012).

The DEGs associated with the expression of calpastatin type I in MDA-MB-231 cells predicted a significant activation of Integrin signalling and cell cycle control of chromosomal replication signalling pathways. Integrin signalling has been shown to be intimately linked to regulation by the calpain system (Storr *et al.*, 2011a). Endoplasmic reticulum (ER) stress

pathway was predicted to be significantly activated by the DEGs associated with calpastatin type II in MDA-MD-231 cells. However, it was reported that overexpression of calpastatin has protective affects following myocardial infarction by suppressing ER stress pathway in mouse models (Li *et al.*, 2018). The DEGs associated with the expression of calpastatin type III in MDA-MB-231 cells predicted a significant inhibition of CREB signalling in neurons, Pulmonary fibrosis, idiopathic signalling pathway, coronavirus pathogenesis, wound healing signalling, TREM1 signalling, pyroptosis signalling pathways and several more. A study by Soong et al, demonstrated a relationship between calpains and pyroptosis signalling mediated by inflammosome activation in keratinocytes (Soong *et al.*, 2012).

It is interesting to note that overexpression of calpastatin types I and III predicted the wound healing pathway to be significantly activated in T47D cells. While in MDA-MB-231 cells, this pathway was predicted to be inhibited by the overexpression of calpastatin types I and III. This suggests that the migration ability in breast cancer cells might be regulated by calpastatin isoforms I and III, and that migration ability of cells in luminal and TNBC subtypes of breast cancer may be regulated by calpastatin types I and III differently.

Some of the genes affected from the above pathways include CDT1, PIH1D1 and MTUS2. High expression of CDT1 was significantly associated with poorer survival in the breast cancer cohort (n=1441) (Mahadevappa *et al.*, 2017). Evidence has been reported that the PIH1D1 gene is overexpressed in multiple breast cancer cell lines and that it may have an important role in the regulation of mTORC1 in breast cancer (Kamano *et al.*, 2013). The MTUS2 oncogene has shown to have a mutated status in a large breast cancer cohort (n=6697) (Pongor *et al.*, 2015). There have been no reports suggesting potential regulatory pathways between these genes and the calpain system, therefore these findings are novel and need further investigation and confirmation.

Although the above mentioned genes have been shown to play some role in breast cancer regulation, there are several other genes that have predicted to be significantly altered by the expression of calpastatin types

I, II or II in T47D and MDA-MB-231 cells. Therefore these genes will, in future work, be assessed for their associations with breast cancer clinicopathological parameters and survival using the METABRIC breast cancer dataset. Due to time constraints this part of the analysis could not be done.

The initial aim to assess the effects of overexpressing calpastatin types I, II and III in T47D and MDA-MB-231 cell lines on breast cancer cell proliferation and plating efficiency, and chemotherapeutic drug and radiation response was also not completed due to Covid 19 related lockdown and lab closures.

Suggested future work

Future work for this chapter includes-

1. Assessing the effect of calpastatin isoform I, II and III overexpression on breast cancer cell behaviour, and chemotherapeutic drug and radiation response in T47D and MDA-MB-231 cell lines. The response will be assessed via both cell proliferation and clonogenic cell survival.
2. Investigating the identities of the multiple bands for HA-tagged calpastatin type III expression by mass spectroscopy.
3. Assessing the identity of the perinuclear punctate 'basket-like' structures with calpastatin type II by performing differential IF.
4. Examining patterns of isoform expression following exposure to different pathway activators and inhibitors, including physiological ones such as hypoxia.
5. Conducting assessments to establish associations with breast cancer clinicopathological parameters and survival analysis on the shortlisted genes significantly altered by the expression of calpastatin isoforms I, II and III in T47D and MDA-MB-231 cells using the breast cancer dataset, METABRIC.
6. Validation of the target(s) identified from RNAseq studies in breast cancer tissues by multitarget simultaneous immunohistochemical analysis, combined with calpain system expression (using a multiplex IHC system recently acquired in our institute).

Chapter 3- Small molecule novel calpain inhibitors

3.1 Abstract

Background: The second strategy to inhibit calpain activity was by using small molecule novel calpain inhibitors. To demonstrate inhibition of calpains, intracellular calpain activity should be assessed. Several assays exist that demonstrate calpain activity, however most of them use cellular lysates which lead to inaccurate measurements of the calpain activity. Therefore, this chapter aimed to develop a novel assay to assess calpain activity in live cells and to assess the effect of novel calpain inhibitors on breast cancer cell behaviour and treatment response.

Methods: Intracellular calpain activity and the effect of the novel calpain inhibitors, compound 1, compound 9 and compound 10 was assessed using the tBOC assay in live MDA-MB-231 cells. The assay was discontinued to be used due to its unreliable nature. A novel FRET based bioassay was developed using a FRET plasmid. The FRET plasmid was transiently transfected in MDA-MB-231 cells and the FRET activity was measured using flow cytometry. The FRET plasmid transfected cells were treated with different doses of calcium ionophore A23187 and PD150606 to demonstrate calpain activation and inhibition. Inhibition of calpain activity using compounds 1, 9 and 10 was assessed using the FRET bioassay. Proliferation and clonogenic assays were performed to determine the effect of novel compounds on cell proliferation and survival.

Results: Calpeptin demonstrated an inhibition of 42.56±2.07% (P<0.01) in calpain activity using the tBOC assay in MDA-MB-231 cells. Compounds 1, 9 and 10 did not show an inhibition in calpain activity using the tBOC assay in MDA-MB-231 cells. The tBOC assay is known for producing inconsistent and unreliable results. Therefore, its use was discontinued in this project. Calpeptin has shown to inhibit other cysteine proteases and therefore was not used further in this study.

A novel FRET based bioassay was developed and was used in this study. To demonstrate activation of calpains MDA-MB-231 cells were treated with different doses of calcium ionophore and maximum calpain activity was optimised at 10 μM of calcium ionophore treatment for 2 hours. A time course experiment was done to investigate the length of calcium activation after calcium induction. A sudden decrease in CFP expression indicated that

the calpain activation lasts only until calcium treatment. PD150606 was used to inhibit calpain activity using the FRET bio assay. 100 μM of PD150606 treatment for 2 hours showed significant inhibition (P<0.0001) in calpain activity in MDA-MB-231 cells, suggesting the FRET bioassay is a reliable assay to assess intracellular calpain activity. Compounds 1, 9 and 10 were assessed for inhibition of calpain activity in MDA-MB-231 cells with PD150606 treatment used as a positive comparator. Similar levels of calpain activity inhibition was seen with 10 μM, 20 μM and 40 μM of compounds 1, 9 and 10 compared to 100 μM PD150606 treatment.

The effect of novel calpain inhibitors was assessed on MDA-MB-231 cell proliferation and survival. The compounds 1, 9 and 10 did not have an effect on cell proliferation while they were seen to reduce the clonogenic cell survival significantly, suggesting their anti-cancer properties.

Conclusion- The current chapter demonstrates a novel FRET based assay to determine intracellular calpain activity in live breast cancer cells. Successful calpain activation and inhibition was demonstrated using the FRET bioassay. Compounds 1, 9 and 10 had successfully shown inhibition of calpain activity and did not have effect cell proliferation but reduced the clonogenic survival of the breast cancer cells significantly.

3.2 Introduction

3.2.1 Activation of calpains

There are several mechanisms that promote calpain activation. These include autolysis of the DI domain (Imajoh *et al.*, 1986), interaction with phospholipids and increased cellular calcium levels (Cong *et al.*, 1989). Several phospholipids have shown to enhance autolysis of m-calpain at the plasma membrane including phosphatidylinositol (PI), phosphatidylinositol-4-monophosphate (PIP) and phosphatidylinositol-4,5-bisphosphate (PIP_2) (reviewed in (Storr *et al.*, 2011a)). There have also been reports of an activator protein that is specific for μ-calpain (reviewed in (Storr *et al.*, 2011a)). Protein kinase Cι (PKCι) has been shown to phosphorylate both μ- and m-calpain and is associated with increased migration and invasion in lung cancer cells (Xu *et al.*, 2006a). During EGFR signalling ERK has been shown to directly phosphorylate m-calpain on a specific serine residue that affects cell adhesion and motility (Glading *et al.*, 2001). PIP_2 may also act

as a cofactor for m-calpain and phosphorylation by PKA or ERK may alter the cellular distribution of the enzyme to regulate activity (Leloup *et al.*, 2010). Protein anchorage through PIP2 resulting in localisation of m-calpain at the plasma membrane has been shown to be significant for activation of the protease (Leloup *et al.*, 2010; Shao *et al.*, 2006). Calpains interact with an array of proteolytic substrates that determines its cellular localisation and hence may dictate the mechanism of their activation.

Calpains exist in the cytosol in their inactive form and translocate to membranes in response to increased cellular calcium, with activation occurring via calcium and phospholipids. During activation domain DI undergoes autolytic hydrolysis and the large subunit (80kDa) dissociates from the small subunit (28 kDa) (Suzuki *et al.*, 1995). The protease subdomains IIa and IIb are separated by structural constraints during the absence of calcium. However, increased calcium induces structural changes and releases such constrains. The two protease subdomains move closer to each other and fuse to form a functional catalytic site (Hosfield *et al.*, 1999). Several X-ray structural studies have revealed that there are at least three different calcium binding sites on m-calpain. These include, a protease domain II, an acidic loop region in domain III, and two calmodulin-like domains IV and VI (Moldoveanu *et al.*, 2002; Nakagawa *et al.*, 2001; Reverter *et al.*, 2001). The mechanism of m-calpain activity regulation is proposed to be comprised of two stages. The first stage includes release of constraints imposed by circular domain interactions, abolishing the interaction between the N-terminal α-helix of domain I and the second EF hand of domain VI, stimulating conformational changes in domain III and the dissociation of the small from the large subunit. The second stage includes binding of two calcium atoms to the protease domain (one each to subdomains IIa and IIb) and restructuring of the active site cleft (Moldoveanu *et al.*, 2002). The subdomains IIa and IIb move close to each other and fuse to form a functional protease core. (Moldoveanu *et al.*, 2004).

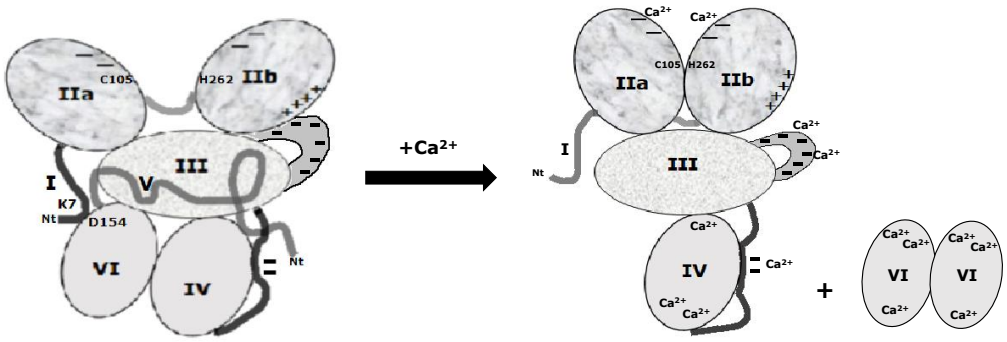

Figure 3. 1 Activation of calpain by calcium. Calcium binding to m-calpain leads to the dissociation of two subunits and brings the domains IIa and IIb together form a functional catalytic site. Reproduced from (Suzuki *et al.*, 2004)**.** Copyright© 2004 by American Diabetes Association with permission conveyed through Copyright Clearance Centre Inc.

Calcium binding of domain III causes translocation of calpains to the membranes, as seen with protein kinase C and phospholipase C (Tompa *et al.*, 2001), and that domain I autolysis promotes dissociation of the small subunit from the large subunit (Nakagawa *et al.*, 2001). In addition, it has been shown that in the calcium-bound calpain structure the relative positions of the domains were changed. The two PEF domains in particular move closer to the core and the N-terminal anchor helix was shown to be displaced in the calcium bound structure of calpain. However, it is not known to what degree release of the anchor helix results in bringing the PEF domains closer to the core and what degree of domain movement results in the displacement of the helix (Hanna *et al.*, 2008).

3.2.2 Calpain inhibitors

Upregulated calpain activity has been implicated in several pathological disorders including neurodegenerative diseases and cancer. Inhibition of calpain activity may reduce the severity of these diseases. Several calpain inhibitors have been designed and developed to target calpains, with variable selectivity and potency. Many commercially available calpain inhibitors have been used in various studies, such as calpeptin, leupeptin, calpain inhibitor I, PD150606, E-64 and MDL28170. The majority of the agents however, do not specifically inhibit calpains as they are targeted against the active sites common to other proteases such as papain and cathepsins. These are also known to have low cell permeability. Most calpain inhibitors are either synthesised chemically or derived from natural compounds (Donkor, 2015).

Calpeptin is the most widely used cell permeable calpain inhibitor. It is a synthetic peptide inhibitor that can penetrate into the cells and bind to the active site of calpain and can reversibly inhibit its activity. Calpeptin was originally developed to inhibit calpain activity in calcium ionophore treated intact platelets where leupeptin did not have an inhibitory effect. It has been shown to be more specific to calpain 1 than leupeptin and has no effect on trypsin (Tsujinaka *et al.*, 1988).

3.2.3 Allosteric inhibition of calpains

The active site cleft is homologous among the cysteine proteases and therefore it can be challenging to increase the specificity of inhibitors for calpains over other proteases. Allosteric inhibition includes binding of the compounds to other sites in the enzyme. The first allosteric inhibitor against calpain 1 was identified from a 150,000 library screening (Wang *et al.*, 1996).

The structure of the first allosteric inhibitor, a-mercaptoacrylic acid based compound, was refined and shown to be an efficient calpain specific inhibitor, PD150606 (3-(4-iodophenyl)-2-mercapto-(Z)-2-propenoic acid). Crystal structure analysis of the calcium bound domain VI of calpain and PD150606 complex demonstrated the binding mechanism of the inhibitor to the penta-EF hand (Lin *et al.*, 1997).

The compound showed an uncompetitive mode of binding and involved chelation of the bound calcium. (Wang *et al.*, 1996). The crystal structure of PD150606 inhibitor bound to the small subunit of calpains revealed binding of the compound to the hydrophobic pocket away from the enzyme's active site (Lin *et al.*, 1997; Todd *et al.*, 2003). The binding of calcium to the small subunit PEF domain leads to the opening of a small hydrophobic pocket near the EF-hand 1 where PD150606 compound was observed to bind (Blanchard *et al.*, 1997; Lin *et al.*, 1997; Todd *et al.*, 2003). The binding of the inhibitor included hydrophobic interactions and no other interactions were observed with the –SH group of the inhibitor. It is thought that by occupying this site, PD150606 sterically interferes with the linking of domain III with calcium bound domain IV and obstructs the release of domain II and subsequent proteolysis (Thompson *et al.*, 1990).

3.2.4 Novel small molecule calpain inhibitors

Novel small molecule calpain inhibitors were used in the current study and were provided by our collaborator Professor R. Allemann, Cardiff University. To identify novel calpain inhibitors the Allemann group used calpain 1 small subunit penta-EF domain in a structure-based virtual screening protocol to determine if the novel compounds would bind to the allosteric pocket. This approach was validated *in silico*, using ligand or protein docking against the penta-EF domain of the small subunit (Kalash *et al.*, 2018).

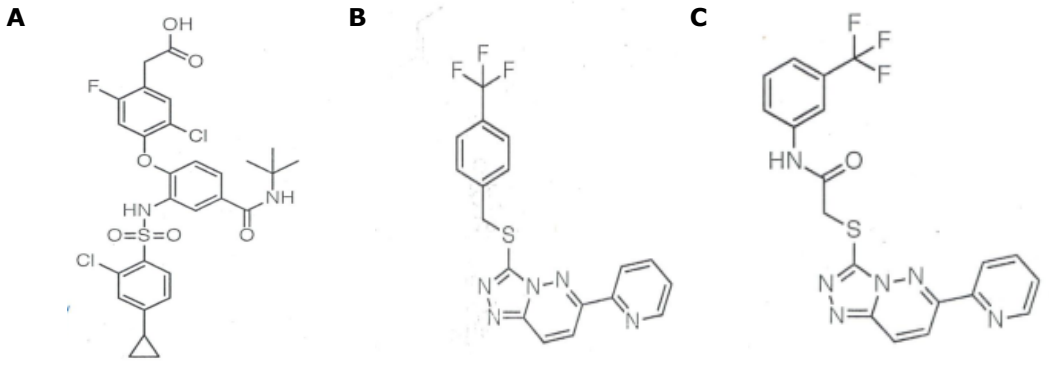

Figure 3. 2 Novel calpain inhibitor structures. (A) Compound 1, (B) Compound 9 and (C) Compound 10. (Obtained through personal communication with Professor Allemann).

To assess the small molecule chemical structure, that would change the geometry of the active site of calpain 1 to inhibit its activity allosterically, compounds with diverse structures were investigated computationally. The penta-EF of the small subunit binding candidates were shortlisted by structure based virtual screening (Kalash *et al.*, 2018). These compounds were also shown to bind to small subunit penta-EF domain experimentally by TNS displacement (Wang *et al.*, 1996). Three compounds, compound 1 ($C_{28}H_{27}Cl_2FN_2O_6S$), compound 9 ($C_{18}H_{12}F_3N_5S$) and compound 10 ($C_{19}H_{13}F_3N_6OS$) were identified (Figure 3.2) and were shown to inhibit full length calpain 1 complex allosterically (small subunit penta-EF and the protease core (CysPc)). These compounds did not bind to the active site domain of calpain 1 in the absence of the small subunit penta-EF domain. The novel compounds thus showed specificity in their mode of action, which is not seen in classical allosteric inhibitors and possess different scaffolds from the classical allosteric inhibitors (Kalash *et al.*, 2018). A summary of binding of different calpain inhibitors is shown in figure 3.3.

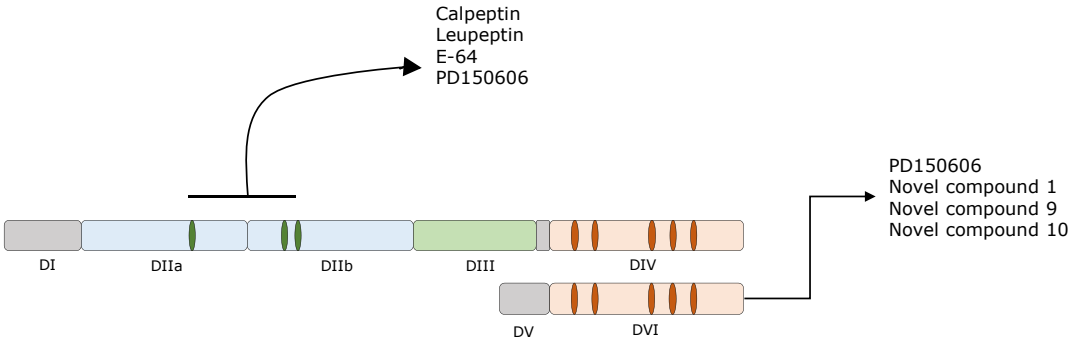

Figure 3. 3 Binding domains of different calpain inhibitors. Commercially available inhibitors of calpains including calpeptin, leupeptin and E-61 bind to the active site of the molecule. PD150606 has shown to bind to the active site as well as allosterically to the calpain molecule. Novel compounds 1, 9 and 10 bind allosterically to the small subunit of the molecule.

3.2.5 Measurement of calpain activity

Intracellular calpain activity can be measured using by a number of assays. The majority detect calpain activity in cell lysates. However, in the process of preparing lysates, the subcellular structure is disrupted which leads to rapid binding of calpastatin with active calpain (Han *et al.*, 1999). Therefore to avoid false measurement of calpain activity, live cell assays were used in this study to measure calpain activity. The t-BOC reagent was used to measure calpain activity in live breast cancer cells. t-BOC-Leu-Met (tert-Butyloxycarbonyl-L-Leucyl-L-Methionine-7-Amino-4-Chloromethylcoumarin or CMAC) is a calpain substrate with an excitation/emission maxima of ~330/403. After cleavage by calpain, the substrate produces blue fluorescence with excitation/emission maxima ~351/430, allowing the measurement of intracellular calpain activity (Rosser *et al.*, 1993).

Variability is a common criticism of the tBOC assay so another, entirely novel, technique to measure calpain activity in breast cancer cells, was used that is reliant on the phenomenon of energy transfer. Föster or fluorescence resonance energy transfer (FRET) was first described by Theodore Föster in 1946. It is a physical phenomenon by which a donor fluorophore when excited non-radiatively, transfers its excitation energy to acceptor fluorophore causing the acceptor to emit its characteristic fluorescence (Forster, 1946). FRET is dependent on the distance between the two molecules, it is highly sensitive when the distance between the donor and acceptor dipoles is within 1-10 nm range. FRET based biosensors composed

of fluorophores and sensing domains have been used widely as spectroscopic rulers to examine a number of biochemical activities that cause changes in molecular proximity such as enzyme activities, conformational changes, intracellular ion concentrations and protein-protein interactions (Lam *et al.*, 2012; Miyawaki, 2011). FRET bio sensing assays are performed optically that enables interrogation of live cells in a non-destructive and minimally invasive way, which is an advantage over biochemical assays (Miyawaki, 2011).

To determine the optimal cleavage site of calpains concerted efforts have been made because calpains do not recognise a discreet consensus sequence. However, calpains have some preferences for residues in the positions that flank the substrate cleavage site, such as an aliphatic residue, leucine in the P2 position (Tompa *et al.*, 2004). Turk et al. and Cuerrier et al. produced an optimal peptide cleavage sequence PLFAER by peptide library based approach (Cuerrier *et al.*, 2005; Turk *et al.*, 2001). They demonstrated that the calpain 1 protease core cleaved PLFAER 18 times more rapidly than the cleavage site EVYGMM, the naturally occurring hexapeptide substrate from α-spectrin and 300 fold faster than SLY-MCA, the unprimed side targeting amino-coumarin-based substrate. Kelly et al. showed that PLFAAR was a better cleavage sequence than PLFAER, by alanine scanning substitutions (Kelly *et al.*, 2009). Several studies have used fluorescent proteins as the FRET pairs to measure protease activity *in vivo* (He *et al.*, 2004; Neefjes *et al.*, 2004; Tyas *et al.*, 2000). McCartney et al. described a set of PLFAAR-based fluorescent protein FRET substrates designed to be calpain specific using Cyan Fluorescent Protein (CFP) and its FRET partner Yellow Fluorescent Protein (YFP) (McCartney *et al.*, 2018) (Figure 3.4) and it is this, via a research collaboration, that is used in the current study. The construct for the CFP-16PLFAAR-YFP on a lentiviral backbone was kindly sent to us by our collaborator Professor P. Davies, Queen's University, Canada.

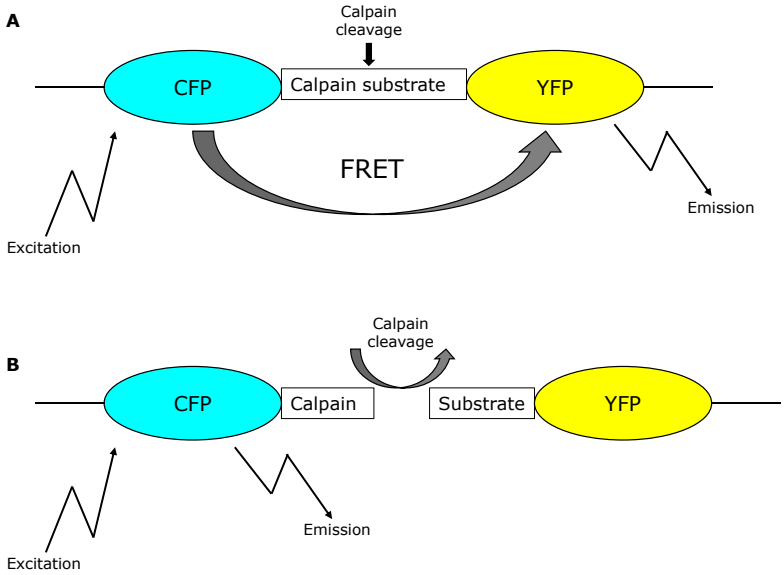

Figure 3. 4 Design of the FRET based biosensor to assess calpain activity in live cells. (A) In the inactive calpain state, the vector in intact, excitation of CFP leads to emission of fluorescence form both CFP and as a consequence of FRET, YFP. (B) Following calpain activation, substrate cleavage occurs, stopping FRET, and emission of CFP only. Reproduced from (Carragher, 2007). Copyright© 2007 by Springer Nature with permission conveyed through Copyright Clearance Centre Inc.

3.2.6 Hypothesis and aims

As mentioned, a number of reasons make accurate measurement of intracellular calpain activity in live cells challenging. In addition, whilst there are several calpain inhibitors available the majority do not selectively inhibit calpains and do not show efficient cell permeability. Therefore in this chapter we hypothesise-

Hypotheses

1. FRET based biosensing is an accurate and reproducible way of determining calpain activity and is suitable to measure efficacy of novel small molecule calpain-1 inhibitors.
2. Small molecule calpain-1 inhibitors will alter cellular behaviour and render breast cancer cells more sensitive to conventional forms of therapy.

Aims

1. To assess calpain activity inhibition by the commercially available inhibitor, calpeptin, using the conventional tBOC assay in MDA-MB-231 cell line.

2. To develop a novel FRET based bio assay to assess calpain activity in live breast cancer cells.
3. To demonstrate activation of calpain activity in MDA-MB-231 cell line using the FRET bio assay.
4. To assess inhibition of calpain activity by the commercially available inhibitor, PD150606 drug, using the novel FRET bio assay in MDA-MB-231 cell line.
5. To demonstrate the inhibition of calpain activity by novel calpain inhibitors using the FRET bio assay in MDA-MB-231 cell line.
6. To assess the affect novel calpain inhibitors on cell behaviour in terms of cell proliferation and clonogenic survival.
7. To determine the specificity of novel calpain inhibitors for calpain 1 using CRISPR/Cas9 calpain 1 knockout MDA-MB-231 cell lines.
8. To determine the effect of calpain activity inhibition by novel calpain inhibitors on chemotherapeutic drug and radiation response in breast cancer cell lines.

3.3 Materials and Methods

3.3.1 Cell lines, growth media and cell culture

The breast cancer cell line MDA-MB-231 was used in the current chapter to assess calpain activity in different treatment conditions. Cell culture media recipe, culture conditions, and storage and recovery were as described in sections 2.3.1, 2.3.2 and 2.3.3.

3.3.2 t-BOC calpain activity assay

To assess calpain activity, via the t-BOC assay, in breast cancer cells, $5x10^5$/ml MDA-MB-231 cells were seeded in T-25cm^2 culture flasks and allowed to grow overnight in a humidified incubator with 5% CO_2 at 37°C. Cells were treated with 100 µM calpeptin (Merck, UK) for 30 minutes. This dose was selected as it has previously demonstrated to significantly reduce calpain activity in MDA-MB-231 cells by 20-30% (Pu, 2016a; Sukkarn, 2020). DMSO was used as a negative control. Following treatment cells were trypsinised, harvested, counted and resuspended at $5x10^5$ cells/ml in 600 µl serum free RPMI 1540 media. The suspension was divided into two aliquots of 250 µl. Pre-warmed t-BOC-Leu-Met (Invitrogen) (2 mM stock)

or DMSO was added (2 µl) to the aliquots. The samples were transferred to duplicate wells (100 µl/well) in a 96-well optical bottom plates. The plates were read using the BMG FLUOstar OPTIMA microplate reader (Germany), preheated to 37°C. The fluorescence produced was measured continuously in a 10 cycle kinetic window with excitation/emission of 350/430, gain 2000 and approximately 4 minute intervals at 37°C.

Background fluorescence, from the medium containing DMSO, was subtracted from the total fluorescence for each sample to obtain the absolute fluorescence intensity of the cleaved t-BOC representing calpain activity. The first cycle baseline measurement was then subtracted from the measurement at each cycle. The percentage calpain activity was calculated using the formula-

$$\text{Percentage calpain activity} = \frac{\text{Fluorescence intensity of treated cells}}{\text{Fluorescence intensity of untreated cells}} \text{x100}$$

Data represent the average ± SD of at least three independent experiments each conducted in triplicate.

3.3.3 Development of the FRET bioassay system

The FRET plasmid containing the calpain specific PLFAAR substrate linked with the Cyan Fluorescence Protein (CFP) and the Yellow Fluorescence Protein (YFP) was received from our collaborator Professor Peter L Davies, Queens University, Canada, spotted onto filter paper. The plasmid was retrieved from the filter paper by immersing the cut out of the plasmid in 30 µl of distilled water. The suspension was pipetted to mix and was stored at -80°C. The vector sequence and map can be found in Appendix B (Section B2.2.1 and Figure B2.2A).

Agar plates were prepared by dissolving LB (Lysogeny broth) media (Sigma Aldrich) (2.5 g/100 ml), and bacteriological agar (Sigma Aldrich) in distilled water. This solution was autoclaved. Once cooled, 100 µg/µl ampicillin (Thermo Fisher) was added into the medium. Approximately 20 ml media was poured in each plate and allowed to solidify. The solidified plates were sealed and stored at 4°C.

Bacterial transformation was performed by the heat shock method. One Shot TOP TEN Competent cells (Thermo Fisher Scientific) were used for bacterial transformation according to the manufacturer's instructions. The transformation reaction (plasmid) was centrifuged and allowed to thaw on ice. One vial of the bacterial competent cells was used per reaction. 1-5 µl of the plasmid was added to one vial of cells. The reaction was kept on ice for 30 minutes. The vial was then placed in the water bath at 42°C for exactly 30 seconds after which it was placed back on ice. To each reaction mixture 250 µl of S.O.C. media was added. This is a nutrient rich media that enhances bacterial growth. The reaction mixtures were placed inside a shaking incubator at 37°C for 1 hour at 225 rpm. After incubation 100 µl of reaction mixture was spread onto agar plates, containing the selection antibiotic as previously described. Untransformed competent cells were used as negative control while the supercoiled pUC19 vector was used as a positive control. Agar plates were then incubated in an inverted position overnight at 37°C.

To generate monoclonal populations, single colonies were picked and inoculated in 3 ml of sterile LB media supplemented with ampicillin and placed in an orbital shaker at 37°C for 12-16 hours and checked for cloudiness. Plasmid was isolated using a Plasmid Mini Kit (Qiagen) according to the manufacturer's protocol. Specific primers were designed and the isolated plasmid was sent for DNA sequencing to the DNA sequencing facility in the School of Life Sciences, University of Nottingham. The sequenced DNA was checked for correct alignment. After confirmation of the correct sequence and alignment, the transformed colonies were picked and the bacterial cell culture scaled up using 500 ml LB media. The plasmid was isolated and endotoxins removed using the Endofree Plasmid Maxi Kit (Qiagen) according to the manufacturer's protocol. The isolated plasmid with the CFP-calpain substrate-YFP had a total yield of 50-60 µg. The plasmid was then stored at -80°C in 10 µl aliquots.

The FRET plasmid was then transfected in the breast cancer cell line, MDA-MB-231 cells line according to the protocol mentioned in section 2.3.6 The transfection efficiency was calculated by using the formula-

$$\frac{\text{Number of fluorescent cells in the dark field}}{\text{Total number of cells}} \times 100$$

The maximum transfection efficiency was optimised to a ratio of 1:3 (DNA: transfection reagent) and 48 hour time point after transfection (Figure B2.2B).

Transfected cells were analysed for calpain activity using flow cytometry. MDA-MB-231 FRET transfected cells were washed and harvested by trysinisation after each treatment. The harvested cells were centrifuged at 1000 rpm for 2 minutes and resuspended in 500 µl of PBS for analysis by a MACSQuant 9 flow cytometer (Miltenyi Biotec). The laser channels used for detection of samples were FITC to detect YFP and Vio-Blue to detect CFP. The voltages were set to Forward Scatter- 244V and Side Scatter- 456V. Data were analysed using FlowJo (BD biosciences) software. Data was gated to exclude dead cells and doublets. To determine the percentage of cells expressing either CFP or YFP, cell population peaks were constructed with cell counts on Y-axis and either CFP or YFP on the X-axis. Gates were created for each channel for untransfected cells showing a single cell population <1% for both CFP and YFP. The same gates were then applied to all the other samples to get a true population percentage expressing CFP and YFP.

3.3.4 Preparation of drugs

Drugs and reagents were reconstituted in Dimethyl sulfoxide (DMSO) (Sigma-Aldrich) to produce stock solutions of 100 mM of calpeptin (Calbiochem, EMD Milipore), 2 mM t-Boc-Leu-Met-CMAC (Invitrogen), 10 mM A23187 calcium ionophore (Sigma-Aldrich), 10 mM PD150606 calpain inhibitor (Sigma-Aldrich) and 50 mM doxorubicin (Sigma-Aldrich). Novel calpain inhibitors were also reconstituted in DMSO to stock solutions of 50 mM of Compound 1, 40 mM of Compound 9 and 40 mM of Compound 10. The stock solutions for all the drugs and reagents were stored at -20°C (except doxorubicin at 4°C). The stock concentrations of the reagents were added to complete culture medium to achieve the desired concentration for use in experiments. For vehicle controls, DMSO was diluted in the cell culture medium at the same ratio of as drug treatment.

3.3.5 Cell proliferation and clonogenic assays

Cell growth and clonogenic assays were conducted to assess the effect of novel compounds on breast cancer cell proliferation and survival. $1x10^5$ MDA-MB-231 cells per well were seeded in triplicate in 6-well plates and left to adhere overnight at 37°C with 5% CO_2 in a humidified incubator. The following day cells were treated with different doses of novel compounds 1, 9 or 10 (at 10, 20, and 40 μM) for 24 hours. DMSO was used as a vehicular control at the same ratio equivalent to that of the drug treatment group. After 24 hours of treatment cells were washed with PBS, trypsinised and counted using a haemocytometer. Treated cells were normalised as a percentage of untreated control cells for each time point. The average percentage of cells (on y-axis) were plotted against the drug concentration (on x-axis) to obtain dose response curves. Treatment with an IC_{50} proliferation dose of doxorubicin was used as a positive control and comparator for these novel compounds. The data in this chapter represent the average percentage of cells ± SD of three independent experiments.

For determination of clonogenic survival, MDA-MB-231 cells treated with 10, 20, or 40 μM of novel compounds 1, 9 and 10 for 24 hours were harvested and counted and serially diluted at the required low seeding densities. Cells were plated in T-25 cm^2 flasks and were incubated at 37°C at 5% CO2 for 14 days to form colonies. Clonogenic flasks were incubated in a separate designated incubator to allow colony formation without any disruption. After 14 days of incubation, the colonies formed were washed with PBS, fixed with 50% methanol for 15 minutes followed by 100% methanol for another 15 minutes. After fixation, colonies were stained with 0.5% crystal violet. After staining with crystal violet, colonies were gently washed with tap water and allowed to dry completely before counting. Colonies having more than 50 cells were counted as surviving colonies. The surviving fraction (SF) of the drug treatment, for each concentration, was calculated using the following equation:

$$S.F. = \frac{\text{Number of colonies counted}}{(\text{Cell seeding density} \times \text{P.E.})}$$

The surviving fraction was plotted (on Y axis) against the drug concentration (on X axis). Treatment with an IC_{50} clonogenic survival dose of doxorubicin was used as a positive control and comparator for these novel compounds. The data in this chapter represent the average surviving fraction ± SD of three independent experiments, having six parallel sets each.

3.3.6 Statistical analysis

All graphs were constructed using GraphPad Prism 9 software. Data are presented as the mean values ± Standard Deviation (SD) of at least two independent experiments, each performed in duplicate or triplicate (or six replicates for clonogenic assay). Student's *t*-test was performed for comparing two variables and a *P*-value< 0.05 was considered to be statistically significant.

3.4 Results

3.4.1 Inhibition of calpain activity using the t-BOC assay

Inhibition of calpain activity by calpeptin in MDA-MB-231 cells was initially demonstrated using the t-BOC assay. MDA-MB-231 cells were treated with 100 µM of calpeptin for 30 minutes and the inhibition in calpain activity was assessed by the addition of the t-BOC reagent (Figure 3.4). The t-BOC is a substrate for calpains and produces fluorescence when cleaved which is a measure of calpain activity.

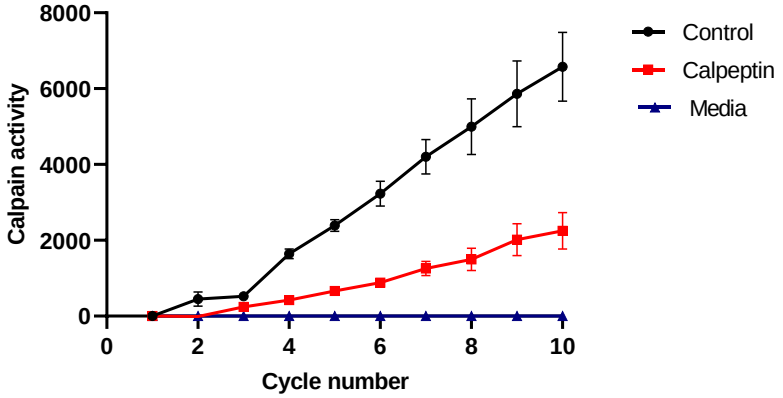

Figure 3. 5 Calpain activity inhibition by calpeptin using t-BOC assay. MDA-MB-231 cell lines were treated with 100 µM of calpeptin and calpain activity was assessed using the t-BOC assay. The inhibition seen was measured at cycle 7. Data represents the average doubling times ± SD of three independent experiments.

The calpain activity inhibition was calculated by normalising the mean fluorescent intensities of calpeptin with the mean fluorescent intensities of control at cycle number 7. The inhibition of calpain activity was determined to be 42.56±2.07% (P<0.01) by calpeptin compared to the control. In a previous study by the group, it was indicated that treatment of MDA-MB-231 cells with 100 µM of calpeptin for 30 minutes, significantly inhibited calpain activity by 34% (Pu, 2016a). Similar results were obtained in another study by Dr. Sukkarn (Sukkarn, 2020), with an inhibition of 21.89 ± 4.49% (P = 0.0011) with 100 µM of calpeptin treatment for 30 minutes. However, the assay was unreliable as the results were not reproducible. Only 3 out of 7 experiments produced reliable results (Figure 3.4) the remaining data is presented in Appendix B (Figure B2.1). Therefore, despite showing significant inhibition in calpain activity, the assay was not reliable to be used routinely for future experiments. In addition, it has been shown that calpeptin is not a specific inhibitor of calpains. Calpeptin is also known to inhibit other cysteine proteases like cathepsins (Siklos *et al.*, 2015).

Novel compounds 1, 9 and 10 were assessed for inhibition of calpain activity using the tBOC assay in MDA-MB-231 cells. The cells were treated with 100 µM of compound 1 (Figure 3.5A), compound 9 (Figure 3.5B), and compound 10 (Figure 3.5C) for 30 minutes and calpain inhibition was assessed using the tBOC reagent. No inhibition in calpain activity was seen by compound 1, compound 9 or compound 10.

This was followed by assessing the fluorescence of these compounds. The fluorescence was measured from MDA-MB-231 cells treated with the novel compounds for 10 cycles for each compound and compared with the fluorescence of cells alone as controls (Figure 3.5D).

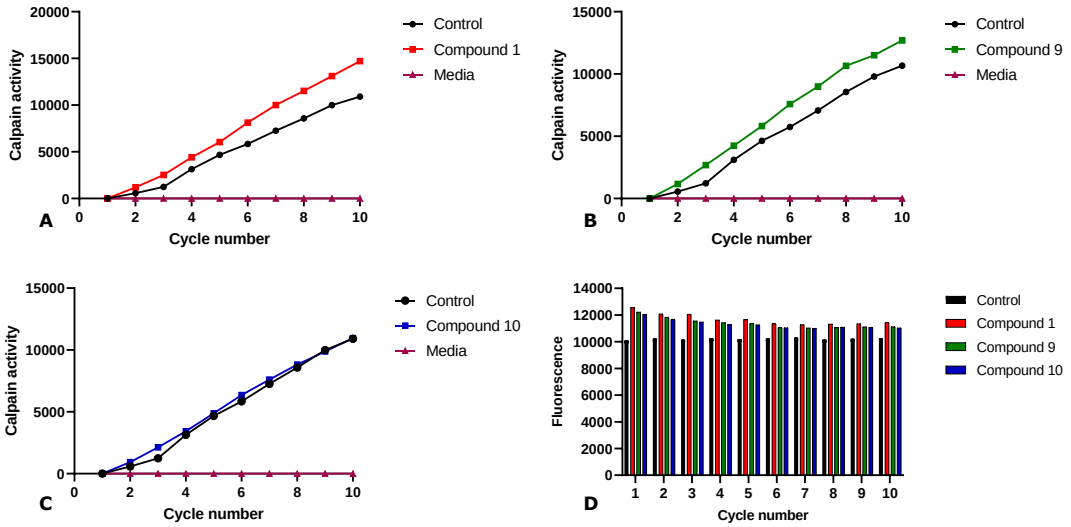

Figure 3. 6 Inhibition of calpain activity by the novel compounds using the tBOC assay and fluorescence. MDA-MB-231 cell lines were treated with 100 µM of the novel compound 1 (A), compound 9 (B) and compound 10 (C) and the calpain activity was assessed using the t-BOC. (D) The novel compounds 1, 9 and 10 were assessed for their fluorescence.

No inhibition in calpain activity was seen by compound 1, compound 9 or compound 10. The compounds were seen to have higher fluorescent intensities compared to the control, as seen in all the cycle numbers (Figure 3.5D). It was therefore predicted that these novel compounds interfered with the fluorescence produced from the interaction of calpains and the t-BOC reagent. Due to the fluorescent nature of these compounds, assessment of inhibition of calpain activity using the tBOC assay produced inaccurate results.

In addition, the t-BOC assay has shown previously to produce inconsistent results (Figure B2.1, Appendix B). Therefore, the use of the t-BOC assay was discontinued to demonstrate the inhibitory activity of the novel compound 1, 9 and 10, and a novel FRET based bio assay was developed.

3.4.2 Development of the FRET bio assay

The novel FRET vector, containing the calpain specific substrate linked by CFP and YFP proteins on both the ends, was used to determine intracellular calpain activity in live cells. The CFP and the novel compounds had different excitation/emission spectra, therefore the fluorescence of the compounds should not interfere with the FRET emission.

After transfection of cells with plasmid they were observed by fluorescent microscopy every 24 hours over a 144 hour timeframe. The transfection efficiency was calculated by counting the number of cells producing fluorescence against the total number of cells in the dark field (Figure 3.6A). The percentage of cells expressing YFP and CFP after transfection was determined by flow cytometry (Figure 3.6B).

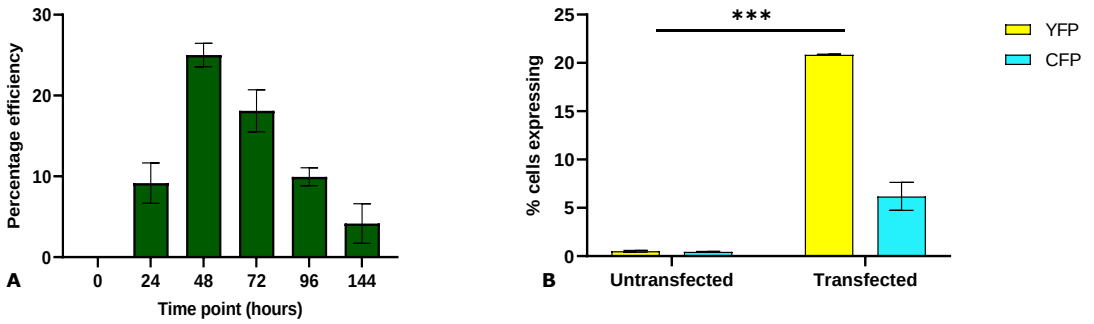

Figure 3. 7 FRET vector transfection efficiency. (A) MDA-MB-231 cell lines transfected with the FRET vector were examined for fluorescence under the microscope. The maximum transfection efficiency was observed at the 48 hour time point. (B) Flow cytometry analysis of untransfected and transfected MDA-MB-231 cells at 48 hour time point showing percentage cells expressing YFP and CFP. Data represents the average expression± SD of three independent experiments. Statistical analysis was carried out using the Student's *t*-test *(P<0.05), ** (P<0.01), *** (P<0.001).

The transfection efficiency was seen to be maximum at 48 hours after transfection, 25±1.46% (Figure 3.6A). This time point was used in all subsequent experiments. The percentage of MDA-MB-231 cells expressing YFP and CFP after transfection was assessed by flow cytometry. The percentage of cells expressing YFP and CFP was increased significantly after transfection 20.85±0.05% (YFP) and 6.185±1.45% (CFP) compared to their expression in untransfected cells (P<0.001) (Figure 3.6B). Due to the absence of a selection marker gene, the FRET vector could not be stably

transfected. Therefore, transient transfections were performed for all subsequent experiments.

3.4.3 Induction of calpain activity using the FRET bio assay

To induce calpain activity in breast cancer cells, FRET transfected MDA-MB-231 cells were treated with 2 µM, 5 µM or 10 µM of calcium ionophore (A23187) for either 30 minutes or 2 hours. Induction of calpain activity was assessed by flow cytometry (Figure 3.7A). To determine the duration of induction of calpain activity FRET transfected MDA-MB-231 cells were treated with calcium ionophore (A23187) for 2 hours after which the cells were washed and analysed for every two hours thereafter (Figure 3.7B). Calpain activity was presented as normalised expression against the control DMSO treated cells.

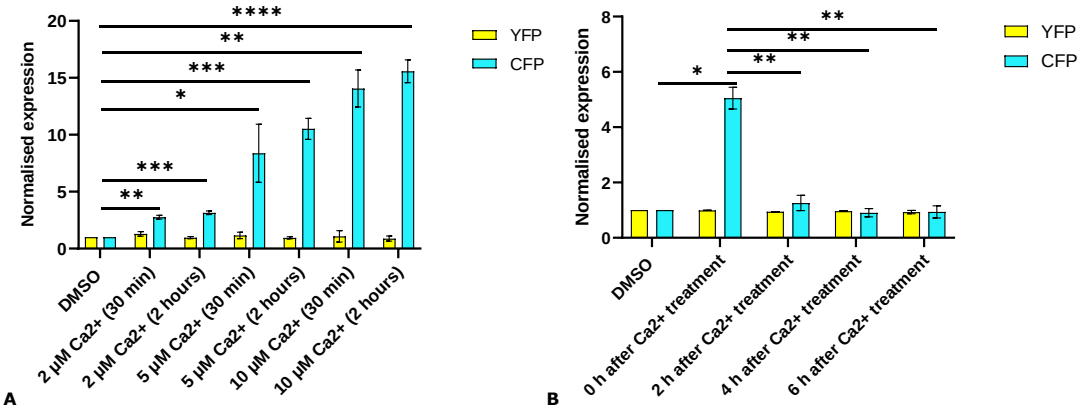

Figure 3. 8 Activation of calpains. (A) FRET transfected MDA-MB-231 cells were treated with 2 µM, 5 µM and 10 µM of calcium ionophore A23187 for 30 minutes or 2 hours. Maximum CFP expression was seen at 10 µM (2 hours). (B) FRET transfected MDA-MB-231 cells were treated with 10 µM of A23187 and the cells were assessed for CFP and YFP expression every 2 hours until 6 hours after removal of A23187. DMSO was used as a treatment control. Calpain activity expression is represented as normalised values to treatment controls. Data represents the average expression± SD of three independent experiments. Statistical analysis was carried out using the Student's *t*-test *(P<0.05), ** (P<0.01), *** (P<0.001).

The transfected and untransfected MDA-MB-231 cells were analysed by flow cytometry and 48 hour time point. The percentage cells expressing YFP and CFP was significantly higher in transfected cells compared to the untransfected cells. Different doses of calcium ionophore A23187 for 30 minutes or 2 hours increased CFP expression after every treatment indicating calpain activation. An increase in CFP expression is directly proportional to an increase in calpain activity. There was a dose dependent

increase in CFP expression after treatment with 2 μM of calcium ionophore for 30 minutes (P<0.01) and for 2 hours (P=0.001), with 5 μM for 30 minutes (P=0.05) and 2 hours (P<0.001), and with 10 μM for 30 minutes (P<0.01) and 2 hours (P<0.0001). The maximum CFP expression was observed with 10 μM of calcium ionophore A23187 treatment for 2 hours. Similar levels of calpain activity induction was observed with 10 μM calcium ionophore treatment between 30 minutes and 2 hours. However, 2 hour treatment with demonstrated a stronger statistically and biologically significant induction of calpain activity (P<0.01 and P<0.0001). Therefore, 10 μM of calcium ionophore A23187 treatment for 2 hours was optimised and used in subsequent experiments for induction of calpain activity. Data suggests that the FRET bioassay is an appropriate system to demonstrate calpain activity in live breast cancer cells.

To determine the duration of calpain activity induction, FRET vector transfected MDA-MB-231 cells were induced for calpain activity followed by removal of calcium ions and flow cytometry analysis every two hours for 6 hours. The CFP expression was seen to be increased significantly (P<0.05) at 0 hours of calpain activity induction with the calcium ionophore A23187. However, CFP expression decreased significantly (P=0.01) 2 hours after the removal of calcium ionophore. Similar levels of CFP expression was observed after 4 hours (P<0.01) and 6 hours (P<0.01) of removal of calcium ionophore A23187, indicating that activation of calpain activity is a direct effect of calcium influx and is short lived. Due to the lack of a selection marker on the vector, the FRET plasmid was transiently transfected in MDA-MB-231 cells for each experiment. This may explain different levels of calpain activity induction in between different sets of experiments.

3.4.4 Inhibition of calpain activity using the FRET bio assay

To demonstrate inhibition of calpain activity in live MDA-MB-231 cells by FRET bio assay, cells were first treated with 10 μM of calcium ionophore A23187 for 2 hours for calpain activity induction, with either treatment with DMSO as controls or 100 μM of PD150606 calpain inhibitor for 30 minutes before the end of 2 hour calcium ionophore treatment or for 2 hours, treated at the same time as calcium ionophore treatment (Figure 3.8). Calpain

activity was presented normalised expression to the respective controls for each treatment.

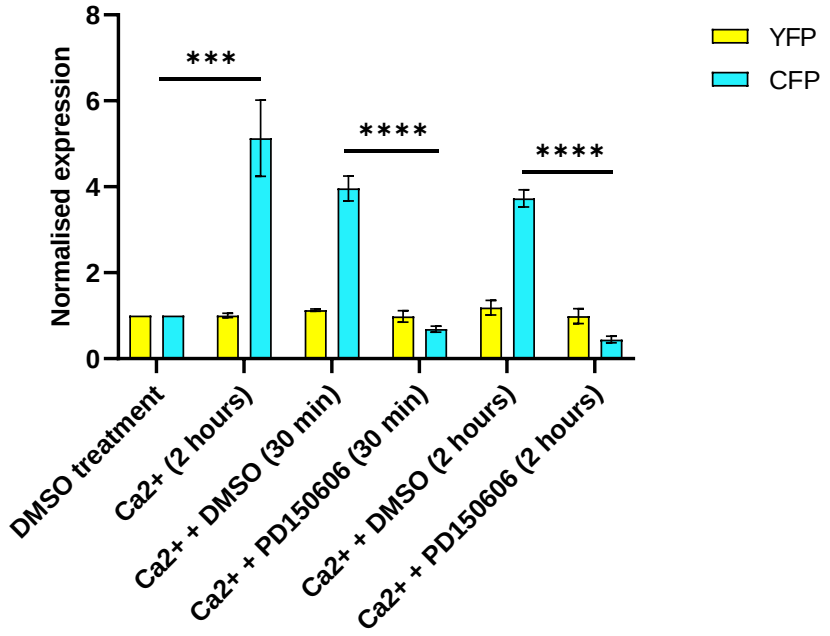

Figure 3. 9 Inhibition of calpains by PD150606. FRET transfected MDA-MB-231 cells were treated with 10 µM for 2 hours and 100 µM PD150606 for 30 minutes before the end of 2 hour calcium ionophore treatment and for 2 hours, treated at the same time as calcium ionophore treatment. The CFP expression was determined by flow cytometry. DMSO was used as treatment control. Calpain activity expression is represented as normalised values to their respective controls. Data represents the average expression± SD of three independent experiments. Statistical analysis was carried out using the Student's *t*-test *(P<0.05), ** (P<0.01), *** (P<0.001).

The CFP expression increased significantly (P=0.001) after calcium ionophore treatment indicating an increase in calpain activity. The treatment with 100 µM PD150606 following calpain activity induction reduced expression of CFP significantly for both 30 minutes and 2 hours (P<0.0001) compared to their respective DMSO treated controls. This data suggest that the calpain inhibitor PD150606 successfully inhibited calpain activity in MDA-MB-231 cells and therefore can be used as a comparator for novel calpain inhibitors. Such data also suggests that the novel FRET bioassay is an appropriate assay to demonstrate calpain activity inhibition.

To examine the inhibitory potential of the novel compounds 1, 9 and 10, FRET transfected MDA-MB-231 cells were treated with 10 µM of calcium ionophore A23187 for 2 hours for induction of calpain activity. Cells were treated with compounds 1, 9 and 10 in different doses for 2 hours, at the

same time as calcium ionophore treatment (Figure 3.9). PD150606 (given together with calcium ionophore for 2 hours) was used as a positive control and calpain activity was represented as normalised expression to the respective controls for each treatment.

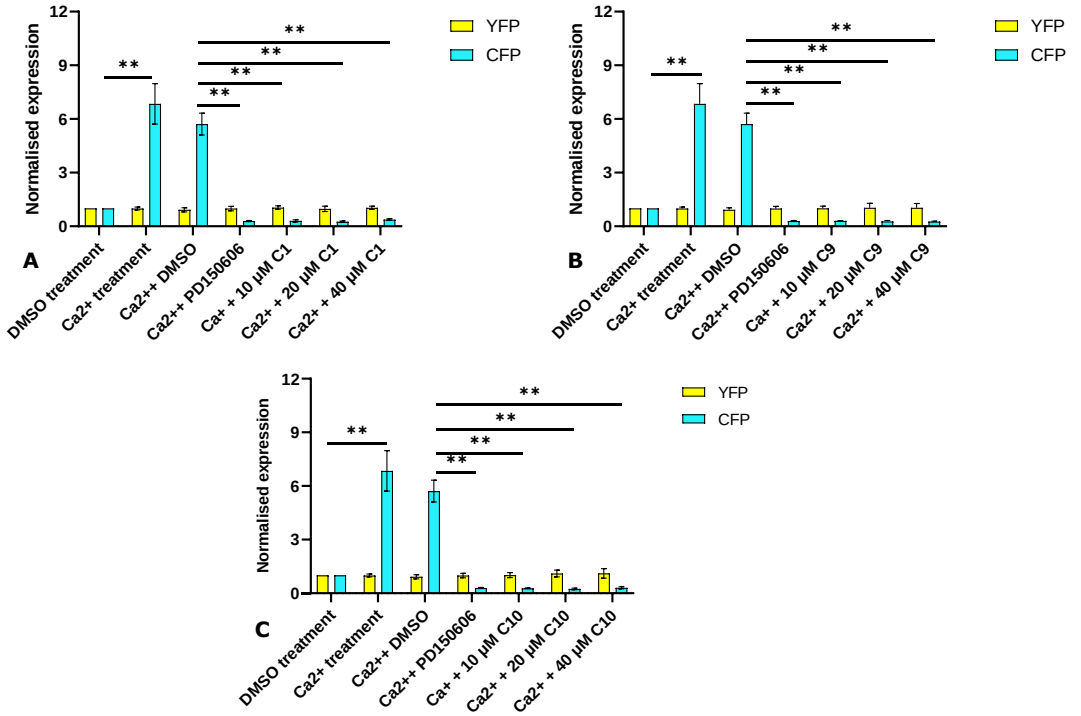

Figure 3. 10 Inhibition of calpains using novel compounds. FRET transfected MDA-MB-231 cells were treated with 10 µM of A23187 for 2 hours together with 10 µM, 20 µM or 40 µM of novel compound 1, C1 (A), compound 9, C9 (B) and compound 10, C10 (C) for 2 hours. 100 µM of PD150606 for 2 hours, given at the same time as calcium ionophore treatment was used as a positive control. DMSO was used as a treatment control. The CFP expression was determined by flow cytometry. Calpain activity expression is represented as normalised values to their respective controls. Data represents the average expression± SD of three independent experiments. Statistical analysis was carried out using the Student's *t*-test *(*P*<0.05), ** (*P*<0.01), *** (*P*<0.001).

Induction of calpain activity for 2 hours, resulted in significant activation of calpain, shown by the increase in CFP expression (*P*<0.01) before inhibitor treatment. The treatment with 100 µM of PD15606 for 2 hours (positive control) reduced the expression of CFP significantly (*P*<0.01) suggesting inhibition in calpain activity.

Calcium activated MDA-MB-231 cells treated with 10 µM, 20 µM or 40 µM of novel compound 1 resulted in significant reduction of CFP expression (P<0.01, P<0.01 and P<0.01, respectively) (Figure 3.9A), indicating inhibition in calpain activity. Calcium activated MDA-MB-231 cells treated

with 10 μM, 20 μM and 40 μM of novel compound 9 resulted in significant reduction of CFP expression ($P<0.01$, $P<0.01$ and $P<0.01$, respectively) (Figure 3.9B), indicating inhibition in calpain activity.

A similar pattern was seen with the novel compound 10 treatment. Calcium activated MDA-MB-231 cells treated with 10 μM, 20 μM and 40 μM of novel compound 10 resulted in significant reduction of CFP expression ($P<0.01$, $P<0.01$ and $P<0.01$, respectively) (Figure 3.9C), indicating inhibition in calpain activity.

It was interesting to note that the degree of reduction in CFP expression with treatment of 10 μM, 20 μM and 40 μM of novel compounds 1, 9 and 10 for 2 hours was comparable with the degree of reduction in calpain activity with 100 μM of PD150606 treatment for 2 hours ($P<0.01$, $P<0.01$ and $P<0.01$ vs $P<0.01$, respectively). These findings suggest that lower doses of novel compounds 1, 9 and 10 result in similar levels of calpain inhibition as seen with the 100 μM of PD150606 treatment suggesting that novel compound 1, 9 and 10 may be more potent calpain inhibitors as demonstrated by the FRET bio assay.

3.4.5 Effect of novel compounds on cell proliferation and survival

The effect of novel compound treatment on breast cancer cell behaviour was determined. MDA-MB-231 cells were treated with 10 μM, 20 μM and 40 μM of compounds 1, 9 and 10 for 24 hours, followed by performing proliferation and clonogenic assays. Doxorubicin IC_{50} doses were used as comparators. As expected, treatment with the IC_{50} dose of doxorubicin resulted in approximately 50% reduction in percentage cell number (Figure 3.10A). Compounds 1 and 10 had comparable effects, however only small anti-proliferative effects were observed with compound 1, 9 or 10 treatments. The effect seen with the calpain inhibitors treatment was small in comparison to the cytotoxic and anti-proliferative effects seen with doxorubicin.

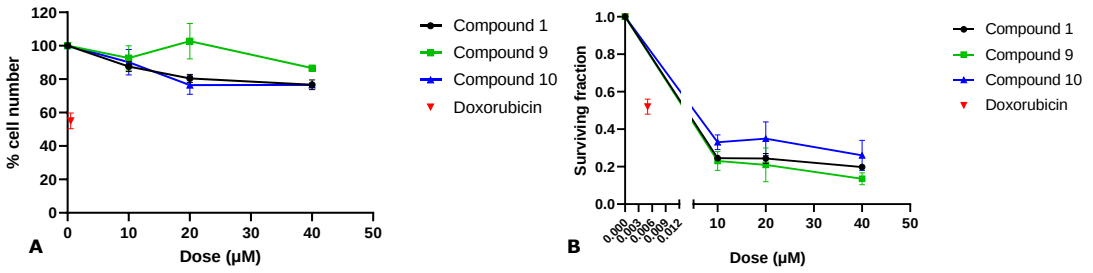

Figure 3. 11 Effect of novel compounds on cell proliferation and survival. MDA-MB-231 cells were treated with 10 μM, 20 μM and 40 μM of novel compounds 1, 9 and 10 for 24 hours and proliferation (A) and clonogenic (B) assays were performed. Doxorubicin proliferation and clonogenic IC_{50} doses were used as positive controls. Data represents the average values ± SD of three independent experiments.

In terms of effect on cell survival, treatment with the IC_{50} dose of doxorubicin yielded the expected level of survival. Interestingly whilst treatment with 10 μM, 20 μM and 40 μM of novel compounds 1, 9 and 10 for 24 hours, had little effect on proliferation they significantly reduced surviving fraction to 20-40% (Figure 3.10B). Such data suggests that the novel compounds 1, 9 and 10 may have anti-cancer properties causing direct cell lethality rather than any short term effects on proliferation.

3.4.6 Specificity of the novel compounds 1, 9 and 10

Novel compounds 1, 9 and 10 were previously shown to inhibit full length calpain 1 complex (Kalash *et al.*, 2018). To assess the inhibition specificity of compounds 1, 9 and 10, demonstration of calpain activity inhibition using the FRET bioassay was performed on calpain 1 KO (Capn1 KO) MDA-MB-231 cells. These cells were provided by our collaborator Dr. P Greer, Queen's University, Canada. Capn1 KO MDA-MB-231 cells were treated with 10 μM of calcium ionophore A23187 for 2 hours for the induction of calpain activity and 10 μM, 20 μM or 40 μM of novel compounds 1, 9 and 10, or 100 μM of P150606 for 2 hour, at the same time (Figure 3.11). Calpain activity was represented normalised expression to the respective controls for each treatment.

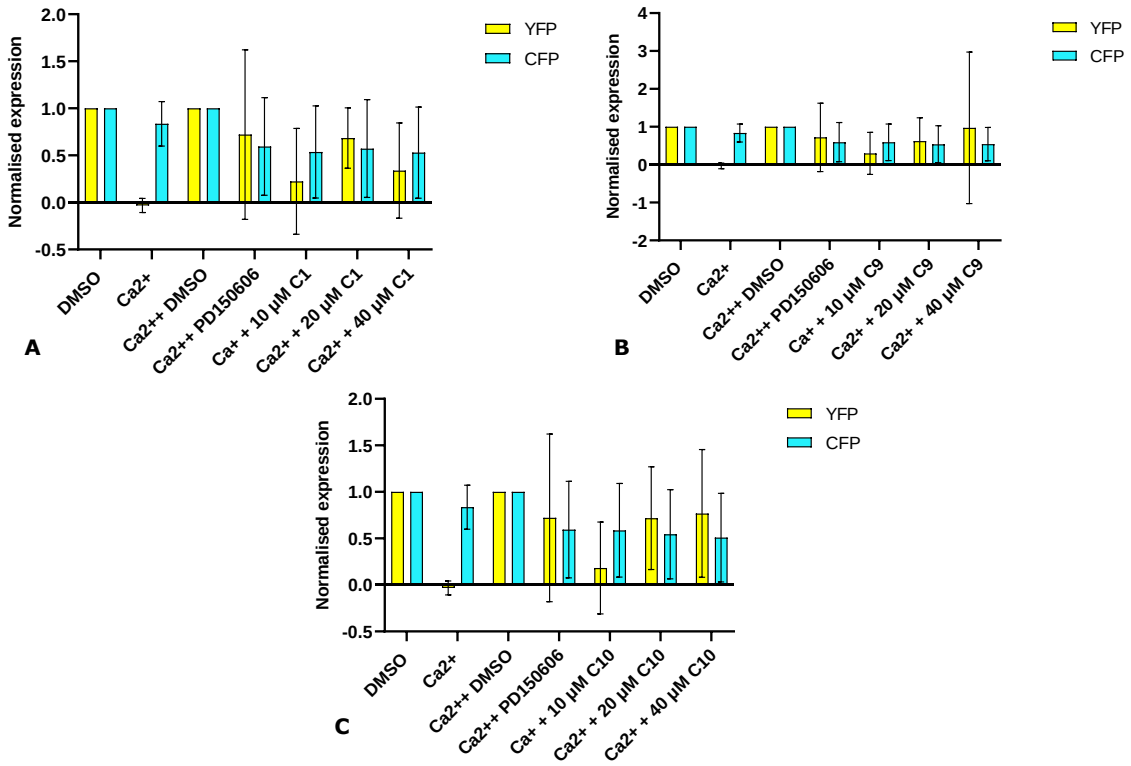

Figure 3. 12 Inhibition of calpain activity by novel compounds on calpain 1 KO cells. FRET transfected Capn1 KO MDA-MB-231 cells were treated with 10 µM of calcium ionophore for 2 hours followed by treatment with 10 µM, 20 µM and 40 µM of (A) compound 1, (B) compound 9 or (C) compound 10 and 100 µM of PD150606 (positive control) for 2 hours. DMSO was used as treatment control. The CFP expression was determined by flow cytometry. Calpain activity expression is represented as normalised values to their respective controls. Data represents the average expression± SD of three independent experiments.

It was subsequently discovered, following discussion with our collaborator, that there is a GFP tag in calpain 1 KO MDA-MB-231 cells, explaining why no activation or inhibition in calpain activity was seen with these cells. Fluorescence produced from GFP tagged Capn1 KO MDA-MB-231 cells, interfered with the CFP and YFP produced as a result of activation or inhibition of calpain activity by the calcium ionophore A23187 or PD150606 or novel compounds 1, 9 and 10 treatment. No conclusions could therefore be drawn from this subsection. As other KO's also had GFP tags present no further work with KO cells (eg. with Calpain-2 or -4 KO's) was conducted to assess the specificity of novel compounds 1, 9 and 10.

3.5 Discussion

Several assays have been developed to assess intracellular calpain activity. The majority of these assays are colorimetric and fluorimetric in nature and

require cell lysates for their analysis. Using cell lysates can often lead to inaccurate measurements of calpain activity as the subcellular structures are disrupted during the preparation of lysates that leads to rapid association of calpains with calpastatin (Han *et al.*, 1999). Therefore, to determine accurate measurement of calpain activity in the intact live cells, the t-BOC-Leu-Met reagent was used, which is a cell permeable calpain substrate. The coumarin moiety of t-BOC-Leu-Met conjugates with glutathione which results in the formation of t-Boc-Leu-Met-MAC-SG conjugate which is a non-fluorescent, membrane impermeable compound. However, proteolytic cleavage of Boc-Leu-Met-MAC-SG between Met and MAC-SG moieties by calpains liberates and unquenches the highly fluorescent, membrane impermeable compound MAC-SG which produces a blue fluorescence within the cell can be measured as a reflection of protease activity (Rosser *et al.*, 1993).

Calpeptin, a commercially available calpain inhibitor was used to show inhibition of calpain activity in MDA-MB-231 cells using the t-BOC assay. The inhibition in calpain activity was calculated by normalising the fluorescent intensity of calpeptin treated cells with that of the control cells at cycle number 7. The cycle number 7 was equivalent to 30 minute treatment with 100 μM of calpeptin. The percentage inhibition in calpain activity was calculated to be 42.56±2.07% ($P<0.01$). This level of inhibition is similar to previously reported data in the lab, inhibition by 34% (Pu, 2016a) and 21.89± 4.49% ($P = 0.0011$) with 100 μM of calpeptin treatment for 30 minutes in MDA-MB-231 cells. The calpain inhibitor calpeptin, however, has been shown not to have selectivity for calpains over other proteases. Designed to bind to the protease core (CysPc), calpeptin has also been shown to inhibit other cysteine proteases such as cathepsins (Siklos *et al.*, 2015). Therefore to inhibit intracellular calpain activity specifically, novel small molecule calpain inhibitors were used.

The novel small molecule calpain inhibitors, compound 1, compound 9 and compound 10 were obtained from our collaborator Professor R. Allemann, Cardiff University. These compounds were developed from a novel structure based virtual screening protocol to identify candidates that bind to the small subunit penta-EF domain and have shown to inhibit full length calpain 1

complex (Kalash *et al.*, 2018). Compounds 1, 9 and 10 were assessed for their potential to inhibit calpain activity using the t-BOC assay. No inhibition in calpain activity was observed with compounds 1, 9 and 10 compared to the untreated control cells. Following which their fluorescence was assessed. MDA-MB-231 cells were treated with novel compounds 1, 9 and 10 and the fluorescence was measured. Cells treated with the novel compounds had marginally higher fluorescence compared to control cells. This indicated that these novel compounds had some fluorescence that could interfere with the detection of inhibition of calpain activity by the t-BOC assay. The t-BOC assay, however useful to provide an indication of calpain activity, is an unreliable assay to determine the inhibition of calpain activity as it has shown to produce inconsistent and inconclusive results. Several experiments were performed to demonstrate inhibition of calpain activity by calpeptin however, data from only three independent experiments demonstrated reliable results and inhibition in calpain activity. As mentioned previously, the assay is known to generate irreproducible results and hence was discontinued to demonstrate inhibition of calpain activity in this study.

To investigate calpain activity in live breast MDA-MB-231 cells, a novel FRET based bioassay was developed using the methods described in the section 3.3.3. The FRET plasmid containing the construct for CFP-16PLFAAR-YFP was transfected into the MDA-MB-231 cell line. The DNA to transfection reagent ratio was optimised to 1:3 and the maximum transfection efficiency was seen at 48 hour time point after transfection. This time point and the DNA: transfection reagent ratio was used in all the experiments to assess intracellular calpain activity. Due to the lack of a selection antibiotic on the construct, the MDA-MB-231 cell line could not be stably transfected with the FRET vector. The cell line was transfected transiently and all the experiments were performed 48 hours after vector transfection as the transfection efficiency declined after the 48 hour time point post transfection. Percentage cells expressing YFP and CFP after transfection was analysed by flow cytometry. The percentage cells expressing YFP (20.85±0.05%) and CFP (6.185±1.45%) in transfected cells was significantly higher (P<0.001) in transfected cells compared to the

untransfected cells. As expected the percentage cells expressing YFP was higher than the percentage of cells expressing CFP in transfected cell population. In the absence of calcium influx, calpains are inactive and do not cleave the substrate. The FRET construct remains intact allowing FRET to occur and subsequently an increased YFP expression.

To demonstrate the inhibition of calpain activity in breast cancer cells using the FRET based bio assay, calpains were activated using calcium ionophore A23187. FRET transfected breast cancer cell line MDA-MB-231 cells were treated with a range of doses of calcium ionophore for 30 minutes and 2 hours following which YFP and CFP expression was analysed. In the presence of Ca^{2+} calpains are activated. The activated calpains cleave the 16PLFAAR substrate on the FRET construct and the CFP and YFP fluorophores are separated reducing FRET and resulting in an increase in CFP expression. After calcium ionophore treatment the CFP expression was significantly increased at all the doses with the maximum expression observed at 10 μM treatment for 2 hours. Enomoto et al. demonstrated activation of calpains using similar doses of calcium ionophore (A23187) in HeLa cells (Enomoto *et al.*, 2019). To assess the length of calpain activity induction, FRET transfected MDA-MB-231 cells were stimulated with 10 μM of calcium ionophore for 2 hours for calpain activation followed by the removal of calcium ionophore and assessment of CFP and YFP expressions every two hours. CFP expression was seen increased at only the 0 hour time point, however it reduced significantly after the 0 hour time point. This suggests that calpains are activated as a direct result of calcium ion influx intracellularly and this activation is reversed on removal of the calcium ionophore.

The commercially available calpain inhibitor calpeptin used in the tBOC assay to demonstrate calpain activity inhibition was discontinued to be used in the FRET based bioassay, as it has shown to inhibit other cysteine proteases like cathepsins by binding to their conserved protease core (Siklos *et al.*, 2015). Therefore, a more specific, commercially available calpain inhibitor, PD150606 was used to demonstrate inhibition of calpain activity in MDA-MB-231 cells using the FRET bio-assay. PD150606 has been shown to have better selectivity for calpains over other cysteine proteases

owing to its allosteric mode of inhibition by binding to the penta-EF domain (Lin *et al.*, 1997). It was later shown that PD150606 can also to bind to the protease core (CysPc) of calpain 1 (Low *et al.*, 2014). FRET transfected MDA-MB-231 cells were induced for calpain activity alongside PD150606 treatment. CFP expression was increased significantly after calcium ionophore treatment indicating activation of calpains. Following PD150606 treatment, it was seen that the calpain activity was reduced significantly after 30 minute and 2 hours treatment of 100 µM of PD150606 ($P<0.0001$, respectively) compared to the DMSO treated controls. The concentration of 100 µM was used to replicate the inhibition in calpain activity shown by calpeptin. In addition, there have been previous reports on significant inhibition of calpain activity in rat renal proximal tubules by 100 µM of PD150606 calpain inhibitor treatment (Edelstein *et al.*, 1996).

Calpain activity induction and inhibition was successfully demonstrated using the novel FRET bio-assay. Therefore, it is an appropriate assay to show the inhibition potential of the novel compounds 1, 9 and 10.

The FRET transfected MDA-MB-231 cells were treated with calcium ionophore and compound 1, 9 and 10 treatment at different doses. The PD150606 drug was used as a positive comparator in these experiments. Calcium ionophore induction resulted in a significant increase in CFP expression ($P<0.01$) indicating calpain activation. The CFP expression was reduced significantly ($P<0.01$) after PD150606 treatment.

Comparable levels of CFP expression were seen with of compound 1 treatment compared to the 100 µM of PD150606 treatment indicating a significant inhibition of calpain activity at 10 µM ($P<0.01$), 20 µM ($P<0.01$) and 40 µM ($P<0.01$). Treatment with compounds 9 and 10 also resulted in reduction in CFP expression indicating significant inhibition of calpain activity at 10 µM ($P<0.01$), 20 µM ($P<0.01$) and 40 µM ($P<0.01$). The levels of decrease with compound 9 and 10 was comparable with the reduction in CFP expression with 100 µM of PD150606 treatment. These findings indicate that the novel compounds 1, 9 and 10 are more potent inhibitors of calpain. Kalash et al. demonstrated that compounds 1, 9 and 10 inhibited calpain 1 with IC_{50} values of 7.5±1.1 µM, 20.5±1.9 µM and 29.7±5.2 µM,

respectively. Compound 1 showed very weak inhibition of the active site CysPc with an IC_{50} value >100 μM, while compounds 9 and 10 did not inhibit the CysPc domain of calpain 1 in the absence of the small subunit penta-EF domain. Compounds 1, 9 and 10 showed specificity for calpain 1 in their allosteric mode of action than the classical a-mercaptoacrylic acid based calpain inhibitor PD150606 as they did not inhibit the active site domain in the absence of the small subunit penta-EF domain (Kalash *et al.*, 2018).

To assess the effect of novel calpain inhibitors on cell behaviour, MDA-MB-231 cells were treated with different doses of novel compounds 1, 9 and 10 for 24 hours and the effect on cell behaviour was assessed in terms of cell proliferation and clonogenic survival. The conventional chemotherapeutic agent doxorubicin was used as positive control and comparator. Marginal anti-proliferative activity was observed with compounds 1 and 10. However, no significant effect on cell proliferation was seen in cells treated with the novel compounds compared to doxorubicin treatment. The effect on survival was assessed by clonogenic assay. Treatment with 10 μM, 20 μM and 40 μM of compounds 1, 9 and 10 for 24 hours significantly reduced the clonogenic surviving fraction in MDA-MB-231 cells. Doxorubicin clonogenic IC_{50} was used as a positive comparator that reduced the surviving fraction of the doxorubicin treated cells was reduced by 50%.

The novel calpain inhibitors did not have an effect on cell proliferation however, they reduced the surviving fraction of the cells significantly, indicating their direct cell lethality effects. This data indicates that the novel compounds may have useful anti-cancer properties.

To assess the specificity of the novel compounds CRISPR/Cas9 calpain 1 knock out cells were treated with calcium ionophore and compounds 1, 9 and 10. The unexpected data caused us to further examine the cell lines used. No conclusions were made from this assessment as it transpired that these cells were tagged with GFP which interfered with the accurate detection of CFP and YFP following different treatments.

Suggested future work

Future work suggested from this chapter includes:

1. Optimise the dose to obtain maximal inhibition of calpain activity using novel compounds 1, 9 and 10.
2. Assess of compound 1, 9 and 10 specificity using calpain-1, -2 and -4 KO cells without a GFP tag.
3. Assess the potential sensitising effect of compounds 1, 9 and 10 on chemotherapeutic drug and radiation response.
4. Asses calpain activity (activation and inhibition) in additional breast cancer cell lines to more fully understand the effect on different breast cancer subtypes, and under different physiological conditions that may alter calpain activity e.g. hypoxia.

Chapter 4- Use of CRISPR/Cas9 calpain knock out cell lines

4.1 Abstract

Background: The third strategy to inhibit calpain activity was by using CRISPR/Cas9 calpain KO breast cancer cells. Calpains are known to be long lived very stable molecules. Genetic deletion of calpains would lead to a complete loss of calpain activity. MDA-MB-231 WT, Capn1, Capn2 and Capns1 KO cells were provided by Dr. Greer's laboratory, Queen's University, Canada. This chapter aimed to assess the effect of knocking out calpain 1, calpain 2 and calpain 4 on breast cancer cellular behaviour and treatment response to the chemotherapeutic agent doxorubicin, radiation in normoxic (21% O2) and hypoxic (1% O2) conditions.

Methods: The calpain 1, 2 and 4, and CA9 protein expression were assessed by performing Western blotting. Proliferation and clonogenic assays were conducted to determine the effect of knocking out calpains on cell proliferation and plating efficiency in normoxia (21% O2). To determine the effect on doxorubicin response in normoxia (21% O2), cells were treated with different doses of doxorubicin and proliferation and clonogenic assays were performed. To determine the effect of knocking out calpains on cell proliferation and plating efficiency in hypoxia (1% O2), cells were grown in hypoxia followed by conducting proliferation and clonogenic assays. To assess the effect on doxorubicin response in the presence of hypoxia (1% O2), the MDA-MB-231 WT and calpain KO cells were pre-treated with hypoxia (1% O2) for 24 hours followed by treatment of different doses of doxorubicin followed by performing proliferation and clonogenic assays. The radiation response in normoxia (21% O2) was assessed by treating cells with different doses of radiation and performing clonogenic assays. While the radiation response in hypoxia (1% O2) was assessed by pre-treating MDA-MB-231 WT and calpain KO cells with hypoxia (1% O2) followed by radiation treatment of different doses and performing clonogenic assay.

Results: The cells lines were confirmed for their expression of calpain proteins, no protein bands were seen in their respective knock out cell line, confirming that these cells were calpain KO cells. MDA-MB-231 WT cells had a growth rate, doubling time (DT) and plating efficiency (PE) (27±2.45 hours and 51.2±1.2%) similar to previously obtained data and published

literature. Capn1 KO cells did not influence cell growth rate or PE compared to the WT cells. Capn2 KO cells did not influence the growth rate but had a significantly reduced PE (22.2±6.5%, *P*=0.001). While Capns1 KO cells had a significantly reduced cell growth rate and a high doubling time, and lower PE (82.6±5.4 hours, P=0.0001 and 32.1±5.2%, *P*<0.01). In normoxia (21% O2), 24 hour doxorubicin treatment reduced percentage number of Capn2 KO and Capns1 KO cells which was not carried over to 48 h or 72 h treatment. In terms of doxorubicin survival, the Capn2 KO and Capns1 KO cells had significantly reduced surviving fractions at 5 nM, 10 nM and 20 nM (*P*<0.001, *P*<0.0001 and *P*=0.01, respectively) for Capn2 KO and (*P*=0.06, *P*<0.001 and *P*<0.001) for Capns1 KO cells.

The effect on cell proliferation and PE was assessed in the presence of hypoxia (1% O2) in MDA-MB-231 WT and calpain KO cell lines. All the cell lines had significantly reduced rate of cell proliferation in the presence of hypoxia, and this was reflected in DT and PEs. MDA-MB-231 WT, Capn1 KO and Capn2 KO cells had significantly higher DT in the presence of hypoxia (1% O2) compared to normoxia (21% O2) (*P*<0.01, *P*<0.01 and *P*<0.05, respectively). While MDA-MB-231 WT, Capn2 KO and Capns1 KO cells had a significantly lower PE in hypoxia (1% O2) compared to normoxia (21% O2) (*P*<0.01). The hypoxic MDA-MB-231 WT and the calpain KO cells were seen to more resistant to doxorubicin treatment compared to the normoxic cells. No significant difference in doxorubicin response was seen in the calpain KO cells compared to the WT cells in the presence of hypoxia.

In addition, radiation response was assessed in the presence of normoxia (21% O2) and hypoxia (1% O2 for 24 h). It was interesting to see that Capn1 KO and Capn2 KO cells were significantly sensitised to radiation in hypoxia (1% O2 for 24 h) compared to normoxia (21% O2). Capn1 KO and Capn2 KO cells had significantly reduced surviving fractions at all the doses, *P*<0.0001 for 2 Gy, *P*<0.05 for 4 Gy, *P*<0.001 for 6 Gy and *P*<0.05 for 8 Gy, and *P*<0.0001 for 2 Gy, *P*<0.05 for 4 Gy, *P*<0.001 for 6 Gy and *P*=0.01 for 8 Gy, for Capn1 KO and Capn2 KO, respectively.

Conclusion: The effect of knocking out calpains was assessed on breast cancer cellular behaviour and treatment response in normoxic (21% O2) and hypoxic (1% O2) conditions. Knocking out calpain 4 reduced cell proliferation significantly while knocking calpain 2 reduced the plating

efficiency of the cells significantly. Knocking out calpains 2 and 4 may sensitise breast cancer cells to doxorubicin in terms of clonogenic cell survival in normoxia (21% O2). In the presence of hypoxia (1% O2), significant delays in growth were seen in all the cell lines. It was interesting to see that in normoxia (21% O2), knocking out calpain 1 has no effect and knocking out calpain 2 made MDA-MB-231 cells resistant to radiation. While in the presence of hypoxia (1% O2 for 24 h), knocking out calpains 1 and 2 significantly sensitised MDA-MB-231 cells to radiation.

4.2 Introduction and aims

4.2.1 Calpains and cancer

The ubiquitously expressed calpains μ- and m- are the most intensively studied calpain types. Calpain activity is strictly regulated intracellularly and its deregulation is involved in the pathogenesis of several diseased states including cancer. Alterations in calpain activity have been shown to be implicated in several cancer types. Calpains have been shown to be involved in cell survival and death in cancer cells. A mechanism crucial for the development of carcinomas is the escape from the programmed cell death machinery, apoptosis, which is often combined with uncontrolled proliferation. Both μ- and m-calpain are known to be involved in apoptosis by regulation of caspases. Calpains can activate caspase 3, 7 and 12 and inactivate caspase 8 and 9 (Chua *et al.*, 2000). Calpain inhibition led to the blocking cell death induced by dexamethasone, cycloheximide and irradiation (Squìer *et al.*, 1994).

Apoptotic induction is often a critical component of certain cancer treatments. Several agents are known to induce apoptosis either directly or indirectly. These include chemotherapeutic drugs such as cisplatin, 5-fluorouracil, irinotecan and paclitaxel. In MCF-7 breast cancer cells treated with genistein, μ-calpain was shown to be activated by increased intracellular calcium which led to cleavage and activation of caspase 12 triggering apoptosis (Sergeev, 2004). This activation of caspase 12 by calpain was a result of ER stress induced apoptosis, reported previously (Martinez *et al.*, 2010; Tan *et al.*, 2006). The chemotherapeutic agents cisplatin and oxaliplatin were also shown to induce calpain-mediated apoptosis. Treatment of lung adenocarcinoma cells with cisplatin induced a

significant increase in μ-calpain activity leading to Bid and caspase 3 mediated cell death (Liu *et al.*, 2009; Liu *et al.*, 2008). A similar mechanism was observed with oxaliplatin treated HeLa cells (Anguissola *et al.*, 2009).

Calpains have shown to cleave wild-type p53 in survival pathways, regulating its protein stability to prevent p53-mediated apoptosis (Atencio *et al.*, 2000; Pariat *et al.*, 1997). Calpains can induce activation of NF-κB by cleaving its inhibitor IκBα. A number of factors can induce cleavage of IκBα including, tumour necrosis factor (TNF) and HER2 activation (Han *et al.*, 1999; Pianetti *et al.*, 2001). In a study of the proteasome inhibitor, bortezomib, treated lung cancer cells showed calpain-dependent induced degradation of IκBα (Li *et al.*, 2010). Calpains have also shown to be involved in many other survival related pathways. The driver of oncogenic transformation, Myc, is often overexpressed in cancers. Under stress conditions such as hypoxia, calpain mediated cleavage of Myc converts the active protein to Myc-Nick, a transcriptionally inactive cleavage product of Myc, which results in cell death evasion and cell survival (Conacci-Sorrell *et al.*, 2014). Calpains have shown to regulate the cell cycle in particular the transition between G1 and S phase (Jánossy *et al.*, 2004; Joy *et al.*, 2006; Mellgren 1997). The cell cycle regulators cyclin D1 and cyclin E are substrates of μ- and m-calpains (Choi *et al.*, 1997; Wang *et al.*, 2003). Degradation of these cyclins by calpain 1 and 2 induces cell cycle arrest in normal cells however the opposite seems to occur in cancer cells where calpains can promote cell cycle progression.

4.2.2 Conventional treatments for breast cancer

Conventional forms of treatment strategies for breast cancer depend on the clinical presentation and the molecular subtype of the disease. As mentioned in section 1.1.5, treatment is generally administered as a multimodal form of therapy that includes a combination of surgery, chemotherapy, hormonal therapy, targeted therapy and radiotherapy. Strategies for treatment include local and systemic therapies.

Local therapy includes surgery and radiotherapy. Surgery includes breast conserving surgery and mastectomy. Radiation is administered to breast cancer patients in the UK as hypofractionated radiotherapy. It is generally

administered as a total dose of 40 Gy in 15 fractions in a period of 3 weeks (NICE, 2018). Recently reviewed, the hypofractionated radiotherapy regimen for breast cancer mentioned in the FAST-Forward RCT is now becoming a routine practice with 26 Gy being delivered in five fractions over a one week period (Bockel *et al.*, 2021). Local therapy is given as an aim to remove primary tumours and is given to patients with early stage breast cancer including stages I and II. Although radiotherapy is generally administered to early stage disease, it is also administered to patients with stage 3 LABC before surgery to enhance tumour accessibility for better resection (van der Leij *et al.*, 2015) and stage 4 MBC patients with bone and brain metastasis to relieve tumour related symptoms (Cardoso *et al.*, 2014).

Whilst systemic therapy can be administered to patients with early stage invasive breast cancer it is usually given to those patients with locally advanced or metastatic disease. The type of systemic treatment for breast cancer depends upon the molecular subtype of the tumour. Patients with TNBC are often treated with cytotoxic chemotherapy. Systemic therapy can be given as an adjuvant to treat early invasive breast cancer. Neo-adjuvant systemic therapy is administered to reduce tumour size and minimise surgery complications for patients with locally advanced disease. In metastatic breast cancer it is given to reduce disease burden and to improve quality of life (Gemignani *et al.*, 2014).

Whilst there are some exciting new developments and new breast cancer chemotherapy options including antibody drug conjugates like Sacituzumab govitecan, VEGF inhibitors like Bevacizumab, EGFR inhibitors like Cetuximab, mTORC1 inhibitors like Everolimus, and several others including Akt inhibitors, androgen receptor inhibitors, CYP17 inhibitors and several more (Burguin *et al.*, 2021), conventional cytotoxic chemotherapeutic agents include platinum compounds, alkylating agents and anthracyclins. The polychemotherapeutic routine is described in detail in section 1.1.5.2.1.

Doxorubicin is a commonly used chemotherapeutic agent in breast cancer and was used in the current project as a control, a drug comparator and in combination studies. It is a nonselective class I anthracycline, having

aglyconic and sugar moieties, and is regarded as one of the most potent chemotherapeutic drugs approved by the Food and Drug Administration (FDA) as it has shown great treatment potential (Carvalho *et al.*, 2009).

Doxorubicin acts by intercalating into the DNA base pairs but also binds to many molecular targets such as topoisomerase I and II, resulting in a range of cytotoxic and anti-proliferative effects and causing damage to the DNA (Buchholz *et al.*, 2002). When the repair of DNA breaks fails, the apoptosis pathway is triggered and cell growth inhibited at G1 and G2 phases. It can also intercalate into the DNA and inhibit DNA and RNA polymerases which ultimately terminates DNA replication and RNA transcription (Buchholz *et al.*, 2002).
Doxorubicin has a higher affinity to bind to the cytoplasm's proteasome and enters the cell by diffusion. It forms a doxorubicin proteasome complex by binding to the 20S subunit of the proteasome and is translocated into the nucleus through the nuclear pore complexes. Due to its high affinity for the DNA, doxorubicin dissociates from the proteasome to bind to DNA. It can also act by generating free radicals that cause further damage to the DNA. It has also been shown to intercalate into mitochondrial DNA. In addition, doxorubicin has the potential to directly bind to plasma proteins effecting the cell membrane by undergoing enzymatic electron reduction and causing production of highly reactive hydroxyl free radicals. These free radicals are also cytotoxic and make doxorubicin a potent anticancer drug for various cancer types (reviewed in (Tacar *et al.*, 2013)).

Doxorubicin has also been shown to initiate autophagy indicating a cytoprotective response to DNA damage. The enzyme (poly (ADP-ribose) polymerase-1) or PARP1 activation is crucial for induction of autophagy. The genotoxic stress causes hyperactivation of PARP1 that can exhaust both NAD+ and ATP, which will result in an irreversible loss of energy in the cell leading to cell death (Minotti *et al.*, 2004). PARP1 deficient cells showed that moderately high dose of doxorubicin was unable to induce cell death. This indicates that PARP1 plays a crucial role in doxorubicin induced autophagy. During doxorubicin hyperactivation of PARP1 the cell undergoes cell death with characteristics of autophagy and necrosis. As a result of PARP1 hyperactivation, there is a collapse of cellular energy which triggers

the cell to enter into autophagy. Inhibition of PARP1 can avert depletion of cellular energy that protects the cells from necrosis and can delay doxorubicin induced autophagy, which results in apoptosis. Thus, PARP1 activation is an important regulator of a cell's fate. PARP1 can repair lesions caused by doxorubicin treatment and inhibition of PARP1 is unable to repair DNA damage, resulting in cell death. In conclusion, PARP1 needs a state of equilibrium between energy crisis and DNA damage, which is effected by doxorubicin dose and activation of PARP1. Therefore, doxorubicin induced type of cell death varies depending on the dose and the treatment duration of the drug and the type of cancer (Tacar *et al.*, 2013).

Radiotherapy for cancer is administered to deliver a toxic dose of radiation to kill the tumour but also to minimise the exposure to the healthy tissues (Emami *et al.*, 1991; Nikjoo *et al.*, 1998). It routinely uses external beam ionising radiation (IR) producing ions and free radicals that deposit energy in biological tissue on its path through the absorber/tissue. This energy can produce huge amounts of ions and free radicals that can kill cancer cells or can cause genetic alterations in the cell (Baskar *et al.*, 2012).

The amount of energy deposited by the radiation determines the biological effects. The amount of energy deposited per unit path length is called the linear energy transfer (LET) and is measured in keV/μm. Ionising radiations that deposit large amounts of energy per unit path length are called high-LET radiations, and include α-particles, neutrons and heavy charged ions. The radiations that deposit less energy per unit path length are called low-LET radiations, and include x-rays, γ-rays, electrons and protons (Franken *et al.*, 2011; Hunter *et al.*, 2009). All radiation types are used to treat cancer however it is external beam electromagnetic radiations (EMR), x-rays and γ-rays that are routinely used. In conventional external beam radiotherapy the X-rays are generated by linear accelerators (Baskar *et al.*, 2012).

Ionising radiation can cause damage to cells that can be a direct and/or indirect effect. The direct action of ionising radiation is where the radiation track interacts with the biological target, such as DNA, directly, causing a physical disruption in the molecular structure that leads to cell damage and death (Pinto *et al.*, 2005). High-LET radiation particles mostly cause damage to the target molecules by direct action (Hall *et al.*, 2006). Low-

LET ionising radiations act mostly via indirect action as they are involved in generation of ions and free radicals formed by the radiolysis of water molecules present close to the target molecules, like DNA (Chapman *et al.*, 1973). These ions and free radicals diffuse to the critical sites and cause damage as they have sufficient biological half-lives. Most of the damage caused by low-LET radiations are a result of their interaction with cellular water which constitutes 70% of cell. This interaction results in the following reactions-

Reaction 1: $H_2O \longrightarrow H_2O+ + e^-$

Reaction 2: $H_2O+ + H_2O \longrightarrow H_3O+ + OH^\circ$

Reaction 3: $OH^\circ + OH^\circ \longrightarrow H_2O_2$

The ionising radiation production of free radicals that have highly reactive unpaired electrons oxidises biological molecules such as proteins, lipids and cellular DNA to cause structural and biological damage (Chapman *et al.*, 1973).

The low-LET radiation induced DNA damage interacts with molecular oxygen which causes the formation of peroxinitrite lesions in the DNA that cannot be repaired followed by cell damage and death. This is called oxygen fixation hypothesis (OFH) (Grimes *et al.*, 2015; Oronsky *et al.*, 2011). Therefore, it is crucial that the molecular oxygen is present to improve the therapeutic efficiency of ionising radiation. This is known as the oxygen enhancement ratio (OER) (Rockwell *et al.*, 2009). Hypoxic cells can repair radiation induced DNA damage much more efficiently and so are relatively radioresistant.

4.2.3 Hypoxia and cancer and the calpain system

The microenvironment of tissues has different levels of oxygen. The normal atmospheric levels of oxygen of 20-21% is termed as normoxia. It is the condition in which cells are routinely cultured in vitro however physoxia, or physiological hypoxia, is the state that describes the physiological levels of oxygen (1-13%) in tissues. Oxygen concentration can vary in normal tissues between 2% oxygen and 10% oxygen depending upon the tissue type (Vaupel *et al.*, 2007). Hypoxia is the state where the oxygen levels are below 1-2% and occurs in tumours. It occurs due to the uncontrolled

proliferation of cancer cells that happens in the absence of an efficient blood supply. When the tumour cells proliferate uncontrollably, they become distanced from the vasculature and nutrients and oxygen are depleted rapidly. This creates an imbalance between oxygen demand and supply, which causes decrease in oxygen generating a hypoxic environment in the tumours (Brown *et al.*, 2004).

Hypoxia in tumours cause resistance to radiation and chemotherapy (Brown, 2007). It is also a predictor of poor clinical outcome and has been associated with increased risk of mortality, independent of other prognostic factors (Vaupel *et al.*, 2007). The transcription factor hypoxia-inducible factor (HIF) is upregulated in the presence of hypoxia. It transcribes several hypoxia related genes such vascular endothelial growth factor (VEGF), and carbonic anhydrase 9 (CA9), to promote adaptive response in cells (Swinson *et al.*, 2003). Some studies have also shown hypoxia as a driver of metastasis by upregulation of metastatic-related genes such as CXCR4, IL8, and VEGF (Rofstad, 2000). In breast cancer hypoxia is seen in approximately 40% of cases (Vaupel *et al.*, 2005). It occurs in all stages of breast cancer form in situ carcinomas to invasive cancers (Hohenberger *et al.*, 1998). The normal breast has a pO2 of 8%, whereas studies have shown a pO2 range between 0.3-3.5%, with a median of 1.3% in breast cancer (Vaupel *et al.*, 1991). Studies show that primary breast cancers with hypoxia were linked with the presence of hypoxic markers in their lymph node metastases (Van den Eynden *et al.*, 2005). Hypoxia in breast cancer also reduces the efficacy of hormonal therapy due to loss of ERα (Kurebayashi *et al.*, 2001). In addition, in patients with DCIS, occurrence of hypoxia is associated with a shorter recurrence period (Cornfield *et al.*, 2004).

Several studies have shown a relationship between hypoxia and the calpain system. In macrophages, calpains have shown to proteolyse the central signalling component of TGFβ signalling by hypoxic interference (Cui *et al.*, 2015). Another study showed that in monkey retinal cells it was calpain and not capase-3 that was involved in hypoxic damage (Nakajima *et al.*, 2011). Intermittent hypoxia down regulates HIF-2α via a calpain dependent signalling pathway leading to oxidative stress and autonomic morbidities (Nanduri *et al.*, 2009). Hypoxia has shown to upregulate calpastatin which

acts as a suicide substrate to calpain after neonatal cerebral hypoxia-ischemia (Blomgren *et al.*, 1999).Presence of hypoxia (0% O2) for 1h-12 h has also shown to activate calpains significantly ($P<0.01$ for 1h and 12 h) in porcine pulmonary artery endothelial cell (PAEC) (Zhang *et al.*, 1998). In human umbilical vein endothelial cells (HUVECs) it was shown that expression of Hypoxia-Inducible factor 1α (HIF-1α) caused an increase in the expression and activity of calpains leading to enhanced proliferation and migration (Mo *et al.*, 2011).

In cancer the calpain system plays role with several important cellular pathways including hypoxic responses. As mentioned previously presence of hypoxia is linked to poor clinical outcome, angiogenesis and metastasis. Presence of hypoxia in melanoma cells, can lead to the induction of calpain-mediated cleavage of a large cytoskeletal binding protein, filamin A (FLNA), and upregulates hypoxia inducible factor-1α (HIF-1α) which results in angiogenesis and tumour progression (Zheng *et al.*, 2014). In hepatoblastoma cells, calpains have also shown to be involved in hypoxia-induced cell death (Kim *et al.*, 2007). In a recent study, it was shown that the presence of hypoxia induced amoeboid migration by activation of calpain 2 which led to cleavage of talin-1 subsequently reducing integrin β1 activity in murine breast cancer cells (Te Boekhorst *et al.*, 2022).

4.2.4 Hypothesis and aims

The above mentioned treatment strategies are effective but not all patients respond well and resistance is often encountered due to the presence of hypoxia. Therefore, there is an interest in predictive biomarkers and approaches to target hypoxia and the processes/pathways regulated by it, such as the calpain system.

Our collaborator Prof. P. Greer from Queen's University, Ontario, Canada kindly supplied us with CRISPR/Cas9 Calpain 1 knock out (Capn1 KO), Calpain 2 knock out (Capn2 KO), and Calpain 4 knock out (Capns1 KO) MDA-MB-231 cell lines. These cells were used in this chapter to assess the effect of knocking out the ubiquitously expressing forms of calpains on chemotherapeutic drug and radiation response. The chemotherapy drug doxorubicin was used in this study as it is easily commercially available, and is one of the most potent and efficient anthracyclines used against triple

negative form of breast cancer. Hypoxia is known to have an influence on calpain activation hence these cells were also used to assess treatment response in the presence of hypoxia (1% O_2).

Hypothesis

Altering calpain activity will alter cell behaviour and breast cancer cellular response to conventional forms of therapy. The strategy of knocking out calpains will alter breast cancer cell behaviour and make them more sensitive to conventional forms of therapy.

Aims

1. To assess the effect of knocking out calpain 1, 2, and 4 on cell proliferation and clonogenic plating efficiency in MDA-MB-231 cell line.
2. To assess the effect on knocking out calpain 1, 2, and 4 on normoxic (21% O2) doxorubicin treatment response in terms of cell proliferation and survival MDA-MB-231 cell line.
3. To assess the effect of knocking out calpains 1, 2, and 4 on cell proliferation and clonogenic plating efficiency in MDA-MB-231 cells under hypoxia (1% O2).
4. To assess the effect of knocking out calpains 1, 2, and 4 on doxorubicin treatment response in terms of cell proliferation and survival in MDA-MB-231 cells under hypoxia (1% O2).
5. To assess the effect of knocking out calpains 1, 2, and 4 on radiation treatment response in MDA-MB-231 cells under hypoxia (1% O2) and normoxia (21% O2).

4.3 Material and methods

4.3.1 Cell lines, reagents, and subculture

MDA-MB-231 Calpain 1 KO (Capn1 KO), MDA-MB-231 Calpain 2 KO (Capn2 KO), and MDA-MB-231 Calpain 4 KO (Capns1 KO) and their parental (MDA-MB-231 WT) breast cancer cell lines were used for the experiments in this chapter. These cell lines were cultured in DMEM (Sigma, UK) supplemented with 2mM L-glutamine (Sigma, UK), 1% penicillin/ streptomycin and 10% donor bovine serum. Cell cultures were maintained in a humidified incubator

with 5% CO_2 at 37°C. Sub culturing was limited within 15 times. The subculture was performed using the method described in section 2.3.2

4.3.2 Cell storage, recovery and mycoplasma checks

Cell storage and recovery was done according to the methods described in section 2.3.3. For the preservation of cells for long term, cells were frozen in liquid nitrogen.

Cells in culture were checked for mycoplasma contamination. Following initial experimental characterisations the MDA-MB-231 WT, Capn1 KO, Capn2 KO and Capns1 KO cells tested positive for mycoplasma and were cleaned using Plasmocin® Treatment-Mycoplasma Elimination Reagent (InvivoGen). Mycoplasma infected cells were transferred to a separate incubator. The media was removed and the cells were washed twice with PBS. Media containing Plasmocin® was prepared (final concentration in T-75 cm2 flask was 25 µg/ml). The cells were split in the ratio 1:10 and were allowed to culture in the media containing Plasmocin®. The cells were treated for three weeks with the antibiotic with replacing the media every 3-4 days. After the three weeks of treatment with Plasmocin®, the cells were allowed to grow for another two weeks in media without Plasmocin®, following which the media was tested again for mycoplasma. The cells were cleaned successfully after Plasmocin® treatment. Infection was ultimately tracked back to the originator lab who also initiated a clean-up procedure.

4.3.3 Western blotting

The MDA-MB-231 WT and the calpain KO cell lines were checked the expression of calpain 1, calpain 2 and calpain 4 by preparing cell lysates and performing Western blotting according to the methods described in section 2.3.7.

The presence of hypoxia in the current chapter's experiments was confirmed by assessing CA9 expression from cells treated with hypoxia (1% O_2 for 24 hours) and normoxia (21% O_2 for 24 hours), using Western blotting as described in section 2.3.7. To detect the expression of CA9, membranes were blocked with 5% non-fat milk in 0.05% PBS-Tween 20 after SDS-PAGE. Following blocking, membranes were probed with primary antibody for CA9 and β-actin (loading control) overnight at 4°C. The

following day membranes were probed with the respective horseradish peroxidase (HRP)-conjugated secondary antibodies (DAKO), for 1 hour at room temperature. After incubation the membranes were washed 3 times with PBS/T for 5 minutes and developed using the Enhanced Chemiluminescence detection method (ECL) (Amersham). Bands were detected using Image Studio Version 4.1 (LI-COR Biosciences) software using the ECL channel. Table 4.1 lists the antibodies for calpain proteins and CA9 their dilutions used.

Table 4. 1 List of antibodies and dilutions

Antibodies	Source	Catalogue number	Molecular weight	Dilution
Anti-Calpain 1	Millipore	MAB3104	~80 kDa	1:500
Anti-Calpain 2	Novus Biologicals	NBP246063	~80 kDa	1:1000
Anti-Calpain small subunit	Millipore	MAB3083	~28 kDa	1:1000
Anti-CA9	2BScientific	ab00414-1.1	49 kDa	1:1000
Anti-β-actin	Abcam	ab8227	42 kDa	1:2000
IRDye® 800 CW Donkey anti-rabbit	LI-COR	926-32213	-	1:10000
IRDye® 680RD Donkey anti-mouse	LI-COR	926-68072	-	1:10000
Rabbit anti-mouse HRP	DAKO	P0260	-	1:1000
Goat anti-rabbit HRP	DAKO	P0448	-	1:1000

4.3.4 Cell growth curves and plating efficiency

To assess the effect of knocking out calpain 1, calpain 2 and calpain 4 in breast cancer cells, proliferation assays were conducted using MDA-MB-231 WT, Capn1 KO, Capn2 KO and Capns1 KO cells using the methods described in section 2.3.4. The effect of knocking out calpains on clonogenic plating efficiency of breast cancer cells was assessed using the methods described in section 2.3.5. The data in this chapter represent the average number of cells ± SD of three independent experiments.

4.3.5 Doxorubicin treatment proliferation and clonogenic response

The effect of knocking out calpains on chemotherapeutic response was assessed by performing cell growth assays on cells treated with doxorubicin. Doxorubicin (Sigma-Aldrich) was reconstituted in DMSO to a stock solution of 50 mM. The stock solution was stored at 4°C. The doxorubicin stock was diluted to working solutions. Proliferation assay was performed on MDA-MB-231 WT, Capn1 KO, Capn2 KO and Capns1 KO cells were treated with 0.25, 0.5 and 1 µM of doxorubicin for 24 h, 48 h and 72 h using the methods described in section 3.3.5. Clonogenic assay was performed on the WT and calpain KO cells treated with 0, 5, 10, 20, 50, 100 nM of doxorubicin for 24 hours using the methods described in section 3.3.5. The IC_{50} values calculated where possible. The data in this chapter represent the average percentage of cells/average S.F. ± SD of three independent experiments.

4.3.6 Cell growth curves and plating efficiency in hypoxia

To assess the effect of hypoxia on cell proliferation and plating efficiency on calpain KO cells cell proliferation and clonogenic assays were performed. $1x10^5$ MDA-MB-231 WT, Capn1 KO, Capn2 KO and Capns1 KO were seeded per well in triplicates in 6-well plates and allowed to attach in normoxia (21% O2) for 3 hours, to allow attachment. Cells were then placed in a HypoxyLab™ hypoxia workstation (Oxford Optronix) for 24-96 hours. The HypoxyLab work station was continuously flushed with gas of 1% O2, 5% CO2 and 94% N_2. At each time point the cells were processed and growth curves were generated according to the methods mentioned in section 2.3.4. For clonogenic assays, hypoxia treated cells from the 24 hour time point above were processed according to the methods described in section 2.3.5. Hypoxic and normoxic proliferation and clonogenic experiments were run in parallel. The data in this chapter represent the PE ± SD of three independent experiments.

4.3.7 Doxorubicin treatment proliferation and survival response in hypoxia

To assess the effect of hypoxia on doxorubicin response in calpain knock out cell proliferation essay was performed. $1x10^5$ cells were seeded per well in triplicate in 6-well plates and were allowed to attach in a normoxic (21% O_2) incubator for three hours, to allow attachment. Following which the plates were transferred to the HypoxyLab work station for 24 hours. After which the cells were treated with 0, 0.25, 0.5, and 1 μM of doxorubicin for 24 hours, 48 hours or 72 hours for proliferation assay, and with 0, 5, 10, 20, 50, 100 nM of doxorubicin for 24 hours for clonogenic assay, in hypoxia (1% O2). DMSO was used as a vehicular control. After each time point, the cells were trypsinised, counted and dose response curves plotted according to the methods described in section 3.3.5 and IC_{50} values were calculated where possible. The data in this chapter represent the average percentage of cells ± SD of three independent experiments.

4.3.8 Cell radiation response in hypoxia vs normoxia

The radiation response of knockouts, +/- hypoxia, was assessed by clonogenic assay. MDA-MB-231 WT, Capn1 KO, Capn2 KO and Capns1 KO cells were seeded in T-25 cm^2 flasks at a density of $5x10^4$ cells/ml and allowed to attach in a normoxic (21% O_2) incubator for three hours. Following which one set of flasks were transferred to the HypoxyLab work station for 24 hours at 1% O_2 After 24 hours, cells were irradiated using a RS225 Xstrahl X-ray cabinet irradiation system (Xstrahl Limited, UK). Cells were irradiated with single doses of 2, 4, 6, or 8 Gy given at 195 kV, 10 mA, at a dose rate of 0.97 Gy/minutes and with the irradiation cabinet fitted with a 0.5 mm copper filter. Control cells were sham irradiated. After radiation, cells were trypsinised immediately, counted, serially diluted, plated at low density and allowed to form colonies for 14 days in a designated clonogenic incubator. Colonies were washed, fixed and stained and counted to calculate the surviving fraction for each dose. The survival curves were fitted to the linear-quadratic model (LQM) using the CS-Cal software (DKFZ, Germany).

Hypoxic and normoxic experiments were run in parallel. The data in this chapter represent the average surviving fraction ± SD of three independent experiments, having six parallel sets each for clonogenic assays.

4.3.9 Statistical analysis

All the graphs were constructed using GraphPad Prism 9 software. Data is represented as the mean values ± Standard Deviation (SD) of at least two independent experiments, each performed in duplicate or triplicate (or six replicates for clonogenic assay). Student's *t*-test was performed for comparing two variables and a *P*-value <0.05 was considered to be statistically significant. The following formula was used for combining errors from each experiment to combine the data-

$$\text{SD combined} = \sqrt{\frac{\{(n_1 - 1) \times SD_1^2 + (n_2 - 1) \times SD_2^2\}}{n_1 + n_2 - y}}$$

Where SD combined is the combined standard deviation from y number of experiments. SD_1 and SD_2 are the standard deviation values from individual experiments, and n_1 and n_2 are the number of replicates in each experiment (Mukherjee *et al.*, 2007).

4.4 Results

4.4.1 Effect of knocking out calpains 1, 2 and 4 on cell proliferation and plating efficiency

MDA-MB-231 WT and calpain KO cells tested positive for mycoplasma after initial cell characterisation, some doxorubicin and radiation treatment experiments were conducted. Mycoplasma positive cells behaved differently to mycoplasma free populations - appendix C shows the comparison of data between mycoplasma negative and positive cells. The following experiments were conducted once cells were cleaned for mycoplasma and proven to be infection free using the method mentioned in section 4.3.2. Infection was traced back to the original stock and confirmed by our collaborator to be an issue with the batch of cells sent out.

The CRISPR/Cas9 calpain 1, 2 and 4 KO MDA-MB-231 cells were tested for calpain 1, 2 and 4 expression by Western blotting and knockout status confirmed (Figure 4.1A). To assess the effect knocking out calpain 1, 2 and

4 on cell proliferation WT and KO lines were grown for a period of 0-96 hours. At every 24 hour time point cell were counted and growth curves were plotted (Figure 4.1B). Cell doubling times were calculated from the growth curves for each cell line (Fig 4.1C). Data is summarised in figure 4.1 but also described in greater detail below.

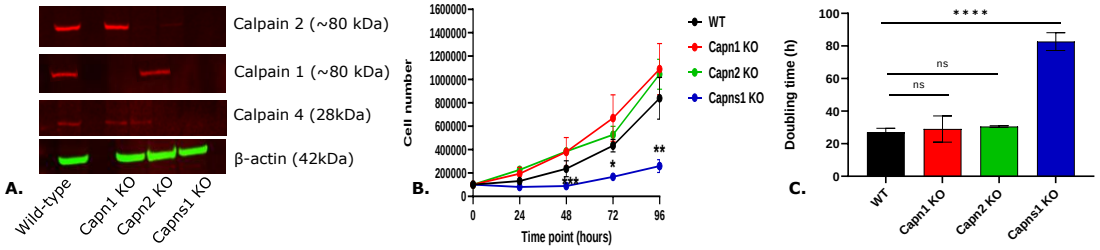

Figure 4. 1 Cell line characterisation of the MDA-MB-231 WT and calpain KO cell lines. (A) Representative blots showing the expression of Calpain 1, 2 and 4 in MDA-MB-231 WT and calpain KO cell lines. B-actin was used as a loading control. (B) Cell growth curves for the cell lines in normoxic growth conditions. Data represent the average number of cells/well ± SD of three independent experiments each conducted in triplicate. (C) Doubling times for each cell line were calculated from the growth curves and plotted. Data represents the average doubling times ± SD of three independent experiments. Statistical analysis was carried out using the Student's *t*-test *****(*P*<0.05), ****** (*P*<0.01), ******* (*P*<0.001).

For Western blotting, B-actin was used as a loading control and with expression indicated by a band at 42kDa (Figure 4.1A). Calpain 1 protein expression, with a band at approx. 80 kDa, was seen in MDA-MB-231 WT and Capn2 KO cells, but not in Capn1 or Capns1 KO cells. Calpain 2 protein expression was seen in MDA-MB-231 WT and Capn1 KO, but not in Capn2 or Capns1 KO cells, by the presence of bands at approx. 80 kDa. Calpain 4 expression was seen in MDA-MB-231 WT, Capn1 KO and Capn2 KO cells, but not in Capns1 KO cells, by the presence of a band at 28 kDa. No bands were seen in Capns1 KO cells lines, indicating that knocking out Capns1 also disrupts Capn1 and Capn2 expression. This confirms that these Capn1, Capn2 and Capns1 CRISPR/Cas9 KO cell lines were knocked out for their respective genes.

Growth curves were constructed for MDA-MB-231 WT, Capn1 KO, Capn2 KO and Capns1 KO (Figure 4.1B). Capn1 and Capn2 KO cell lines did not show any altered proliferation compared to their WT counterpart. However, the Capns1 KO cell line showed decreased proliferation compared to WT cells. Doubling time for each line was calculated from the growth curves (Figure 4.1C). The average cell doubling times was 27±2.45 hours in MDA-

MB-231 WT which is in agreement with results obtained previously by our group using a separate population of MDA-MB-231's (doubling time of 20±2.47 hours in MDA-MB-231 cells (Aiyappa, 2020)) and with the published literature (Watanabe *et al.*, 2001)). Capn1 KO cells had an average doubling time of 29±8.04 hours, Capn2 KO cells had an average doubling time of 30.5±0.5 hours and Capns1 KO cells had a significantly higher average doubling time of 82.67±5.44 hours (P=0.0001). Table 4.2 shows a summary of average doubling times of each of the cell lines.

The plating efficiency is defined as the inherent quality of cells to reproduce when the growth conditions remain constant (Franken *et al.*, 2006; Pomp *et al.*, 1996). The PEs of the lines were assessed by clonogenic survival assay (Figure 4.2).

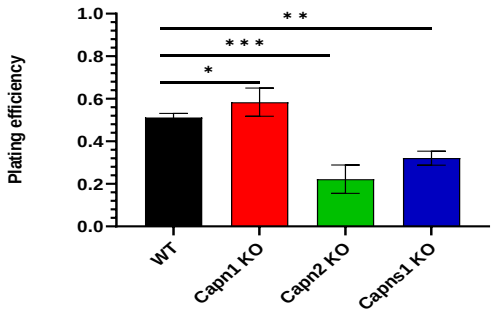

Figure 4. 2 Plating efficiencies for the MDA-MB-231 WT and calpain KO cell lines. Data represents the average plating efficiencies ± SD of three independent experiments, each conducted in triplicate. Statistical analysis was carried out using the Student's *t*-test * (P<0.05), ** (P<0.01), *** (P<0.001).

MDA-MB-231 WT had a plating efficiency of 51.2±1.2%. which is comparable with results previously obtained in the lab with a different MDA-MB-231 WT population (51.5±5.7% (Aiyappa, 2020)) and with the published literature (52.83±7.41% (Zhang *et al.*, 2014)). Capn1 KO cells had a marginally higher plating efficiency of 58.4±1.3% (P=0.05). Capn2 KO and Capns1 KO cells had significantly reduced colony forming abilities, PE's 22.2±6.5% (P=0.001) and 32.1±5.2% (P<0.01) respectively, compared to the WT cells. Table 4.2 summarises the doubling times and the plating efficiency for each of the cell lines.

Table 4. 2 Table summarising the DT and PE for WT and calpain KO cells.

Cell lines	Doubling time	Plating efficiency
MDA-MB-231 WT	27±2.45 hours	51.2±1.2%
Capn1 KO	29±8.04 hours	58.4±1.3%
Capn2 KO	30.5±0.5 hours	22.2±6.5%
Capns1 KO	82.6±5.4 hours	32.1±5.2%

To summarise knocking out either calpain 1 or 2 in human breast cancer cells does not affect cell proliferation however, knocking out both via calpain 4 renders a significant growth reduction. Knocking out calpain 1 does not have an effect on the colony forming ability of cells, but knocking out calpain 2 significantly reduces the plating efficiency of these cells. This may, as regulation of cellular adhesion and migration is partially dependent on intracellular calpain 2 activity, be due to low attachment of these cells. Calpain 4 KO cells also demonstrated a significant lower plating efficiency but this may be due to reduced proliferation in addition to decreased attachment in this cell line. It would be interesting to extend the incubation time to over 14 days to further investigate this.

4.4.2 Effect of knocking out calpains on doxorubicin response

Calpain 1, calpain 2, and calpain 4 KO breast cancer cell lines were treated with the chemotherapeutic drug doxorubicin to test the effect on treatment response. The effect of doxorubicin response was assessed in terms cell proliferation and clonogenic cell survival. Proliferation dose response curves are shown in Figure 4.3.

As expected, treatment of WT MDA-MB-231 cells with doxorubicin for 24 hours (Figure 4.3A) reduced the percentage cell number and this effect was also seen at 48 hours (Figure 4.3B) and 72 hours (Figure 4.3C) compared to the respective untreated control. Calpain 1 KO cells treated with doxorubicin did not show a significantly different effect on doxorubicin response at 24 hour (Figure 4.3A), 48 hour (Figure 4.3B) or 72 hour (Figure 4.3C) time points compared to the WT cells. Doxorubicin treatment of calpain 2 and calpain 4 KO cells resulted in significant reduction in cell number at 24 hour time point (Figure 4.3A) compared to the WT cells but

this effect was however not maintained at 48 hour or 72 hour time points suggesting it may be of marginal biological significance.

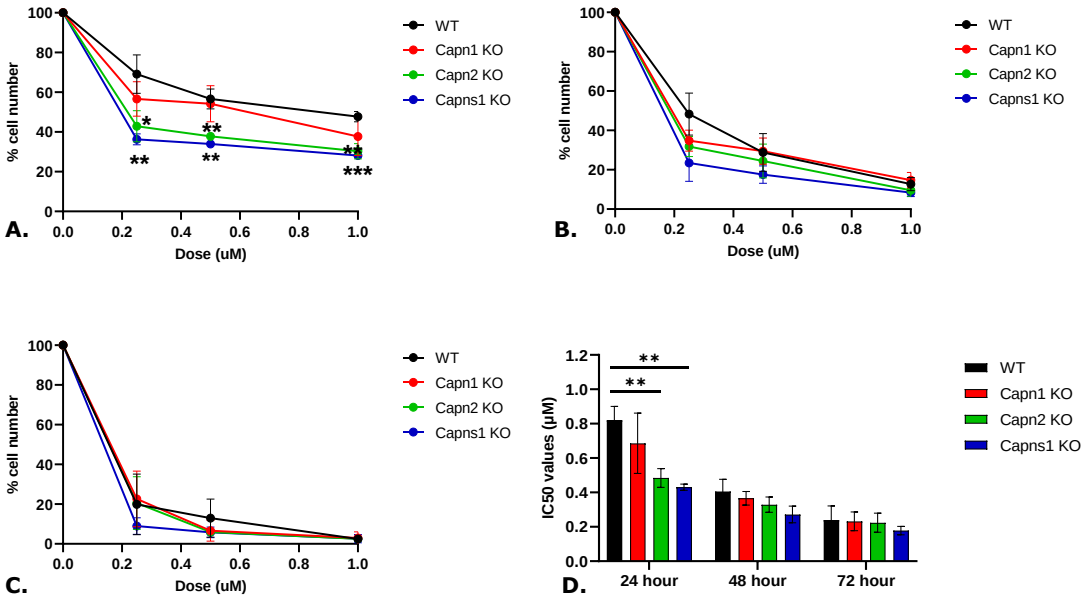

Figure 4. 3 Effect of knocking out calpains on doxorubicin response on cell proliferation. MDA-MB-231 WT and calpain KO cells were treated with doxorubicin for (A) 24 hours, (B) 48 hours, and (C) 72 hours. The IC50 values (D) were plotted for each time point for each cell line. The graphs represent the average data ± SD from three independent experiments, each conducted in triplicate. Statistical analysis was carried out using the Student's *t*-test *($P<0.05$), ** ($P<0.01$), *** ($P<0.001$).

The IC_{50} values for each time point was calculated from the dose response curves (Figure 4.3D). The effect seen above was reflected in the IC_{50} values. The average IC_{50} values were 0.82±0.08 µM at 24 hour, 0.41±0.07 µM at 48 hour, and 0.24±0.08 µM at 72 hour time points for the MDA-MB-231 WT cell line. These values are similar to the results obtained previously by the colleagues in the lab (Abdullah, 2019) and in the published literature (Abdullah, 2019; Pichot *et al.*, 2009; Pilco-Ferreto *et al.*, 2016; Wu *et al.*, 2013). The average IC_{50} values for the Capn1 KO, Capn2 KO and Capns1 KO cells were- 0.69±0.18 µM, 0.37±0.04 and 0.23±0.05 µM; 0.48±0.05 µM, 0.33±0.04 µM and 0.22±0.06 µM; 0.43±0.02 µM, 0.27±0.05 µM and 0.18±0.02 µM for 24 h, 48 h and 72 h time points, respectively. The IC_{50} values for Capn2 KO cells and Capns1 KO cells were significantly lower than the MDA-MB-231 WT cells at 24 h $P<0.01$ and $P<0.01$, respectively. No significant difference was seen between the IC_{50} values at 48 hour or 72 hour time points (Fig 4.3D).

The effect of knocking out calpains on doxorubicin response in terms of clonogenic survival was determined in MDA-MB-231 WT and calpain KO cells treated with different doses (0, 5, 10, 20, 50, and 100 nM) of doxorubicin for 24 hours. Results are shown in Figure 4.4.

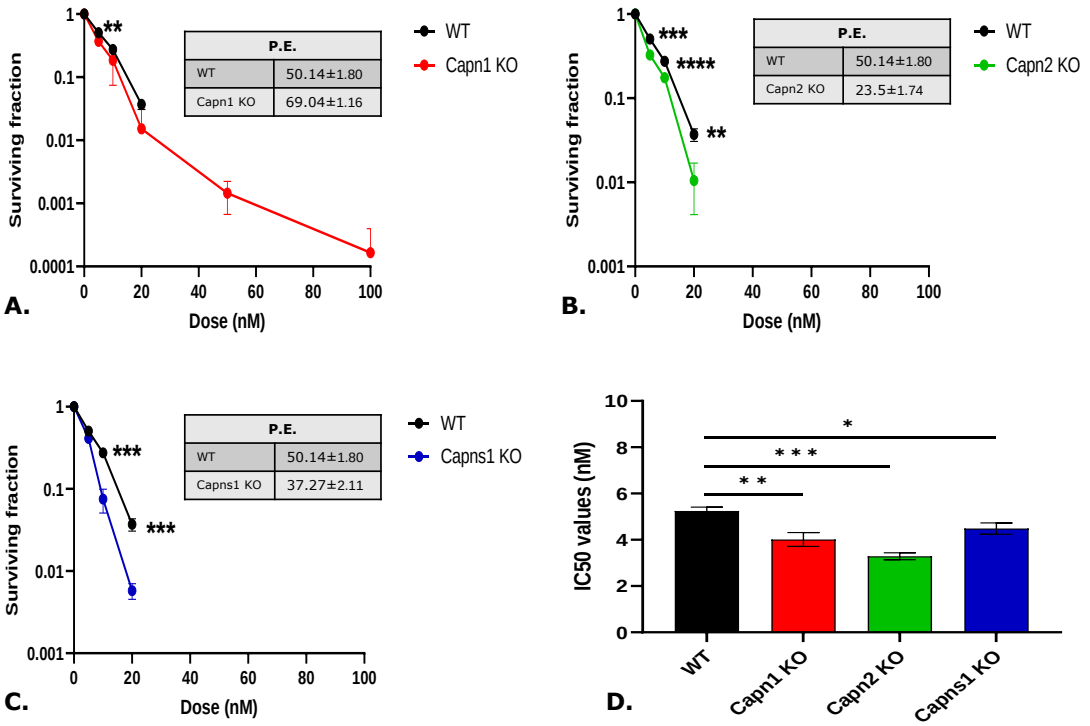

Figure 4. 4 Effect of knocking out calpains on doxorubicin response on cell survival. MDA-MB-231 WT and calpain KO cells were treated with doxorubicin for 24 hours and clonogenic assays were done to assess the effect on cell survival. The surviving fractions were plotted (A) WT vs Capn1 KO, (B) WT vs Capn2 KO, and (C) WT vs Capns1 KO. The IC50 values (D) were calculated for each cell line. The inset table shows the plating efficiencies for each cell line. The graphs represent the average data ± SD from three independent experiments, each conducted in triplicate. Statistical analysis was carried out using the Student's *t*-test *(P<0.05), ** (P<0.01), *** (P<0.001).

The PE calculated for the MDA-MB-231 WT cells was 50.14±1.80% which was in agreement with previously reported data in the lab and in the literature (mentioned in section 4.4.1). Doxorubicin treatment for 24 hours reduced the surviving fraction significantly in the MDA-MB-231 WT cells compared to their untreated controls. Capn1 KO cells were sensitive at lower doses of doxorubicin however had no effect on overall response compared to the WT cells. Capn2 and Capns1 KO caused significant sensitisation to doxorubicin treatment with surviving fractions of 0.3±0.01 (P<0.001), 0.2±0.01 (P<0.0001) and 0.01±0.01 (P=0.01) in Capn2 KO cells and 0.4±0.06 (P=0.06), 0.07±0.02 (P<0.001) and 0.01 (P<0.001) in

Capns1 KO cells at 5 nM, 10 nM and 20 nM, respectively compared to the WT surviving fractions. The IC_{50} values were calculated from using survival curves for all the cell lines (Figure 4.4D). MDA-MB-231 WT cells had an IC_{50} of 5.2±0.17 nM. Capn1 KO, Capn2 KO and Capns1 KO cells had significantly lower IC_{50} values of 4.0±0.30 (P<0.01), 3.3±0.15 (P<0.001) and 4.5±0.25 (P<0.05), respectively.

To summarise, knocking out calpain 2 and calpain 4 caused significantly decreased cell counts at 24 hours of treatment, which was not carried on to 48 and 72 hour treatments. While marginal chemosensitisation was seen with Capn2 and Capns1 KO cells with them having significantly lower surviving fractions compared to the WT cells. Knocking out calpain 1 had no effect on doxorubicin cell proliferation or clonogenic survival.

4.4.3 Cell proliferation and plating efficiency in hypoxic growth conditions

Cells were grown in the hypoxic chamber (1% O_2) for a period of 0-96 hours with cells harvested and counted every 24 hours. Growth curves were plotted (Figure 4.5A) and doubling times were calculated where possible (Figure 4.5C). The presence of hypoxia was confirmed by CA9 protein expression, analysed by Western blotting (Figure 4.5B). β-actin was used as a loading control. Effect of hypoxia on plating efficiency was assessed by clonogenic assays (Figure 4.5D). Parallel experiments were performed in normoxic conditions (21% O_2) for comparison (Figure 4.5).

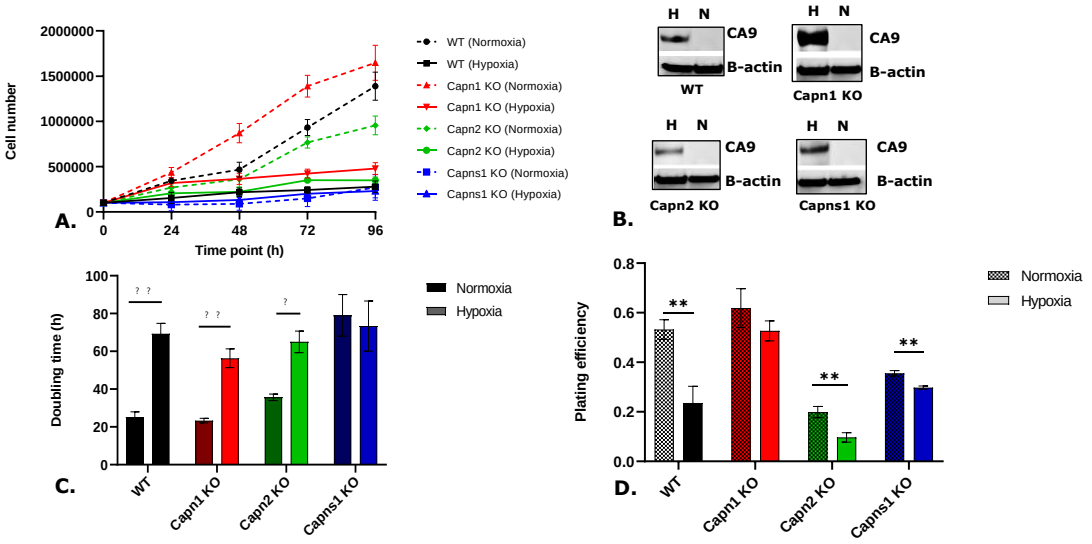

Figure 4. 5 Cell growth curves, doubling times and Plating efficiencies of the MDA-MB-231 WT and calpain KO cell lines in the presence of normoxia (21% O2) and hypoxia (1% O2). (A) Cell growth curves for the WT and calpain KO cells (B) Representative images for blots showing expression of CA9 in (H) hypoxia and (N) normoxia with B-actin used as a loading control (C) Doubling times for each cell line were calculated form the growth curves (D) Plating efficiencies for the WT calpain KO cell lines. The graphs represent the average data ± SD from three independent experiments, each conducted in triplicate. Statistical analysis was carried out using the Student's *t*-test *(P<0.05), ** (P<0.01), *** (P<0.001).

In normoxia (21%O2), the MDA-MB-231 WT and the calpain KO cells had similar growth rates as seen previously in section 4.4.1. The Capn1 KO and Capn2 KO cells had growth rates similar to the WT cells while the Capns1 KO cells had a significant reduced rate of proliferation compared to the WT cells. After hypoxic treatment (1% O2), growth rate was significantly reduced in MDA-MB-231 WT, Capn1 KO and Capn2 KO cells when compared to growth in normoxia (21% O_2). Capns1 KO cells had a similar rate of proliferation in normoxic (21%O_2) and hypoxic (1%O_2) growth conditions (Fig.4.5A). CA9 protein expression was seen in all the cell lines grown in hypoxia. No CA9 bands were observed for cells in normoxia (Figure 4.5B). The cell doubling times were calculated from the growth curves constructed (Figure 4.5C). The hypoxic doubling times were significantly higher than the normoxic doubling times. The doubling times in hypoxia vs normoxia were - 69.34±5.44 hours and 25±2.94 hours (P=0.01) for MDA-MB-231 WT cells, 56.34±4.92 hours and 23.34±1.25 hours (P<0.01) for Capn1 KO cells, 65±5.72 hours and 35.67±1.70 hours (P=0.03) for Capn2 KO cells. No difference in was observed in Capns1 KO doubling times between normoxia

and hypoxia, 73.34±13.3 and 79±11, respectively. The above values have been presented in Table 4.3. As expected, these results indicate that hypoxia reduces the rate of cell proliferation.

The effect of hypoxia on the colony forming ability of cells (PE) was also assessed (1% O2 24 h v normoxia, 21% O2) (Figure 4.5D). PEs of hypoxic cells were significantly lower than that of the normoxic cells for MDA-MB-231 WT 23.56±6.72% and 53.23±3.97% (P<0.01), Capn2 KO 9.67±1.91% and 19.89±2.28% (P<0.01) and Capns1 KO 29.78±0.68% and 35.56±1.1% (P<0.01) for hypoxia and normoxia, respectively. No difference in the PEs was seen for the Capn1 KO cells with the PEs of 52.67±4.03% and 61.89±7.82% (P=0.21) in hypoxia and normoxia, respectively. The above values are presented in Table 4.3.

Table 4. 3 Summary of doubling times and plating efficiencies hypoxia (1%O2) vs normoxia (21% O2)

Cell lines	**Doubling time (hours)**		**Plating efficiency (%)**	
	Normoxia (21% O2)	Hypoxia (1% O2)	Normoxia (21% O2)	Hypoxia (1% O2)
WT	25±2.94	69.34±5.44 **(*P*<0.01)**	53.23±3.97	23.56±6.72 **(*P*<0.01)**
Capn1 KO	23.34±1.25	56.34±4.92 **(*P*<0.01)**	61.89±7.82	52.67±4.03
Capn2 KO	35.67±1.70	65±5.72 **(*P*<0.05)**	19.89±2.28	9.67±1.91 **(*P*<0.01)**
Capns1 KO	79±11	73.34±13.3	35.56±1.1	29.78±0.68 **(*P*<0.01)**

The above results suggest that hypoxia reduces the rate of cell proliferation and the ability of cells to form colonies, with effects particularly evident in the WT, Capn1 KO and Capn2 KO cells which had a significantly reduced rate of cell growth and a significantly higher doubling times (Table 4.3) in hypoxia. The PEs were also seen to be significantly lower in MDA-MB-231 WT, Capn2 KO and Capns1 KO cells in hypoxia compared to their normoxia counterparts.

4.4.4 Effect of knocking out calpains on doxorubicin response in hypoxia

Cells were grown in hypoxic conditions (1% O_2) for a period of 24 hours then treated with different doses of doxorubicin (0, 0.25, 0.5, and 1 μM) for a period of 24-72 hours. After every 24 hours of doxorubicin treatment, cells were harvested, counted and dose response curves constructed, and IC_{50} values were calculated where possible (Figure 4.6).

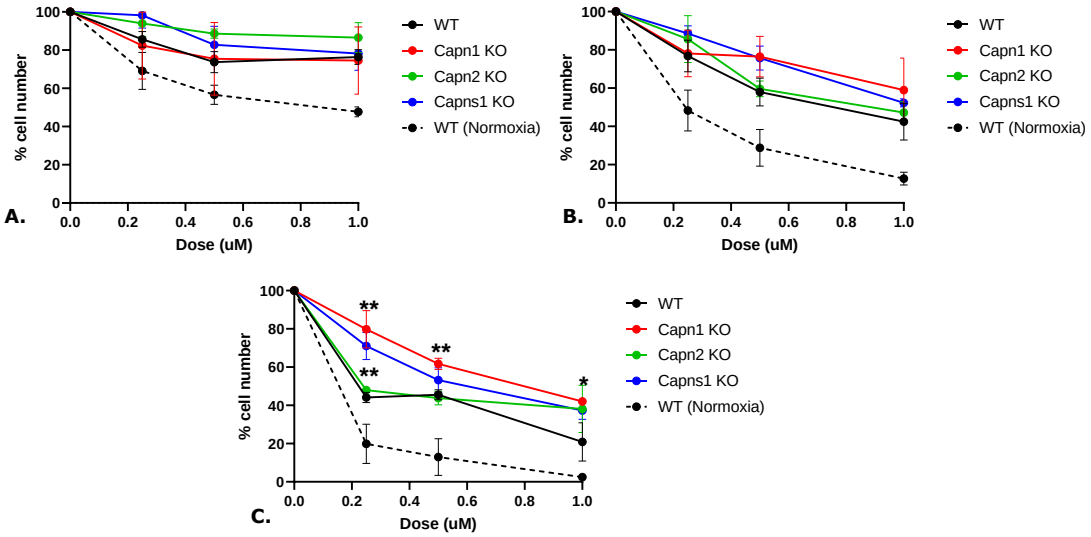

Figure 4. 6 Effect of knocking out calpains on doxorubicin response on cell proliferation in hypoxia (1% O2). MDA-MB-231 WT and calpain KO cells were treated with doxorubicin for (A) 24 hours, (B) 48 hours, and (C) 72 hours in the presence of 1% of O2. The graphs represent the average percentage number of cells ± SD from three independent experiments, each conducted in triplicate. Statistical analysis was carried out using the Student's *t*-test *(P<0.05), ** (P<0.01), *** (P<0.001).

MDA-MB-231 WT dose response in hypoxia was compared with the MDA-MB-231 WT dose response in normoxia (black dotted curve, Figure 4.6). The hypoxic WT cells showed approximately 20% inhibition in cell proliferation. While the normoxic WT cells had approximately 40% inhibition of cell proliferation at 0.5 μM doxorubicin treatment for 24 hours. At 48 hour and 72 hour time points, the hypoxic WT cells had approximately 40% and 50% inhibition in cell proliferation respectively, while the normoxic counterparts had approximately 70% and 80% inhibition in cell proliferation, respectively at 0.5 μM of doxorubicin treatment. The WT cells were relatively resistant to doxorubicin treatment at 24, 48 and 72 hours in hypoxia, compared to the WT response in normoxia. The Capn1, Capn2

and Capns1 KO cells did not alter doxorubicin proliferation response compared to WT cells in hypoxia at 24 and 48 hour time points. However at 72 hours Capn1 KO cell lines were seen to be significantly overall resistant to doxorubicin compared to the WT cells in the presence of hypoxia, while Capns1 KO cells were seen to resistant only at the low dose. The hypoxic IC_{50} doses were calculated where possible and compared with the normoxic IC_{50} doses. The calculated hypoxic IC_{50} doses were significantly higher than the normoxic doses. Table 4.4 summarises the normoxic and hypoxic IC_{50} values for 24 h, 48 h, and the 72 h time points for all the cell lines.

Table 4. 4 Normoxic (21% O2) vs hypoxic (1% O2) proliferation IC_{50} values.

Cell line	24 hour IC50 values (µM)		48 hour IC50 values (µM)		72 hour IC50 values (µM)	
	Normoxia	Hypoxia	Normoxia	Hypoxia	Normoxia	Hypoxia
WT	0.82 ± 0.08	> 1	0.40 ± 0.07	> 1	0.23 ± 0.08	0.60 ± 0.1
Capn1 KO	0.69 ± 0.18	> 1	0.37 ± 0.04	> 1	0.23 ± 0.05	0.80 ± 0.05
Capn2 KO	0.48 ± 0.05	> 1	0.33 ± 0.04	0.89 ± 0.03	0.22 ± 0.05	0.62 ± 0.15
Capns1 KO	0.43 ± 0.02	> 1	0.27 ± 0.04	> 1	0.17 ± 0.01	0.70 ± 0.08

To test the effect of hypoxia (1%O_2) on doxorubicin clonogenic survival cells were treated with 1% O_2 for 24 hours following which the cells were treated with different doses of doxorubicin for 24 hours then plated and allowed to form colonies for two weeks (Figure 4.7).

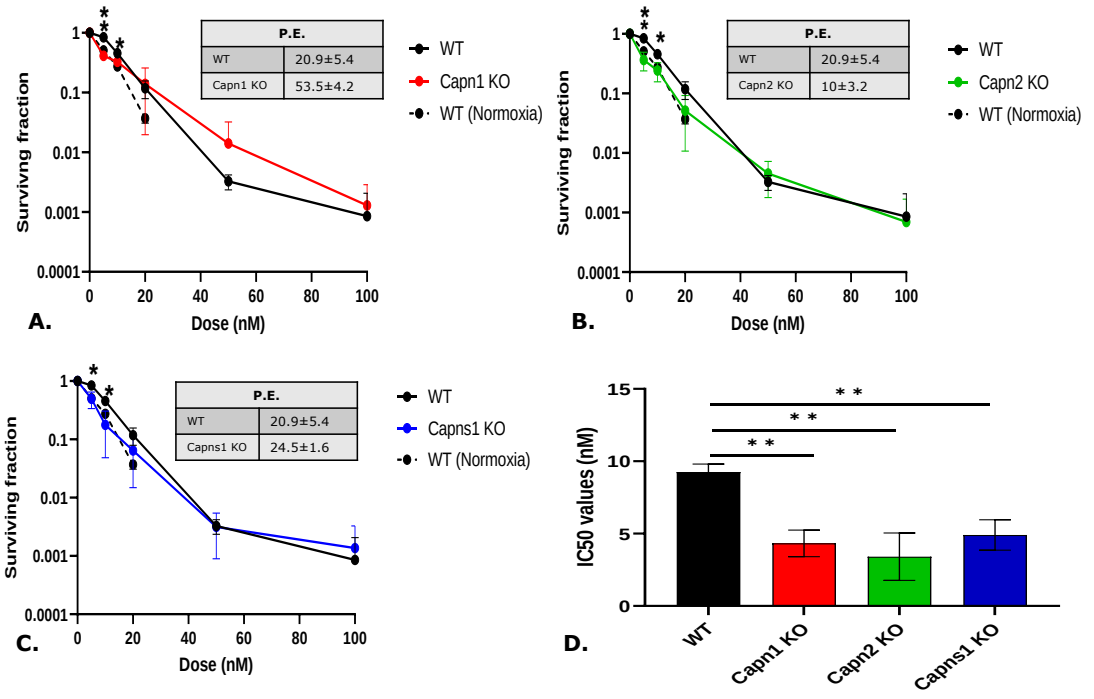

Figure 4. 7 Effect of knocking out calpains on doxorubicin response on clonogenic cell survival in hypoxia (1% O2). MDA-MB-231 WT and calpain KO cells were tested for the effect on doxorubicin survival under hypoxic conditions. The surviving fractions were plotted (A) WT vs Capn1 KO, (B) WT vs Capn2 KO, and (C) WT vs Capns1 KO. The IC50 values (D) were calculated for each cell line. The graphs represent the average data ± SD from three independent experiments, each conducted in triplicate. Statistical analysis was carried out using the Student's *t*-test *(*P*<0.05), ** (*P*<0.01), *** (*P*<0.001).

The MDA-MB-231 WT cells treated with doxorubicin in hypoxia were slightly more resistant compared to their normoxic counterparts. Calpain KO response did not vary substantially from WT responses, however there was evidence of some altered sensitivity at lower doses; *P*<0.01 and *P*<0.05 for Capn1 KO cell line, *P*=0.01 and *P*<0.05 for Capn2 KO cell line and *P*=0.05 and *P*<0.04 for Capns1 KO cell line for 5 nM and 10 nM doses. However, no difference in overall response was observed between the calpain KO cells and the WT cells in the presence of hypoxia. The IC_{50} doses were calculated from the survival curves and were compared between the WT and the calpain KO cell lines (Figure 4.7D). Capn1 KO, Capn2 KO and Capns1 KO cells had small but significantly lower (*P*<0.01) IC_{50} doses compared to WT cells.

To summarise MDA-MB-231 WT cells showed significant resistance to doxorubicin treatment in the presence of hypoxia compared to normoxia. However, no overall difference was observed in Capn1 KO, Capn2 KO and

Capns1 KO cells compared to the WT cells for doxorubicin proliferation and clonogenic survival response in the presence of hypoxia (1% O2).

4.4.5 Effect of hypoxia and normoxia on radiation response in calpain knock out cells

The response to radiotherapy on the MDA-MB-231 WT and calpain KO cells was assessed in the presence of hypoxia (1% O_2 for 24h) and normoxia (21% O_2). MDA-MB-231 WT, Capn1 KO, Capn2 KO and Capns1 KO cells were exposed to different doses of radiation. The surviving fraction dose response curves were plotted using the Linear Quadratic Model. Radiation treatments were conducted in parallel for hypoxia and normoxia grown cells

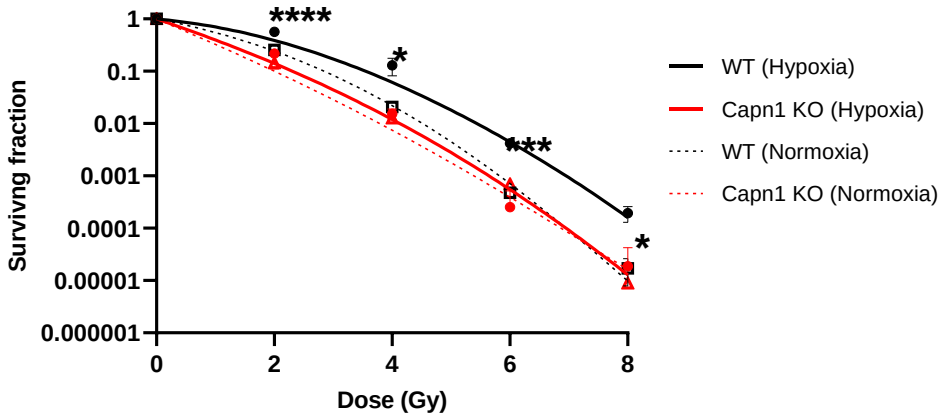

Figure 4. 8 MDA-MB-231 WT and calpain 1 KO cell lines response to radiotherapy. Radiation response in normoxic (21% O2) and hypoxic conditions (1% O2). The survival curves for each cell lines were fitted according to the Linear Quadratic Model. Data represent the average surviving fraction ± SD of three independent experiments each conducted in triplicate. Statistical analysis was carried out using the Student's *t*-test *(*P*<0.05), ** (*P*<0.01), *** (*P*<0.001).

In normoxia, the WT cells had a PE of 50.67±3.8%, an α/β value of 6.23±5.67% and a SF2 of 0.24±0.08 (Table 4.5). These parameters are in agreement with the previously generated data in the lab by Dr. Aiyappa with an α/β value of 7.50±5.35 and an SF2 value of 0.33±0.10 (Aiyappa, 2020). In hypoxia WT cells were, as expected, more resistant to radiation with an $OER_{0.01}$ of 1.42±0.29 (Table 4.8) (Figure C3.7, Appendix C) a PE of 18.4±2.05% an α/β of 2.36±1.82 and an SF2 of 0.39±0.09 (Table 4.5).

Table 4. 5 PEs and radiobiological parameters for WT and Capn1 KO cells.

		PE	Radiobiological parameters			
			α	β	α/β	SF2
WT	Normoxia Hypoxia	50.67±3.8% 18.43±2.05%	0.51±0.28 0.24±0.15	0.12±0.04 0.12±0.03	6.23±5.67 2.36±1.82	0.24±0.08 0.39±0.09
Capn1 KO	Normoxia Hypoxia	57.67±4.2% 49.1±2.9%	0.86± 0.06 0.89±0.25	0.07±0.01 0.07±0.02	19.29±9.47 19.09±9.32	0.14±0.02 0.14±0.06

Such data is in agreement with the previously generated data in the lab with the hypoxic α/β value of 3.69±91 and an SF2 of 0.61±0.10 for MDA-MB-231 WT cells treated with hypoxia (1% O2) for 24 hours followed by radiation treatment. The $OER_{0.01}$ value for MDA-MB-231 WT cells in normoxic and hypoxic conditions was 1.40±0.06 (Aiyappa, 2020).

In normoxic conditions (21% O2) Capn1 KO had no effect on radiation response compared to WT cells. However, in hypoxic conditions (1% O2) the Capn1 KO cells exhibited a significant increased radiosensitisation all doses (P<0.0001 for 2 Gy, P<0.05 for 4 Gy, P<0.001 for 6 Gy and P<0.05 for 8 Gy) (Figure 4.8). Capn1 KO cells were therefore sensitised to radiation treatment compared to the WT cells in hypoxia with the SF2 of 0.39±0.09 for WT cells and 0.14±0.06 for Capn1 KO cells (P<0.05) (Table 4.5), but not in normoxia with an $OER_{0.01}$ of 0.96±0.12 (Table 4.8, Figure C3.7, Appendix C).

Capn2 KO cells were resistant to radiation response compared to WT cells, especially evident at higher doses, in normoxic conditions (21% O2) (Figure 4.9). However, as with Capn1 KO's Capn2 KO cells had a significant overall radiosensitisation at all doses in hypoxia (P<0.0001 for 2 Gy, P<0.05 for 4 Gy, P<0.001 for 6 Gy and P=0.01 for 8 Gy) (Figure 4.9) yielding an SF2 of 0.39±0.09 for WT cells and 0.14±0.08 for Capn2 KO cells (P<0.05) (Table 4.6), and an $OER_{0.01}$ of 0.84±0.16 (Table 4.8, Figure C3.7, Appendix C).

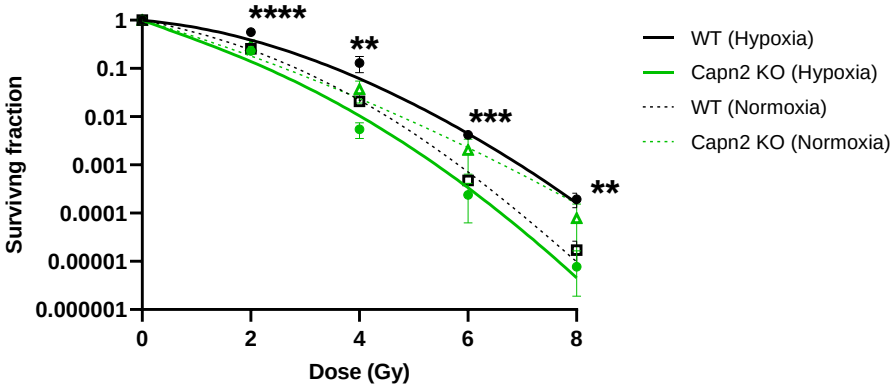

Figure 4. 9 MDA-MB-231 WT and calpain 2 KO cell lines response to radiotherapy. Radiation response in normoxic conditions (21% O2) and hypoxic conditions (1% O2). The survival curves for each cell lines were fitted according to the Linear Quadratic Model. Data represent the average surviving fraction ± SD of three independent experiments each conducted in triplicate. Statistical analysis was carried out using the Student's *t*-test *(*P*<0.05), ** (*P*<0.01), *** (*P*<0.001).

Table 4. 6 PEs and radiobiological parameters for WT and Capn2 KO cells.

		PE	Radiobiological parameters			
			α	β	α/β	SF2
WT	Normoxia Hypoxia	50.67±3.8% 18.43±2.05 %	0.51±0.28 0.24±0.15	0.12±0.04 0.12±0.03	6.23±5.67 2.361±1.82	0.24±0.08 0.39±0.09
Capn2 KO	Normoxia Hypoxia	26±2.9% 14.8±3.0%	0.72± 0.29 0.97±0.52	0.07±0.03 0.08±0.05	15.38±13.36 14.25±12.72	0.20±0.10 0.14±0.08

Capns1 KO cells were resistant to radiation response compared to the WT cells, in normoxic condition (21% O2) (Figure 4.10). However, in hypoxic conditions (1% O2) the Capns1 KO cells had sensitisation to radiation treatment but only at only lower doses (P<0.001 for 2 Gy and P<0.05 for 4 Gy) with no overall effect was seen compared to the WT cells (Figure 4.10); SF2 of 0.39±0.09 for WT cells and 0.19±0.10 for Capns1 KO cells (Table 4.7).

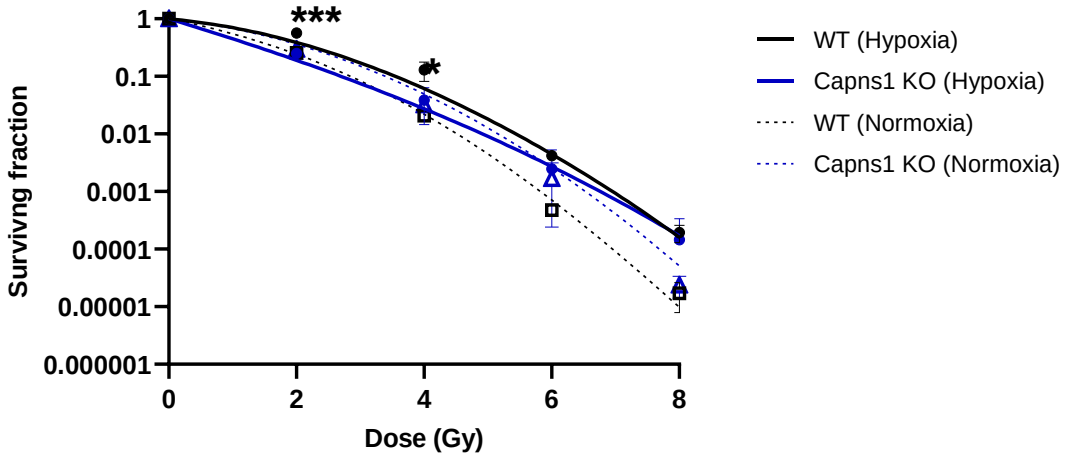

Figure 4. 10 MDA-MB-231 WT and calpain 4 KO cell lines response to radiotherapy. Radiation response in normoxic conditions (21% O2) and hypoxic conditions (1% O2). The survival curves for each cell lines were fitted according to the Linear Quadratic Model. Data represent the average surviving fraction ± SD of three independent experiments each conducted in triplicate. Statistical analysis was carried out using the Student's *t*-test *(*P*<0.05), ** (*P*<0.01), *** (*P*<0.001).

Table 4. 7 PEs and radiobiological parameters for WT and Capns1 KO cells.

		PE	Radiobiological parameters			
			α	β	α/β	SF2
WT	Normoxia Hypoxia	50.67±3.8% 18.43±2.05%	0.51±0.28 0.24±0.15	0.12±0.04 0.12±0.03	6.23±5.67 2.361±1.82	0.24±0.08 0.39±0.09
Capns1 KO	Normoxia Hypoxia	37.67±4.50% 22.34±2.35%	0.06±0.04 0.06±0.02	0.07±0.01 0.07±0.02	15.02±15.13 17.21±12.53	0.21±0.11 0.19±0.10

The Capns1 KO cells had an $OER_{0.01}$ of 1.03±0.07 (Table 4.8, Figure C3.7, Appendix C).

Table 4. 8 MDA-MB-231 WT and Calpain KO OER and SF8 values in normoxia and hypoxia

Cell line	OER	SF8	
		Normoxia	Hypoxia
MDA-MB-231 WT	1.42±0.29	9.81E-06±3.1E-06	1.6E-04±1.1E-04
Capn1 KO	0.96±0.12	2E-05±1E-05	1E-05±1E-05
Capn2 KO	0.84±0.16	6.44E-05±6.3E-05	4.57E-06±3.66E-06
Capns1 KO	1.03±0.07	2.5E-05±1.9E-05	1.7E-04±2E-04

Table 4. 9 MDA-MB-231 WT and Calpain KO radio enhancement values at 1% survival in normoxia and hypoxia

	Normoxia	Hypoxia
WT vs Capn1 KO	1.09±0.10	1.35±0.08
WT vs Capn2 KO	1.03±0.20	1.47±0.27
WT vs Capns1 KO	1.05±0.20	1.19±0.11

The SF8 values mentioned in the table 4.8 indicate the surviving fraction at 8 Gy for all the cell lines in normoxia (21% O2) and hypoxia (1% O2 for 24 h). The SF8 values of Capn1 KO and Capn2 KO cells were much lower compared to that of WT cells in hypoxic growth conditions (1% O2 for 24 h). The radio enhancement ratios were calculated at 1% survival between the WT and the calpain KO cells in normoxia (21% O2) and hypoxia (1% O2 for 24h) growth conditions (Table 4.9). The hypoxic enhancement ratios were much higher compared to the normoxic enhancement ratios between WT and Capn1 KO and WT and Capn2 KO cells, indicating a significant sensitisation in hypoxic growth conditions (1% O2 for 24 h).

To summarise, knocking out calpain 1 does not have an effect on radiation response in normoxia but makes cells sensitive to radiation in hypoxia. Knocking out calpain 2 and calpain 4 makes breast cancer cells somewhat resistant to radiation treatment in normoxia. However in hypoxia, knocking out calpain 2 makes breast cancer cells sensitive to radiation treatment and knocking out calpain 4 has little effect on hypoxic radiation response in breast cancer cells. Therefore, Calpain 1 and calpain 2 could potentially be used as therapeutic targets to sensitise hypoxic breast cancer cells to radiation.

4.5 Discussion

Calpain 1, calpain 2 and calpain 4 CRISPR/Cas9 knock out (KO) breast cancer MDA-MB-231 cells lines were used to assess the effect on cell behaviour and cellular treatment response. These cell lines were provided by our collaborator Professor P. Greer's at Queen's University, Ontario, Canada.

Several experiments were performed on these cell lines including cell characterisation, doxorubicin and radiation sensitivity assessments. Initial experiments with cell lines were unreliable when lines tested positive for

mycoplasma, with this being traced back to, and confirmed by, the originating lab. The cells were cleaned using the method described in section 4.3.2 and all experiments repeated or conducted anew with the cleaned population. Appendix C shows the comparison of data with mycoplasma negative and positive cell lines. Several significant differences were observed between the mycoplasma negative and positive cells. It is therefore critical to conduct regular mycoplasma checks to obtain reliable data.

The MDA-MB-231 WT and calpain KO cells were tested for calpain1, 2 and 4 protein expression by Western blotting. Calpain 1 bands were observed for WT and Capn2 KO cell lysates. Calpain 2 bands were observed in WT and Capn1 KO cell lysates, and calpain 4 bands were seen in the WT, Capn1 and Capn2 KO cell lysates. No bands were seen for calpain 4 KO cell lysates, indicating that knocking out the small subunit, calpain 4 results in the loss of both calpain 1 and calpain 2. Calpain 4 is the common small subunit for both μ- and m-calpain (Storr *et al.*, 2011a), so depleting calpain 4 abolishes expression of calpain 1 and calpain 2. Once cells were confirmed for their expression of calpains 1, 2 and 4 the effect of KO on cellular behaviour was assessed. The effect knocking out calpains on cell proliferation was assessed by proliferation assay. MDA-MB-231 WT, Capn1 KO and Capn2 KO cells had similar growth rates. However, Capns1 KO cells had a significantly inhibited rate of cell proliferation, as reflected by the cell doubling times. MDA-MB-231 WT cells had a doubling time of 27±2.45 hours. This data is in agreement with results previously obtained in the group, Dr. Aiyappa demonstrated that MDA-MB-231 WT cells had a doubling time of 20±2.47 hours (Aiyappa, 2020). In a study by Watanabe et al, the doubling time was 28.1±1.2 hours in MDA-MB-231 cells (Watanabe *et al.*, 2001). Knocking out calpain1 and calpain 2 in breast cancer cells did not have any significant effect on rate of cell proliferation. However, with a significantly high doubling time of 82.6±5.4 hours, Capns1 KO cells had significant reduced rate of cell proliferation. Knocking out calpain 4 destabilises both the subunits, Capn1 and Capn2 and hence has a significant effect on certain cellular activities. MacLeod et al. demonstrated that deletion of Capns1 effectively lead to the loss of calpain 1 and calpain 2 activity, blocked

tumorigenesis in mammary tumour epithelial cell line (MTEC) in an orthotropic engraftment model, and delayed the onset of tumours to a mean of 79 days, while the WT had tumour onset with the mean time of 29 days (MacLeod *et al.*, 2018). In another study, Grieve et al. showed that knocking down calpain 4 lead to attenuated growth of tumours at the orthotopic site in a human triple negative breast cancer xenograft model (Grieve *et al.*, 2016).

Plating efficiency is described as the inherent ability of the cells to reproduce, retaining clonogenic potential. The MDA-MB-231 WT cells had a plating efficiency of 51.2±1.2%, which was in agreement with the previously obtained data in the lab, 51±5.70% (Aiyappa, 2020) and in literature, 52.83±7.43% (Zhang *et al.*, 2014). Capn1 KO MDA-MB-231 cells had a marginally increased PE of 58.4±1.3%. Although this was statistically significant (P=0.05) there may be no difference biologically while the Capn2 KO cells had a significantly lower PE (22.2±6.5%, P=0.001) compared to the WT cells. Calpain 2 has shown to be associated with regulating focal adhesion dynamics (Chan *et al.*, 2010; Franco *et al.*, 2004; Saraiva *et al.*, 2013). It is thought that knocking out of calpain 2 may lead to reduced cell adhesion or attachment. Therefore a reduced plating efficiency in calpain 2 KO cell lines may be a consequence of reduced adhesion in these cells. In a study, Xu and colleagues have reported that the colony forming ability of A549 and 95D cells was significantly reduced by the siRNA knock down of calpain 2 (Xu *et al.*, 2019). Capns1 KO cells also had a reduced plating efficiency of 32.1±5.2% (P<0.01) compared to the WT cells. Owing to their reduced rate of cell proliferation, (Grieve *et al.*, 2016; MacLeod *et al.*, 2018) they may not have been able to develop into colonies within the 2-week period. In addition knocking out calpain 4 also results in disruption of calpain 2 expression. Disruption in calpain 2 expression may also have a knock on effect on calpain 4 KO cells and contribute to decreased plating efficiency.

The effect of knocking out calpains on breast cancer cellular response to doxorubicin was assessed in MDA-MB-231 WT and calpain KO cells. MDA-MB-231 WT and Capn1 KO, Capn2 KO and Capns1 KO cells were treated with doxorubicin for 24-72 hours. MDA-MB-231 WT had reduced percentage

cell number, with approximately 40% inhibition of cell proliferation seen at 0.5 μM after 24 hours of doxorubicin treatment. This effect was seen to carry on to 48 hour and 72 hour treatments with a notable increase in cell kill of approximately 70% and 80%, respectively. The IC_{50} doses were 0.81±0.08 μM for 24 hour, 0.40±0.07 μM for 48 hour, and 0.23±0.08 μM for 72 hour doxorubicin. This data is in agreement with the previously published work with doxorubicin proliferation IC_{50} values ranging from 0.02-1 μM for a period of 72 hours in MDA-MB-231 cells (Pichot *et al.*, 2009; Pilco-Ferreto *et al.*, 2016; Wu *et al.*, 2013).

Knocking out calpain 1 did not have an effect on doxorubicin proliferation response at 24 hour, 48 hour or 72 hour time points when compared to the WT cells which was reflected in the IC_{50} values, 0.69±0.18 μM for 24 hour, 0.37±0.04 μM for 48 hour, and 0.23±0.05 μM for 72 hour doxorubicin treatments. The Capn2 KO and Capns1 KO cells however, had a significant inhibition in cell proliferation (about 60%) with 0.5 μM doxorubicin treatment for 24 hours compared to the WT cells (40% inhibition). This effect was not seen at 48 and 72 hour time points for these cells. A significant reduction ($P<0.01$) in the IC_{50} doses was observed at only 24 hour doxorubicin treatment compared to the WT cells suggesting that inhibition seen at 24 hour treatment may be a result of the lower plating efficiency of the calpain 2 KO cells but once established and growing there is little effect seen. Similar data was obtained with calpain 4 KO ie no effect was seen at 48 hours and 72 hours of doxorubicin treatment. MacLeod and colleagues demonstrated, however, that knocking out calpain 4 significantly sensitised MTECs to 72 hour doxorubicin treatment (MacLeod *et al.*, 2018). This discrepancy in data could be attributed to the use of different assays, endpoints, and cell lines.

Proliferation assays may not reflect the overall effect on cell survival. Therefore to assess the effect of knocking out calpains on doxorubicin cell survival, clonogenic assays were done on the MDA-MB-231 WT and calpain KO cells were treated with doxorubicin for 24 hours. The plating efficiency for MDA-MB-231 WT cells was 50.14±1.80% which was in agreement with previously reported data in the lab and in the literature (mentioned in section 4.4.1). The Plating efficiencies for all the calpain KO cell lines were

in agreement with the results obtained in section 4.4.1. A sharp decrease in the surviving fraction of MDA-MB-231 WT cells was seen compared to the untreated cells, with no colonies surviving at higher doses ie WT cells appear much more sensitive to doxorubicin when clonogenic survival is used as an endpoint rather than short-term proliferation. A similar pattern was observed previously in the group by Dr. Abdullah (Abdullah, 2019), reinforcing the necessity of conducting both proliferation and clonogenic survival assays when investigating drug sensitivities. Calpain 1 KO cells showed significant sensitisation at 5 nM of doxorubicin treatment, however no overall effect was observed in the calpain 1 KO response compared to the WT cells. Knocking out calpain 2 resulted in significant sensitisation of the MDA-MB-231 cells line compared to the WT cells at 5 nM ($P<0.001$), 10 nM ($P<0.0001$) and 20 nM ($P=0.01$) with no surviving colonies for 50 nM or 100 nM. However statistically significant, the separation in surviving curves suggests that the biological effect may be small. The Capns1 KO cells treated with doxorubicin for 24 hours demonstrated significant sensitisation at 10 nM ($P<0.001$) and 20 nM ($P<0.001$) compared to the WT cells, with no surviving colonies at 50 nM or 100 nM treatment. Such data suggests that knocking out calpain 4 may have a sensitising effect on doxorubicin cell survival.

The presence of hypoxia determines the response to many therapies in cancer. Hypoxia has also shown to regulate calpain activation in cells (Storr *et al.*, 2011a). MDA-MB-231 WT and calpain KO cell lines were grown in the presence of hypoxia (1% O2) for 96 hours and growth curves constructed to determine the effect of hypoxia on cell proliferation. Normoxic experiments were run in parallel. Normoxic MDA-MB-231 WT cells were seen to have an expected proliferation rate and doubling time, similar to the results obtained in section 4.4.1 and in the published literature. The hypoxic WT cells had a significantly reduced rate of cell proliferation and a higher doubling time (69.34±5.44 hours, $P=0.01$). Normoxic Capn1 KO and Capn 2 KO cells had expected cell growth rates and doubling times from experiments conducted previously in section 4.4.1 however, when grown in hypoxia they had significantly reduced growth rates and higher doubling times (56.34±4.92 hours, $P<0.01$) and (65±5.72 hours, $P=0.03$).

Normoxic Capns1 KO cells had similar growth rate and doubling times as obtained previously in section 4.4.1. However, when grown in hypoxia they showed little change in proliferation or doubling time compared to those grown in normoxia (73.34±13.3 hours). This may be a reflection of cells altered growing at a much reduced rate, due to Calpain 4 KO, with hypoxia causing little additional effect.

Such data are in agreement with previously published literature which suggests that presence of hypoxia results in decreased cell proliferation and higher doubling times in breast cancer cells (Song *et al.*, 2018). It has been shown that depletion of oxygen concentration below 10 mmHg leads to acidosis, depletion of ATP and energy supply which may affect proliferation in hypoxic cell culture (Höckel *et al.*, 1991). The presence of hypoxia is known to modulate proliferation in cells as an increased number of cells would cause an increase in demand of oxygen leading to further aggravation of hypoxic stress. To compensate, cells respond by reducing their rate of proliferation (Hubbi *et al.*, 2015; Ortmann *et al.*, 2014). Hypoxia Inducible factor alpha (HIF-1α) regulates this cellular adaptation and induces cell cycle arrest in hypoxic cells by direct repression of cell cycle associated genes (Ortmann *et al.*, 2014). In addition, the inhibitor of HIF-1α, prolyl hydroxylases (PHD) is inactivated under hypoxia which results in reduced cyclin D1 levels and hence, reduced proliferation in breast cancer cells (Zhang *et al.*, 2009).

HIF-1α regulates expression of a variety of genes involved in proliferation, apoptosis, angiogenesis, metastasis and invasion (Kumar *et al.*, 2015). It targets genes such as VEGF and its receptors, CA9, glycolytic pathway enzymes such as lactate dehydrogenase, glucose transporters 1 and 3, and hexokinase 2 (Chan *et al.*, 2003). Expression of CA9 is considered a marker for the presence of hypoxia and it is extensively upregulated under hypoxic conditions. It can promote tumour growth and metastasis by lowering pH levels, acidosis, inside the cells (Potter *et al.*, 2004). Expression of CA9 was used as a marker to demonstrate the presence of hypoxia in MDA-MB-231 WT and calpain KO cell lines. CA9 bands were observed only for the cell lysates prepared form cells grown in hypoxia (1% O2).

The effect of hypoxia on the ability of breast cancer cells to form colonies of the cells was assessed and compared with normoxic cultures. The plating efficiency for normoxic MDA-MB-231 WT cells was 53.23±3.97% which was in agreement with the previously obtained data in section 4.4.1 and the published literature. The plating efficiency of the hypoxic MDA-MB-231 WT cells was significantly lower (23.56±6.72%, $P<0.01$). This was marginally lower than previously reported in the lab by Dr. Aiyappa which was 43.0±2.64% in MDA-MB-231 cells grown in hypoxia (1% O2 for 48h). The plating efficiencies for calpain 1, 2 and 4 KO cells in normoxia were 61.89±7.82%, 19.89±2.28% and 35.56±1.1%, respectively. These values were in agreement and within the range of results obtained in section 4.4.1. The hypoxic Capn2 and Capns1 KO cells had significantly reduced plating efficiencies of 9.67±1.91% ($P<0.01$) and 29.78±0.68% ($P<0.01$), respectively. The reduced plating efficiency may be a reflection of reduced cell proliferation of hypoxic cells and perhaps, in retrospect, longer incubation, over the 2 weeks, may have been useful, to differentiate altered adhesion from altered proliferation. Previous studies have shown reduced plating efficiencies in cancer cells in the presence of hypoxia that may be due to cellular stress caused as a result of oxygen deprivation (Guo *et al.*, 2019). Hypoxia has been known to promote cell death by upregulating apoptotic markers, increased production of ROS and inducing mitochondrial damage. All of the above factors can lead to reduced clonogenic survival (Semenza, 2012).

Doxorubicin proliferation response was also assessed for MDA-MB-231 WT and calpain KO cell lines in the presence of hypoxia (1% O2 pre-treatment for 24h followed by 24-72h treatment with doxorubicin in hypoxia). As expected hypoxic WT cells were relatively resistant at 24 hours, 48 hours and 72 hours of doxorubicin treatment compared to the normoxic (21% O2) doxorubicin treated WT cells. There was no difference in response observed between the calpain KO and WT hypoxic doxorubicin treated cells at 24 hours or 48 hours. However, at 72 hours of doxorubicin treatment, hypoxic calpain 4 KO cells were significantly more resistant compared to their WT counterparts. The hypoxic IC_{50} doses were calculated where possible and were compared to the normoxic doxorubicin proliferation IC_{50} doses. At 72

hours of doxorubicin treatment, the hypoxic IC_{50} values for the WT and calpain KO cells were significantly higher compared to the normoxic IC_{50} values. A previous study by Jeon and colleagues demonstrated that doxorubicin treatment led to an increase in intracellular calcium and ROS which led to hyperactivation of m- calpain but not μ-calpain. This specifically induced cleavage of topoisomerase IIα followed by its accumulation in the cytoplasm which reduced the efficacy of doxorubicin (Jeon *et al.*, 2018). Such a mechanism may explain the increased resistance seen in calpain 1 KO cells treated with doxorubicin for 72 hours in hypoxia.

Doxorubicin survival response was also assessed in the presence of hypoxia (1% O2). Hypoxic WT cells were more resistant to doxorubicin treatment compared to the normoxic controls. Calpain 1, 2 and 4 KO cells had significantly lower surviving fractions at lower doses however no overall differences in relation to doxorubicin survival was observed between the calpain KO and the WT hypoxic cells. Time permitting it would have been interesting to see the doxorubicin survival response with cell treated at lower dose ranges. Chemotherapy resistance is linked with the presence of hypoxia and there can be several reasons. As mentioned previously presence of hypoxia promotes acidosis inside the cells that can compromise the uptake of certain drugs widely used for TNBC treatment (Gerweck *et al.*, 2006), a number of drugs depend on availability of oxygen and need cells to be in actively proliferation stage for their cytotoxic effects (Cosse *et al.*, 2008). Hypoxic cells have upregulated DNA repair and survival pathways that leads to increased rate of DNA repair and reduction in cell death induced by chemotherapeutic agents (Jongen *et al.*, 2017). In addition, hypoxia upregulates the expression of the multidrug transport P-glycoprotein (multidrug resistance 1 gene), an efflux pump that actively can export drugs out of the cells contributing to resistance towards a wide array of chemotherapeutic agents (Lv *et al.*, 2015).

Radiation therapy is given as an adjuvant to patients with breast cancer. Breast cancer cellular radiation response was determined in MDA-MB-231 WT and the calpain KO cells under normoxic (21% O2) and hypoxic conditions (1% O2). WT and calpain KO cells were treated with radiation and surviving fractions plotted against dose in semi-log plots then fitted to

the Linear Quadratic Model (LQM), for normoxia (21%O2) and hypoxia (1%O2) exposures. Normoxic WT cells had a plating efficiency of 50.67±3.8% while the hypoxic WT cells had a significantly reduced plating efficiency of 18.43±2.05%, which was in agreement with, and within the range of, previously obtained data in the group and in the published literature. Hypoxic WT cells were, as expected, significantly more resistant to radiation doses compared to the normoxic controls. The hypoxic and the normoxic WT cells had an α value of 0.24±0.15 and 0.51±0.28 and an α/β value of 2.36±1.82 and 6.23±5.67. The α and β elements of the LQM model signifiy the inherent sensitivity of cells to radiation. The linear element, α, describes single-hit killing and establishes radiation response at low doses, while the quadratic element, β, describes multiple-hit killing that causes the curve to bend at higher doses. The ratio α/β is described as the ratio of cell kill obtained from the α (linear) component is equal to that obtained from the β (quadratic) component. When the cells are sensitive to radiation, the survival curve is linear at low doses and the α value is higher (Fowler, 1992). The α and α/β values for normoxic WT cells higher than those of the hypoxic WT cells, suggesting the hypoxic WT cells were more resistant to radiation treatment. The SF2 for hypoxic WT cells was also seen to be higher than for the normoxic SF2 cells.

Normoxic Capn1 KO cells had higher α and α/β values compared to those of normoxic WT suggesting sensitisation at low doses, however no change in overall radiation response was seen in normoxic Capn1 KO cells. In hypoxia, the α and α/β values of Capn1 KO cells were higher compared to those of WT cells, suggesting sensitisation in hypoxic conditions. This was also evident when comparing SF2 values for both the cells lines. Knocking out calpain 1 did not have, however, a marked effect on radiation response in normoxia, yet in hypoxia it demonstrated significant radiosensitisation.

Normoxic Capn2 KO cells had higher α and α/β values compared to those of normoxic WT suggesting radiosensitisation at low doses, however calpain 2 KO cells were more resistant compared to WT cells especially at higher doses. In hypoxia, the α and α/β values of Capn2 KO cells were higher compared to those of WT cells, indicating radiosensitisation in hypoxic conditions. This was also evident when comparing SF2 values for both the cells lines. Knocking out calpain 2 made MDA-MB-231 cells more resistant

to radiation in normoxia however, in hypoxia it demonstrated significant radiosensitisation. And, as mentioned previously, the SF8 values indicated that Capn1 KO and Capn2 KO cells had significant radiosensitisation in hypoxic conditions (1% O2 for 24 h) compared to the WT cells as opposed to radiosensitisation in normoxic conditions (21% O2).

The normoxic Capns1 KO cells had a lower α value compared to that of the normoxic WT, and seemed more radioresistant compared to WT control. In hypoxia, Capns1 KO cells were sensitive to radiation at lower doses compared to WT cells however, no overall change in radiation response was observed. This was also evident when comparing SF2 and SF8 values for both the cells lines. Knocking out calpain 4 made MDA-MB-231 cells more resistant to radiation in normoxia however, in hypoxia no change in response to radiation was observed.

The WT cells were more resistant to radiation in hypoxia than the cells grown in normoxia. The difference in radiation response between normoxic and hypoxic cells is known as the oxygen enhancement ratio (OER). In the presence of oxygen the radiation induced free radical DNA damage lesions are not restored, and is known as the oxygen fixation hypothesis (Brown *et al.*, 2004; Roots *et al.*, 1974). However, in hypoxic conditions, the DNA based free radicals are reduced by sulfhydryl groups containing compounds which renders DNA to its undamaged state leading to resistance to radiotherapy (Brown *et al.*, 2004).

Knocking out calpains 1 did not have an effect on radiation response and knocking out calpain 2 made cells resistant to radiation treatment at higher doses, in normoxic state (21% O2), while in hypoxia, significant radiosensitisation was observed in both the cell lines compared to the WT cells. This was also reflected in the SF8 values. The SF8 values for Capn1 KO and Capn2 KO cells were 10 fold lower than the WT cell in the presence of hypoxia (1% O2 for 24h) than in normoxia (21% O2), suggesting a significant radiosensitisation in the presence of hypoxia (1% O2 for 24 h). Therefore targeting calpain 1 and calpain 2 can lead to radiosensitisation in breast cancer cells in hypoxic state.

Knocking out calpain 4 made MDA-MB-231 cells overall resistant to radiation treatment in normoxic state (21% O2), however no overall difference in response was observed in hypoxia (1% O2). This might be due

to the cell lines low rate of proliferation. In retrospect the clonogenic flasks should have been incubated for another 2 weeks to allow colony formation in cases where cells have significantly reduced rates of proliferation. It might have been interesting to observe a similar effect in Capns1 KO cells.

Suggested future work-

Results in the current chapter need further confirmation and additional work to elucidate the role of the calpain system in therapeutic response, especially in hypoxia and radiosensitivity. Suggestions for future work in includes-

1. Determining calpain activity in hypoxia treated cells CRISPR/Cas9 calpain KO cells without GFP tags using the FRET based bioassay.
2. Determining clonogenic radiation response in calpain 4 KO cells incubated for 3-4 weeks to form colonies.
3. Determining cellular chemotherapeutic response using other chemotherapeutic drugs in normoxia (21% O2) and hypoxia (1% O2).
4. Determining treatment response (chemotherapeutic and radiation) in 3D spheroids and comparing the results with 2D normoxia and 2D hypoxia.

Chapter 5- Bioinformatic analyses

5.1 Abstract

Background: Bioinformatic analyses were conducted using gene expression information on publicly available breast cancer datasets. The current chapter aimed to identify genes altered by differential expression of calpain system genes, namely CAPN1, CAPN2, CAPNS1 and CAST.

Methods: Each calpain system gene was queried on the cBioportal database and the publicly available breast cancer datasets, TCGA and METABRIC, and DEG lists were produced. Pathway enrichment analysis was performed on these DEGS using the online package, WEBGESTALT. Commonalities in pathways were assessed and analysed for survival analysis using Xena browser using the GDC TCGA cohort. Survival analysis data was validated using the METABRIC cohort. Correlations were assessed, using the METABRIC cohort, between associated DEGs and the calpain system genes. This was followed by assessing associations with breast cancer clinicopathological variables and validation of protein expression of one of the identified genes, RBBP4, conducted in breast cancer cells and tissues by Western blotting and Immunohistochemistry respectively.

Results: The number of DEGs associated with altered expression of calpain system genes were 63 and 759 in the METABRIC and TCGA cohort, respectively for CAPN1, 2455 and 1369 in the METABRIC and TCGA cohort, respectively for CAPN2, 2614 and 3446 in the METABRIC and TCGA cohort, respectively for CAPNS1, and 1999 and 1221 in the in the METABRIC and TCGA cohort, respectively for CAST.

CAPN1 gene associated DEGs significantly enriched pathways including cell cycle, proteasome, DNA replication and several others. The tight junction, cell cycle, and Hippo signalling pathways were significantly enriched by CAPN2 associated DEGs. CAPNS1 associated DEGs significantly enriched pathways such as cell cycle, DNA replication, senescence, and Mismatch repair. CAST associated DEGs significantly enriched pathways including RNA transport, nucleotide excision repair, and cell cycle pathways. The common genes in these pathways analysed for overall survival in the GDC TCGA database.

The genes seen significant in terms of overall survival were taken forward for validation in the METABRIC dataset where gene probe level information

was available. These genes included, PPP1CA for altered CAPN1; AMOT, PRKAB2, AMOTL1 and RAB13 for altered CAPN2; MAGOH and POLE2 for altered CAPNS1, and YWHAG, HDAC1, RBBP4 and PSMB5 for altered CAST expression.

Correlation analysis of these genes revealed some statistically significant and intermediate to strong biological correlations seen between the expression of CAST probe 4 and YWHAG probe 1, CAST probe 4 and RBBP4 probe 2, CAST probe 6 and RBBP4 probe 2, and YWHAG probe 2 and RBBP4 probe 1. Survival analysis on the METABRIC breast cancer cohort revealed that high expressions of PPP1CA probe 2, PRKAB2, POLE2, RBBP4 probe 1 and PSMB5 were significantly associated with poor breast cancer specific survival. While, high expression of CAST probes 4 and 6 were associated with better breast cancer specific survival.

From the above-mentioned genes RBBP4 was selected to be validated in breast cancer cells and tissues. RBBP4 protein expression was assessed in two luminal and two TNBC cell types. Breast cancer tissue stained with RBBP4 protein demonstrated that it was predominantly located in the nuclear region.

Conclusions: PPP1CA, PRKAB2, POLE2, YWHAG, RBBP4 and PSMB5 genes were identified as the significant DEGs associated with altered expression of calpain system genes and were associated with overall survival and breast cancer specific survival in GDC TCGA and METABRIC breast cancer cohorts. RBBP4 protein was expressed in TNBC and luminal cell lines and was seen to have a predominantly nuclear localisation in the breast cancer tissues.

5.2 Introduction

5.2.1 Bioinformatics analyses

Bioinformatics analyses were conducted during the shutdown of labs, using publically available information retrieved from breast cancer datasets

5.2.2 Cancer datasets

Several datasets exist that contain gene expression information across many different cancer types. The METABRIC and TCGA datasets were used in this study. The Molecular Taxonomy of Breast Cancer International Consortium (METABRIC) database is a UK-Canada project that includes data

collected by Professor C. Caldas (Cambridge, UK) and Professor S. Aparicio (Canada) (Pereira *et al.*, 2016). The data contains clinical traits, copy number aberration (CNA) profiles, and single nucleotide polymorphisms (SNP) genotypes acquired from the participants of the METABRIC trial consisting of 1980 primary breast cancer samples. The clinical and genomic data was obtained from cBioPortal (cBioPortal, 2022).

The Cancer Genome Atlas (TCGA) is a publically available cancer genomics program that began in 2006 as a joint effort between the NCI and the National Human Genome Research. The database consists of molecular characterisation of over 20,000 primary cancers and their respective normal samples including over 33 cancer types. Over the years the TCGA has generated over 2.5 petabytes of genomic, epigenomic, transcriptomic and proteomic data leading to enhancements in cancer diagnosis, treatment and prevention (TCGA, 2022).

Another dataset, the Pan-Cancer Atlas provides a comprehensive and in-depth understanding of tumour formation in humans, from the analysis of over 11,000 tumours from 33 forms of cancer. To develop new forms of treatment, the Pan-Cancer Atlas is a singular and unified resource. The database represents a collection of 27 papers classified into three main categories including, cell of origin patterns, oncogenic processes, and signalling pathways. Each category consists of a leading articles that summarises the core findings for that category that are supported by other papers that explore the subtopics in detail (PCA, 2022).

THE METABRIC and TCGA datasets were accessed on the cBioPortal database to identify the targeted differentially expressed genes associated with the altered expression of the calpain system genes, calpain 1, calpain 2, calpain 4 and calpastatin.

5.2.3 Pathway analysis

Pathway enrichment analyses were done on the differentially expressed genes, with altered expression of the calpain system genes, to study the affected pathways using WebGestalt and KEGG pathway browser. The KEGG pathway is a library of pathway maps representing molecular interactions, reaction and relation networks for carbohydrate, lipid, amino

acid, nucleotide metabolism; cellular processing; organismal systems; human diseases and drug development. The KEGG pathway browser uses the KEGG Mapper to map network pathways .

One of the differentially expressed genes identified by the altered calpain system expression was the Retinoblastoma binding protein 4 (RBBP4) gene which was significantly correlated with Calpastatin and breast cancer survival in both METABRIC and TCGA datasets.

5.2.4 RBBP4

RBBP4 is a 48 kDa tumour specific protein that identified in HeLa cell lysates (Qian *et al.*, 1993). The protein has a nuclear localisation, belonging to a highly conserved subfamily with four WD-repeat sequences that bind to the retinoblastoma protein in vivo and in vitro, hence the name (Nowak *et al.*, 2011). The protein is part of several chromatin modified protein complexes, including nucleosome remodelling and deacetylation complex (Zhang *et al.*, 1999), polycomb repressor complex (Kouznetsova *et al.*, 2019), and SIN3-chromatin modulating complexes (Vermaak *et al.*, 1999). It has been shown to play an important role in chromatin metabolism, nucleosome assembly and histone modification that regulates gene transcription, and cell proliferation (Burkhart *et al.*, 2008). RBBP4 has shown to be involved in cell cycle regulation by interacting with the transcription factor E2F in the presence of retinoblastoma protein and histone deacetylase 1 (Guo *et al.*, 2020; Qian *et al.*, 1993). In a recent study, RBBP4 was shown to be essential in early embryonic development in mice (Miao *et al.*, 2020). Accumulated research in the past decades have demonstrated that RBBP4 plays a significant role in the pathogenesis of cancers.

Overexpression of RBBP4 in gastric cancer was shown to increase the radiosensitivity by downregulating the PI3K/AKT pathway in vitro (Jin *et al.*, 2018). In cervical cancer cells, overexpression of RBBP4 led to the induction of cell cycle arrest and apoptosis by upregulating the expression of p53, caspase 8 and retinoblastoma (Zheng *et al.*, 2013) and upregulation in DNA replication was observed in lung adenocarcinoma cells (Wang *et al.*, 2021). Upregulation in RBBP4 expression was shown to be significantly correlated with adverse clinicopathological characteristics and prognosis in

colon cancer with hepatic metastasis and involvement of lymph node (Li *et al.*, 2019b). RBBP4 silencing demonstrated an enhanced sensitivity to the chemotherapeutic agent temozolomide by inducing H2AX phosphorylation, in glioblastoma cells (Kitange *et al.*, 2016). RBBP4 knockdown was also shown to reduce cell invasion and migration by regulating proteins involved in EMT in colon cancer cells (Li *et al.*, 2020b).

Till date only a few studies have reported expression of RBBP4 in breast cancer. Its involvement in the formation of histone deacetylation complex has been reported to contribute to the progression of breast cancer and expression of histone deacetylase 1 (HDAC1) has been shown to be positively correlated with expression of RBBP4 in breast cancer (Guo *et al.*, 2020). The study reported a significant correlation between high RBBP4 expression and lymph node metastasis. The study also showed that high RBBP4 expression was also associated with worse overall survival in a cohort of 240 breast cancer patients treated with no neoadjuvant therapy (Guo *et al.*, 2020). However, these findings remain to be confirmed in a larger patient cohort.

5.2.5 Hypothesis and aims

The altered expression of the calpain system has been implicated in a number of pathological conditions, as indicated previously. The altered expression of calpain 1, calpain 2, calpain 4 and calpastatin may lead to a change in expression of several other genes intracellularly which may lead to altered cellular phenotypes. The regulation of these genes by the calpain system may also shed light on the interaction patterns, target molecules, and localised functions of the calpain system genes.

Hypothesis

In the current chapter we hypothesise that altered expression of calpain system genes leads to the differential expression of other genes. The genes correlated with calpain 1, calpain 2, calpain 4 and calpastatin in breast cancer, will affect clinicopathological variables of the disease and be associated with patient clinical outcome.

Aims

1. To identify the DEGs associated with altered expression of calpain 1, calpain 2, calpain 4 and calpastatin using publically available breast cancer datasets.
2. Identification and mapping of cellular pathways enriched by these DEGs.
3. To perform survival analysis on these DEGs using breast cancer cohorts.
4. To perform correlation analyses on DEGS with calpain 1, calpain 2, calpain 4 and calpastatin.
5. Validation of target genes in breast cancer tissue by immunohistochemistry.
6. Investigation of associations with clinicopathological criteria and breast cancer clinical outcomes.

5.3 Materials and methods

5.3.1 Differentially expressed genes

The cBioportal database (https://www.cbioportal.org/) was used to obtain mRNA expression data, METABRIC and TCGA were used. Calpain 1, calpain 2, calpain 4 and calpastatin genes were queried. The comparison/survival tab was selected and the list of genes obtained under the mRNA section. The gene list for each gene queried per calpain system gene was set to the 'altered group' and 'significant only' genes. This DEG list was downloaded for each queried gene.

5.3.2 Pathway enrichment analysis

Pathway enrichment analyses were done on DEG lists obtained from section 5.3.1. Pathway enrichment analysis was performed using the WEB-based GEne SeT AnaLysis Toolkit (WebGestalt) available for free on the internet (http://www.webgestalt.org/). The basic parameters were set to- Homo sapiens for the organism of interest; Over Representation Analysis (ORA) was selected from the drop down list for the method of interest; for the functional database, pathway was selected from the drop down list and the KEGG browser used. For the gene list parameters, gene symbol was selected from the drop down menu, for Select gene ID type the gene lists

obtained from the section 5.3.1 were uploaded and the reference gene set was selected to genome. For the advanced parameters, the multiple test adjustment was set to BH and the significance level set to an FDR of 0.05 following which the gene lists were submitted. The submitted lists were run and the enrichment results obtained with the overlap value between the number of genes in the gene set and the mapped genes, FDR, p-values and enrichment ratios.

The enriched pathways were mapped using the KEGG pathway database (https://www.genome.jp/kegg/).

5.3.3 Survival analysis on TCGA data

The TCGA data set was used to predict the breast cancer survival of the genes. The Xena browser tool (https://xenabrowser.net/) (UCSC, USA) was used to predict the overall survival. On the website, in column A Sample ID, the GDC TCGA Breast Cancer study was selected. In column B, the data type was set to genomic followed by inputting the gene symbol. The dataset was set to gene expression. Under advanced settings, the gene expression RNA-seq was set to HT-seq count. In column C, phenotypic datatype was selected and phenotype was set to sample_type.samples. The data summary and tumour distribution was visualised using the graph icon. The survival KM plots were obtained from the list of options in column B. The gene expression was divided into two groups low and high based on the gene's median expression.

5.3.4 Patient cohorts

A total of 1655 early stage invasive breast cancer patients, treated at Nottingham University Hospitals between 1998 and 2006 were included in the current study. All patients were treated in a standard manner. Depending on the disease characteristics or patient's choice, all patients underwent a mastectomy or wide local excision followed by radiotherapy if indicated. Systemic adjuvant treatment was given on the basis of NPI, ER, and menopausal status. Combination chemotherapy, CMF (cyclophosphamide, methotrexate and 5-fluorouracil) was given to patients with an NPI score of 3.4 and above, if they were premenopausal or ER

negative, and hormonal therapy was given if the patients were ER positive. Patients with an NPI score less than 3.4 did not receive adjuvant treatment.

The METABRIC patient cohort was used in this study to perform survival analysis and assess RBBP4 mRNA associations with the available clinicopathological data. The dataset consists of gene expression profiles from 1980 primary breast tumour and normal tissue samples. This data was generated from mRNA hybridised to illumina HT-12v3 platform described by Curtis and colleagues (Curtis *et al.*, 2012). Adjuvant chemotherapy was given to patients with ER negative and lymph node positive disease, while patients with ER positive disease did not receive adjuvant chemotherapy. Information on disease-specific survival was also available. The average age of patients was 61.10 and the tumours were collected in the UK and Canada between 1977 and 2005. The median follow up was 141 months. Protocol for sample acquisition followed appropriate ethical guidelines (Curtis *et al.*, 2012).

5.3.5 Tissue microarray

RBBP4 protein expression was determined in a breast cancer tissue microarray (TMA) by conducting Immunohistochemical staining. The TMAs were constructed by the Breast Pathology Group at the University of Nottingham. A single tissue core of 0.6 mm from a, breast cancer histopathologist assessed, representative tumour area was used for each patient sample. Freshly cut (4 µm) TMA sections mounted on slides (done by a specialist technician) were used for immunohistochemistry.

5.3.6 Antibody specification and optimisation

The primary antibodies for RBBP4 (Table 5.1) were used in this study. The antibody specificities were determined by Western Blotting on breast cancer cell line lysates prepared from MDA-MB-231, MDA-MB-468, T47D and MCF7 cell lines according to the methods described in Chapter 2 section 2.3.7.

The antibody was then optimised to determine the concentrations to stain the breast cancer tissue by immunohistochemistry. The antibody optimisations were performed using the Novolink Polymer Detection Kit (Leica). Different concentrations for RBBP4 (1 in 5000, 1 in 10,000 and 1 in 15,000) were used to stain the TMA. DARPP32 antibody (Abcam), used

previously in the lab by was used as a positive control (1:500 dilution) and the sections with no primary antibody treatments were used as negative controls (Saidy *et al.*, 2021).

Table 5. 1 List of antibodies and dilutions.

Antibodies	Source	Catalogue number	Molecular weight	Dilution
Anti-RBBP4	Abcam	epr3411	48 kDa	1:10000
Anti-β-actin	Abcam	ab8227	42 kDa	1:2000
IRDye® 800 CW Donkey anti-rabbit	LI-COR	926-32213	-	1:10000
IRDye® 680RD Donkey anti-mouse	LI-COR	926-68072	-	1:10000

5.3.6 Immunohistochemistry

RBBP4 protein expression was detected in breast tumour tissue microarrays by immunohistochemistry (IHC) using the Novolink Polymer Detection Kit (Leica) and the tissues were stained according to the manufacturer's instructions. The tissues were dewaxed in xylene and rehydrated in ethanol and distilled water. Antigen retrieval was done using 0.01 mol/L sodium citrate buffer with a pH of 6.0. The slides were rinsed in Tris Buffered Saline (TBS) with a pH of 7.6. The Novolink Peroxidase Block was used to block the tissues.

For staining, anti-rabbit RBBP4 (Abcam) was diluted at 1:5000, in the Leica Primary Antibody Diluent. The tissues were incubated with diluted antibodies for 1 hour at room temperature followed by a TBS rinse and blocking with the Novolink Post Primary Block for 30 minutes. The Novolink Polymer solution was added after blocking. The tissues were counterstained with haematoxylin and the chromogenic substrate 3,3'-diaminobenzidine was used after which the tissues were dehydrated in ethanol and cleaned using xylene. The sections were mounted in DPX mounting medium (Sigma) and the breast tumour composite sections of grade 1 and grade 2 early-stage invasive tumours were used as positive and negative controls.

The stained tissue sections were scanned at x200 magnification using a Nanozoomer Digital Pathology Scanner (Hamamatsu Photonics) following which the staining intensity was assessed. Nuclear expression was assessed by both, by assigning a percentage of tumour cells stained and H-scores. H scores from 0-3 were given where 0 is no expression, 1 is weak expression,

2 is moderate expression and 3 is strong expression over the percentage are for each staining intensity. While, the cytoplasmic expression of RBBP4 was assessed as the percentage of tumour cells stained compared to unstained.

Greater that 30% of the cores for each TMA were assessed by two assessors blinded to each other's scores and the clinical outcome. The Interclass Correlation Coefficients (ICC) were calculated between the scores from two assessors for concordance and the values greater than 0.7 were accepted for good concordance.

5.4 Results

5.4.1 Differentially expressed genes

The list of differentially expressed genes obtained from cBioportal for each of the calpain system genes, CAPN1, CAPN2, CAPNS1 and CAST was retrieved from the METABRIC and TCGA publically available datasets. The differentially expressed gene lists obtained were based on differential mRNA expression of CAPN1, CAPN2, CAPNS1 and CAST genes. Table 5.2 shows the number of differentially expressed genes associated with altered expression of calpain system genes.

Table 5. 2 Number of DEGs obtained from METABRIC and TCGA

Calpain system gene	METABRIC	TCGA
CAPN1	63	759
CAPN2	2455	1369
CAPNS1	2614	3446
CAST	1999	1221

5.4.2 Pathway enrichment analysis

The pathways with a FDR of 0.05 were shortlisted for the significantly DEGs associated with the altered expression of CAPN1, CAPN2, CAPNS1 and CAST (Tables 5.3-5.6). The pathways enriched were arranged in the order of their significant enrichment, from the most significantly enriched pathway to the least significantly enriched pathway.

Table 5. 3 Pathways enriched by altered CAPN1 expression

Pathways	FDR	Pathways	FDR
Cell cycle	2.692e-9	Progesterone mediated oocyte maturation	0.0061290
Proteasome	9.6690e-8	Epstein-Barr virus infection	0.011908
DNA replication	2.9966e-7	Homologous recombination	0.014709
Oocyte meiosis	0.000058901	Base excision repair	0.017905
Pyrimidine metabolism	0.00078295	Purine metabolism	0.026483
Fanconi anemia pathway	0.0013957	p53 signaling pathway	0.0066012
Spliceosome	0.0016530	Cellular senescence	0.029785

Table 5. 4 Pathways enriched by altered CAPN2 expression

Pathways	FDR	Pathways	FDR
Tight junction	0.0035473	Protein signalling in ER	0.0048535
Hippo signalling pathway	0.0048535	Cell cycle	0.028080

Table 5. 5 Pathways enriched by altered CAPNS1 expression

Pathways	FDR	Pathways	FDR
Cell cycle	9.472e-9	T cell receptor signaling pathway	0.0016831
Ribosome biogenesis in eukaryotes	9.9195e-9	Viral carcinogenesis	0.016276
DNA replication	0.0000032882	Base excision repair	0.022265
Spliceosome	0.0000058382	Proteasome	0.043999
Homologous recombination	0.00064662	Glycosphingolipid biosynthesis	0.043999
Cellular senescence	0.0013221	Non-alcoholic fatty liver disease	8.1435e-14
Fanconi anemia pathway	0.0014675	Metabolic pathway	4.7823e-9
Oocyte meiosis	0.0020796	Protein processing in ER	0.00011288
RNA transport	0.0025674	RNA polymerase	0.00085438
Mismatch repair	0.0058821	Vibrio Cholerae infection	0.0022338
Adherens junction	0.016776	Shigellosis	0.018532
Biosynthesis of amino acids	0.022468	Pathogenic E.coli infection	0.024925
Pentose phosphate pathway	0.026748	Amino sugar and nucleotide sugar metabolism	0.026938
Lysine degradation	0.032855	Retrograde endocannabionoid signaling	0.037645
Purine metabolism	0.034814	Proteasome	0.043999
Carbon metabolism	0.038668	Glycosphingolipid biosynthesis	0.043999
Human T cell leukemia virus 1 infection	0.00011355	Pyrimidine metabolism	0.0019912
TNF signaling pathway	0.00011355	Bladder cancer	0.021570
Epstein Barr virus	0.00033661		

Table 5. 6 Pathways enriched by altered CAST expression

Pathway	FDR	Pathway	FDR
RNA transport	0.00018858	Proteasome	0.040599
Alzheimer disease	0.00018858	Pyrimidine metabolism	0.00017068
Oxidative phosphorylation	0.00056325	DNA replication	0.0040800
Huntington disease	0.00087301	Aminoacyl t-RNA biosynthesis	0.0063412
Nucleotide excision repair	0.0010906	Base excision repair	0.014034
Non-alcoholic fatty liver disease (NAFLD)	0.0032579	Epstein-Barr virus infection	0.041107
Cell cycle	0.0042626	Viral carcinogenesis	0.041107
Basal transcription factors	0.0080654	Central carbon metabolism in cancer	0.00076957
RNA degradation	0.012512	Pathways in cancer	0.0073063
Parkinson disease	0.012512	Colorectal cancer	0.0074027
Ubiquitin mediated proteolysis	0.014445	Pancreatic cancer	0.0074027
Thermogenesis	0.014445	HIF-1 signaling pathway	0.028566
Spliceosome	0.047528	Small cell lung cancer	0.035357
Oocyte meiosis	1.6540e-7	Apoptosis	0.041950
Progesterone-mediated oocyte maturation	0.000027908	Adherens junction	0.041950
Ribosome biogenesis in eukaryotes	0.031887	Oocyte meiosis	0.041950
Cellular senescence	0.040599		

5.4.3 Pathway commonalities in datasets

The pathways significantly enriched by the DEGs associated with altered expression of calpain system genes were assessed for commonalities. The pathways and the genes that were common in between the METABRIC and TCGA dataset for each of the calpain system genes were shortlisted below and mapped using the KEGG pathway dataset (https://github.com/RichaVasan/Calpain-system-pathway-mapping.git).

Table 5. 7 Common DEGs between datasets for CAPN1

ESPL1	CDC25A	CDC6	ANAPC7	PPPICA	PLK1
PTTG1	BUB1B	CCNB1	CCNB2	ANAP7	AURKA
CDK1	CDC25C	BUB1			

Table 5. 8 Common DEGs between datasets for CAPN2

F11R	RAB13	ARHGEF2	CLDN7	AMOTL1
PRKAB2	AMOT	OCLN	DLG3	

Table 5. 9 Common DEGs between datasets for CAPNS1

AAAS	GEMIN4	POLD2	RPP21	WDR3	RAD54L
ADRM1	GEMIN6	POLR2G	RPP25	WDR43	RPIA
ALYREF	GNL2	POP4	RPP38	XPO5	SGO1
BMS1	GNL3	POP7	RPP40	YWHAE	SHMT2
BUD31	GTPBP4	PPIH	SEC13	ADSL	TALDO1
CCNA2	HEATR1	PRPF38A	SEH1L	AK2	TKT
CDC16	HSPA1B	PSMA7	SF3A3	ASNS	TPI1
CDC25A	ISY1	PSMB10	SF3B3	AURKA	UBE2T
CDC25B	LIN37	PSMB2	SF3B4	BLM	USP1
CDC45	LIN9	PSMB3	SF3B6	DGUOK	XRCC2
CDC7	LSM2	PSMB4	SFN	EME1	XRCC3
CDKN2A	MAGOH	PSMB7	SKP2	ENO1	YWHAQ
CDKN2D	MAGOHB	PSMC2	SMAD2	FANCA	BUB1
CHEK1	MCM2	PSMC3	SNRPA	FANCB	CCNB1
CHEK2	MCM4	PSMC4	SNRPA1	FANCD2	CCNB2
CHERP	MCM5	PSMD13	SNRPC	FANCE	CCNE1
CSNK2A2	MCM6	PSMD14	SNRPD1	FANCG	CDC20
CSNK2B	MCM7	PSMD8	SNRPD2	FANCL	CDC25C
DDX39B	MPHOSPH10	PSME4	SNRPD3	GAPDH	CDK1
DKC1	MSH2	PUF60	SNRPG	GART	CUL1
DNA2	MSH6	PWP2	SRSF4	GMPS	ESPL1
DTYMK	MYBL2	RAN	STAG1	GPT2	PKMYT1
E2F1	NAT10	RANGAP1	STRAP	HPRT1	PLK1
E2F2	NOB1	RBM17	SUMO1	IMPDH1	POLD1
E2F3	NOP56	RBM28	SUMO2	MAD2L1	POLE2
E2F4	NRAS	RBM8A	TACC3	NT5C2	POLR1C
EIF3B	NUP205	RCL1	TCOF1	NUDT5	POLR1E
EIF3I	NUP37	RFC2	TTK	PAPSS1	POLR2F
EIF4EBP1	NUP93	RFC4	TXNL4A	PDE7A	POLR2I
EIF5B	ORC1	RHEB	U2AF1L4	PFKL	PPP1CB
EMG1	ORC6	RIOK1	UCK2	POLR1B	PPP3R1
EXO1	PABPC4	RNASEH2A	UPF3A	POLR3C	PTTG1
FBL	PCBP1	RNASEH2B	UPF3B	PSAT1	SEM1
FEN1	PHF5A	RP9	USP39	RAD51	SSBP1

Table 5. 10 Common DEGs between datasets for CAST

PSMA7	RAD21	MAD2L1	ORC6	ESPL1	E2F2
ADRM1	PTTG1	YWHAG	CDC25A	DBF4	PPP3R1
PSMD14	CDK1	E2F1	BUB1B	YWHAZ	RBBP4
PSMB5	HDAC2	CDC20	BUB	MYBL2	ORC1
CCNB1	TTK	PLK1	HDAC1	FOXM1	CCNB2
PCNA	CDC23				

5.4.4 Survival analysis on TCGA

The differentially expressed genes associated with the altered expression of calpain system genes were assessed for survival analysis using the methods described in section 5.3.3 using the publically available GDC TCGA breast cancer cohort. The DEGs shortlisted in section 5.4.3 were assessed and only the genes which were significant in terms of survival were taken forward. The DEG expression was also shown in breast cancer patients grouped into solid tissue normal (n=113), primary tumour (n=1097) and metastatic tumours (n=7).

The PPP1CA gene was the only gene associated with altered CAPN1 expression that was seen to be significant in terms of overall breast cancer survival. It was seen that high expression of PPP1CA was significantly associated with better overall survival (P<0.01) (Figure 5.1).

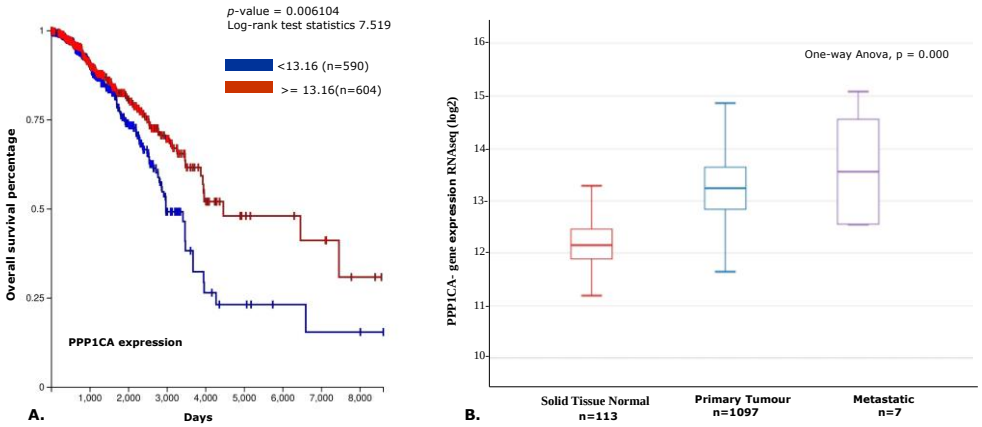

Figure 5. 1 Survival analysis for PPP1CA gene. (A) Kaplan-Meier plot showing low expression (blue) and high expression (red) of PPP1CA. (B) PPP1CA gene expression in normal solid tissue, primary tumour and metastatic samples.

The AMOT, PRKAB2, AMOTL1 and RAB13 genes were the differentially expressed gene associated with altered CAPN2 expression that were seen to be significant in terms of overall breast cancer survival. It was seen that high expression of AMOT was significantly associated with poor overall survival (P<0.01) (Figure 5.2). High PRKAB2 expression was also significantly associated with poor overall survival (P<0.001) (Figure 5.3). High AMOTL1 expression was significantly associated with poor overall survival (P<0.05) (Figure 5.4) with high expression of RAB13 significantly associated with better overall survival (P=0.001) (Figure 5.5).

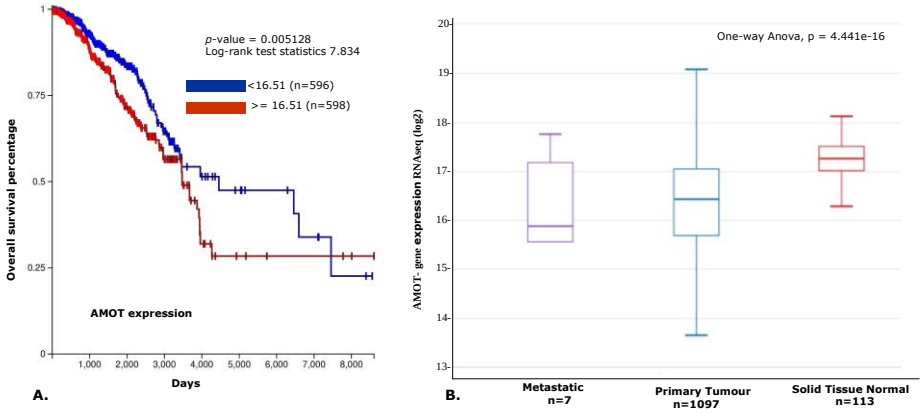

Figure 5. 2 Survival analysis for AMOT gene. (A) Kaplan-Meier plot showing low expression (blue) and high expression (red) of AMOT. (B) AMOT gene expression in normal solid tissue, primary tumour and metastatic samples.

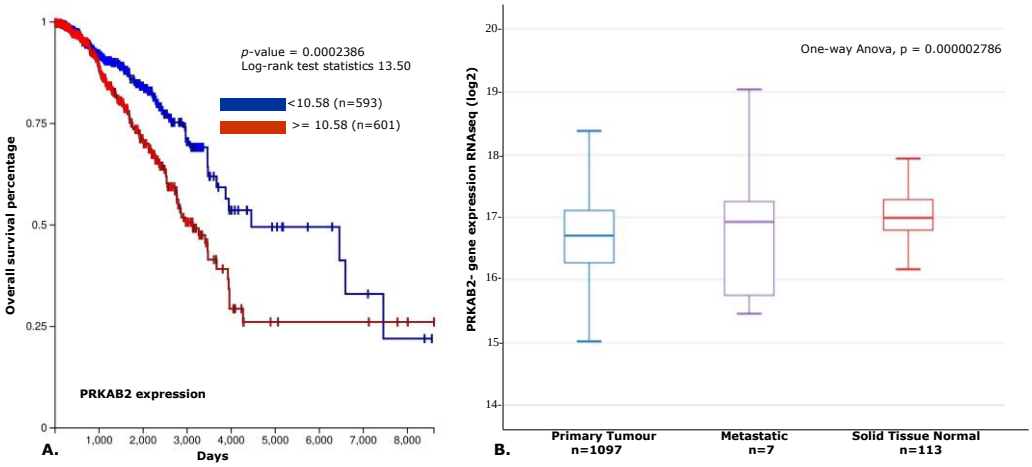

Figure 5. 3 Survival analysis for PRKAB2 gene. (A) Kaplan-Meier plot showing low expression (blue) and high expression (red) of PRKAB2. (B) PRKAB2 gene expression in normal solid tissue, primary tumour and metastatic samples.

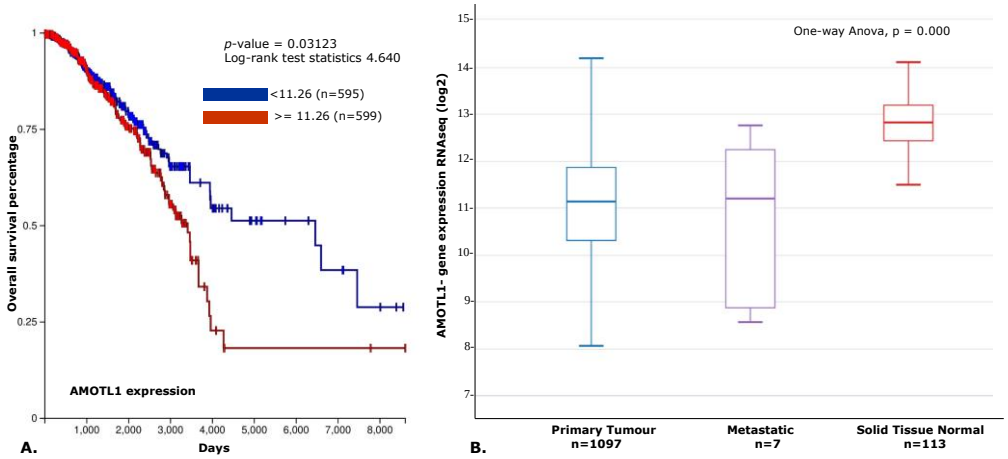

Figure 5. 4 Survival analysis for AMOTL1 gene. (A) Kaplan-Meier plot showing low expression (blue) and high expression (red) of AMOTL1. (B) AMOTL1 gene expression in normal solid tissue, primary tumour and metastatic samples.

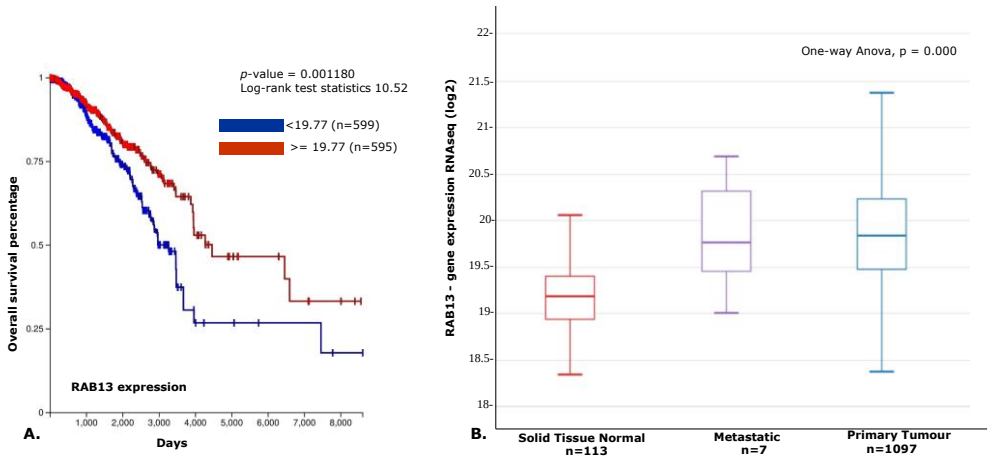

Figure 5. 5 Survival analysis for RAB13 gene. (A) Kaplan-Meier plot showing low expression (blue) and high expression (red) of RAB13. (B) RAB13 gene expression in normal solid tissue, primary tumour and metastatic samples.

The MAGOH and POLE2 genes were the only genes associated with altered CAPNS1 expression that was seen to be significant in terms of overall breast cancer survival. It was seen that high expression of MAGOH was significantly associated with better overall survival (*P*=0.01) (Figure 5.6). High POLE2 expression was significantly associated with better overall survival in the GDC TCGA breast cancer cohort (*P*<0.01) (Figure 5.7).

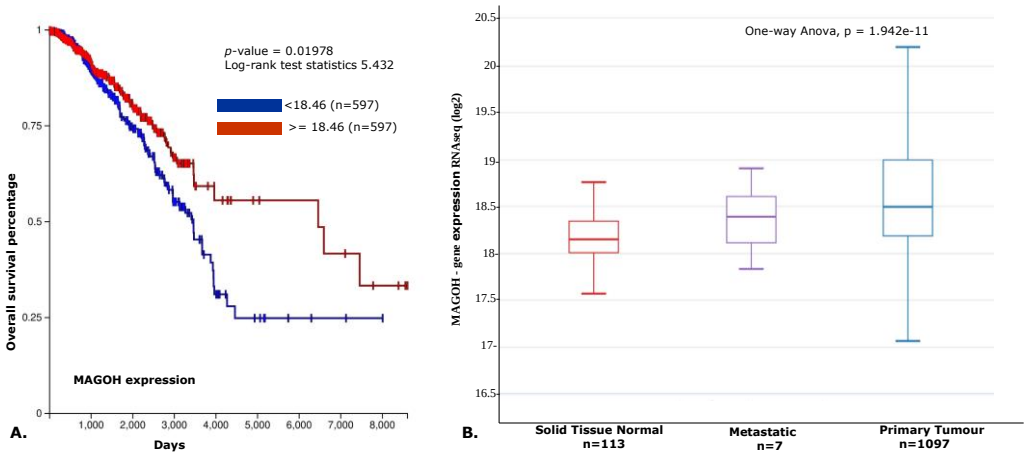

Figure 5. 6 Survival analysis for MAGOH gene. (A) Kaplan-Meier plot showing low expression (blue) and high expression (red) of MAGOH. (B) MAGOH gene expression in normal solid tissue, primary tumour and metastatic samples.

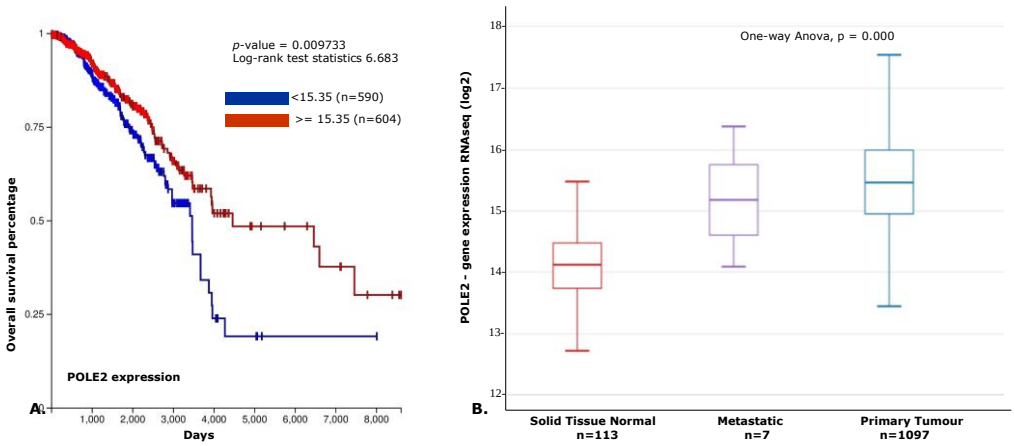

Figure 5. 7 Survival analysis for POLE2 gene. (A) Kaplan-Meier plot showing low expression (blue) and high expression (red) of POLE2. (B) POLE2 gene expression in normal solid tissue, primary tumour and metastatic samples.

The YWHAG, HDAC1, RBBP4 and PSMB5 genes were the only genes associated with altered CAST expression that were seen to be significant in terms of overall breast cancer survival. High expression of YWHAG was significantly associated with poor overall survival (P<0.05) (Figure 5.8). High HDAC1 expression was significantly associated with better overall survival (P=0.01) (Figure 5.9). High RBBP4 expression was also significantly associated with better overall survival (P<0.01) (Figure 5.10) as was expression of PSMB5 (P<0.05) (Figure 5.11).

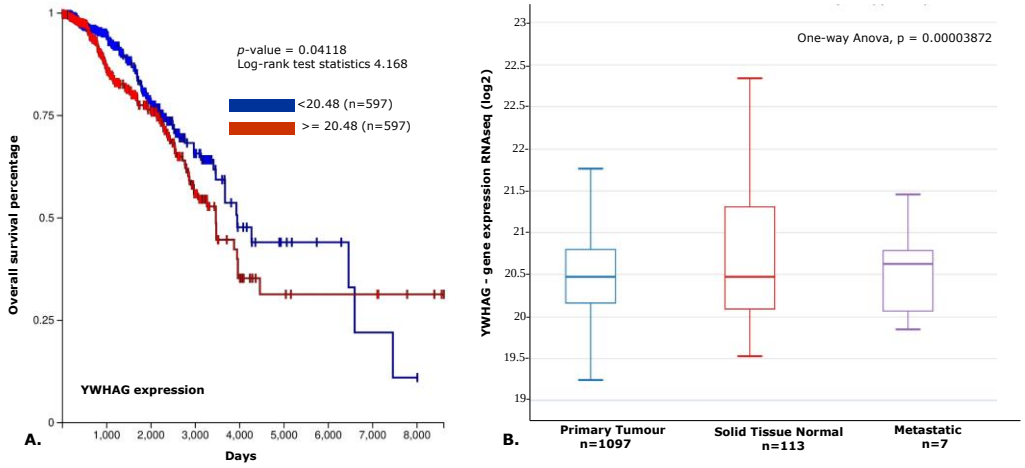

Figure 5. 8 Survival analysis for YWHAG gene. (A) Kaplan-Meier plot showing low expression (blue) and high expression (red) of YWHAG. (B) YWHAG gene expression in normal solid tissue, primary tumour and metastatic samples.

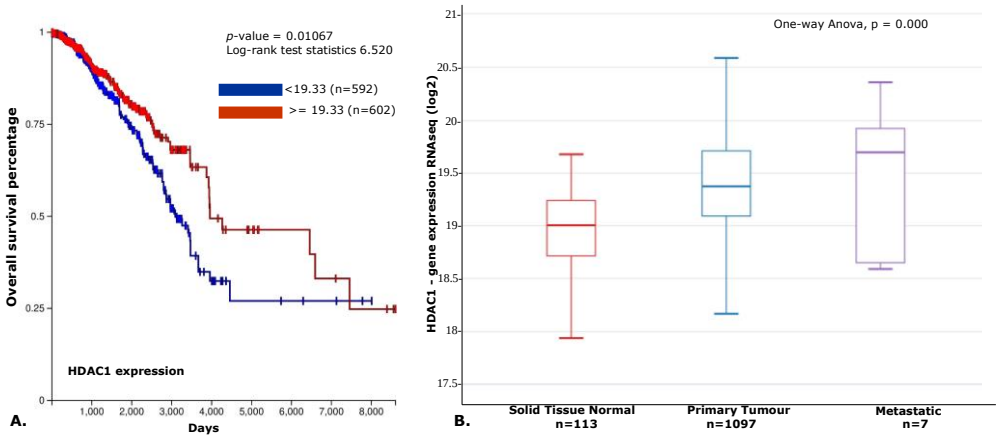

Figure 5. 9 Survival analysis for HDAC1 gene. (A) Kaplan-Meier plot showing low expression (blue) and high expression (red) of HDAC1. (B) HDAC1 gene expression in normal solid tissue, primary tumour and metastatic samples.

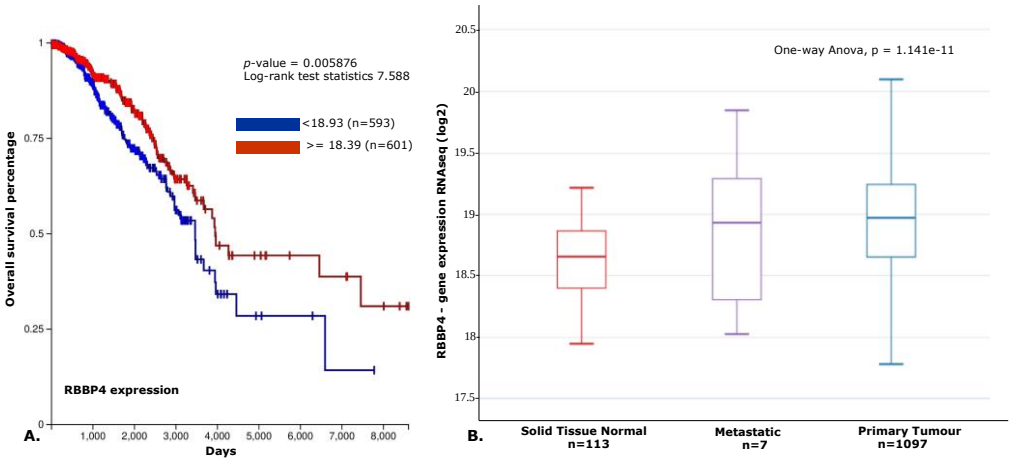

Figure 5. 10 Survival analysis for RBBP4 gene. (A) Kaplan-Meier plot showing low expression (blue) and high expression (red) of RBBP4. (B) RBBP4 gene expression in normal solid tissue, primary tumour and metastatic samples.

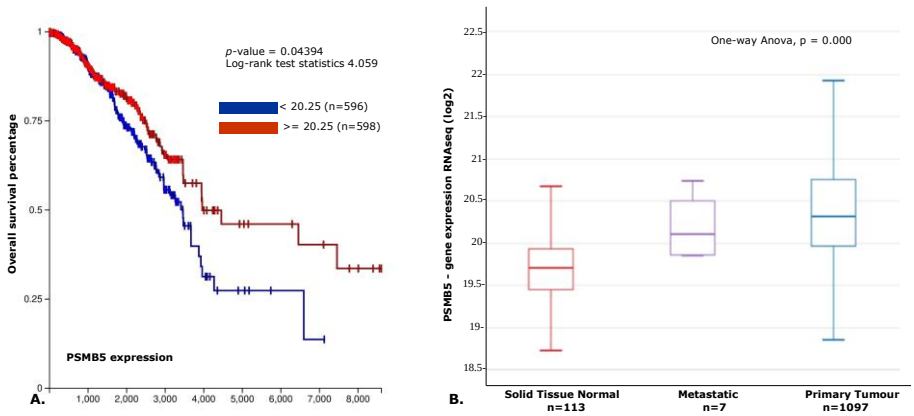

Figure 5. 11 Survival analysis for PSMB5 gene. (A) Kaplan-Meier plot showing low expression (blue) and high expression (red) of PSMB5. (B) PSMB5 gene expression in normal solid tissue, primary tumour and metastatic samples.

The DEGs listed in table 5.11 were shortlisted as they were significantly DEGs associated with the altered expression of calpain system genes that

were also seen to be significant with overall survival using the GDC TCGA breast cancer cohort. These DEGs were taken forward for assessment in the METABRIC cohort.

Table 5. 11 List of calpain system associated genes

Calpain system gene	Gene showing significance in overall survival on Xena browser
Calpain 1	PPP1CA- Serine/threonine-protein phosphatase PP1-alpha catalytic subunit
Calpain 2	AMOT- Angiomotin
	PRKAB2- protein kinase AMP-activated non-catalytic subunit beta 2
	AMOTL1- Angiomotin-like protein 1
	RAB13- RAB13, member RAS oncogene family
Calpain 4	MAGOH- mago homolog, exon junction complex subunit
	POLE2- DNA polymerase epsilon 2, accessory subunit
Calpastatin	YWHAG- tyrosine 3-monooxygenase/tryptophan 5-monooxygenase activation protein gamma
	HDAC1- histone deacetylase 1
	RBBP4- RB binding protein 4, chromatin remodelling factor
	PSMB5- proteasome subunit beta 5

The gene expression information available in the METABRIC cohort was at probe level while the TCGA cohort provided the overall mRNA expression level information.

5.4.5 Analysis with the METABRIC dataset

As mentioned previously, the METABRIC dataset had probe level information available for each gene that binds to specific sites on the gene. The number of probes and their sequences for the calpain system and the associated DEGs shortlisted in the table 5.11 are mentioned in section D4.3, appendix D.

Correlation analysis

Correlation assessments were performed between the shortlisted significant DEGs associated with altered calpain system gene expression using the Spearman's rank correlation test. Correlation analysis was performed (Figure 5.12) between each of the calpain system gene probes to their associated DEGs and their probes mentioned in Table 5.11.

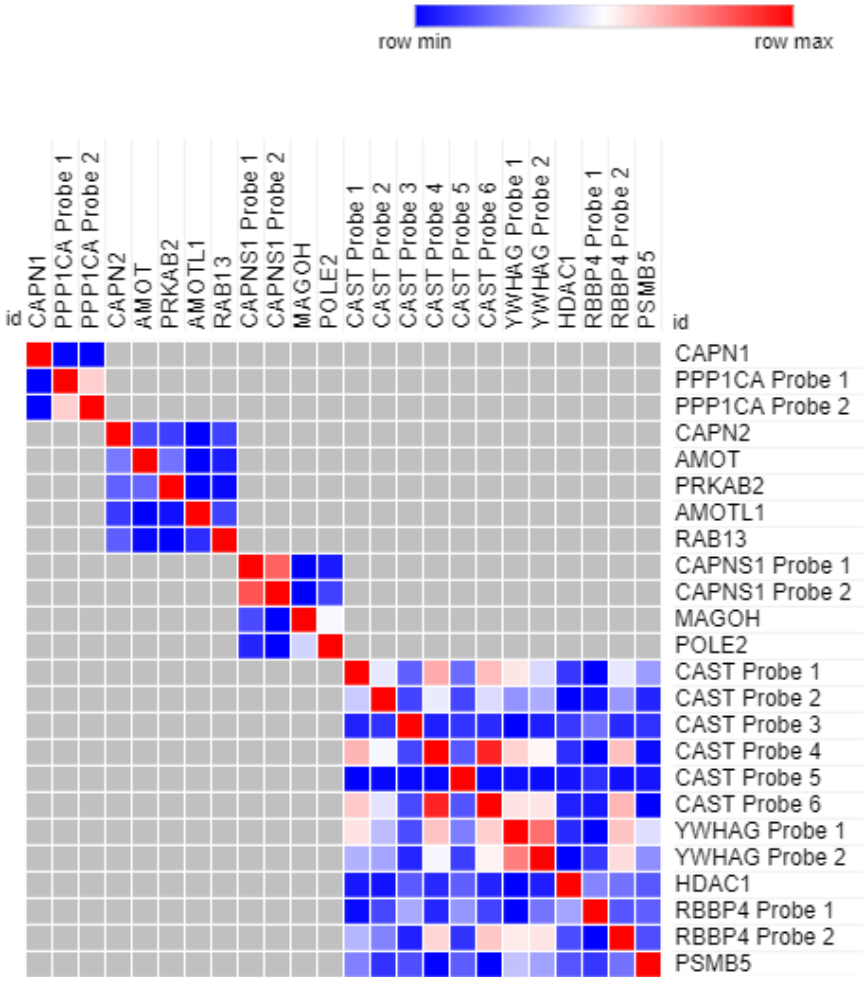

Figure 5. 12 Correlation between the calpain system and associated DEGs. A Morpheus map demonstrating correlations between CAPN1, CAPN2, CAPNS1 and CAST gene probes with the associated genes and probes.

Expression of CAPN1 was significantly correlated with PPP1CA probe 1 (P<0.001, r^2=0.091), PPP1CA probe 2 (P<0.001, r^2=0.086) expression. Expression of PP1CA probe 1 was significantly correlated with PP1CA probe 2 expression (P<0.001, r^2=0.631).

Expression of CAPN2 was significantly correlated with AMOT (P<0.001, r^2=0.194), PRKAB2 (P<0.001, r^2=0.171), AMOTL1 (P=0.01, r^2=0.058), RAB13 (P<0.001, r^2=0.174) expression. Expression of AMOT was significantly correlated with PRKAB2 (P<0.001, r^2=0.181), AMOTL1 (P<0.05, r^2=-0.058) expression. Expression of AMOTL1 was significantly correlated with RAB13 expression (P=0.001, r^2=0.075).

CAPNS1 probe 1 expression was significantly correlated with CAPNS1 probe 2 (P<0.001, r^2=0.794), MAGOH (P=0.001, r^2=-0.076) expression. Expression of CAPNS1 probe 2 was significantly correlated with MAGOH

(P<0.001, r^2=-0.260) and POLE2 (P<0.001, r^2=-0.101) expression. MAGOH expression was significantly correlated with POLE2 expression (P<0.001, r^2=0.354).

Expression of CAST probe 1 was significantly correlated with CAST probe 2 (P<0.001, r^2=0.287), CAST probe 3 (P=0.002, r^2=-0.069), CAST probe 4 (P<0.001, r^2=0.563), CAST probe 6 (P=0.004, r^2=-0.064), YWHAG probe 1 (P<0.001 and r^2=0.408), YWHAG probe 2 (P<0.001 and r^2=0.248), HDAC1 (P<0.001 and r^2=-0.169), RBBP4 probe 1 (P<0.001, r^2=-0.310), RBBP4 probe 2 (P<0.001, r^2=0.284) and PSMB5 (P<0.001, r^2=0.092). Expression of CAST probe 2 was significantly correlated with CAST probe 4 (P<0.001, r^2=0.363), CAST probe 6 (P<0.001, r^2=0.325), YWHAG probe 1 (P<0.001, r^2=0.159), YWHAG probe 2 (P<0.001,r^2=0.220), HDAC1 (P<0.001, r^2=-0.182), RBBP4 probe 1 (P<0.001, r^2=-0.151), RBBP4 probe 2 (P<0.001, r^2=0.171) and PSMB5 (P<0.001, r^2=-0.098). CAST probe 3 expression was significantly correlated with CAST probe 4 (P<0.05, r^2=-0.069), YWHAG probe 1 (P<0.001, r^2=-0.135), YWHAG probe 2 (P<0.01, r^2=-0.070), RBBP4 probe 1 (P<0.001 and r^2=0.110) and RBBP4 probe 2 (P=0.051, r^2=-0.044). CAST probe 4 expression was significantly correlated with CAST probe 6 (P<0.001, r^2=0.914), YWHAG probe 1 (P<0.001, r^2=0.493), YWHAG probe 2 (P<0.001, r^2=0.405), HDAC1 (P<0.001, r^2=-0.130), RBBP4 probe 1 (P<0.001, r^2=-0.236), RBBP4 probe 2 (P<0.001, r^2=0.536) and PSMB5 (P<0.001, r^2=-0.209). CAST probe 5 expression was significantly correlated with RBBP4 probe 1 (P=0.011, r^2=0.057). Expression of CAST probe 6 was significantly correlated with YWHAG probe 1 (P<0.001, r^2=0.460), YWHAG probe 2 (P<0.001, r^2=0.452), HDAC1 (P<0.001, r^2=-0.140), RBBP4 probe 1 (P<0.001, r^2=-0.163), RBBP4 probe 2 (P<0.001, r^2=0.566) and PSMB5 (P<0.001, r^2=-0.215). Expression of YWHAG probe 1 were significantly correlated with YWHAG probe 2 (P<0.001, r^2=0.712), HDAC1 (P<0.001, r^2=-0.225), RBBP4 probe 1 (P<0.001, r^2=-0.333), RBBP4 probe 2 (P<0.001, r^2=0.489) and PSMB5 (P<0.001, r^2=0.247). Expression of YWHAG probe 2 was significantly correlated with HDAC1 (P<0.001, r^2=-0.153), RBBP4 probe 2 (P<0.001, r^2=0.503) and PSMB5 (P<0.001, r^2=0.169). Expression of HDAC1 was significantly correlated with RBBP4 probe 1 (P<0.001, r^2=0.095), RBBP4

probe 2 (P<0.05, r^2=0.051). Expression of RBBP4 probe 1 was significantly correlated with RBBP4 probe 2 (P<0.001, r^2=-0.112) and PSMB5 (P<0.001, r^2=-0.085). Expression of RBBP4 probe 2 was significantly correlated with PSMB5 (P=0.01, r^2=0.057).

Survival analysis

The calpain system gene probes and associated DEGs were assessed for breast cancer specific survival using the METABRIC breast cancer cohort to determine the effect of their expression as independent biomarkers on patient survival. Kaplan-Meier plots were produced for each gene probes.

High expression of PPP1CA probe 2 was significantly associated with poor disease specific survival (P<0.001) (Figure 5.13C), while high expression of CAPN1 and PPP1CA probe 1 was not associated with disease specific survival (Figure 5.13A and 5.13B).

High PRKAB2 expression was significantly associated with poor disease specific survival (P<0.05) (Figure 5.14C). High expression of CAPN2, AMOT, AMOTL1 and RAB13 was not associated with breast cancer specific survival (Figure 5.14) in the METABRIC breast cancer cohort.

High expression of POLE2 gene was significantly associated with poor disease specific survival in the METABRIC breast cancer cohort (P<0.001) (Figure 5.15D). High expression of CAPNS1 probe1, CAPNS1 probe 2 and MAGOH was not associated with breast cancer specific survival (Figure 5.15).

High expression of CAST probe 4 and CAST probe 6 was significantly associated with better disease specific survival in the METABRIC breast cancer cohort (P<0.01 and <0.05, respectively). While high expression of YWHAG probe 2, RBBP4 probe 1 and PSMB5 was significantly associated with adverse disease specific survival (P<0.05, <0.001, =0.001, respectively). High expression of CAST probes 1, 2, 3, 5, YWHAG probe 1, HDAC1, and RBBP4 probe 2 was not associated with breast cancer specific survival (Figure 5.16).

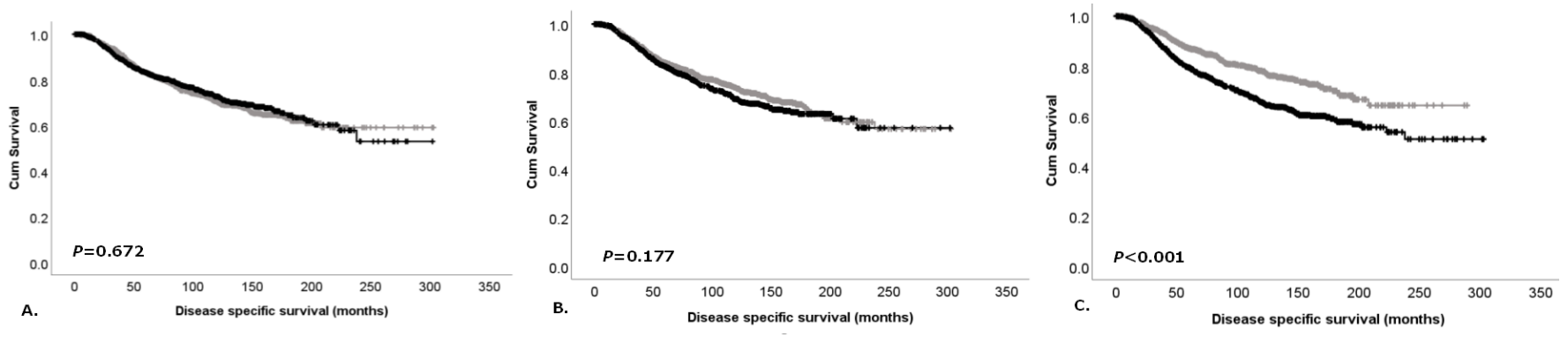

Figure 5. 13 Survival analysis of Calpain 1 and associated DEG probes. Kaplan-Meier analysis of (A) CAPN1, (B) PPP1CA probe 1 and (C) PPP1CA probe 2 showing association with high (black line) and low (grey line) expression on breast cancer specific survival. Log-rank test was used to determine the *P*-value.

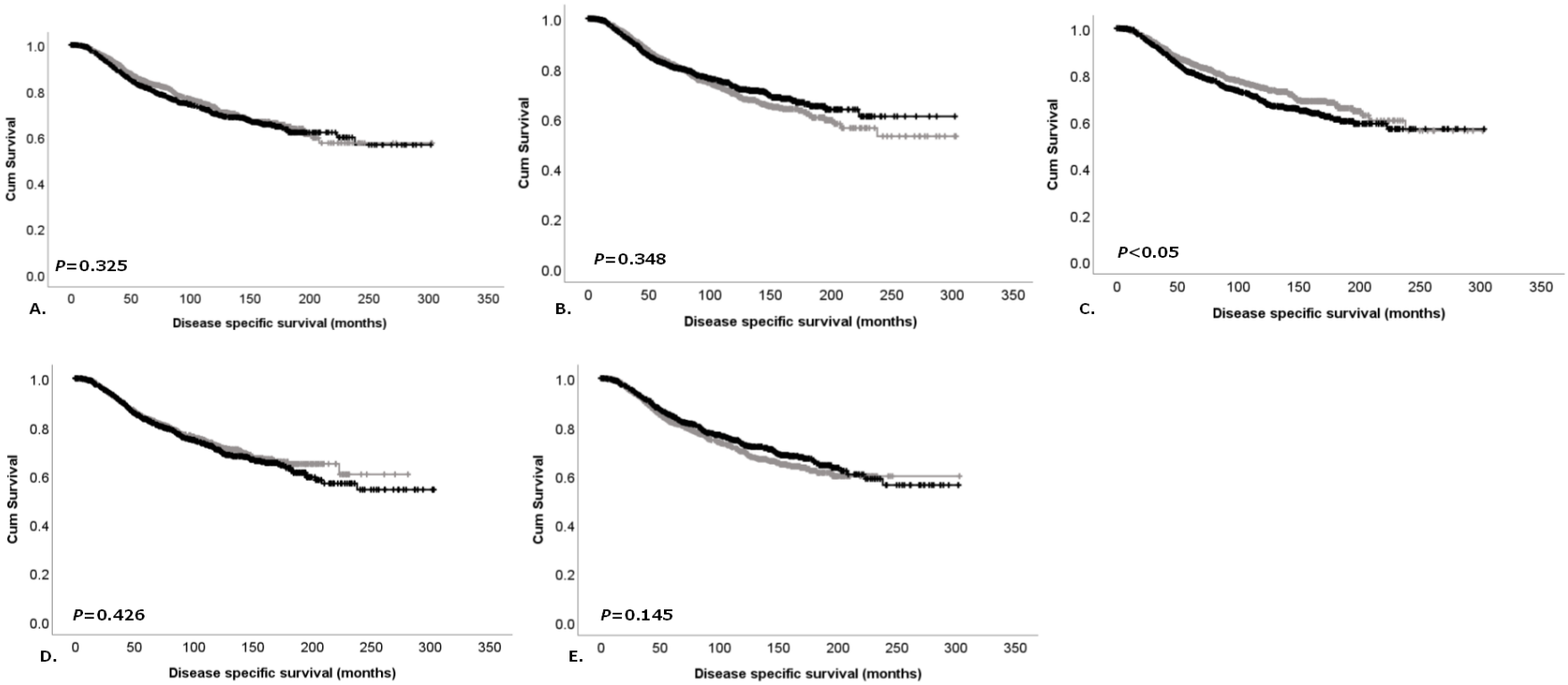

Figure 5. 14 Survival analysis of Calpain 2 and associated DEG probes. Kaplan-Meier analysis of (A) CAPN2, (B) AMOT, (C) PRKAB2, (D) AMOTL1 and (E) RAB13 gene showing association with high (black line) and low (grey line) expression on breast cancer specific survival. Log-rank test was used to determine the *P*-value.

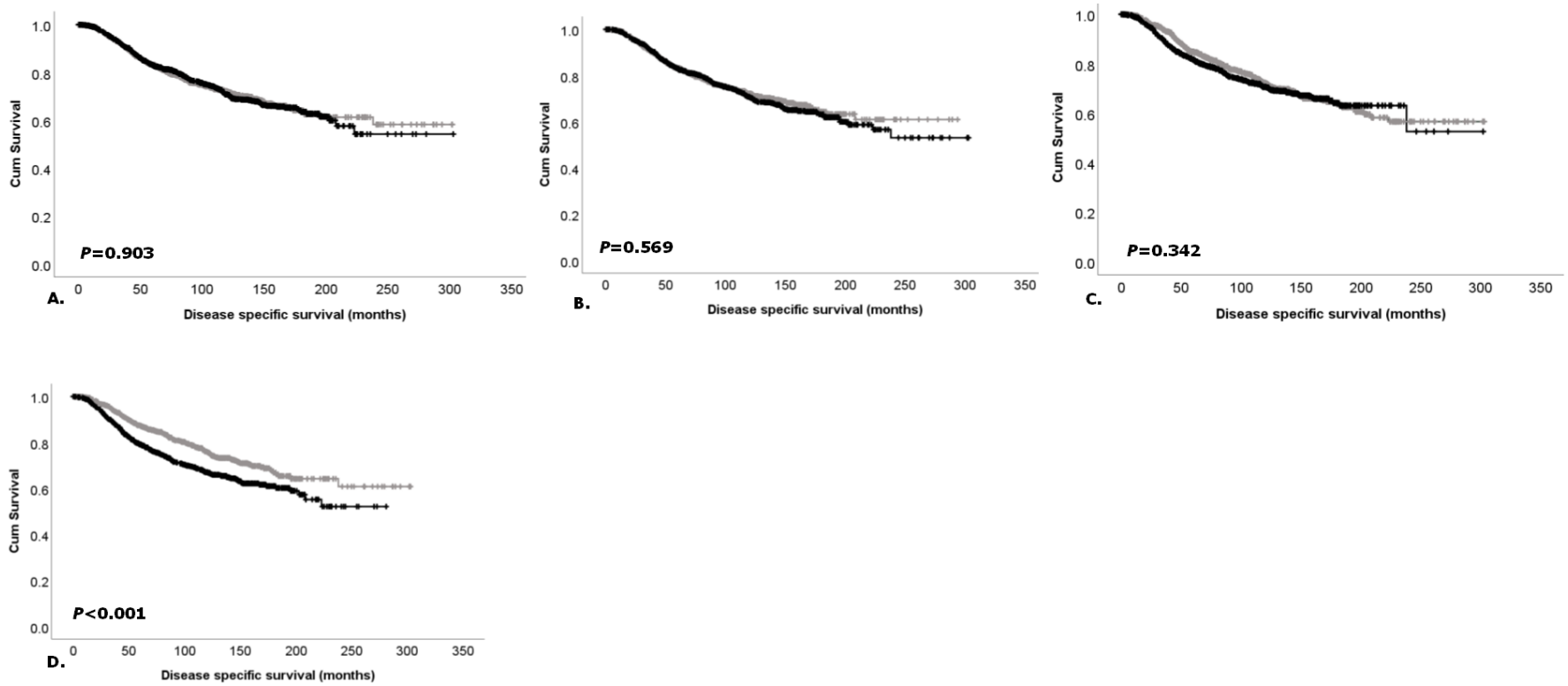

Figure 5. 15 Survival analysis of Calpain 4 probes and associated DEG probes. Kaplan-Meier analysis of (A) CAPNS1 probe 1, (B) CAPNS1 probe 2, (C) MAGOH and (D) POLE2 gene showing association with high (black line) and low (grey line) expression on breast cancer specific survival. Log-rank test was used to determine the *P*-value.

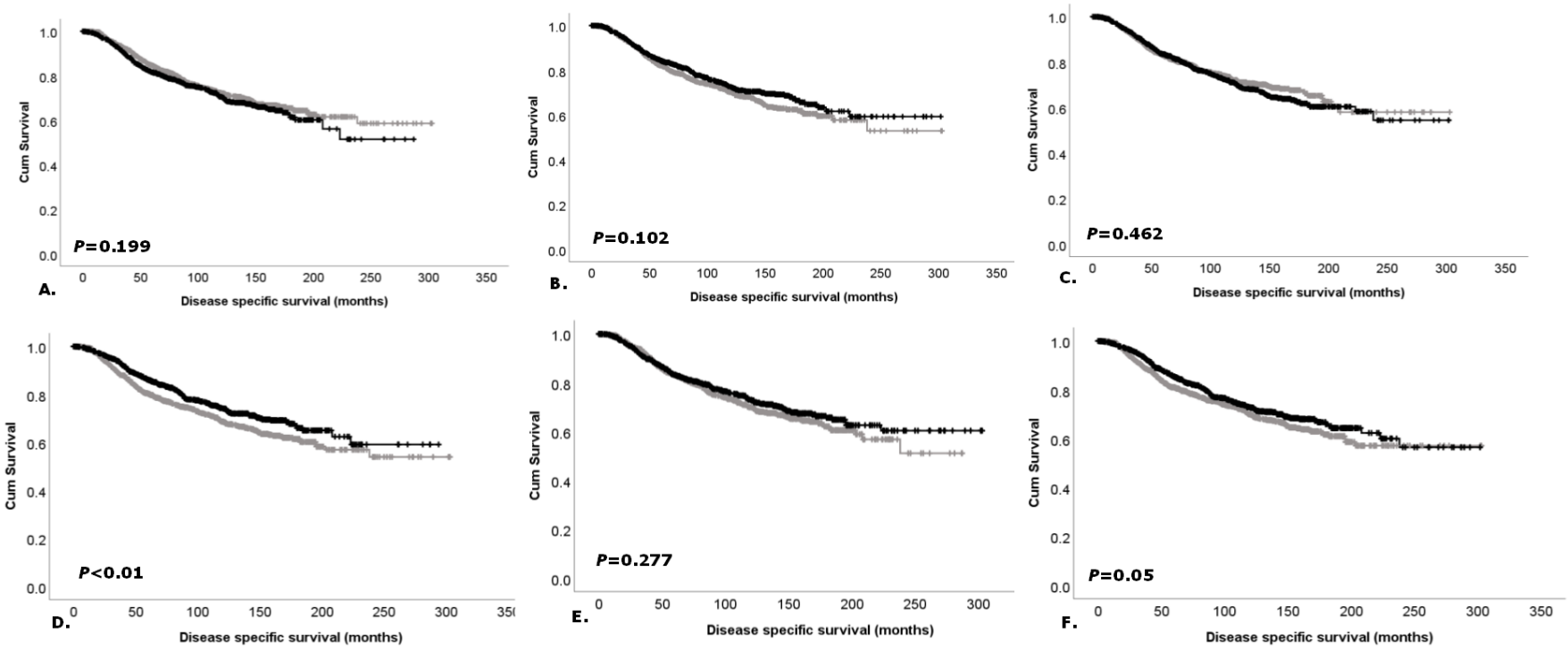
A.
P=0.199
B.
P=0.102
C.
P=0.462
D.
P<0.01
E.
P=0.277
F.
P=0.05
Cum Survival
Disease specific survival (months)

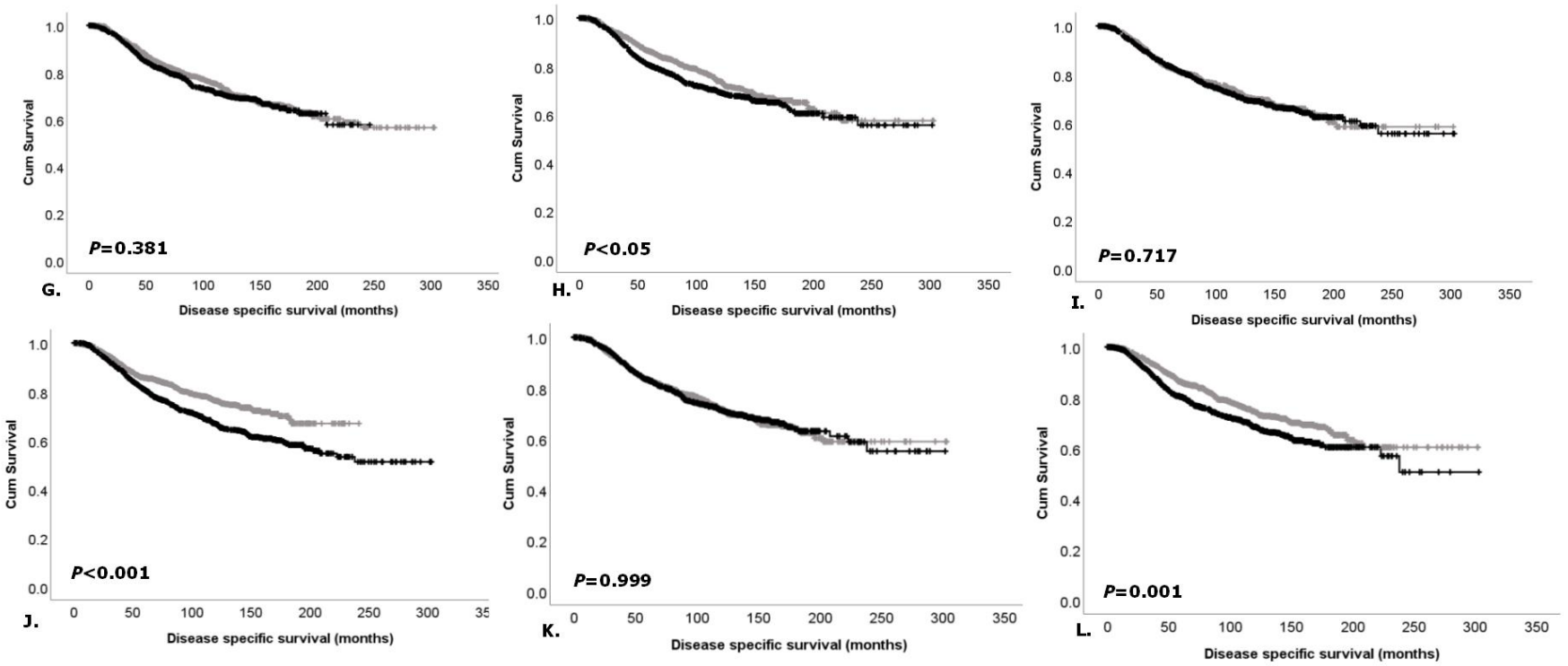

Figure 5. 16 Survival analysis of CAST probes and associated DEG probes. Kaplan-Meier analysis of (A) CAST probe 1, (B) CAST probe 2, (C) CAST probe 3, (D) CAST probe 4, (E) CAST probe 5, (F) CAST probe 6, (G) YWHAG probe 1, (H) YWHAG probe 2, (I) HDAC1, (J) RBBP4 probe 1, (K) RBBP4 probe 2,and (L) PSMB5 gene showing association with high (black line) and low (grey line) expression on breast cancer specific survival. Log-rank test was used to determine the *P*-value.

Due to a striking localisation observed for calpastatin type II, mentioned in Chapter 2 section 2.4.3, the CAST gene probes and the associated DEG probes were taken forward to assess their protein expression in breast cancer cells and tissues. The RBBP4 gene was selected to be taken forward for assessment of protein expression in breast cancer tissues as compared to the other shortlisted DEGs RBBP4 probe 2 had a biologically intermediate but statically significant correlation with CAST probes 4 and 6. This was the highest and significant correlation observed between the CAST gene probes and their associated DEGs and their probes. High expression of RBBP4 probe 1 was also seen to be significantly associated with adverse breast cancer specific survival. In addition, RBBP4 has been reported previously to be associated with cancer but no associations previously reported with the calpain system. It was therefore selected as the biomarker to assess protein expression in breast cancer tissues and its associations with breast cancer clinical outcomes. The RBBP4 protein was stained in the Nottingham cohort of breast cancer patients to determine the associations between its expression and different breast cancer subtypes and their clinical outcomes.

The different CAST probes 1-6 and the RBBP4 probes 1-2 were assessed for their binding on their respective genes using the *Ensemble* database. Table D4.2, appendix D demonstrates the CAST and RBBP4 transcripts with which each probes bind.

Categorised RBBP4 probes were assessed against clinicopathological variables (Table 5.12). As can be seen, high RBBP4 probe 1 expression was significantly associated with Pam50 subtype (χ^2=47.254, d.f. =5, P<0.001) and tumour stage (χ^2= 29.655, d.f. =4, P< 0.001). While high expression of RBBP4 probe 2 was significantly associated with negative ER (χ^2= 7.522, d.f.=1, P<0.01), positive HER2 (χ^2 = 7.427, d.f.=1, P<0.01), negative PR (χ^2= 19.456, d.f. =1,P<0.001), p53 mutation (χ^2= 7.437, d.f.=1, P=0.006) status, grade 3 tumours (χ^2 = 13.553, d.f.=2, P=0.001), poor NPI (χ^2= 8.95, d.f. =2, P=0.011), HER2 and basal subtypes (χ^2= 32.947, d.f.=5, P<0.01), tumour stage (χ^2= 50.025, d.f.=4, P<0.001), and in patient's above the age of 60 (χ^2 = 5.336, d.f.=1, P=0.021).

Table 5. 12 Associations between the expression of RBBP4 probes 1 and 2 and the breast cancer clinicopathological variables.

		RBBP4 probe 1			RBBP4 probe 2		
		Low	**High**	**P value**	**Low**	**High**	**P value**
Age at diagnosis	<60	445 (22.5%)	426 (21.5%)		461 (23.3%)	410 (20.7%)	
	≥60	544 (27.5%)	563 (28.5%)	0.389	528 (26.7%)	579 (29.3%)	**0.021**
Size	<2cm	8 (0.4%)	7 (0.4%)		7 (0.4%)	8 (0.4%)	
	≥2cm	970 (49.5%)	975 (49.7%)	0.789	975 (49.7%)	970 (49.5%)	0.789
Grade	1	74 (3.9%)	95 (5%)		96 (5.1%)	73 (3.9%)	
	2	400 (21.2%)	370 (19.6%)	0.127	414 (21.9%)	356 (18.8%)	
	3	466 (24.6%)	486 (25.7)		438 (23.2%)	514 (27.2%)	**<0.001**
NPI	Good	342 (17.3%)	339 (17.1%)		372 (18.8%)	309 (15.6%)	
	Moderate	554 (28%)	546 (27.6%)		525 (26.5%)	575 (29%)	
	Poor	94 (4.7%)	105 (5.3%)	0.712	93 (4.7%)	106 (5.4%)	**0.011**
ER expression	Low	238 (12%)	234 (11.8%)		210 (10.6%)	262 (13.2%)	
	High	752 (38%)	756 (38.2%)	0.833	780 (39.4%)	728 (36.8%)	**0.006**
Her 2 Expr	Negative	862 (43.5%)	872 (44%)		887 (44.8%)	847 (42.8%)	
	Positive	128 (6.5%)	118 (6%)	0.496	103 (5.2%)	143 (7.2%)	**0.006**
PR Expression	Negative	487 (24.6%)	451 (22.8%)		420 (21.2%)	518 (26.2%)	
	Positive	503 (25.4%)	539 (27.2%)	0.105	570 (28.8%)	472 (23.8%)	**<0.001**
Pam50subtype	Basal	163 (8.2%)	168 (8.5%)		163 (8.2%)	168 (8.5%)	
	Her2	117 (5.9%)	122 (6.2%)		83 (4.2%)	156 (7.9%)	
	Lum A	358 (18.1%)	357 (18%)		393 (19.8%)	322 (16.3%)	
	Lum B	207 (10.5%)	283 (14.3%)		244 (12.3%)	246 (12.4%)	
	NC	4 (0.2%)	2 (0.1%)		1 (0.1%)	5 (0.3%)	
	Normal	141 (7.1%)	58 (2.9%)	**<0.001**	106 (5.4%)	93 (4.7%)	**<0.001**
Lymph node	Negative	513 (26%)	522 (26.5%)		528 (26.8%)	507 (25.7%)	
	Positive	473 (24%)	465 (23.6%)	0.702	455 (23.1%)	483 (24.5%)	0.266
Stage	0	276 (18%)	214 (14%)		190 (12.4%)	300 (19.6%)	
	1	149 (9.7%)	222 (14.5%)		228 (14.9%)	143 (9.3%)	
	2	281 (18.3%)	290 (18.9%)		281 (18.3 %)	290 (18.9%)	
	3	35 (2.3%)	55 (3.6%)		56 (3.7%)	34 (2.2%)	
	4	8 (0.5%)	2 (0.1%)	**<0.001**	6 (0.4%)	4 (0.3%)	**<0.001**
Menopausal status	Post	772 (39.2%)	762 (38.7%)		759 (38.5%)	775 (39.4%)	
	Pre	213 (10.8%)	222 (11.3%)	0.616	227 (11.5%)	208 (10.6%)	0.319
P53 mutation status	MUT	52 (6.4%)	47 (5.8%)		42 (5.1%)	57 (7%)	
	WT	344 (42.1%)	374 (45.8%)	0.389	409 (50.1%)	309 (37.8%)	**0.006**

5.4.6 RBBP4 protein expression

RBBP4 protein expression was assessed on breast tumour tissues. Before staining the breast cancer tissues, the RBBP4 antibody was checked for specificity. Western blot analysis was conducted on cell lysates prepared form MDA-MB-231, MDA-MB-468, T47D and MCF-7 cell lines. Presence of single bands at 48 kDa confirmed the presence of RBBP4 expression in all the cell lines and specificity of the antibody (Figure 5.17A). RBBP4 protein expression was then assessed in breast cancer tissues by immunohistochemical staining. It was seen the RBBP4 was mainly localised in the nuclear region of the breast cancer cells (Figure 5.17B). The stained cells were scored by assigning a percentage score for staining intensities. The percentage intensities were however, seen to be approximately 100% for most of the cases (with an ICC of 0.57). Due to which the cores were rescored by assigning H-scores. This was conducted by two independent observers. The calculated ICC score was 0.52. As the ICC scores were <0.7 (using both the methods), no further analysis could be done to produce reliable data. Hence, further analysis was discontinued.

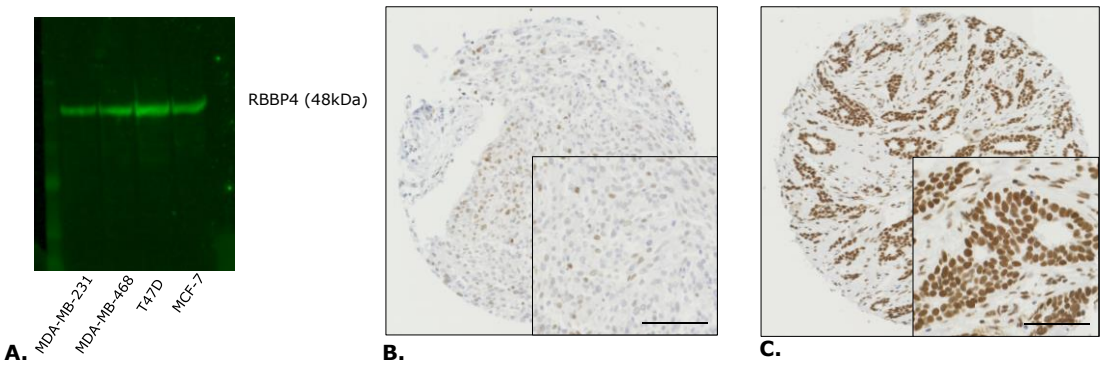

Figure 5. 17 RBBP4 expression in breast cancer cells and tissue. (A) Representative blot of a single RBBP4 bands showing antibody specificity. Representative microphotograph of RBBP4 expression in breast cancer tissue showing (B) low and (C) high expression at 10x magnification with a 20x magnification inset box. Scale bar represents 100 µm.

5.5 Discussion

The calpain system associated DEGs enriched several pathways. The pathways enriched by DEGs associated with altered expression of CAPN1 included the cell cycle, proteasome, DNA replication and DNA repair pathways like homologous recombination and base excision repair pathways. As mentioned previously calpains have been shown to regulate the cell cycle and the G1/S phase transition (Jánossy *et al.*, 2004; Joy *et al.*, 2006). In normal cells, calpain 1 and calpain 2 induce cell cycle arrest. However in cancer cells, they can promote cell cycle progression (Choi *et al.*, 1997; Wang *et al.*, 2003). DNA polymerase η (pol η) is a known substrate of the calpains and is involved in translesion DNA synthesis across UV-induced DNA lesions (Nettersheim *et al.*, 2021). Pathways enriched by the DEGs associated with the altered expression of CAPN2 included tight junction pathways, Hippo signalling and cell cycle pathway. Calpains 1 and 2 have been shown to be involved in cell cycle progression, as mentioned previously (Choi *et al.*, 1997; Wang *et al.*, 2003). The DEGs associated with the altered expression of CAPNS1 enriched several pathways including cell cycle, DNA replication, cellular senescence, mismatch repair, adherens junction. And the pathways enriched by the DEGs associated with the altered expression of calpastatin included nucleotide excision repair, cell cycle, cellular senescence, DNA replication, apoptosis and several more.

These enriched pathways were assessed for common genes between the two datasets and the common DEGs were shortlisted for the common pathways. These DEGs were then mapped on to the pathways using the KEGG pathway dataset. The shortlisted DEGs associated with altered expression of CAPN1 mentioned in table 5.7 included several genes viz PTTG1, CDC25A and several more. Pituitary Tumour-Transforming Gene 1 (PTTG1) has been shown to have an effect on the stability of p53 by modulation of susceptibility by calpains (Bernal *et al.*, 2007). Sadeghi et al demonstrated that the Cell Division Cycle 25A (CDC25A) gene was involved in cell proliferation and tumorigenesis and that silencing of CDC25A led to reduced proliferation and a change in expression of proteins involved in regulation of cyclin D1 and G1/S transition including calpains (Sadeghi *et al.*, 2019). The shortlisted DEGs associated with the altered expression of

CAPN2 mentioned in table 5.8 enlisted several genes including OCLN. In human cervical epithelial CaSki cells, it was seen that calpains were involved in disassembly of tight junction by calpain mediated breakdown of Occludin (OCLN) from 65-kDa form to a 50-kDa form (Zhu *et al.*, 2006). The DEGs associated with altered expression of CAPNS1 mentioned in table 5.9 included CDC25C, E2F3 and SMAD2 among several others. Cell Division Cycle 25C (CDC25C) has been shown to be proteolysed by calpains and not by the proteasome in glioblastoma cells leading to the rescue of downregulated CDC25C in the presence of ansamycins (García-Morales *et al.*, 2007). A study suggested that the activated calpains may have an involvement in the overexpression of E2F Transcription Factor 3 (E2F3) that in turn could lead to the urothelial tumour cell proliferation (Roperto *et al.*, 2010). A study showed that calpain 4 mediated proteolysis of the central signalling component of the SMAD family member 2 (SMAD2) in macrophages causes a reduction in TGFβ transcriptional activity in the presence of hypoxia (Cui *et al.*, 2015). Altered expression of CAST led to the differential expression of the genes shortlisted in table 5.10 which included genes viz PSMA7, PCNA, CCNB1, CCNB2 and several more. These shortlisted DEGs associated with altered expression of different calpain system genes were mapped onto their respective pathways.

The above mentioned shortlisted DEGs demonstrated that they were expressed differently by the altered expression of the queried calpain system gene in the breast cancer cohorts. To assess the effect of their expression on survival, survival analysis were done using the GDC TCGA cohort. Survival analysis would also identify the genes that were significantly associated with survival and independently of the calpain system genes in the GDC TCGA breast cancer cohort. The DEG expression was also shown in breast cancer patients grouped into solid normal tissue (n=113), primary tumour (n=1097) and metastatic tumours (n=7). Only the DEGs associated significantly with the altered expression of calpain system genes and were with survival were further shortlisted and taken forward for analysis in the METABRIC cohort. The Protein Phosphatase 1 Catalytic Subunit Alpha (PPP1CA) gene was identified as the only DEG associated with the altered expression of CAPN1 and significantly associated

with overall survival in the GDC TCGA cohort. High expression of PPP1CA was associated with better overall survival (P<0.01). PPP1CA gene encodes for one of the three catalytic subunits of the multifunctional protein PP1 which is involved in a numbers of important cellular pathways. It has been shown to play a role in steering cell migration and in the tumour microenvironment. Expression of PPP1CA mRNA has shown to be associated with breast cancer specific survival (Saidy *et al.*, 2021). In addition, it has been shown that siRNA knockdown of the gene led to inhibition of cell proliferation and migration in breast cancer cells (Xie *et al.*, 2022). Calpain 1 and calpain 2 have been shown to be inactivated by phosphatases like PP2A, however there is less evidence of the direct association of PPP1CA and calpains (L. Xu *et al.*, 2006b).

The significant DEGs associated with the altered expression of CAPN2 and survival were AMOT, PRKAB2, AMOTL1 and RAB13 genes. High expression of Angiomotin (AMOT) was significantly associated with poor overall survival in the GDC TCGA breast cancer cohort (P<0.01). The AMOT is a membrane protein that plays a central role in the maintenance of tight junctions that regulate cell shaping, migration and has been linked to angiogenesis (Jiang *et al.*, 2006; Sang *et al.*, 2021). It has been shown previously that AMOT is overexpressed in breast cancer cells and plays an important role in breast cancer cell proliferation and invasion (Lv *et al.*, 2015). In addition, the AMOT transcript has been shown to be associated with shorter overall survival (P<0.05) (Jiang *et al.*, 2006). High expression of Protein Kinase AMP-Activated Non-Catalytic Subunit Beta 2 (PRKAB2) was significantly associated with poor overall survival in the GDC TCGA breast cancer cohort (P<0.01). The PRKAB2 protein encoded by PRKAB2 gene is a regulatory subunit of AMPK which is an energy sensor protein kinase that plays an important role in regulating cellular energy. The PRKAB2 gene has shown to be overexpressed in breast cancer patients and was associated with poor overall survival in a breast cancer cohort (Li *et al.*, 2021). It has been reported that activation of the AMPK pathway is mediated by calpain 2, however the direct association of calpains with PRKAB2 is unclear (Zhang *et al.*, 2017). High expression of the Angiomotin like 1 (AMOTL1) gene was significantly associated with poor overall survival in the GDC TCGA cohort

(P<0.05). AMOTL1 is a member of the motin family. It plays a key role in the modulation of the endothelial cell polarity and migration (Moleirinho *et al.*, 2014). AMOTL1 expression modulated by Hippo signalling has been shown to promote progression of breast cancer (Couderc *et al.*, 2016). High expression of RAB13, a member of the RAS Oncogene Family, was significantly associated with better overall survival in the GDC TCGA breast cancer cohort (P=0.001). RAB13 is a GTPase found at the trans-Golgi network, on endosomes and at the plasma membrane. It has been shown to stimulate migration, metabolism and cell proliferation in cancer cells (Chen *et al.*, 2019). It has been reported to be highly expressed in breast cancer stem cells and its depletion leads to suppression of breast cancer cell stemness, tumorigenesis and chemoresistance (Wang *et al.*, 2022).

The significant DEGs associated with altered expression of CAPNS1 and that were significantly associated with survival were MAGOH and POLE2. High expression of Mago-nashi Homolog, (MAGOH) was associated significantly with better overall survival in the GDC TCGA breast cancer cohort (P<0.05). It is an important component of the exon junction complex (EJC) that mediates mRNA processing like splicing, translocation and localisation (Zhou *et al.*, 2020). MAGOH has shown to be upregulated in breast cancer and is expressed differentially between the ER positive and TN tumour subtypes (Stricker *et al.*, 2017). High expression of DNA Polymerase Epsilon 2 (POLE2), was significantly associated with better overall survival in the GDC TCGA breast cancer cohort (P<0.05). It belongs to the DNA polymerase B family and is its second largest subunit with a molecular weight of 59 kDa. It plays a key role in cellular functions including DNA replication, DNA repair and regulation of the cell cycle (Zhu *et al.*, 2020). It was reported that altered expression of POLE2 was predictive of survival in the METABRIC breast cancer cohort (Pearlman *et al.*, 2019).

The significant DEGs associated with altered expression of CAST and with survival were YWHAG, HDAC1, RBBP4 and PSMB5. High expression of the Tyrosine 3-Monooxygenase/Tryptophan 5-Monooxygenase Activation protein Gamma (YWHAG) was significantly associated with overall survival in the GDC TCGA breast cancer cohort (P<0.05). The gene product belongs to the 14-3-3 family. The protein regulates a vast range of cell signalling

pathways by forming protein-protein complexes with signalling proteins within a specific sequence motif (Ye *et al.*, 2021). A study showed that YWHAG was located in the pseudopodia of MDA-MB-231 cells and knockdown of the gene resulted in decreased pseudopod formation, migration and wound healing. In addition, YWHAG was also shown to be expressed in lymphatic invasion sites than the centre and periphery of the human breast cancer tissue (Hiraoka *et al.*, 2019). High expression of the Histone Deacetylase 1 (HDAC1) was significantly associated with better overall survival in the GDC TCGA breast cancer cohort (P=0.01). It is a member of the histone deacetylase family that catalyses the deacetylation of lysine residues on the N-terminal part of the core histones. They regulate major endothelial functions such as inflammatory signalling, redox homeostasis and angiogenesis (Dunaway *et al.*, 2021). HDAC1 expression was shown to be negatively correlated with ER and PR expression in breast cancer (Guo *et al.*, 2020). High expression of the Retinoblastoma Binding Protein 4 (RBBP4) was significantly associated with better overall survival in the GDC TCGA breast cancer cohort (P<0.01). RBBP4 is a nuclear protein which belongs to a highly conserved subfamily and plays a key role in nucleosome assembly, chromatin metabolism and histone modification. In a small cohort of 240 breast cancer patients and it was seen that RBBP4 expression was significantly higher in breast cancer than the normal tissues and was significantly correlated with lymph node metastasis (Guo *et al.*, 2020). High expression of the Proteasome 20S Subunit Beta 5 (PSMB5) was associated with better overall survival in the GDC TCGA breast cancer cohort (P<0.05). PSMB5 is the component of the 20S core of the proteasome complex that is involved in the proteolytic degradation of intracellular proteins. The proteasome has shown to be significantly activated in the TNBC and that PSMB5 was overexpressed in the TNBC tissue. It has been predictive of poor prognosis of breast cancer. In addition it was reported that knockdown of PSMB5 led to induction of apoptosis and significantly enhanced chemo sensitivity to bortezomib and paclitaxel (Wei *et al.*, 2018).

The DEGs shortlisted in table 5.11 were assessed for correlations with the calpain system genes in the METABRIC cohort (n=1980). In the METABRIC

cohort the mRNA expression data was available using ILLUMINA probes. These probes are 50 nucleotide long sequences that bind to a complimentary region on the gene. The CAPN1 gene had one probe and its associated DEG, PPP1CA had two probes available. One probe was available for the CAPN2 and associated DEGs (AMOT, PRKAB2, AMOTL1 and RAB13). Two probes were available for the CAPNS1 gene and one probe was available for its associated DEGs (MAGOH and POLE2). The CAST gene had six probes available, two probes were available for its associated DEGs, YWHAG and RBBP4, and one probe was available for CAST associated DEGs HDAC1 and PSMB5.

To assess the correlation between the calpain system genes and their associated DEGs mRNA expression data available from the METABRIC cohort was used. Several correlations were statically significant, however they were of a weak biological significance. However, statistically significant and biologically intermediate to strong relevance was seen between the expressions of different probes of the gene including, PPP1CA probes 1 and 2, CAPNS1 probes 1 and 2, CAST probes 1 and 4, CAST probes 4 and 6. Interestingly, statistically significant and biologically intermediate to strong correlations were seen between the expressions of CAST probe 4 and YWHAG probe 1, CAST probe 4 and RBBP4 probe 2, CAST probe 6 and RBBP4 probe 2, and YWHAG probe 2 and RBBP4 probe 1. It is interesting to note that CAST probe 4 was found to be located on the L-domain and CAST probe 6 was located on the inhibitory domain region.

Survival analysis was performed on the calpain system gene probes and their associated DEGs and probes to determine the association between their expression and breast cancer specific survival. The mRNA expression was categorised around the median expression of the probe. High expressions of PPP1CA probe 2, PRKAB2, POLE2, RBBP4 probe 1 and PSMB5 were significantly associated with poor breast cancer specific survival. While, high expression of CAST probes 4 and 6 were associated with better breast cancer specific survival. No association were observed between the remaining probes and breast cancer specific survival.

The CAST gene and its associated DEGs were selected to be taken for analysis for protein expression, due to the unique intracellular localisation of Calpastatin type II. Amongst the DEGs associated with the altered expression of CAST, RBBP4 was selected to assess its protein expression in breast cancer cells and tissues. High expression of RBBP4 probe 1 was significantly associated with adverse breast cancer specific survival and expression of RBBP4 probe 2 had a statically significant and biologically intermediate correlation to CAST probes 4 and 6. RBBP4 has been studied in a small breast cancer cohort previously and its high expression was shown to be associated with poor overall survival. To confirm these results in a bigger cohort and to establish associations between the expression of RBBP4 and different breast cancer subtypes and their clinical outcomes, RBBP4 was selected to assess its expression in the breast cancer tissue. Several alignment assessments showed that CAST probe 1 is located in an untranslated region, CAST probes 2 and 4 are located in the L-domain, and CAST probes 3, 5 and 6 are located within the inhibitory domains of CAST gene. RBBP4 probes 1 and 2 may be located in the untranslated region.

RBBP4 probe mRNA expressions were assessed for their associations with different breast cancer clinicopathological parameters. High RBBP4 probe 1 expression was significantly associated with Pam50 subtype and tumour stage, and high RBBP4 probe 2 expression was significantly associated with negative ER and PR, positive HER2, mutated p53 status, grade 3 tumours, tumour stage, HER2 and basal subtypes and older age at diagnosis.

To assess the RBBP4 protein expression, the antibody was validated in breast cancer cell lines. Cell lysates prepared from MDA-MB-231, MDA-MB-468, T47D and MCF7 cell lines were used to assess the expression of RBBP4 and the antibody specificity. Single bands were observed in both the TNBC cell lines (MDA-MB-231 and MBA-MB-468) and the luminal cell lines (T47D and MCF7) suggesting that RBBP4 is expressed in Luminal and TNBC subtypes of breast cancer. RBBP4 was taken forward to assess its expression in breast cancer tissue by immunohistochemistry. In the tissues, its expression was localised predominantly in the nucleus of the breast cancer cells. RBBP4 expression was observed in most of the patients however, there was some variation between the patient cores. To quantify

RBBP4 staining, percentage intensity scoring was done by two individual scorers. However, the percentage scores were seen to be largely around 100% in most of the cases. In addition, the ICC calculated was 0.57. To differentiate this, the tissue cores were therefore, rescored using the H-scoring method with the ICC between two individual scorers of 0.52. Two attempts were made with different approaches to score the expression of RBBP4 and both resulted in an ICC score of <0.7. It was therefore concluded, as time was limited during the final month of the project, that further analysis on the expression of RBBP4 could not be conducted. The associations with survival and other clinicopathological parameters could not be reliably established. As mentioned previously, RBBP4 was seen to be expressed in most of the patient cores with some variation. These variations however, could not be assessed reproducibly. Given the time constraints, further re-training and re-scoring could not be done.

Suggested future work

Future work includes-

1. Rescoring the RBBP4 biomarker in the breast cancer tissues and establishing associations between its expression and different breast cancer subtypes and their clinical outcomes.
2. Assessing protein expression of another calpain system associated DEG in breast cancer cell lines and tissue.

Chapter 6- General Discussion, limitations and suggestions for future work

6.1 General discussion

Conventional therapeutic strategies are effective however not all patients respond. Treatment resistance, resulting from multiple mechanisms, is often encountered. As result, there is an interest in predictive biomarkers, such as the calpain system of proteins. Previous data from our group has shown that Calpain 1 expression is associated with adverse relapse free survival in HER2 positive breast cancer patients treated with trastuzumab following adjuvant therapy (Pu *et al.*, 2016b). In addition to playing a role in response to trastuzumab our group has also shown a role in breast cancer disease progression, overall survival across various cancer types and also resistance to other anticancer treatments (Storr *et al.*, 2013; Storr *et al.*, 2012b; Storr *et al.*, 2012c). The aim of this current study was to assess the role of the calpain system in breast cancer progression and treatment response. This aim was fulfilled using three strategies. The first strategy included molecular overexpression of calpastatin isoforms in breast cancer cells.

Calpastatin, the endogenous inhibitor of calpains can reversibly inhibit up to four calpain molecules. The current group performed multiple studies with calpastatin, results from which suggest that modulation of calpastatin isoform expression may play a crucial role in progression and treatment response in breast cancer (Storr *et al.*, 2012a; Storr *et al.*, 2011b; Storr *et al.*, 2016).

As mentioned previously, alternative splicing and different promoter usage leads to the production of several calpastatin transcripts (Parr *et al.*, 2001). Calpastatin types I, II, III and IV are summarised in the section 2.1.4. DNA constructs containing calpastatin types I, II and III were stably transfected into MDA-MB-231 and T47D cells. These two cell lines were selected as they showed low protein and mRNA calpastatin levels, short doubling times and suitable clonogenic plating efficiencies.

A monoclonal population was generated for each cell line by performing single cell cloning. HA-tagged calpastatin type I protein was detected as a single band, type II was seen as a duplet band and multiple bands were observed for type III in both lines. It is thought that the presence of multiple

bands might represent proteolytic products or observed as a result of protease degradation at the N-terminal of the transcript (Goll *et al.*, 2003). It would have been useful to identify these proteolytic products by pull down (Co-IP) and mass spectrometry technique. This however could not be done due to time and funding constraints.

As no antibodies against specific isoforms exist the level of overexpression of calpastatin isoforms in T47D and MDA-MB-231 cell lines was determined using RT-qPCR. The fold change in mRNA calpastatin type I expression was determined previously by Dr. Sukkarn (Sukkarn, 2020). Calpastatin type I had a 6.22 fold ($P<0.0001$) and 2.60 fold ($P<0.01$) higher expression in T47D and MDA-MB-231 cells, respectively, compared to their mock-transfected control cells. Higher expression in the luminal line as opposed to the TNBC was confirmed by examining HA-tagged calpastatin I protein levels. CAST II transfected cells had a 3.1 fold ($P=0.01$) and 5.8 fold ($P<0.01$) higher mRNA expression in T47D and MDA-MB-231 cells, respectively, compared to their mock-transfected control cells. As with CAST I, the marginally higher level of CAST II in TNBC's as opposed to the luminal line was confirmed by assessing levels of HA-tagged calpastatin type II protein expression.

It was noted that HA-tagged calpastatin type I protein and calpastatin type I mRNA expression was generally higher in both lines compared to calpastatin type II expression, suggesting that the promoter for calpastatin type I may be more active in breast cancer cells compared to calpastatin type II or that calpastatin type II may be degraded rapidly. Such data indicates a differential level of control for different products of calpastatin gene. Whilst, the fold change in calpastatin type III mRNA expression could not be measured due to the absence of exon 1u on the construct, HA-tagged calpastatin type III protein was expressed significantly in both the cell lines ($P<0.05$) compared to their respective mock-transfected controls and had similar levels of expression in both the cell lines. In summary, calpastatin types I, II and III were successfully expressed in two different breast cancer cell lines and provide good models to assess effects on calpain system proteolytic activity and subsequent effects on phenotypic behaviour.

The subcellular distribution of calpastatin types were studied and calpastatin type I and III had a generally diffused cytoplasmic localisation in both cell lines. Storr et al. had previously reported that calpastatin was principally distributed in the cytoplasm in breast cancer tissues (Storr *et al.*, 2012a; Storr *et al.*, 2011b; Storr *et al.*, 2015). Calpastatin type II, however, had a unique punctate and predominantly perinuclear localisation. Similar results were reported previously in the neuroblastoma LAN-5 cells where total calpastatin was observed to be distributed as an aggregate confined in two granule-like structures without membranes, that was nearly absent in nucleus and the cytosol (De Tullio *et al.*, 1999). Interestingly, these calpastatin aggregates were affected by the increase in intracellular Ca^{2+} levels leading to a gradual diffusion of calpastatin in the cytosol (De Tullio *et al.*, 1999). The perinuclear localisation of calpastatin type II observed in T47D and MDA-MB-231 cells observed in this study might be a consequence of aggregation of calpastatin before or after stimulation by calcium. This could also potentially indicate that calpastatin types I and III are the isoforms that get diffused into cytoplasm after calcium stimulation. It would be therefore interesting to investigate and study the effects of calcium ionophore treatment and presence of hypoxia on calpastatin type II localisation.

To understand the differential localisation, cells overexpressing calpastatin types I, II and III and were sent for RNA-sequencing to Novogene, UK. The number of DEGs associated with the overexpression of calpastatin type I and II were comparable, while calpastatin type III overexpression had considerably lower DEGs in T47D cells. In MDA-MB-231 cells the number of DEGs associated with calpastatin type I and II overexpression were comparable, while calpastatin type III had considerably higher DEGs, perhaps suggesting calpastatin isoforms have different roles in each cell type. In basal like cells calpastatin types I and II may have fewer intercellular associations than in luminal cell type. While the reverse may be true for calpastatin type III.

The entire DEG lists were too extensive to present in the current thesis, however, can be accessed at https://github.com/RichaVasan/CAST-DEGs.git. A number of the identified DEGs have previously been shown to

have associations with breast cancer however, very few have been reported to have associations with the calpain system. The number of DEGs overlapping with the expression of calpastatin type I/II was considerably higher than the number of overlapping DEGs with the expression of calpastatin types I/III, and calpastatin types II/III, suggesting that calpastatin type I and II may have a considerably higher number of gene associations together and therefore, may have roles in a higher number of cellular functions compared to calpastatin type III in the luminal subtype of breast cancer. The number of DEGs unique to expression of calpastatin type III was considerably lower than those of calpastatin type I and II, suggesting that calpastatin type III may have a role in fewer cellular functions compared to calpastatin type I and type II in luminal breast cancer subtype. In MDA-MB-231 cells, the number of DEGs overlapping with calpastatin types II/III expression was much higher than the number of overlapping DEGs with the expression of calpastatin types I/II, and calpastatin types I/III, suggesting that calpastatin types II and III may have a higher number of associations together and hence may play a more varied role in cellular functions compared to calpastatin type I in TNBC subtype. The number of DEGs unique to calpastatin type III expression was considerably higher than those of type I and II expression, potentially suggesting that calpastatin type III may play greater role in regulation of cellular functions in the TNBC subtype compared to calpastatin types I and II.

The DEGs overlapping and unique to the expression of different calpastatin isoforms between the two cell lines were also assessed. The numbers of DEGs overlapping with calpastatin type I, II and III expression were comparable between T47D and MDA-MB-231. Caution should be used when comparing results as only a single luminal and only a single TNBC cell line was used but with this limitation in mind the number of DEGs unique to calpastatin type I expression was much lower in MDA-MB-231 cells than those in T47D cells, perhaps suggesting that calpastatin type I might play a role in more cellular functions in the luminal subtype compared to the TNBC subtype. The DEGs associated with calpastatin type II expression in MDA-MB-231 cells were much lower than those in T47D cells similarly

suggesting that calpastatin type II might play a more important role in the luminal subtype compared to the TNBC subtype. Finally, the DEGs associated with calpastatin type III expression in MDA-MB-231 cells was much higher than those associated in T47D cells suggesting that calpastatin type III may be involved in more cellular functions in the TNBC subtype compared to the luminal subtype. Such observations require confirmation and validation before any firm conclusions can be drawn but they provide avenues for future studies to progress (ie by using additional cell lines, identifying the pathways involved, and checking/confirming data by qRT-PCR, Western blotting etc).

The pathways significantly enriched and affected (inhibited or activated) by the DEGs were taken forward to assess their associations with different calpastatin types. RhoGDI protein signalling was the most significantly inhibited, and the wound healing pathway was the significantly activated pathways enriched by the DEGs associated with the expression of calpastatin type I in T47D. Both the pathways have known regulatory roles involving the calpain system mentioned previously. Pathways significantly enriched and inhibited by the DEGs associated with calpastatin type II expression in T47D cells included CD5 signalling, while the significantly enriched and activated pathways included PD-1, and PD-L1 cancer immunotherapy pathway, PI3K/AKT signalling. Several studies have reported these pathways to be linked to the calpain system (Bockel *et al.*, 2021; Pianetti *et al.*, 2001; Sato *et al.*, 2011). The pathways significantly enriched and predicted to be inhibited by calpastatin type III associated DEGs included cyclins and cell cycle regulation pathway, and the pathways activated included wound healing signalling pathway. These pathways were mapped for associations with calpastatin and the genes having association with calpastatin were shortlisted, including a few novel genes whose regulatory associations with the calpain system have not been reported previously, such as PRNP, FNTB and PLCG1.

In MDA-MB-231 cells, pathways enriched significantly and activated by the DEGs associated with calpastatin type I included Integrin signalling. Calpains have been implicated in the regulation of cell adhesion mediated by Integrins. It was reported that m-calpains localised to integrin associated

focal adhesion structures directly cleaved talin (reviewed in (Storr *et al.*, 2011a). The endoplasmic reticulum (ER) stress pathway was predicted to be significantly activated by the DEGs associated with calpastatin type II. However in mouse models, it was reported that calpastatin overexpression has protective affects following myocardial infarction by suppression of ER stress pathway (Li *et al.*, 2018). The pyroptosis signalling and wound healing pathways were two examples from several pathways significantly enriched and inhibited by calpastatin type III expression in MDA-MB-231 cells. As mentioned previously, both the pathways have known regulatory roles involving the calpain system. It was interesting to note that calpastatin types I and III overexpression predicted significant activation of the wound healing pathway in T47D cells, while it was predicted to be significantly inhibited in MDA-MB-231 cells. Such findings may suggest that overexpression of calpastatin types I and III in Luminal cells have opposing actions to those found in TNBC's, ie overexpression in Luminal's upregulates migratory abilities whilst in MDA-MB-231 cells overexpression downregulates the migratory ability. Previous caveats apply but it would be interesting to examine this further by additional phenotypic characterisations of the overexpressing lines. These pathways were mapped for associations with calpastatin and the genes having association with calpastatin were shortlisted, including a few novel genes whose regulatory associations with the calpain system have not been reported previously, such as CDT1, PIH1D1 and MTUS2. These genes should be further assessed for their associations with breast cancer clinicopathological parameters and survival using the METABRIC breast cancer dataset.

The second strategy used in this project was to inhibit calpains by using novel inhibitors. There are currently few assays available to determine intracellular calpain activity in intact live cells. One such assay is the tBOC assay that uses tBOC a calpain substrate. The proteolytic cleavage of the substrate produces a blue fluorescence within the cell which can be measured as a reflection of protease activity (Rosser *et al.*, 1993). The commercial calpain inhibitor calpeptin demonstrated an inhibition in calpain activity of 42.56±2.07% (P<0.01). Similar levels of calpain activity inhibition have been observed previously in the lab, with an inhibition of

34% and 21.89± 4.49% (P = 0.0011) with 100 µM of calpeptin treatment for 30 minutes in MDA-MB-231 cells (Pu, 2016a).The assay however, could only generate reliable data from 3 out of 7 independent experiments. The inherent variability of the assay results in difficult interpretation. Similar problems have been reported previously with experimental results being inconclusive due to generation of inconsistent data (Pu, 2016a; S. Zhang, 2018). Therefore, as the tBOC assay is notoriously known to generate irreproducible and unreliable data, its further use was discontinued in the current project. Calpeptin has, as it is designed to bind to the protease core (CysPC), been shown to inhibit other cysteine proteases such as the cathepsins and therefore does not offer selectivity for calpains over other proteases (Siklos *et al.*, 2015). Therefore to specifically inhibit intracellular calpain activity novel small molecule calpain inhibitors were used.

Small molecule novel calpain inhibitors, compound 1, compound 9 and compound 10 were obtained from our collaborator Professor R. Allemann, Cardiff University. Developed from a novel structure based virtual screening protocol, these compounds were shown to inhibit full length calpain 1 complex (Kalash *et al.*, 2018). These compounds did not show inhibition in calpain activity using the t-BOC assay in the MDA-MB-231 cells. From further investigation it was discovered that these compounds were fluorescent and had a marginally higher fluorescence compared to control cells, and so interfered with detection.

A novel FRET based bio-assay was developed and used to determine calpain activity in live cells. To demonstrate activation of calpains, FRET transfected MDA-MB-231 cells were treated with the calcium ionophore A23187. The calcium ionophore treatment dose and time were optimised to 10 µM for 2 hours in FRET transfected MDA-MB-231 cells. In the presence of Ca^{2+} calpains are activated which resulted in an increase in CFP expression. Enomoto et al. demonstrated activation of calpains using similar doses of calcium ionophore (A23187) in HeLa cells (Enomoto *et al.*, 2019). The length of calpain activity induction was also optimised by stimulating the FRET transfected MDA-MB-231 cells with A233187 followed by flow cytometry assessment every two hours. The increased CFP expression was observed only at the 0 hour time point and was reduced significantly after

the 0 hour time point indicating that activation of calpains may be a direct result of intracellular calcium influx and can be reversed by the removal of calcium treatment. Calpains are believed to be activated transiently by increased concentration of intracellular calcium which is quickly followed by its deactivation after the depletion of high calcium levels (Shapovalov *et al.*, 2022).

As a comparator to inhibit calpain activity, and to use for initial optimisations, the commercially available calpain inhibitor PD150606 was used as it has shown to have improved selectivity for calpains over other cysteine proteases owing to its allosteric mode of inhibition by binding to the penta-EF domain (Lin *et al.*, 1997). FRET transfected MDA-MB-231 cells were stimulated for calpain activity and treated with 100 μM calpain inhibitor PD150606. The dose was used to replicate the inhibition in calpain activity by calpeptin. After calcium ionophore treatment, CFP expression was significantly increased showing calpain activation. Significant reduction in CFP expression was seen after PD150606 treatment at both 30 minutes and 2 hours (P=0.001 and P<0.001, respectively). The α-mercaptoacrylic acid derivative PD150606 has shown to have better selectivity for calpains over other cysteine proteases due to binding to the penta-EF domain (Lin *et al.*, 1997). Several studies have shown the efficacy of the PD150606 compound on inhibition of calpains with a treatment dose range of 20 μM-100 μM in mouse cardiomyocytes, lymphoma cells and rat renal proximal tubules (Edelstein *et al.*, 1996; Li *et al.*, 2012; Luo *et al.*, 2015). The FRET bio-assay demonstrated successful activation and inhibition of calpain activity in live breast cancer cells and therefore it was used to assess the inhibitory potential of the novel compounds.

Using PD150606 as a comparator, the novel Compounds 1, 9 and 10 showed significant inhibition at 10 μM (P<0.01), 20 μM (P<0.01) and 40 μM (P<0.01) in calpain activity, with the level of inhibition being similar to 100 μM PD150606 treatment suggesting that the novel compounds are potent calpain inhibitors. Kalash et al. has shown previously that compounds 1, 9 and 10 inhibited calpain 1 with IC_{50} values of 7.5±1.1 μM, 20.5±1.9 μM and 29.7±5.2 μM, respectively. The novel compounds showed specificity for calpain 1 in the allosteric mode of action than the classical α-

mercaptoacrylic acid based calpain inhibitor PD150606 (Kalash *et al.*, 2018).

The effect of the novel calpain inhibitors on cell behaviour was assessed in terms of cell proliferation and clonogenic survival. Using the conventional chemotherapeutic agent doxorubicin as a positive comparator, MDA-MB-231 cells were treated with different doses of compounds 1, 9 and 10 for 24 hours. The novel compounds had no significant effect on cell proliferation compared to the doxorubicin treatment in MDA-MB-231 cells. However from clonogenic survival assessments, the novel compounds significantly reduced the surviving fraction of cells. The chemotherapeutic drug doxorubicin IC_{50} dose was used as a positive comparator and, as expected, reduced clonogenic survival by 50%. To summarise, the novel calpain inhibitors did not have an effect on cell proliferation, but they significantly reduced the surviving fraction of the cells, suggesting that the compounds may have useful anti-cancer properties. The clonogenic assay is a gold standard assay to determine the effectiveness of a treatment. In cancer cells, the primary mechanism of cell kill may not be apoptosis therefore, it is crucial to conduct long term survival assays when assessing the efficiency of a treatment as short term assays may not provide information on overall cytotoxicity of an agent (Woolston *et al.*, 2011).

The specificity of compounds 1, 9 and 10 were assessed using CRISPR/Cas9 calpain knock out cells. These MDA-MB-231 calpain knock out cells were induced for calpain activation followed by treatment with compound 1, compound 9 and compound 10. No conclusions could be drawn from experiments as it transpired that cells were GFP tagged and this interfered with accurate CFP and YFP detection after different treatments. It would be useful to obtain non-GFP tagged KO cells with which to continue specificity assessments and assess the potential utility of these compounds in a variety of phenotypic endpoints in which calpain activity is known to play an important role.

Calpains are well known as very long-lived stable proteins, so genetic deletion of the gene is needed to ensure complete depletion of protein expression. Therefore, the third strategy used in the current thesis was to

use CRISPR/Cas9 calpain knock out breast cancer cell lines and examine behaviour and treatment response.

Capn1, Capn2 and Capns1 KO MDA-MB-231 cells were received from our collaborator Prof. P. Greer's lab at Queen's University, Ontario, Canada, and used to assess the effect on cell behaviour and treatment response. However, all four cell lines tested positive for mycoplasma and required to be cleared of infection using Plasmocin treatment. Knock out status was confirmed by performing Western blotting of the mycoplasma free cells. The effect on cell behaviour in terms of cell proliferation and plating efficiency was assessed using proliferation and clonogenic assays. MDA-MB-231 WT, Capn1 KO and Capn2 KO cells had similar rates of growth while Capns1 KO cells had a significantly inhibited rate of cell proliferation, which was also reflected in the cell doubling times. The doubling time for the WT cells was 27±2.45 hours which was in line with the results obtained previously in the lab, 20±2.47 hours (Aiyappa, 2020) and in the literature, 28.1±1.2 hours (Watanabe *et al.*, 2001). Capn1 KO and Capn2 KO cells had doubling times similar to the WT cells, 29±8.04 hours and 30.5±0.5 hours, respectively. While, Capns1 KO cells had a significantly higher doubling time compared to the WT cells suggesting knocking out calpain 4 reduced the rate of cell proliferation significantly. Inhibition of calpain 1 by calpain inhibitor ZLLY-CHN_2 in Chinese hamster ovary (CHO) cell line led to a reduction in cell proliferation rate, which was believed to be as a result of prolonged G1 phase (Mellgren *et al.*, 1996). SiRNA knockdown of calpain 2 also led to a significant inhibition in proliferation rate in non-small cell lung cancer cells (Xu *et al.*, 2019). These differences in finding can be because of use of different cell types and different assays to determine effect on cell proliferation. MacLeod et al, demonstrated that deletion of calpain 4 in MTEC lead to the loss of calpain 1 and 2 activity, blocked tumorigenesis in an orthotropic engraftment model, and led to delayed tumour onset (MacLeod *et al.*, 2018). Grieve et al. showed that knock down of calpain 4 lead to attenuated growth of tumours at the orthotopic site in a human triple negative breast cancer xenograft model (Grieve *et al.*, 2016). The effect of knocking out calpains on plating efficiency of the WT, Capn1 KO, Capn2 KO and Capns1 KO cells was also assessed. WT cells had a plating efficiency of

51.2±1.2% which was similar to the results obtained previously by the group, 51±5.70% (Aiyappa, 2020) and 52.83±7.43% demonstrated by Zhang et al. (Zhang *et al.*, 2014). Capn1 KO cells had a marginally higher PE of 58.±1.3% compared to WT cells. Whilst this difference was statistically significant such a small different is likely to be of marginal biological significance. Mellgren et al. also demonstrated that the CHO cells with inhibited calpain 1 had an increased PE compared to the untreated CHO cells (Mellgren *et al.*, 1996). Capn2 KO cells had, however, a significantly lower PE of 22.2±6.5% (P=0.001) compared to the WT cells. This might be due to calpain 2 KO causing lower attachment and adhesion in cells as calpain 2 has been shown to be associated with regulating focal adhesion dynamics (Chan *et al.*, 2010; Franco *et al.*, 2004; Saraiva *et al.*, 2013). Xu et al previously reported that colony forming ability was significantly reduced in A549 and 95D cells with siRNA knocked down of calpain 2 (Xu *et al.*, 2019). The Capns1 KO cells also had a reduced plating efficiency of 32.1±5.2% (P<0.01) compared to the WT cells. Cells with knocked out calpain 4 have previously been shown to have significantly reduced cell proliferation (Grieve *et al.*, 2016; MacLeod *et al.*, 2018) and hence may not have developed into colonies in a period of two weeks. Disruption in calpain 2 expression, as a results of calpain 4 KO, may also have had an effect on calpain 4 KO cells and contributed to the decreased PE.

The conventionally used chemotherapeutic agent doxorubicin was used in this study to determine the effect of knocking out calpains on chemotherapeutic drug response. The MDA-MB-231 WT and calpain KO cells treated with different doses of doxorubicin were assessed for response in terms of cell proliferation and clonogenic survival. The WT cells showed an approximately 40% inhibition in cell proliferation in cells treated with 0.5 µM for 24 hours with inhibitory effects increasing at 48 and 72 hours of doxorubicin treatment. The IC_{50} values calculated were 0.81±0.08 µM for 24 hour, 0.40±0.07 µM for 48 hour, and 0.23±0.08 µM for 72 hour doxorubicin. This data is in agreement with the previously published work with doxorubicin proliferation IC_{50} values ranging from 0.02-1 µM for a period of 72 hours in MDA-MB-231 cells (Pichot *et al.*, 2009; Pilco-Ferreto *et al.*, 2016; Wu *et al.*, 2013). Capn1 KO did not have an effect on

proliferation response at 24, 48 or 72 hour doxorubicin treatment compared to the WT cells. A significant inhibition in cell proliferation of approximately 60% was observed in Capn2 KO and Capns1 KO cells treated with 0.5 μM of doxorubicin for 24 hours compared to the WT cells however this effect was not observed at 48 or 72 hour doxorubicin treatments suggesting that the inhibition in percentage cell number seen at 24 hour treatment may be a result of low plating efficiency of the Capn2 KO cells. Whilst knocking out calpain 4 may have a sensitising effect on MDA-MB-231 cells, the effect was not seen at 48 hour or 72 hour treatment. MacLeod and colleagues demonstrated, however, that Capns1 KO MTEC cells were significantly sensitised to 72 hour doxorubicin treatment (MacLeod *et al.*, 2018). This discrepancy might be attributed to the use of different assays and cell lines. As mentioned previously, proliferation assays do not reflect the effect on cell survival, hence clonogenic assays were also performed. The PE for the MDA-MB-231 WT cells was 50.14±1.80 which was in line with previously obtained data in the lab and mentioned in the literature. The calpain KO cells also had their plating efficiencies in line with the ones obtained previously in section 4.4.1. The doxorubicin treated WT cells had a significantly lower surviving fraction at high doses compared to the untreated cells, which is in line with the results obtained previously by the group (Abdullah, 2019). Capn1 KO had no overall effect on doxorubicin survival response compared to the WT cells however knocking out calpain 2 significantly sensitised cells at 5 nM ($P<0.001$), 10 nM ($P<0.0001$) and 20 nM ($P=0.01$) with no surviving colonies at higher doses. Although statistically significant, the separation between the survival response curves (KO v WT) suggests that there may only be a small effect biologically. Capns1 KO cells also showed significant sensitisation to doxorubicin at 10 nM ($P<0.001$) and 20 nM ($P<0.001$) compared to WT cells with no colonies surviving at higher doses, suggesting that knocking out calpain 4 may sensitise cells to doxorubicin biologically.

Hypoxia is an important parameter that determines response to cancer therapy. The presence of hypoxia has also shown to regulate calpain activity (Storr *et al.*, 2011). The effect of presence of hypoxia (1% O2) on MDA-MB-231 WT and calpain KO cell proliferation was assessed with experiments

in normoxia (21% O2) run in parallel. As expected hypoxic WT cells had a significantly reduced rate of cell proliferation and a higher doubling time (69.34±5.44 hours). Capn1 KO and Capn2 KO also had significantly reduced growth rates and higher doubling times (56.34±4.92 hours and 65±5.72 hours, respectively), while Capns1 KO cells had a similar rate of proliferation and doubling times (73.34±13.3 hours), compared to cells grown in normoxia (21% O2). Calpains enhance cell proliferation with several studies showing a reduced rate of proliferation when calpains are silenced using antisense nucleotides or use of calpain inhibitors by blocking cell cycle progression into S-phase (Mellgren *et al.*, 1996; Zhang *et al.*, 1996; Zhang *et al.*, 1997). Presence of hypoxia is known to activate the calpains leading to enhanced cell proliferation and migration (Mo *et al.*, 2011). This was however, not observed in the WT or calpain KO cell lines in the presence of hypoxia. The presence of hypoxia is known to modulate proliferation as a higher number of cells would lead to an increase in oxygen demand causing an increased hypoxic stress and cells combat this by reduced proliferation rate (Hubbi *et al.*, 2015; Ortmann *et al.*, 2014). Depletion of oxygen concentration below 10 mmHg leads to acidosis, depletion of ATP and supply of energy that may affect cell proliferation in hypoxic cell culture (Höckel *et al.*, 1991). The data mentioned above indicates that presence of hypoxia results in reduced cell proliferation and hence higher doubling times in breast cancer cells (Song *et al.*, 2018). HIF-1α is known to regulate this cellular adaptation and leads to induction of cell cycle arrest in hypoxic cells by directly repressing genes associated with the cell cycle (Ortmann *et al.*, 2014). Expression of CA9 was used as a marker to verify the presence of hypoxia with its expression seen as bands in cell lysates prepared from cells grown in hypoxia. The effect of hypoxia on the plating efficiencies of MDA-MB-231 WT and calpain knock out cells was assessed and hypoxic and normoxic experiments were carried out in parallel. The WT cells grown in normoxia had a plating efficiency of 53.23±3.97% which is in line with the previously obtained data and published literature. The WT cells grown in hypoxic (1% O2) growth conditions had a significantly lower plating efficiency of 23.56±6.72%, $P<0.01$. Capn2 KO and Capns1 KO cells grown in hypoxia (1% O2) also had significantly lower plating efficiencies of 9.67±1.91% ($P<0.01$) and

29.78±0.68% (<0.01), respectively, compared to the normoxic PEs. Due to the presence of hypoxia production of ATP is limited leading to activation cell death pathways and/or induction of cell cycle arrest (Iida *et al.*, 2002). Reduced PEs of cancer cells in hypoxia may also be due to cellular stress caused by deprivation of oxygen (Guo *et al.*, 2019).

Assessment of doxorubicin treatment in WT and calpain KO cells in the presence of hypoxia did not show a difference in terms of proliferation response. Albeit some sensitisation was observed at lower doses in calpain KO cells compared to the WTs, there was no overall difference in doxorubicin clonogenic survival in hypoxic (1% O2) Capn1 KO, Capn2 KO and Capns1 KO cells. Time permitting it would have been interesting to see the doxorubicin survival response with cells treated with a lower doxorubicin dose range. It has been established that presence of hypoxia is linked with chemotherapy resistance which can be a result of several factors. Presence of hypoxia leads to acidosis inside the cells that can cause a reduced uptake of certain drugs used widely for the treatment of TNBC (Gerweck *et al.*, 2006), a number of agents require cells in actively proliferating state for their cytotoxic activity (Cosse *et al.*, 2008). Hypoxia upregulates the MDR1 gene expression that contributes resistance towards a wide range of chemotherapeutic agents (Lv *et al.*, 2015).

Breast cancer cellular radiation response was also assessed using MDA-MB-231 WT and calpain 1, 2 and 4 knock out cells under both normoxic (21% O2) and hypoxic conditions (1% O2 for 24h). The PEs of normoxic and hypoxic WT cells were in agreement with and within the range of previously obtained data and the published literature. Hypoxic WT cells were, as expected, significantly more resistant to radiation treatment compared to the normoxic controls. The radiobiological parameters, α and α/β values demonstrated and confirmed that the hypoxic WT cells were more resistant to radiation. Knocking out calpain 1 did not alter response in MDA-MB-231 cells grown in normoxic (21% O2) growth conditions. However, in hypoxic (1% O2 for 24h) conditions Capn1 KO cells demonstrated significant sensitisation to radiation treatment compared to the WT cells. The radiobiological parameters α and α/β of the hypoxic Capn1 KO cells compared to those of the WT cells, confirmed sensitisation in hypoxic

conditions. Knocking out calpain 2 had a radio-resistant effect in MDA-MB-231 cells compared to the WT cells grown in normoxic (21% O2) growth conditions. However, in hypoxia (1% O2 for 24h) Capn2 KO cells also showed significant sensitisation to radiation treatment compared to the WT cells. The radiobiological parameters α and α/β of the hypoxic Capn2 KO cells compared to those of the WT cells confirmed sensitisation in calpain 2 KO cells in hypoxic conditions. The Capns1 KO cells were resistant to radiation treatment compared to WT cells under normoxic (21% O2) conditions whilst, in hypoxic (1% O2 for 24h) conditions, no overall effect in radiation response was observed in Capns1 KO cells compared to the WT cells. As mentioned previously, presence of hypoxia leads to activation of calpains and hence, may lead to activation of calpain 2 in Capn1 KO and calpain 1 in Capn2 KO cell lines. Studies have shown calpains interaction with the caspase cysteine protease machinery, BCL-2 family in the induction of apoptosis. Calpains also lead to the activation of several substrates that promote apoptosis including APAF1, CDK5, JUN, FOS and cabin 1 (Storr *et al.*, 2011a), which may lead to enhanced radiosensitivity in Capn1 KO and Capn2 KO cells. In addition, silencing of calpain 1 was seen to enhance the expression of pro-apoptotic genes in skeletal muscle cells (Van Ba *et al.*, 2013). Downregulation of calpain 2 led of significant reduction in NF-κB activation and sensitisation to anticancer therapy (Kovacs *et al.*, 2014), both of which may lead to sensitisation Capn1 KO and Capn2 KO cells. MDA-MB-231 Capn1 KO and Capn2 KO cells grown in hypoxic conditions showed significant sensitisation to radiation treatment compared to the WT cells, suggesting that targeting calpain 1 and calpain 2 might be a useful potential radiosensitising strategy to treat hypoxic breast cancer cells for example in the potential treatment of locally advanced or metastatic patient tumours where hypoxia may be problematic. The fact that no overall effect was observed in Capns1 KO cells compared to the WT cells grown in hypoxia may reflect their low rate of proliferation as radiosensitivity is linked to rates of proliferation with certain cell cycle phases being more resistant/sensitive than others ie proliferating cells are more sensitive than quiescent cells, with cells in G2/M phase being most sensitive, less sensitive in the G1 phase and least sensitive in the late-S phase of the cell cycle (Pawlik *et al.*, 2004). In retrospect, as these cells proliferated much slower than all others the

incubation period for these cells to form colonies perhaps should also have been longer. This should be conducted in any future work, along with cell cycle analyses, that seeks to confirm current observations.

Several bioinformatic analyses were conducted using publically available breast cancer datasets. The cBioportal website provides detailed gene information from publically available breast cancer datasets. The calpain system genes CAPN1, CAPN2, CAPNS1 and CAST were queried using the database and mRNA gene expression data assessed using the TCGA and METABRIC datasets. DEG lists associated with each calpain system gene were obtained and analysed for pathway enrichment. Several pathways were enriched by those DEGs associated with altered expression of calpain system genes. The pathways were assessed for commonalities between the datasets and the DEGs were further shortlisted. A few of these have shown to be associated with the calpain system and breast cancer previously mentioned in section 5.5.

Genes from the above mentioned lists were assessed for breast cancer specific and overall survival using the METABRIC and GDC TCGA breast cancer cohorts. High PPP1CA, POLE2, RBBP4 and PSMB5 mRNA expression was associated with better overall survival and poor breast cancer specific survival. While high expression of PRKAB2 expression was associated with poor overall and breast cancer specific survival. Previous studies have shown that PPP1CA is associated with breast cancer specific survival and that it may play a role in cancer stem cell populations (Ferrer *et al.*, 2016; Saidy *et al.*, 2021). POLE2 overexpression has shown to be associated with reduced metastasis free survival in breast cancer (Pearlman *et al.*, 2019). RBBP4 expression was shown to be significantly higher in breast cancer than the normal tissues and was significantly correlated with lymph node metastasis in a small cohort of patients (Guo *et al.*, 2020). High PSMB5 expression has shown to be associated with poor progression free and overall survival in a group of TNBC patients (n=96) (Wei *et al.*, 2018).

The METABRIC cohort had gene information available at probe level. It was interesting to see that expressions of CAST probe 4 and YWHAG probe 1, CAST probe 4 and RBBP4 probe 2, CAST probe 6 and RBBP4 probe 2, and YWHAG probe 2 and RBBP4 probe 1 had statistically and biologically

significant correlations. Due to the unique intracellular localisation of calpastatin type II, CAST gene and its associated DEGS were selected for further analysis. RBBP4 was selected to be assessed for protein expression in the breast cancer cells and tissues. RBBP4 gene was selected as it has not been reported to have regulatory associations with the calpain system till date. Although protein expression has previously been studied in a small breast cancer cohort (Guo *et al.*, 2020), it was selected to be assessed to confirm the findings and establish association with breast cancer subtypes, survival and clinical outcomes in a large cohort.

RBBP4 mRNA probe expressions were assessed against different breast cancer clinicopathological variables. High RBBP4 probe 1 expression was significantly associated with Pam50 subtype and tumour stage, and high RBBP4 probe 2 expression was significantly associated with negative ER and PR, positive HER2, mutated p53 status, grade 3 tumours, tumour stage, HER2 and basal subtypes and older age at diagnosis.

RBBP4 protein expression was seen in TNBC and luminal type cells as seen by Western blotting and was localised predominantly in nuclear region as observed by performing IHC. The staining was quantified by percentage intensity scoring which failed to establish concordance between individual scorers (ICC- 0.57). As the percentage scores were largely 100% for most of the cases, re-scoring was done by assigning H-scores which again did not establish a decent ICC (ICC-0.52) between two independent scorers. After two attempts using different approaches (both with ICC<0.7), it was concluded, due to time limitations, that further analysis on the expression of RBBP4 could not be conducted and therefore survival and other clinicopathological parameters associations could not be reliably established. Guo et al. have previously established association with breast cancer survival and other parameters in a small cohort (n=240) by assigning H-scores to the stained cores however, it describes limited patterns of staining without stating whether the sections were stained in the cytoplasm or nucleus or both (Guo *et al.*, 2020).

6.2 Limitations and suggestions for future work

Breast cancer is classified into several distinct molecular subtypes including Luminal A and B, HER2 enriched and TNBC (Perou *et al.*, 2000b; Sørlie *et al.*, 2001). The calpastatin types I, II and III were expressed in T47D and MDA-MB-231 cells representing only Luminal A and TNBC subtype of breast cancer, respectively. It would be useful to assess the expression of calpastatin types I, II and III in cell lines representing other breast cancer subtypes including, other Luminal A cells such as, MCF7 and BT483, Luminal B type cells such as, BT474 and UACC812, HER2 enriched cells such as, JIMT1 and SKBR3, and other basal-like cells such as, MDA-MB-468 and SUM149. While calpastatin type I and type II fold change in mRNA expression was determined by using specific primers, the fold change in calpastatin type III was not determined due to the exclusion of the exon 1u from the DNA construct for calpastatin type III. In retrospect, it would have been useful to try and determine the fold change for calpastatin type III in both the cell lines to be able to compare its expression with calpastatin types I and II in both the cell lines. This could be done by performing new sets of transfections with the DNA constructs that were generated at a later stage in Professor Parr's lab. Measuring the differences in HA-tagged protein expression will not have provided accurate measurement of the fold change in calpastatin type III expression.

Intracellular distribution of calpastatin types I, II and III was determined by cell immunofluorescence. As presented earlier calpastatin types I and III had a diffused cytoplasmic localisation in both cell lines. It would have been interesting to assess their distribution in other breast cancer cell types including Luminal B and HER2 enriched cells however this would require performing immunofluorescence on stably transfected BT474 or UACC812 (Luminal B) and JIMT-1 or SKBR3 (HER2 enriched) cells with calpastatin types I, II and III constructs. Calpastatin type II had a distinct perinuclear localisation in both cell lines. It would be interesting to study its localisation in other breast cancer cell types including, if they are eventually available, Luminal A and HER2 enriched cells. Further studies with calpastatin type II include co-localisation experiments; studying the 'basket-like' structures by live imaging, super resolution microscopy, correlative light microscopy;

studying protein interaction by using BioID proteomics. In a previous study it was shown that when calcium dependent calpain activity is not required by the cells, calpastatin associates in large aggregates and is not available for inhibition of calpains. During an increase in intracellular calcium levels, calpastatin becomes available in the cytosol (Averna *et al.*, 2003). Future experiments could involve treatment of calpastatin overexpressing cells with the calcium ionophore A23187 for calpain induction to observe the intracellular distribution of calpastatin type I, II and III. It would also be insightful to study how the external factors, such as hypoxia, affect different calpastatin isoform localisation.

The T47D and MDA-MB-231 cells overexpressing different calpastatin types were treated with 10 µM of the calcium ionophore A23187 for 2 hours to activate the calpain system and sent for RNA sequencing. The DEG lists associated with the expression of calpastatin types I, II and III obtained after sequencing had listed a huge number of genes. The DEG lists were filtered and a reduced number of genes were shortlisted for further assessments. The DEGs shortlisted for each calpastatin type either was a direct 'target' or a 'node' gene association. In future, it would be interesting to study their associations with breast cancer clinicopathological parameters and survival. It would also be interesting to validate some of these protein expression in breast cancer cells and tissues and assess their associations with the clinical outcomes. Due to the shutdown of the labs imposed by the Covid19 pandemic, a few important aims of this study were not fulfilled. These included assessing the effect of overexpression of different calpastatin isoforms on breast cancer cell proliferation and plating efficiency. It would also have been interesting to study the effect on chemotherapeutic drug and radiation treatment response in these cell lines. Future work would include accomplishing the above mentioned aims using the chemotherapeutic drugs such as doxorubicin. Although 2D cell culture models are used widely, they do not accurately represent in vivo models of tumour compared to 3D cell culture models (Breslin *et al.*, 2013). Growing cells in 3D models such as cell aggregates or spheroids, within or on a biologically derived matrix (for e.g collagen, matrigel etc.) will provide more physiologically relevant data with more predictive information for in vivo

studies (Kapałczyńska *et al.*, 2018). 3D models have altered cell proliferation, adhesion, invasion and related protein expression compared to 2D models. These altered cellular phenotypes resemble the in vivo parameters such as oxygen conditions, gradients of immune factor, growth factor, and the tumour microenvironment (Fuller *et al.*, 2014). It would be therefore interesting to investigate the effect of calpastatin types I, II and III overexpression on the regulation of breast cancer cell proliferation, colony formation, adhesion, migration and response to therapy in 3D culture models.

Intracellular calpain activity can be assessed using several assays that use cell lysates. The tBOC assay determines the calpain activity in live cells. However, it is notoriously unreliable as it is difficult to generate reproducible data. Therefore, the FRET based bio-assay was developed to determine intracellular calpain activity in live breast cancer cells. Transient transfections were performed to transfect the FRET plasmid in to the MDA-MB-231 cells. The FRET plasmid could not be stably transfected in the breast cancer cells due to the lack of selection antibiotic for mammalian cells on the plasmid. Therefore, transient transfections were done for each experiment which resulted in some variability between experiments. This could perhaps be overcome by using viral transduction of the FRET plasmid to generate breast cancer cell lines stably expressing the FRET plasmid. The calpain activity in MDA-MB-231 cells was assessed by calcium induction. The calcium ionophore treatment dose and times were optimised using flow cytometry. Calpain activity was also seen to reduce immediately after the removal of calcium ionophore. Thus, there may have been some loss of calpain activity measurement between the removal of calcium ionophore and flow cytometry analysis. It was therefore crucial that all the experiments were done quickly to minimise the loss of calpain activity measurements.

Inhibition of calpain activity was demonstrated using the commercially available calpain inhibitor PD150606. Significant inhibition of calpain activity was observed with 100 μM PD150606 treatment for 2 hours, and was used as a positive comparator for inhibition by the novel calpain inhibitors. Compounds 1, 9 and 10 demonstrated similar levels of calpain

inhibition compared to the PD150606 at lower doses of 10 μM, 20 μM and 40 μM. All the above data was assessed in only one cell line representing only one breast cancer subtype. It would be interesting to investigate the calpain activity in other breast cancer subtype cell lines such as T47D cells (Luminal A subtype), BT474 (Luminal B subtype) and SKBR3 (HER2 enriched subtype). Additional future work can include, assessing intracellular calpain activity in other cell lines and comparing the levels of calpain activity between different breast cancer subtypes, demonstrating inhibition of calpain activity in these cell lines and comparing the levels of inhibition between different breast cancer subtypes and different compounds. Since compounds 1, 9 and 10 showed similar levels of calpain activity inhibition for all the doses, it would be interesting to investigate calpain activity inhibition at a lower range of doses to obtain a dose response curve and titre the concentration for calpain activity inhibition for compounds 1, 9 and 10.

Compounds 1, 9 and 10 were shown to be specific for ex-vivo inhibition of calpain activity by calpain 1 (Kalash *et al.*, 2018). Thus they were tested to assess the inhibition of calpain activity in Capn1 CRISPR/Cas9 KO MDA-MB-231 cells. As mentioned, GFP-tag in the Capn1 KO cells interfered with the expression of CFP and YFP, leading to inaccurate measurements. In future, it would be very interesting to assess the specificity of these compounds on CAPN1 KO cells not tagged with GFP. It would also be insightful to study intracellular calpain activity in 3D cell culture models. The assessments could include investigating how a 3D cell culture model microenvironment effects induction and inhibition of calpain activity. Additionally future work could include assessing the effect of novel calpain inhibitors on cell proliferation and survival in 3D cell culture models.

It would also be very interesting to investigate induction of calpain activity levels in T47D and MDA-MB-231 cells overexpressing calpastatin types I, II and III.

The third strategy was to inhibit calpains was by using CRISPR/Cas9 calpain 1, calpain 2 and calpain 4 KO MDA-MB-231 cells provided by Dr. Greer's laboratory. These cell lines tested positive for mycoplasma infection after

which the cells were cleaned using the reagent Plasmocin. Results obtained from mycoplasma negative cells were significantly different, suggesting that results obtained with mycoplasma positive cells were inaccurate and unreliable. This highlights the significance of conducting regular mycoplasma checks on cells maintained in culture. The effect of knocking out calpains on cell proliferation, plating efficiency, doxorubicin treatment and radiation response was assessed on Capn1, Capn2 and Capns1 KO cells lines in 2D monolayers. The doxorubicin treatment response was assessed in terms of cell proliferation and survival. It has been previously shown, by others and in this thesis, that IC50 concentrations of doxorubicin from clonogenic assays are much lower compared to ones obtained from proliferation assays (Abdullah, 2019). Interestingly, in the current study, no surviving cells were observed at high doses of 50 nM and 100 nM. It would therefore be interesting to conduct clonogenic experiments with calpain KO cells treated with a lower dose range of doxorubicin, to generate a full dose response curve. This may also help in visualising any significant separation between WT and KO curves. In future it will be interesting to investigate the effect of knocking out calpains on initialising 3D cell culture models like spheroids. As mentioned previously, 3D cell culture models have altered cell proliferation, adhesion, and invasion while giving a picture of the tumour microenvironment including factors such as oxygen conditions, gradients of immune factor and growth factors (Fuller *et al.*, 2014). It would therefore be interesting to investigate effect of knocking out calpain on cell proliferation and colony formation in terms spheroid initiation. Although 2D cell culture models are widely used in pre-clinical evaluation of several anticancer agents, when compared to 3D models, they do not accurately represent in vivo tumour response (Breslin *et al.*, 2013). Therefore, it would be interesting to investigate doxorubicin response in calpain KO 3D culture models like spheroids.

The effect of knocking out calpains was also assessed on radiation response in the presence of normoxia (21% O2) and hypoxia (1% O2 for 24 hours). Knocking out calpains 1 and 2 made cells more sensitive to radiation treatment compared to the WT cells in the presence of hypoxia (1% O2 for 24 hours). Knocking out calpain 4 however, unexpectedly did not have an

effect on radiation response compared to the WT cells. This may have been due to a small incubation period for calpain 4 KO cells or reflect their slower cell cycle time and altered cell cycle phases. It was established that calpain 4 KO cells have a significantly reduced rate of proliferation compared to the WT cells in both normoxic and hypoxic conditions. Therefore, in retrospect, it may have been useful to keep the calpain 4 KO cells flasks for a few more weeks to form colonies and to also assess cell cycle parameters. Future experiments could include assessing the radiation response in 3D models of calpain KO cells and also assessing effects on WT breast cancer radiosensitivity with novel calpain inhibitors under both normoxic and hypoxic conditions.

The above data was assessed in one cell line representing one breast cancer cell type using one chemotherapeutic drug. It would be insightful to investigate the effect of knocking out calpains in other cell lines of different breast cancer subtypes including Luminal A, B and HER2 enriched. It would also be interesting to study the normoxic and hypoxic radiation response in breast cancer cell lines of different subtypes knocked out with calpains, and with a range of calpain inhibitors.

Bioinformatic analyses were done on several publically available breast cancer datasets. The genes shortlisted by pathway enrichment and survival analysis on TCGA and METABRIC dataset revealed a few DEGs highly significant and in terms of survival and had a good correlation with the calpain system genes. The RBBP4 gene was assessed for the expression of proteins in the breast cancer tissues and was predominantly seen to be distributed in the nucleus. The stained tissues were scored and the ICC scored obtained between two independent assessors was <0.7, suggesting any further analysis would be unreliable and therefore further analysis was discontinued. In future it would be interesting to validate some other shortlisted DEG associated with the expression of calpain system genes.

6.3 Conclusions

In summary, the current project evaluated the role of the calpain system in breast cancer progression and treatment response by using three strategies including molecular overexpression of the endogenous calpain inhibitor,

calpastatin; use of novel small molecule calpain inhibitors; and the use of CRISPR/Cas9 calpain KO breast cancer cell lines. Although, some of the aims were not fulfilled due to the shutdown of labs, this project highlights differential expression and localisation of different calpastatin isoforms in breast cancer cells. In addition, RNA sequencing of these cell line resulted in the identification of certain novel genes linked to the calpain system for the first time that will be interesting to study further in breast cancer survival and clinical outcomes. This project, for the first time demonstrates activation of calpains in live breast cancer cells using a novel FRET based biosensor that can be taken forward into further studies. The novel calpain inhibitors were also validated as potent inhibitors using the FRET based system. This thesis also highlights that knocking out calpains 2 and 4 results in sensitisation of MDA-MB-231 cells to doxorubicin survival in normoxia (21% O2) and that knocking out calpains 1 and 2 sensitises MDA-MB-231 cells to radiation treatment in hypoxia (1% O2 for 24 h). Therefore, suggesting modulation of the calpain system may lead to improved response to therapy.

References

Abdullah, N. (2019). *The role of redox proteins in the radiotherapeutic response of breast cancer.* University of Nottingham.

ABS. (2009). Surgical guidelines for the management of breast cancer. *Eur J Surg Oncol, 35 Suppl 1*, 1-22. doi:10.1016/j.ejso.2009.01.008

Ai, M., Qiu, S., Lu, Y., & Fan, Z. (2013). HER2 regulates Brk/PTK6 stability via upregulating calpastatin, an inhibitor of calpain. *Cell Signal, 25*(9), 1754-1761. doi:10.1016/j.cellsig.2013.05.010

Aiyappa, R. (2020). *Targetting DNA repair and hypoxia to improve radioresponse in breat cancer.* (Doctor of Philosophy), University of Nottingham.

Albain, K., Allred, D., & Clark, G. (1994). Breast cancer outcome and predictors of outcome: are there age differentials? *J Natl Cancer Inst Monogr*(16), 35-42.

Albrektsen, G., Heuch, I., Hansen, S., & Kvåle, G. (2005). Breast cancer risk by age at birth, time since birth and time intervals between births: exploring interaction effects. *Br J Cancer, 92*(1), 167-175. doi:10.1038/sj.bjc.6602302

Amadori, D., & Silvestrini, R. (1998). Prognostic and predictive value of thymidine labelling index in breast cancer. *Breast Cancer Res Treat, 51*(3), 267-281. doi:10.1023/a:1006140629766

Anguissola, S., Köhler, B., O'Byrne, R., Düssmann, H., Cannon, M., Murray, F., . . . Prehn, J. (2009). Bid and calpains cooperate to trigger oxaliplatin-induced apoptosis of cervical carcinoma HeLa cells. *Mol Pharmacol, 76*(5), 998-1010. doi:10.1124/mol.109.058156

Annis, M., Ouellet, V., Rennhack, J., L'Esperance, S., Rancourt, C., Mes-Masson, A., . . . Siegel, P. (2018). Integrin-uPAR signaling leads to FRA-1 phosphorylation and enhanced breast cancer invasion. *Breast Cancer Res, 20*(1), 9. doi:10.1186/s13058-018-0936-8

Atencio, I., Ramachandra, M., Shabram, P., & Demers, G. (2000). Calpain inhibitor 1 activates p53-dependent apoptosis in tumor cell lines. *Cell Growth Differ, 11*(5), 247-253.

Averna, M., De Tullio, R., Capini, P., Salamino, F., Pontremoli, S., & Melloni, E. (2003). Changes in calpastatin localization and expression during calpain activation: a new mechanism for the regulation of intracellular Ca(2+)-dependent proteolysis. *Cell Mol Life Sci, 60*(12), 2669-2678. doi:10.1007/s00018-003-3288-0

Averna, M., De Tullio, R., Passalacqua, M., Salamino, F., Pontremoli, S., & Melloni, E. (2001). Changes in intracellular calpastatin localization are mediated by reversible phosphorylation. *Biochem J, 354 Pt 1*, 25-30.

Bachmann, H., Jung, D., Link, T., Arnold, A., Kantelhardt, E., Thomssen, C., . . . Kuhlmann, J. D. (2022). FNTB Promoter Polymorphisms Are Independent Predictors of Survival in Patients with Triple Negative Breast Cancer. *Cancers (Basel), 14*(3). doi:10.3390/cancers14030468

Badovinac Črnjević, T., Spagnoli, G., Juretić, A., Jakić-Razumović, J., Podolski, P., & Šarić, N. (2012). High expression of MAGE-A10 cancer-testis antigen in triple-negative breast cancer. *Med Oncol, 29*(3), 1586-1591. doi:10.1007/s12032-011-0120-9

Baghdiguian, S., Martin, M., Richard, I., Pons, F., Astier, C., Bourg, N., . . . Lefranc, G. (1999). Calpain 3 deficiency is associated with myonuclear apoptosis and profound perturbation of the IkappaB alpha/NF-kappaB pathway in limb-girdle muscular dystrophy type 2A. *Nat Med, 5*(5), 503-511. doi:10.1038/8385

Balz, L., Bartkowiak, K., Andreas, A., Pantel, K., Niggemann, B., Zänker, K., . . . Dittmar, T. (2012). The interplay of HER2/HER3/PI3K and EGFR/HER2/PLC-γ1 signalling in breast cancer cell migration and dissemination. *J Pathol, 227*(2), 234-244. doi:10.1002/path.3991

Bao, Y., Wang, A., & Mo, J. (2016). S100A8/A9 is associated with estrogen receptor loss in breast cancer. *Oncol Lett, 11*(3), 1936-1942. doi:10.3892/ol.2016.4134

Bartlett, J., Bayani, J., Marshall, A., Dunn, J., Campbell, A., Cunningham, C., . . . Stein, R. C. (2016). Comparing Breast Cancer Multiparameter Tests in the OPTIMA Prelim Trial: No Test Is More Equal Than the Others. *J Natl Cancer Inst, 108*(9). doi:10.1093/jnci/djw050

Baskar, R., Lee, K., Yeo, R., & Yeoh, K. (2012). Cancer and radiation therapy: current advances and future directions. *Int J Med Sci, 9*(3), 193-199. doi:10.7150/ijms.3635

Benetti, R., Del Sal, G., Monte, M., Paroni, G., Brancolini, C., & Schneider, C. (2001). The death substrate Gas2 binds m-calpain and increases susceptibility to p53-dependent apoptosis. *Embo j, 20*(11), 2702-2714. doi:10.1093/emboj/20.11.2702

Bernal, J., & Hernández, A. (2007). p53 stabilization can be uncoupled from its role in transcriptional activation by loss of PTTG1/securin. *J Biochem, 141*(5), 737-745. doi:10.1093/jb/mvm076

Bernstein, L. (2002). Epidemiology of endocrine-related risk factors for breast cancer. *J Mammary Gland Biol Neoplasia, 7*(1), 3-15. doi:10.1023/a:1015714305420

Blanchard, H., Grochulski, P., Li, Y., Arthur, J., Davies, P., Elce, J., & Cygler, M. (1997). Structure of a calpain Ca(2+)-binding domain reveals a novel EF-hand and Ca(2+)-induced conformational changes. *Nat Struct Biol, 4*(7), 532-538. doi:10.1038/nsb0797-532

Blomgren, K., Hallin, U., Andersson, A., Puka-Sundvall, M., Bahr, B., McRae, A., . . . Hagberg, H. (1999). Calpastatin is up-regulated in response to hypoxia and is a suicide substrate to calpain after neonatal cerebral hypoxia-ischemia. *J Biol Chem, 274*(20), 14046-14052. doi:10.1074/jbc.274.20.14046

Bloom, H., & Richardson, W. (1957). Histological grading and prognosis in breast cancer; a study of 1409 cases of which 359 have been followed for 15 years. *Br J Cancer, 11*(3), 359-377. doi:10.1038/bjc.1957.43

Bockel, S., Louvel, G., Brion, T., Ung, M., Berthelot, K., Villaret, F., . . . Rivera, S. (2021). [Extreme hypofractionation: New indications for breast cancer radiotherapy]. *Cancer Radiother, 25*(6-7), 679-683. doi:10.1016/j.canrad.2021.08.004

Bonadonna, G., Brusamolino, E., Valagussa, P., Rossi, A., Brugnatelli, L., Brambilla, C., . . . Veronesi, U. (1976). Combination chemotherapy as an adjuvant treatment in operable breast cancer. *N Engl J Med, 294*(8), 405-410. doi:10.1056/nejm197602192940801

Bonifazi, M., Franchi, M., Rossi, M., Zambelli, A., Moja, L., Zambon, A., . . . Negri, E. (2014). Long term survival of HER2-positive early breast cancer treated with trastuzumab-based adjuvant regimen: a large cohort study from clinical practice. *Breast, 23*(5), 573-578. doi:10.1016/j.breast.2014.05.022

Bozza, W., Zhang, Y., Hallett, K., Rivera Rosado, L., & Zhang, B. (2015). RhoGDI deficiency induces constitutive activation of Rho GTPases and COX-2 pathways in association with breast cancer progression. *Oncotarget, 6*(32), 32723-32736. doi:10.18632/oncotarget.5416

Braun, C., Engel, M., Seifert, M., Theisinger, B., Seitz, G., Zang, K., & Welter, C. (1999). Expression of calpain I messenger RNA in human renal cell carcinoma: correlation with lymph node metastasis and histological type. *Int J Cancer, 84*(1), 6-9. doi:10.1002/(sici)1097-0215(19990219)84:1<6::aid-ijc2>3.0.co;2-t

Breslin, S., & O'Driscoll, L. (2013). Three-dimensional cell culture: the missing link in drug discovery. *Drug Discov Today, 18*(5-6), 240-249. doi:10.1016/j.drudis.2012.10.003

Brown, J. (2007). Tumor hypoxia in cancer therapy. *Methods Enzymol, 435*, 297-321. doi:10.1016/s0076-6879(07)35015-5

Brown, J., & Wilson, W. (2004). Exploiting tumour hypoxia in cancer treatment. *Nat Rev Cancer, 4*(6), 437-447. doi:10.1038/nrc1367

Brown , R., Allred, C., Clark, G., Osborne, C., & Hilsenbeck, S. (1996). Prognostic value of Ki-67 compared to S-phase fraction in axillary node-negative breast cancer. *Clin Cancer Res, 2*(3), 585-592.

Bryant, J., Fisher, B., Gündüz, N., Costantino, J., & Emir, B. (1998). S-phase fraction combined with other patient and tumor characteristics for the prognosis of node-negative, estrogen-receptor-positive breast cancer. *Breast Cancer Res Treat, 51*(3), 239-253. doi:10.1023/a:1006184428857

Buchholz, T., Stivers, D., Stec, J., Ayers, M., Clark, E., Bolt, A., . . . Pusztai, L. (2002). Global gene expression changes during neoadjuvant chemotherapy for human breast cancer. *Cancer J, 8*(6), 461-468. doi:10.1097/00130404-200211000-00010

Bugide, S., David, D., Nair, A., Kannan, N., Samanthapudi, V., Prabhakar, J., & Manavathi, B. (2015). Hematopoietic PBX-interacting protein (HPIP) is over expressed in breast infiltrative ductal carcinoma and regulates cell adhesion and migration through modulation of focal adhesion dynamics. *Oncogene, 34*(35), 4601-4612.

Burguin, A., Diorio, C., & Durocher, F. (2021). Breast Cancer Treatments: Updates and New Challenges. *J Pers Med, 11*(8). doi:10.3390/jpm11080808

Burkhart, D., & Sage, J. (2008). Cellular mechanisms of tumour suppression by the retinoblastoma gene. *Nat Rev Cancer, 8*(9), 671-682. doi:10.1038/nrc2399

Cardarelli, F., Digiacomo, L., Marchini, C., Amici, A., Salomone, F., Fiume, G., . . . Caracciolo, G. (2016). The intracellular trafficking mechanism of Lipofectamine-based transfection reagents and its implication for gene delivery. *Sci Rep, 6*(1), 25879. doi:10.1038/srep25879

Cardoso, F., Costa, A., Norton, L., Senkus, E., Aapro, M., André, F., . . . Winer, E. (2014). ESO-ESMO 2nd international consensus guidelines for advanced breast cancer (ABC2)†. *Ann Oncol, 25*(10), 1871-1888. doi:10.1093/annonc/mdu385

Cardoso, F., Kyriakides, S., Ohno, S., Penault-Llorca, F., Poortmans, P., Rubio, I., . . . Senkus, E. (2019). Early breast cancer: ESMO Clinical Practice Guidelines for diagnosis, treatment and follow-up. *Ann Oncol, 30*(10), 1674. doi:10.1093/annonc/mdz189

Cardoso, F., van't Veer, L., Bogaerts, J., Slaets, L., Viale, G., Delaloge, S., . . . Piccart, M. (2016). 70-Gene Signature as an Aid to Treatment Decisions in Early-Stage Breast Cancer. *N Engl J Med, 375*(8), 717-729. doi:10.1056/NEJMoa1602253

Carey, L., Perou, C., Livasy, C., Dressler, L., Cowan, D., Conway, K., . . . Millikan, R. (2006). Race, breast cancer subtypes, and survival in the Carolina Breast Cancer Study. *Jama, 295*(21), 2492-2502. doi:10.1001/jama.295.21.2492

Carragher, N. (2007). Assaying calpain activity. *Methods Mol Biol, 370*, 109-120. doi:10.1007/978-1-59745-353-0_9

Carstens, P., Greenberg, R., Francis, D., & Lyon, H. (1985). Tubular carcinoma of the breast. A long term follow-up. *Histopathology, 9*(3), 271-280. doi:10.1111/j.1365-2559.1985.tb02444.x

Carter, C., Allen, C., & Henson, D. (1989). Relation of tumor size, lymph node status, and survival in 24,740 breast cancer cases. *Cancer, 63*(1), 181-187. doi:10.1002/1097-0142(19890101)63:1<181::aid-cncr2820630129>3.0.co;2-h

Carvalho, C., Santos, R., Cardoso, S., Correia, S., Oliveira, P., Santos, M., & Moreira, P. (2009). Doxorubicin: the good, the bad and the ugly effect. *Curr Med Chem, 16*(25), 3267-3285. doi:10.2174/092986709788803312

cBioPortal. (2022). cBioPortal for Cancer Genomics. Retrieved from https://www.cbioportal.org/

CGHFBC. (2001). Familial breast cancer: collaborative reanalysis of individual data from 52 epidemiological studies including 58,209 women with breast cancer and 101,986 women without the disease. *Lancet, 358*(9291), 1389-1399. doi:10.1016/s0140-6736(01)06524-2

Chakraborti, S., Alam, M., Paik, D., Shaikh, S., & Chakraborti, T. (2012). Implications of calpains in health and diseases. *Indian J Biochem Biophys, 49*(5), 316-328.

Chan, Bennin, D., & Huttenlocher, A. (2010). Regulation of adhesion dynamics by calpain-mediated proteolysis of focal adhesion kinase (FAK). *J Biol Chem, 285*(15), 11418-11426. doi:10.1074/jbc.M109.090746

Chan, & Camphausen, K. (2003). Angiogenic tumor markers, antiangiogenic agents and radiation therapy. *Expert Rev Anticancer Ther, 3*(3), 357-366. doi:10.1586/14737140.3.3.357

Chan , A., Delaloge, S., Holmes, F., Moy, B., Iwata, H., Harvey, V., . . . Von Minckwitz, G. (2015). Neratinib after adjuvant chemotherapy and trastuzumab in HER2-positive early breast cancer: Primary analysis at 2 years of a phase 3, randomized, placebo-controlled trial (ExteNET): American Society of Clinical Oncology.

Chang, J., & Fan, W. (2013). Endocrine therapy resistance: current status, possible mechanisms and overcoming strategies. *Anticancer Agents Med Chem, 13*(3), 464-475.

Chapman, J., Reuvers, A., Borsa, J., & Greenstock, C. (1973). Chemical radioprotection and radiosensitization of mammalian cells growing in vitro. *Radiat Res, 56*(2), 291-306.

Checka, C., Chun, J., Schnabel, F., Lee, J., & Toth, H. (2012). The relationship of mammographic density and age: implications for breast cancer screening. *AJR Am J Roentgenol, 198*(3), W292-295. doi:10.2214/ajr.10.6049

Chen, Chen, G., Wang, C., & Mao, C. (2019). RAB13 as a novel prognosis marker promotes proliferation and chemotherapeutic resistance in gastric cancer. *Biochem Biophys Res Commun, 519*(1), 113-120. doi:10.1016/j.bbrc.2019.08.141

Chen, Zhang, L., Yuan, M., Kuang, Z., Zou, Y., Tang, T., . . . Jia, H. (2020). Sam68 Promotes the Progression of Human Breast Cancer through inducing Activation of EphA3. *Curr Cancer Drug Targets, 20*(1), 76-83. doi:10.2174/1568009619666190718124541

Chen , F., Demers, L., Vallyathan, V., Lu, Y., Castranova, V., & Shi, X. (2000a). Impairment of NF-kappaB activation and modulation of gene expression by calpastatin. *Am J Physiol Cell Physiol, 279*(3), C709-716. doi:10.1152/ajpcell.2000.279.3.C709

Cheng, Y., Qiu, F., Huang, J., Tashiro, S., Onodera, S., & Ikejima, T. (2008). Apoptosis-suppressing and autophagy-promoting effects of calpain on oridonin-induced L929 cell death. *Arch Biochem Biophys, 475*(2), 148-155. doi:10.1016/j.abb.2008.04.027

Chetsawang, J., Nudmamud-Thanoi, S., Phonchai, R., Abubakar, Z., Govitrapong, P., & Chetsawang, B. (2018). Methamphetamine toxicity-induced calcineurin activation, nuclear translocation of nuclear factor of activated T-cells and elevation of cyclooxygenase 2 levels are averted by calpastatin overexpression in neuroblastoma SH-SY5Y cells. *Neurotoxicology, 67*, 287-295. doi:10.1016/j.neuro.2018.06.011

Chlebowski, R., Anderson, G., Gass, M., Lane, D., Aragaki, A., Kuller, L., . . . Prentice, R. (2010). Estrogen plus progestin and breast cancer incidence and mortality in postmenopausal women. *Jama, 304*(15), 1684-1692. doi:10.1001/jama.2010.1500

Chlebowski, R., Kuller, L., Prentice, R., Stefanick, M., Manson, J., Gass, M., . . . Anderson, G. (2009). Breast cancer after use of estrogen plus progestin in postmenopausal women. *N Engl J Med, 360*(6), 573-587. doi:10.1056/NEJMoa0807684

Choi, Y., Lee, S., Nguyen, P., Jang, J., Lee, J., Wu, M., . . . Trepel, J. (1997). Regulation of cyclin D1 by calpain protease. *J Biol Chem, 272*(45), 28479-28484. doi:10.1074/jbc.272.45.28479

Chua, B., Guo, K., & Li, P. (2000). Direct cleavage by the calcium-activated protease calpain can lead to inactivation of caspases. *J Biol Chem, 275*(7), 5131-5135. doi:10.1074/jbc.275.7.5131

Cianfrocca, M., & Goldstein, L. (2004). Prognostic and predictive factors in early-stage breast cancer. *Oncologist, 9*(6), 606-616. doi:10.1634/theoncologist.9-6-606

Ciruelos, E., Villagrasa, P., Pascual, T., Oliveira, M., Pernas, S., Paré, L., . . . Prat, A. (2020). Palbociclib and Trastuzumab in HER2-Positive Advanced Breast Cancer: Results from the Phase II SOLTI-1303 PATRICIA Trial. *Clin Cancer Res, 26*(22), 5820-5829. doi:10.1158/1078-0432.ccr-20-0844

Clayton, F. (1986). Pure mucinous carcinomas of breast: morphologic features and prognostic correlates. *Hum Pathol, 17*(1), 34-38. doi:10.1016/s0046-8177(86)80152-6

Coles, C., Choudhury, A., Hoskin, P., Jones, C., O'Leary, B., Roques, T., . . . Yuille, F. (2020). COVID-19: A Catalyst for Change for UK Clinical Oncology. *Int J Radiat Oncol Biol Phys, 108*(2), 462-465. doi:10.1016/j.ijrobp.2020.06.041

Conacci-Sorrell, M., Ngouenet, C., Anderson, S., Brabletz, T., & Eisenman, R. (2014). Stress-induced cleavage of Myc promotes cancer cell survival. *Genes Dev, 28*(7), 689-707. doi:10.1101/gad.231894.113

Conacci-Sorrell, M., Ngouenet, C., & Eisenman, R. (2010). Myc-nick: a cytoplasmic cleavage product of Myc that promotes alpha-tubulin acetylation and cell differentiation. *Cell, 142*(3), 480-493. doi:10.1016/j.cell.2010.06.037

Cong, J., Goll, D., Peterson, A., & Kapprell, H. (1989). The role of autolysis in activity of the Ca2+-dependent proteinases (mu-calpain and m-calpain). *J Biol Chem, 264*(17), 10096-10103.

Cong , M., Thompson, V., Goll, D., & Antin, P. (1998). The bovine calpastatin gene promoter and a new N-terminal region of the protein are targets for cAMP-dependent protein kinase activity. *J Biol Chem, 273*(1), 660-666. doi:10.1074/jbc.273.1.660

Cooke, T., Reeves, J., Lanigan, A., & Stanton, P. (2001). HER2 as a prognostic and predictive marker for breast cancer. *Ann Oncol, 12 Suppl 1*, S23-28. doi:10.1093/annonc/12.suppl_1.s23

Cornfield, D., Palazzo, J., Schwartz, G., Goonewardene, S., Kovatich, A., Chervoneva, I., . . . Schwarting, R. (2004). The prognostic significance of multiple morphologic features and biologic markers in ductal carcinoma in situ of the breast: a study of a large cohort of patients treated with surgery alone. *Cancer, 100*(11), 2317-2327. doi:10.1002/cncr.20260

Cortes, J., Cescon, D., Rugo, H. S., Nowecki, Z., Im, S., Yusof, M., . . . Schmid, P. (2020). Pembrolizumab plus chemotherapy versus placebo plus chemotherapy for previously untreated locally recurrent inoperable or metastatic triple-negative breast cancer (KEYNOTE-355): a randomised, placebo-controlled, double-blind, phase 3 clinical trial. *Lancet, 396*(10265), 1817-1828. doi:10.1016/s0140-6736(20)32531-9

Cosse, J., & Michiels, C. (2008). Tumour hypoxia affects the responsiveness of cancer cells to chemotherapy and promotes cancer progression. *Anticancer Agents Med Chem, 8*(7), 790-797. doi:10.2174/187152008785914798

Couderc, C., Boin, A., Fuhrmann, L., Vincent-Salomon, A., Mandati, V., Kieffer, Y., . . . Lallemand, D. (2016). AMOTL1 Promotes Breast Cancer Progression and Is Antagonized by Merlin. *Neoplasia, 18*(1), 10-24. doi:10.1016/j.neo.2015.11.010

Creagan, E., Green, S., Ahmann, D., Ingle, J., Edmonson, J., & Marschke, R. J. (1984). A phase III clinical trial comparing the combination cyclophosphamide, adriamycin, cisplatin with cyclophosphamide, 5-

fluorouracil, prednisone in patients with advanced breast cancer. *J Clin Oncol, 2*(11), 1260-1265. doi:10.1200/jco.1984.2.11.1260

Croall, D., & DeMartino, G. (1991). Calcium-activated neutral protease (calpain) system: structure, function, and regulation. *Physiol Rev, 71*(3), 813-847. doi:10.1152/physrev.1991.71.3.813

CRUK. (2020). Breast cancer staging. Retrieved from https://www.cancerresearchuk.org/about-cancer/breast-cancer/stages-types-grades/number-stages

CRUK. (2021a). Retrieved from https://www.cancerresearchuk.org/health-professional/cancer-statistics/statistics-by-cancer-type/breast-cancer/survival#heading-Three

CRUK. (2021b). Cancer Research UK statistics. Retrieved from https://www.cancerresearchuk.org/health-professional/cancer-statistics/statistics-by-cancer-type/breast-cancer#heading-Three

Cuerrier, D., Moldoveanu, T., & Davies, P. (2005). Determination of peptide substrate specificity for μ-calpain by a peptide library-based approach: the importance of primed side interactions. *Journal of Biological Chemistry, 280*(49), 40632-40641.

Cui, W., Zhou, J., Dehne, N., & Brüne, B. (2015). Hypoxia induces calpain activity and degrades SMAD2 to attenuate TGFβ signaling in macrophages. *Cell & Bioscience, 5*(1), 36. doi:10.1186/s13578-015-0026-x

Curtis, C., Shah, S., Chin, S., Turashvili, G., Rueda, O., Dunning, M., . . . Aparicio, S. (2012). The genomic and transcriptomic architecture of 2,000 breast tumours reveals novel subgroups. *Nature, 486*(7403), 346-352. doi:10.1038/nature10983

D. E. Cremoux, P., Hamy, A., Lehmann-Che, J., Scott, V., Sigal, B., Mathieu, M., . . . Bièche, I. (2018). COX2/PTGS2 Expression Is Predictive of Response to Neoadjuvant Celecoxib in HER2-negative Breast Cancer Patients. *Anticancer Res, 38*(3), 1485-1490. doi:10.21873/anticanres.12375

Dai, Z., Zhou, S., Zhou, Z., Bai, D., Xu, X., Fu, X., . . . Yu, L. (2014). Capn4 contributes to tumour growth and metastasis of hepatocellular carcinoma by activation of the FAK–Src signalling pathways. *J Pathol, 234*(3), 316-328.

Daly, M., Clark, G., & McGuire, W. (1985). Breast cancer prognosis in a mixed Caucasian-Hispanic population. *J Natl Cancer Inst, 74*(4), 753-757.

Darby, S., McGale, P., Correa, C., Taylor, C., Arriagada, R., Clarke, M., . . . Peto, R. (2011). Effect of radiotherapy after breast-conserving surgery on 10-year recurrence and 15-year breast cancer death: meta-analysis of individual patient data for 10,801 women in 17 randomised trials. *Lancet, 378*(9804), 1707-1716. doi:10.1016/s0140-6736(11)61629-2

Davies, C., Pan, H., Godwin, J., Gray, R., Arriagada, R., Raina, V., . . . Peto, R. (2013). Long-term effects of continuing adjuvant tamoxifen to 10 years versus stopping at 5 years after diagnosis of oestrogen receptor-positive breast cancer: ATLAS, a randomised trial. *Lancet, 381*(9869), 805-816. doi:10.1016/s0140-6736(12)61963-1

Dawson, S., Rueda, O., Aparicio, S., & Caldas, C. (2013). A new genome-driven integrated classification of breast cancer and its implications. *Embo j, 32*(5), 617-628. doi:10.1038/emboj.2013.19

De Tullio, R., Cantoni, C., Broggio, C., Prato, C., Stifanese, R., Averna, M., . . . Melloni, E. (2009). Involvement of exon 6-mediated calpastatin intracellular movements in the modulation of calpain activation. *Biochim Biophys Acta, 1790*(3), 182-187. doi:10.1016/j.bbagen.2008.11.002

De Tullio, R., Passalacqua, M., Averna, M., Salamino, F., Melloni, E., & Pontremoli, S. (1999). Changes in intracellular localization of calpastatin during calpain activation. *Biochem J, 343 Pt 2*(Pt 2), 467-472.

Demarchi, F., Bertoli, C., Copetti, T., Tanida, I., Brancolini, C., Eskelinen, E., & Schneider, C. (2006). Calpain is required for macroautophagy in mammalian cells. *J Cell Biol, 175*(4), 595-605. doi:10.1083/jcb.200601024

Diéras, V., Miles, D., Verma, S., Pegram, M., Welslau, M., Baselga, J., . . . Gianni, L. (2017). Trastuzumab emtansine versus capecitabine plus lapatinib in patients with previously treated HER2-positive advanced breast cancer (EMILIA): a descriptive analysis of final overall survival results from a randomised, open-label, phase 3 trial. *Lancet Oncol, 18*(6), 732-742. doi:10.1016/s1470-2045(17)30312-1

Donkor, I. (2015). An updated patent review of calpain inhibitors (2012 - 2014). *Expert Opin Ther Pat, 25*(1), 17-31. doi:10.1517/13543776.2014.982534

Dunaway, L., & Pollock, J. (2021). HDAC1: an environmental sensor regulating endothelial function. *Cardiovasc Res*. doi:10.1093/cvr/cvab198

EBCTCG. (2015). Adjuvant bisphosphonate treatment in early breast cancer: meta-analyses of individual patient data from randomised trials. *Lancet, 386*(10001), 1353-1361. doi:10.1016/s0140-6736(15)60908-4

Edelstein, C., Yaqoob, M., Alkhunaizi, A., Gengaro, P., Nemenoff, R., Wang, K., & Schrier, R. (1996). Modulation of hypoxia-induced calpain activity in rat renal proximal tubules. *Kidney international, 50*(4), 1150-1157.

Edge, S., & Compton, C. (2010). The American Joint Committee on Cancer: the 7th edition of the AJCC cancer staging manual and the future of TNM. *Ann Surg Oncol, 17*(6), 1471-1474. doi:10.1245/s10434-010-0985-4

Elledge, R., Clark, G., Chamness, G., & Osborne, C. (1994). Tumor biologic factors and breast cancer prognosis among white, Hispanic, and black women in the United States. *J Natl Cancer Inst, 86*(9), 705-712. doi:10.1093/jnci/86.9.705

Elston, C., & Ellis, I. (1991). Pathological prognostic factors in breast cancer. I. The value of histological grade in breast cancer: experience from a large study with long-term follow-up. *Histopathology, 19*(5), 403-410. doi:10.1111/j.1365-2559.1991.tb00229.x

Emami, B., Lyman, J., Brown, A., Coia, L., Goitein, M., Munzenrider, J., . . . Wesson, M. (1991). Tolerance of normal tissue to therapeutic irradiation. *Int J Radiat Oncol Biol Phys, 21*(1), 109-122. doi:10.1016/0360-3016(91)90171-y

Emori, Y., Kawasaki, H., Imajoh, S., Minami, Y., & Suzuki, K. (1988). All four repeating domains of the endogenous inhibitor for calcium-dependent protease independently retain inhibitory activity. Expression of the cDNA fragments in Escherichia coli. *J Biol Chem, 263*(5), 2364-2370.

Enomoto, A., Fukasawa, T., Tsumoto, H., Karube, M., Nakagawa, K., Yoshizaki, A., . . . Miyagawa, K. (2019). Prevention of calpain-dependent degradation of STK38 by MEKK2-mediated phosphorylation. *Sci Rep, 9*(1), 16010. doi:10.1038/s41598-019-52435-8

Erol, A., Ho, A., Winham, S. J., & Karpyak, V. (2019). Sex hormones in alcohol consumption: a systematic review of evidence. *Addict Biol, 24*(2), 157-169. doi:10.1111/adb.12589

Fan, D., Dai, J., Tang, J., Wu, M., Sun, S., Jiang, J., & Fan, Q. (2009). Silencing of calpain expression reduces the metastatic potential of human osteosarcoma cells. *Cell biology international, 33*(12), 1263-1267.

Farkas, O., Polgár, B., Szekeres-Barthó, J., Dóczi, T., Povlishock, J., & Büki, A. (2005). Spectrin breakdown products in the cerebrospinal fluid in severe head injury--preliminary observations. *Acta Neurochir (Wien), 147*(8), 855-861. doi:10.1007/s00701-005-0559-6

FASG. (2001). Benefit of a high-dose epirubicin regimen in adjuvant chemotherapy for node-positive breast cancer patients with poor prognostic factors: 5-year follow-up results of French Adjuvant Study Group 05 randomized trial. *J Clin Oncol, 19*(3), 602-611. doi:10.1200/jco.2001.19.3.602

Ferlay, J., Ervik, M., Lam, F., Colombet, M., Mery, L., Piñeros, M., . . . Bray, F. (2020a). Cancer Today; International Agency for Research on Cancer. Retrieved from https://gco.iarc.fr/today

Ferlay, J., Laversanne, M., Ervik, M., Lam, F., Colombet, M., Mery, L., . . . Bray, F. (2020b). Global Cancer Observatory: Cancer Tomorrow; International

Agency for Research on Cancer. Retrieved from https://gco.iarc.fr/tomorrow

Ferrer, I., Verdugo-Sivianes, E., Castilla, M., Melendez, R., Marin, J., Muñoz-Galvan, S., . . . Carnero, A. (2016). Loss of the tumor suppressor spinophilin (PPP1R9B) increases the cancer stem cell population in breast tumors. *Oncogene, 35*(21), 2777-2788. doi:10.1038/onc.2015.341

FESG. (1988). A prospective randomized phase III trial comparing combination chemotherapy with cyclophosphamide, fluorouracil, and either doxorubicin or epirubicin. French Epirubicin Study Group. *J Clin Oncol, 6*(4), 679-688. doi:10.1200/jco.1988.6.4.679

Finn, R., Crown, J., Lang, I., Boer, K., Bondarenko, I., Kulyk, S., . . . Slamon, D. (2015). The cyclin-dependent kinase 4/6 inhibitor palbociclib in combination with letrozole versus letrozole alone as first-line treatment of oestrogen receptor-positive, HER2-negative, advanced breast cancer (PALOMA-1/TRIO-18): a randomised phase 2 study. *Lancet Oncol, 16*(1), 25-35. doi:10.1016/s1470-2045(14)71159-3

Fisher, B., Bauer, M., Wickerham, D., Redmond, C., Fisher, E., Cruz, A., . . . et al. (1983). Relation of number of positive axillary nodes to the prognosis of patients with primary breast cancer. An NSABP update. *Cancer, 52*(9), 1551-1557. doi:10.1002/1097-0142(19831101)52:9<1551::aid-cncr2820520902>3.0.co;2-3

Fisher, B., Redmond, C., Fisher, E., & Caplan, R. (1988). Relative worth of estrogen or progesterone receptor and pathologic characteristics of differentiation as indicators of prognosis in node negative breast cancer patients: findings from National Surgical Adjuvant Breast and Bowel Project Protocol B-06. *J Clin Oncol, 6*(7), 1076-1087. doi:10.1200/jco.1988.6.7.1076

Fisher, B., Redmond, C., Wickerham, D., Bowman, D., Schipper, H., Wolmark, N., . . . et al. (1989). Doxorubicin-containing regimens for the treatment of stage II breast cancer: The National Surgical Adjuvant Breast and Bowel Project experience. *J Clin Oncol, 7*(5), 572-582. doi:10.1200/jco.1989.7.5.572

Fisher, B., Slack, N., & Bross, I. D. (1969). Cancer of the breast: size of neoplasm and prognosis. *Cancer, 24*(5), 1071-1080. doi:10.1002/1097-0142(196911)24:5<1071::aid-cncr2820240533>3.0.co;2-h

Forster, T. (1946). Energiewanderung und fluoreszenz. *Naturwissenschaften, 33*(6), 166-175.

Fowler, J. (1992). Alpha, beta, and surviving fraction. *Int J Radiat Oncol Biol Phys, 24*(1), 188-189. doi:10.1016/0360-3016(92)91048-r

Franco, S., & Huttenlocher, A. (2005). Regulating cell migration: calpains make the cut. *J Cell Sci, 118*(Pt 17), 3829-3838. doi:10.1242/jcs.02562

Franco, S., Rodgers, M., Perrin, B., Han, J., Bennin, D., Critchley, D., & Huttenlocher, A. (2004). Calpain-mediated proteolysis of talin regulates adhesion dynamics. *Nat Cell Biol, 6*(10), 977-983. doi:10.1038/ncb1175

Franken, N., Rodermond, H., Stap, J., Haveman, J., & van Bree, C. (2006). Clonogenic assay of cells in vitro. *Nat Protoc, 1*(5), 2315-2319. doi:10.1038/nprot.2006.339

Franken, N., ten Cate, R., Krawczyk, P., Stap, J., Haveman, J., Aten, J., & Barendsen, G. (2011). Comparison of RBE values of high-LET α-particles for the induction of DNA-DSBs, chromosome aberrations and cell reproductive death. *Radiat Oncol, 6*, 64. doi:10.1186/1748-717x-6-64

Franklin, M., Carey, K., Vajdos, F., Leahy, D., de Vos, A., & Sliwkowski, M. (2004). Insights into ErbB signaling from the structure of the ErbB2-pertuzumab complex. *Cancer Cell, 5*(4), 317-328. doi:10.1016/s1535-6108(04)00083-2

Fulford, L., Easton, D., Reis-Filho, J., Sofronis, A., Gillett, C., Lakhani, S., & Hanby, A. (2006). Specific morphological features predictive for the basal

phenotype in grade 3 invasive ductal carcinoma of breast. *Histopathology, 49*(1), 22-34. doi:10.1111/j.1365-2559.2006.02453.x

Fuller, E., & Howell, V. (2014). Culture models to define key mediators of cancer matrix remodeling. *Front Oncol, 4*, 57. doi:10.3389/fonc.2014.00057

Gafni, J., Cong, X., Chen, S., Gibson, B., & Ellerby, L. (2009). Calpain-1 cleaves and activates caspase-7. *J Biol Chem, 284*(37), 25441-25449. doi:10.1074/jbc.M109.038174

Gao , G., & Dou, Q. (2000). N-terminal cleavage of bax by calpain generates a potent proapoptotic 18-kDa fragment that promotes bcl-2-independent cytochrome C release and apoptotic cell death. *J Cell Biochem, 80*(1), 53-72. doi:10.1002/1097-4644(20010101)80:1<53::aid-jcb60>3.0.co;2-e

Gao, L., Yang, Q., Zhou, W., Dai, Y., Wang, J., Fu, L., . . . Zou, C. (2021). RNA-Sequencing-Based lncRNA Biomarker Profiling on Triple Negative Breast Cancer. *Journal of Cancer Research Updates, 10*, 1-9. doi:10.30683/1929-2279.2021.10.01

García-Morales, P., Carrasco-García, E., Ruiz-Rico, P., Martínez-Mira, R., Menéndez-Gutiérrez, M., Ferragut, J., . . . Martínez-Lacaci, I. (2007). Inhibition of Hsp90 function by ansamycins causes downregulation of cdc2 and cdc25c and G(2)/M arrest in glioblastoma cell lines. *Oncogene, 26*(51), 7185-7193. doi:10.1038/sj.onc.1210534

Gemignani, M., & Armstrong, D. (2014). Breast cancer. *Gynecol Oncol, 132*(2), 264-267. doi:10.1016/j.ygyno.2014.01.022

Gerweck, L., Vijayappa, S., & Kozin, S. (2006). Tumor pH controls the in vivo efficacy of weak acid and base chemotherapeutics. *Mol Cancer Ther, 5*(5), 1275-1279. doi:10.1158/1535-7163.mct-06-0024

Geyer, C., Forster, J., Lindquist, D., Chan, S., Romieu, C., Pienkowski, T., . . . Cameron, D. (2006). Lapatinib plus capecitabine for HER2-positive advanced breast cancer. *N Engl J Med, 355*(26), 2733-2743. doi:10.1056/NEJMoa064320

Gil-Parrado, S., Fernández-Montalván, A., Assfalg-Machleidt, I., Popp, O., Bestvater, F., Holloschi, A., . . . Machleidt, W. (2002). Ionomycin-activated calpain triggers apoptosis. A probable role for Bcl-2 family members. *J Biol Chem, 277*(30), 27217-27226. doi:10.1074/jbc.M202945200

Gil-Parrado, S., Popp, O., Knoch, T., Zahler, S., Bestvater, F., Felgenträger, M., . . . Spiess, E. (2003). Subcellular localization and in vivo subunit interactions of ubiquitous mu-calpain. *J Biol Chem, 278*(18), 16336-16346. doi:10.1074/jbc.M208657200

Giordano, S. (2018). Breast Cancer in Men. *N Engl J Med, 378*(24), 2311-2320. doi:10.1056/NEJMra1707939

Glading, A., Uberall, F., Keyse, S., Lauffenburger, D., & Wells, A. (2001). Membrane proximal ERK signaling is required for M-calpain activation downstream of epidermal growth factor receptor signaling. *J Biol Chem, 276*(26), 23341-23348. doi:10.1074/jbc.M008847200

Goel, S., Pernas, S., Tan-Wasielewski, Z., Barry, W., Bardia, A., Rees, R., . . . Tolaney, S. (2019). Ribociclib Plus Trastuzumab in Advanced HER2-Positive Breast Cancer: Results of a Phase 1b/2 Trial. *Clin Breast Cancer, 19*(6), 399-404. doi:10.1016/j.clbc.2019.05.010

Goetz, M., Toi, M., Campone, M., Sohn, J., Paluch-Simon, S., Huober, J., . . . Di Leo, A. (2017). MONARCH 3: Abemaciclib As Initial Therapy for Advanced Breast Cancer. *J Clin Oncol, 35*(32), 3638-3646. doi:10.1200/jco.2017.75.6155

Goll, D., Thompson, V., Li, H., Wei, W., & Cong, J. (2003). The calpain system. *Physiol Rev, 83*(3), 731-801. doi:10.1152/physrev.00029.2002

Gombos, A. (2019). Selective oestrogen receptor degraders in breast cancer: a review and perspectives. *Curr Opin Oncol, 31*(5), 424-429. doi:10.1097/cco.0000000000000567

Gonen, H., Shkedy, D., Barnoy, S., Kosower, N., & Ciechanover, A. (1997). On the involvement of calpains in the degradation of the tumor suppressor protein p53. *FEBS Lett, 406*(1-2), 17-22. doi:10.1016/s0014-5793(97)00225-1

Gray, R., Rea, D., Handley, K., Bowden, S., Perry, P., Earl, H., . . . Dewar, J. (2013). aTTom: Long-term effects of continuing adjuvant tamoxifen to 10 years versus stopping at 5 years in 6,953 women with early breast cancer: American Society of Clinical Oncology.

Green, A., Soria, D., Powe, D., Nolan, C., Aleskandarany, M., Szász, M., . . . Ellis, I. (2016). Nottingham prognostic index plus (NPI+) predicts risk of distant metastases in primary breast cancer. *Breast Cancer Res Treat, 157*(1), 65-75. doi:10.1007/s10549-016-3804-1

Grieve, S., Gao, Y., Hall, C., Hu, J., & Greer, P. (2016). Calpain Genetic Disruption and HSP90 Inhibition Combine To Attenuate Mammary Tumorigenesis. *Mol Cell Biol, 36*(15), 2078-2088. doi:10.1128/mcb.01062-15

Grimes, D., & Partridge, M. (2015). A mechanistic investigation of the oxygen fixation hypothesis and oxygen enhancement ratio. *Biomed Phys Eng Express, 1*(4), 045209. doi:10.1088/2057-1976/1/4/045209

Guo, Q., Cheng, K., Wang, X., Li, X., Yu, Y., Hua, Y., & Yang, Z. (2020). Expression of HDAC1 and RBBP4 correlate with clinicopathologic characteristics and prognosis in breast cancer. *Int J Clin Exp Pathol, 13*(3), 563-572.

Guo , Y., Tan, J., Miao, Y., Sun, Z., & Zhang, Q. (2019). Effects of microvesicles on cell apoptosis under hypoxia. *Oxidative Medicine and Cellular Longevity, 2019*.

Guroff, G. (1964). A NEUTRAL, CALCIUM-ACTIVATED PROTEINASE FROM THE SOLUBLE FRACTION OF RAT BRAIN. *J Biol Chem, 239*, 149-155.

Hall, E., & Giaccia, A. (2006). *Radiobiology for the Radiologist* (Vol. 6): Philadelphia.

Han, Y., Weinman, S., Boldogh, I., Walker, R., & Brasier, A. (1999). Tumor necrosis factor-alpha-inducible IkappaBalpha proteolysis mediated by cytosolic m-calpain. A mechanism parallel to the ubiquitin-proteasome pathway for nuclear factor-kappab activation. *J Biol Chem, 274*(2), 787-794. doi:10.1074/jbc.274.2.787

Hanna, H., Campbell, R., & Davies, P. (2008). Calcium-bound structure of calpain and its mechanism of inhibition by calpastatin. *Nature, 456*(7220), 409-412. doi:10.1038/nature07451

Hartmann, L., Sellers, T., Frost, M., Lingle, W., Degnim, A., Ghosh, K., . . . Visscher, D. (2005). Benign breast disease and the risk of breast cancer. *N Engl J Med, 353*(3), 229-237. doi:10.1056/NEJMoa044383

Hassan, M., Ansari, J., Spooner, D., & Hussain, S. (2010). Chemotherapy for breast cancer (Review). *Oncol Rep, 24*(5), 1121-1131. doi:10.3892/or_00000963

Haviland, J., Owen, J., Dewar, J., Agrawal, R., Barrett, J., Barrett-Lee, P., . . . Yarnold, J. (2013). The UK Standardisation of Breast Radiotherapy (START) trials of radiotherapy hypofractionation for treatment of early breast cancer: 10-year follow-up results of two randomised controlled trials. *Lancet Oncol, 14*(11), 1086-1094. doi:10.1016/s1470-2045(13)70386-3

He, L., Wu, X., Meylan, F., Olson, D., Simone, J., Hewgill, D., . . . Lipsky, P. (2004). Monitoring caspase activity in living cells using fluorescent proteins and flow cytometry. *Am J Pathol, 164*(6), 1901-1913.

Hiraoka, E., Mimae, T., Ito, M., Kadoya, T., Miyata, Y., Ito, A., & Okada, M. (2019). Breast cancer cell motility is promoted by 14-3-3γ. *Breast Cancer, 26*(5), 581-593. doi:10.1007/s12282-019-00957-4

Höckel, M., Schlenger, K., Knoop, C., & Vaupel, P. (1991). Oxygenation of carcinomas of the uterine cervix: evaluation by computerized O2 tension measurements. *Cancer Res, 51*(22), 6098-6102.

Hohenberger, P., Felgner, C., Haensch, W., & Schlag, P. (1998). Tumor oxygenation correlates with molecular growth determinants in breast cancer. *Breast Cancer Res Treat, 48*(2), 97-106. doi:10.1023/a:1005921513083

Hörner-Rieber, J., Forster, T., Hommertgen, A., Haefner, M., Arians, N., König, L., . . . Debus, J. (2021). Intensity Modulated Radiation Therapy (IMRT) With Simultaneously Integrated Boost Shortens Treatment Time and Is Noninferior to Conventional Radiation Therapy Followed by Sequential Boost in Adjuvant Breast Cancer Treatment: Results of a Large Randomized Phase III Trial (IMRT-MC2 Trial). *Int J Radiat Oncol Biol Phys, 109*(5), 1311-1324. doi:10.1016/j.ijrobp.2020.12.005

Hortobagyi, G., Blumenschein, G., Spanos, W., Montague, E., Buzdar, A., Yap, H., & Schell, F. (1983). Multimodal treatment of locoregionally advanced breast cancer. *Cancer, 51*(5), 763-768. doi:10.1002/1097-0142(19830301)51:5<763::aid-cncr2820510502>3.0.co;2-c

Hortobagyi, G., Stemmer, S., Burris, H., Yap, Y., Sonke, S., Paluch-Shimon, S., . . . O'Shaughnessy, J. (2018). Updated results from MONALEESA-2, a phase III trial of first-line ribociclib plus letrozole versus placebo plus letrozole in hormone receptor-positive, HER2-negative advanced breast cancer. *Ann Oncol, 29*(7), 1541-1547. doi:10.1093/annonc/mdy155

Hosfield, C., Elce, J., Davies, P., & Jia, Z. (1999). Crystal structure of calpain reveals the structural basis for Ca(2+)-dependent protease activity and a novel mode of enzyme activation. *Embo j, 18*(24), 6880-6889. doi:10.1093/emboj/18.24.6880

Hoskin, V., Szeto, A., Ghaffari, A., Greer, P., Côté, G., & Elliott, B. (2015). Ezrin regulates focal adhesion and invadopodia dynamics by altering calpain activity to promote breast cancer cell invasion. *Molecular biology of the cell, 26*(19), 3464-3479.

Hou, S., Sang, M., Zhao, L., Hou, R., & Shan, B. (2016). The expression of MAGE-C1 and MAGE-C2 in breast cancer and their clinical significance. *Am J Surg, 211*(1), 142-151. doi:10.1016/j.amjsurg.2015.05.028

Howlader, N., Altekruse, S., Li, C., Chen, V., Clarke, C., Ries, L., & Cronin, K. (2014). US incidence of breast cancer subtypes defined by joint hormone receptor and HER2 status. *J Natl Cancer Inst, 106*(5). doi:10.1093/jnci/dju055

Hubbi, M., & Semenza, G. (2015). Regulation of cell proliferation by hypoxia-inducible factors. *Am J Physiol Cell Physiol, 309*(12), C775-782. doi:10.1152/ajpcell.00279.2015

Hudis, C. (2007). Trastuzumab--mechanism of action and use in clinical practice. *N Engl J Med, 357*(1), 39-51. doi:10.1056/NEJMra043186

Hudis , C., & Gianni, L. (2011). Triple-negative breast cancer: an unmet medical need. *Oncologist, 16 Suppl 1*, 1-11. doi:10.1634/theoncologist.2011-S1-01

Hunter, N., & Muirhead, C. (2009). Review of relative biological effectiveness dependence on linear energy transfer for low-LET radiations. *J Radiol Prot, 29*(1), 5-21. doi:10.1088/0952-4746/29/1/r01

Husby, A., Wohlfahrt, J., Øyen, N., & Melbye, M. (2018). Pregnancy duration and breast cancer risk. *Nat Commun, 9*(1), 4255. doi:10.1038/s41467-018-06748-3

Iida, T., Mine, S., Fujimoto, H., Suzuki, Y., Minami, Y., & Tanaka, Y. (2002). Hypoxia-inducible factor-1alpha induces cell cycle arrest of endothelial cells. *Genes Cells, 7*(2), 143-149. doi:10.1046/j.1356-9597.2001.00512.x

Imajoh, S., Kawasaki, H., Emori, Y., & Suzuki, K. (1987). Calcium-activated neutral protease inhibitor from rabbit erythrocytes lacks the N-terminal region of the liver inhibitor but retains three inhibitory units. *Biochem Biophys Res Commun, 146*(2), 630-637. doi:10.1016/0006-291x(87)90575-4

Imajoh, S., Kawasaki, H., & Suzuki, K. (1986). Limited autolysis of calcium-activated neutral protease (CANP): reduction of the Ca2+-requirement is due to the NH2-terminal processing of the large subunit. *J Biochem, 100*(3), 633-642. doi:10.1093/oxfordjournals.jbchem.a121755

Imajoh , S., Kawasaki, H., & Suzuki, K. (1987). The COOH-terminal E-F hand structure of calcium-activated neutral protease (CANP) is important for the

association of subunits and resulting proteolytic activity. *J Biochem, 101*(2), 447-452. doi:10.1093/oxfordjournals.jbchem.a121930

Innes, K., & Byers, T. (1999). Preeclampsia and breast cancer risk. *Epidemiology, 10*(6), 722-732.

Ishida, S., Emori, Y., & Suzuki, K. (1991). Rat calpastatin has diverged primary sequence from other mammalian calpastatins but retains functionally important sequences. *Biochim Biophys Acta, 1088*(3), 436-438. doi:10.1016/0167-4781(91)90139-d

Ishiura, S., Murofushi, H., Suzuki, K., & Imahori, K. (1978). Studies of a calcium-activated neutral protease from chicken skeletal muscle. I. Purification and characterization. *J Biochem, 84*(1), 225-230. doi:10.1093/oxfordjournals.jbchem.a132111

Jánossy, J., Ubezio, P., Apáti, A., Magócsi, M., Tompa, P., & Friedrich, P. (2004). Calpain as a multi-site regulator of cell cycle. *Biochem Pharmacol, 67*(8), 1513-1521. doi:10.1016/j.bcp.2003.12.021

Jeon, K., Yu, H., & Kwon, Y. (2018). Hyperactivated m-calpain affects acquisition of doxorubicin resistance in breast cancer cells. *Biochim Biophys Acta Gen Subj, 1862*(5), 1126-1133. doi:10.1016/j.bbagen.2018.02.002

Jiang, W., Watkins, G., Douglas-Jones, A., Holmgren, L., & Mansel, R. (2006). Angiomotin and angiomotin like proteins, their expression and correlation with angiogenesis and clinical outcome in human breast cancer. *BMC Cancer, 6*, 16. doi:10.1186/1471-2407-6-16

Jin, X., Jiang, R., Xiang, Y., Fan, Z., Wu, Z., Yang, B., . . . Yang, Y. (2018). Overexpression of retinoblastoma-binding protein 4 contributes to the radiosensitivity of AGS gastric cancer cells via phosphoinositide3-kinase/protein kinase B pathway suppression. *Mol Med Rep, 18*(2), 1571-1581. doi:10.3892/mmr.2018.9153

Jin, X., & Mu, P. (2015). Targeting Breast Cancer Metastasis. *Breast Cancer (Auckl), 9*(Suppl 1), 23-34. doi:10.4137/bcbcr.s25460

Jongen, J., van der Waals, L., Trumpi, K., Laoukili, J., Peters, N., Schenning-van Schelven, S., . . . Kranenburg, O. (2017). Downregulation of DNA repair proteins and increased DNA damage in hypoxic colon cancer cells is a therapeutically exploitable vulnerability. *Oncotarget, 8*(49), 86296-86311. doi:10.18632/oncotarget.21145

Joy, J., Nalabothula, N., Ghosh, M., Popp, O., Jochum, M., Machleidt, W., . . . Holak, T. (2006). Identification of calpain cleavage sites in the G1 cyclin-dependent kinase inhibitor p19(INK4d). *Biol Chem, 387*(3), 329-335. doi:10.1515/bc.2006.044

Kaelin, W. (2005). The concept of synthetic lethality in the context of anticancer therapy. *Nat Rev Cancer, 5*(9), 689-698. doi:10.1038/nrc1691

Kalash, L., Cresser-Brown, J., Habchi, J., Morgan, C., Miller, D., Glen, R., . . . Bender, A. (2018). Structure-based design of allosteric calpain-1 inhibitors populating a novel bioactivity space. *Eur J Med Chem, 157*, 1264-1275. doi:10.1016/j.ejmech.2018.08.049

Kamano, Y., Saeki, M., Egusa, H., Kakihara, Y., Houry, W., Yatani, H., & Kamisaki, Y. (2013). PIH1D1 interacts with mTOR complex 1 and enhances ribosome RNA transcription. *FEBS Lett, 587*(20), 3303-3308. doi:10.1016/j.febslet.2013.09.001

Kapałczyńska, M., Kolenda, T., Przybyła, W., Zajączkowska, M., Teresiak, A., Filas, V., . . . Lamperska, K. (2018). 2D and 3D cell cultures - a comparison of different types of cancer cell cultures. *Arch Med Sci, 14*(4), 910-919. doi:10.5114/aoms.2016.63743

KEGG. (2022). KEGG pathway database. Retrieved from https://www.genome.jp/kegg/pathway.html

Kelly, J., Cuerrier, D., Graham, L., Campbell, R., & Davies, P. (2009). Profiling of calpain activity with a series of FRET-based substrates. *Biochimica et Biophysica Acta (BBA)-Proteins and Proteomics, 1794*(10), 1505-1509.

Key, T., Appleby, P., Reeves, G., Travis, R., Alberg, A., Barricarte, A., . . . Vineis, P. (2013). Sex hormones and risk of breast cancer in premenopausal women: a collaborative reanalysis of individual participant data from seven prospective studies. *Lancet Oncol, 14*(10), 1009-1019. doi:10.1016/s1470-2045(13)70301-2

Kim, E., Chang, Y., Ahn, J., Yun, J., Park, Y., Park, C., . . . Ryu, S. (2020). Mammographic breast density, its changes, and breast cancer risk in premenopausal and postmenopausal women. *Cancer, 126*(21), 4687-4696. doi:10.1002/cncr.33138

Kim , M., Oh, S., Park, S., Kang, H., Won, M., Kang, T., . . . Lee, J. (2007). Hypoxia-induced cell death of HepG2 cells involves a necrotic cell death mediated by calpain. *Apoptosis, 12*(4), 707-718. doi:10.1007/s10495-006-0002-3

Kitange, G., Mladek, A., Schroeder, M., Pokorny, J., Carlson, B., Zhang, Y., . . . Sarkaria, J. (2016). Retinoblastoma Binding Protein 4 Modulates Temozolomide Sensitivity in Glioblastoma by Regulating DNA Repair Proteins. *Cell Rep, 14*(11), 2587-2598. doi:10.1016/j.celrep.2016.02.045

Koscielny, S., Tubiana, M., Lê, M., Valleron, A., Mouriesse, H., Contesso, G., & Sarrazin, D. (1984). Breast cancer: relationship between the size of the primary tumour and the probability of metastatic dissemination. *Br J Cancer, 49*(6), 709-715. doi:10.1038/bjc.1984.112

Kouznetsova, V., Tchekanov, A., Li, X., Yan, X., & Tsigelny, I. (2019). Polycomb repressive 2 complex-Molecular mechanisms of function. *Protein Sci, 28*(8), 1387-1399. doi:10.1002/pro.3647

Kovacs, L., & Su, Y. (2014). The Critical Role of Calpain in Cell Proliferation. *J Biomol Res Ther, 3*(3). doi:10.4172/2167-7956.1000112

Kubbutat, M., & Vousden, K. (1997). Proteolytic cleavage of human p53 by calpain: a potential regulator of protein stability. *Mol Cell Biol, 17*(1), 460-468. doi:10.1128/mcb.17.1.460

Kumar, H., & Choi, D. (2015). Hypoxia Inducible Factor Pathway and Physiological Adaptation: A Cell Survival Pathway? *Mediators Inflamm, 2015*, 584758. doi:10.1155/2015/584758

Kurebayashi, J., Otsuki, T., Moriya, T., & Sonoo, H. (2001). Hypoxia reduces hormone responsiveness of human breast cancer cells. *Jpn J Cancer Res, 92*(10), 1093-1101. doi:10.1111/j.1349-7006.2001.tb01064.x

Kwak, J., Lee, N., Lee, H., Hong, I., & Nam, J. (2016). HIF2α/EFEMP1 cascade mediates hypoxic effects on breast cancer stem cell hierarchy. *Oncotarget, 7*(28), 43518-43533. doi:10.18632/oncotarget.9846

Lagadec, C., Dekmezian, C., Bauché, L., & Pajonk, F. (2012). Oxygen levels do not determine radiation survival of breast cancer stem cells. *PLoS One, 7*(3), e34545. doi:10.1371/journal.pone.0034545

Laisné, M., Benlamara, S., Nicolas, A., Djerroudi, L., Gupta, N., Daher, D., . . . Defossez, P. (2021). Cancer/Testis genes are predictive of breast tumor subtypes. *bioRxiv*, 2021.2010.2027.465656. doi:10.1101/2021.10.27.465656

Lakshmikuttyamma, A., Selvakumar, P., Kanthan, R., Kanthan, S., & Sharma, R. (2004). Overexpression of m-calpain in human colorectal adenocarcinomas. *Cancer Epidemiol Biomarkers Prev, 13*(10), 1604-1609.

Lam, A., St-Pierre, F., Gong, Y., Marshall, J., Cranfill, P., Baird, M., . . . Lin, M. (2012). Improving FRET dynamic range with bright green and red fluorescent proteins. *Nat Methods, 9*(10), 1005-1012. doi:10.1038/nmeth.2171

Larsen, A., Lametsch, R., Elce, J., Larsen, J., Thomsen, B., Larsen, M., . . . Ertbjerg, P. (2008). Genetic disruption of calpain correlates with loss of membrane blebbing and differential expression of RhoGDI-1, cofilin and tropomyosin. *Biochem J, 411*(3), 657-666. doi:10.1042/bj20070522

Le Doussal, V., Tubiana-Hulin, M., Friedman, S., Hacene, K., Spyratos, F., & Brunet, M. (1989). Prognostic value of histologic grade nuclear components of

Scarff-Bloom-Richardson (SBR). An improved score modification based on a multivariate analysis of 1262 invasive ductal breast carcinomas. *Cancer, 64*(9), 1914-1921. doi:10.1002/1097-0142(19891101)64:9<1914::aid-cncr2820640926>3.0.co;2-g

LeBeau, A., Duriseti, S., Murphy, S., Pepin, F., Hann, B., Gray, J., . . . Craik, C. (2013). Targeting uPAR with antagonistic recombinant human antibodies in aggressive breast cancer. *Cancer Res, 73*(7), 2070-2081. doi:10.1158/0008-5472.can-12-3526

Lee , A., & Ellis, I. (2008). The Nottingham prognostic index for invasive carcinoma of the breast. *Pathol Oncol Res, 14*(2), 113-115. doi:10.1007/s12253-008-9067-3

Lee, W., Hatanaka, M., & Maki, M. (1992a). Multiple forms of rat calpastatin cDNA in the coding region of functionally unknown amino-terminal domain. *Biochim Biophys Acta, 1129*(2), 251-253. doi:10.1016/0167-4781(92)90500-y

Lee, W., Ma, H., Takano, E., Yang, H., Hatanaka, M., & Maki, M. (1992b). Molecular diversity in amino-terminal domains of human calpastatin by exon skipping. *J Biol Chem, 267*(12), 8437-8442.

Lehmann, B., Bauer, J., Chen, X., Sanders, M., Chakravarthy, A., Shyr, Y., & Pietenpol, J. (2011). Identification of human triple-negative breast cancer subtypes and preclinical models for selection of targeted therapies. *J Clin Invest, 121*(7), 2750-2767. doi:10.1172/jci45014

Leloup, L., Shao, H., Bae, Y., Deasy, B., Stolz, D., Roy, P., & Wells, A. (2010). m-Calpain activation is regulated by its membrane localization and by its binding to phosphatidylinositol 4,5-bisphosphate. *J Biol Chem, 285*(43), 33549-33566. doi:10.1074/jbc.M110.123604

Lester, S., Bose, S., Chen, Y., Connolly, J., de Baca, M., Fitzgibbons, P., . . . Winer, E. (2009). Protocol for the examination of specimens from patients with invasive carcinoma of the breast. *Arch Pathol Lab Med, 133*(10), 1515-1538. doi:10.5858/133.10.1515

Lewis, J., & Jordan, V. (2005). Selective estrogen receptor modulators (SERMs): mechanisms of anticarcinogenesis and drug resistance. *Mutat Res, 591*(1-2), 247-263. doi:10.1016/j.mrfmmm.2005.02.028

Lewis Phillips, G., Li, G., Dugger, D., Crocker, L., Parsons, K., Mai, E., . . . Sliwkowski, M. (2008). Targeting HER2-positive breast cancer with trastuzumab-DM1, an antibody-cytotoxic drug conjugate. *Cancer Res, 68*(22), 9280-9290. doi:10.1158/0008-5472.can-08-1776

Li, Cao, Y., Yu, X., Jin, F., & Li, Y. (2021). A novel autophagy-related genes prognostic risk model and validation of autophagy-related oncogene VPS35 in breast cancer. *Cancer Cell Int, 21*(1), 265. doi:10.1186/s12935-021-01970-4

Li , Chen, S., Yue, P., Deng, X., Lonial, S., Khuri, F., & Sun, S. (2010). Proteasome inhibitor PS-341 (bortezomib) induces calpain-dependent IκBα degradation. *Journal of Biological Chemistry, 285*(21), 16096-16104.

Li , Lv, Z., Xie, H., & Zheng, S. (2019b). Retinoblastoma binding protein 4 up-regulation is correlated with hepatic metastasis and poor prognosis in colon cancer patients. *Hepatobiliary Pancreat Dis Int, 18*(5), 446-451. doi:10.1016/j.hbpd.2019.08.006

Li , Lv, Z., & Zhu, W. (2020b). RBBP4 promotes colon cancer malignant progression via regulating Wnt/β-catenin pathway. *World J Gastroenterol, 26*(35), 5328-5342. doi:10.3748/wjg.v26.i35.5328

Li , Ma, J., Li, J. B., Lacefield, J., Jones, D., Peng, T., & Wei, M. (2018). Over-expression of calpastatin attenuates myocardial injury following myocardial infarction by inhibiting endoplasmic reticulum stress. *J Thorac Dis, 10*(9), 5283-5297. doi:10.21037/jtd.2018.08.133

Li, Nepal, R., Martin, A., & Berger, S. (2012). Induction of apoptosis in Eμ-myc lymphoma cells in vitro and in vivo through calpain inhibition. *Exp Hematol, 40*(7), 548-563.e542. doi:10.1016/j.exphem.2012.02.002

Li, Uribe, D., & Daling, J. (2005). Clinical characteristics of different histologic types of breast cancer. *Br J Cancer, 93*(9), 1046-1052. doi:10.1038/sj.bjc.6602787

Li , H., Zhang, M., Wei, Y., Haider, F., Lin, Y., Guan, W., . . . Wang, H. (2020a). SH3BGRL confers innate drug resistance in breast cancer by stabilizing HER2 activation on cell membrane. *J Exp Clin Cancer Res, 39*(1), 81. doi:10.1186/s13046-020-01577-z

Lin, G., Chattopadhyay, D., Maki, M., Wang, K., Carson, M., Jin, L., . . . Narayana, S. V. (1997). Crystal structure of calcium bound domain VI of calpain at 1.9 A resolution and its role in enzyme assembly, regulation, and inhibitor binding. *Nat Struct Biol, 4*(7), 539-547. doi:10.1038/nsb0797-539

Lin , N., Winer, E., Wheatley, D., Carey, L., Houston, S., Mendelson, D., . . . Garcia, A. (2012). A phase II study of afatinib (BIBW 2992), an irreversible ErbB family blocker, in patients with HER2-positive metastatic breast cancer progressing after trastuzumab. *Breast Cancer Res Treat, 133*(3), 1057-1065.

Lind, M. (2011). Principles of cytotoxic chemotherapy. *Medicine (Baltimore), 39*(12), 711-716.

Liu , B., Zhou, Y., Lu, D., Liu, Y., Zhang, S., Xu, Y., . . . Gu, X. (2017). Comparison of the protein expression of calpain-1, calpain-2, calpastatin and calmodulin between gastric cancer and normal gastric mucosa. *Oncol Lett, 14*(3), 3705-3710. doi:10.3892/ol.2017.6617

Liu, L., Xing, D., & Chen, W. (2009). Micro-calpain regulates caspase-dependent and apoptosis inducing factor-mediated caspase-independent apoptotic pathways in cisplatin-induced apoptosis. *Int J Cancer, 125*(12), 2757-2766. doi:10.1002/ijc.24626

Liu, L., Xing, D., Chen, W., Chen, T., Pei, Y., & Gao, X. (2008). Calpain-mediated pathway dominates cisplatin-induced apoptosis in human lung adenocarcinoma cells as determined by real-time single cell analysis. *Int J Cancer, 122*(10), 2210-2222. doi:10.1002/ijc.23378

Livasy, C., Karaca, G., Nanda, R., Tretiakova, M., Olopade, O., Moore, D., & Perou, C. (2006). Phenotypic evaluation of the basal-like subtype of invasive breast carcinoma. *Mod Pathol, 19*(2), 264-271. doi:10.1038/modpathol.3800528

Loibl, S., Untch, M., Burchardi, N., Huober, J., Sinn, B., Blohmer, J., . . . Schneeweiss, A. (2019). A randomised phase II study investigating durvalumab in addition to an anthracycline taxane-based neoadjuvant therapy in early triple-negative breast cancer: clinical results and biomarker analysis of GeparNuevo study. *Ann Oncol, 30*(8), 1279-1288. doi:10.1093/annonc/mdz158

López-Cortés, A., Cabrera-Andrade, A., Vázquez-Naya, J., Pazos, A., Gonzáles-Díaz, H., Paz, Y., . . . Munteanu, C. (2020). Prediction of breast cancer proteins involved in immunotherapy, metastasis, and RNA-binding using molecular descriptors and artificial neural networks. *Sci Rep, 10*(1), 8515. doi:10.1038/s41598-020-65584-y

Lord, C., Tutt, A., & Ashworth, A. (2015). Synthetic lethality and cancer therapy: lessons learned from the development of PARP inhibitors. *Annual review of medicine, 66*, 455-470.

Low, K., Karunan Partha, S., Davies, P., & Campbell, R. (2014). Allosteric inhibitors of calpains: Reevaluating inhibition by PD150606 and LSEAL. *Biochim Biophys Acta, 1840*(12), 3367-3373. doi:10.1016/j.bbagen.2014.08.014

Lu, X., Xiao, L., Wang, L., & Ruden, D. (2012). Hsp90 inhibitors and drug resistance in cancer: the potential benefits of combination therapies of Hsp90 inhibitors and other anti-cancer drugs. *Biochemical pharmacology, 83*(8), 995-1004.

Łukasiewicz, S., Czeczelewski, M., Forma, A., Baj, J., & Sitarz, R. (2021). Breast Cancer—Epidemiology, Risk Factors, Classification, Prognostic Markers, and Current Treatment Strategies—An Updated Review. Cancers 2021, 13, 4287: s Note: MDPI stays neutral with regard to jurisdictional claims in published ….

Luo, T., Yue, R., Hu, H., Zhou, Z., Yiu, K., Zhang, S., . . . Yu, Z. (2015). PD150606 protects against ischemia/reperfusion injury by preventing μ-calpain-induced mitochondrial apoptosis. *Arch Biochem Biophys, 586*, 1-9. doi:10.1016/j.abb.2015.06.005

Lv, M., Lv, M., Chen, L., Qin, T., Zhang, X., Liu, P., & Yang, J. (2015). Angiomotin promotes breast cancer cell proliferation and invasion. *Oncol Rep, 33*(4), 1938-1946. doi:10.3892/or.2015.3780

Lv , Y., Zhao, S., Han, J., Zheng, L., Yang, Z., & Zhao, L. (2015). Hypoxia-inducible factor-1α induces multidrug resistance protein in colon cancer. *Onco Targets Ther, 8*, 1941-1948. doi:10.2147/ott.s82835

MacLeod, J., Gao, Y., Hall, C., Muller, W., Gujral, T., & Greer, P. (2018). Genetic disruption of calpain-1 and calpain-2 attenuates tumorigenesis in mouse models of HER2+ breast cancer and sensitizes cancer cells to doxorubicin and lapatinib. *Oncotarget, 9*(70), 33382-33395. doi:10.18632/oncotarget.26078

Mahadevappa, R., Neves, H., Yuen, S., Bai, Y., McCrudden, C., Yuen, H., . . . Kwok, H. (2017). The prognostic significance of Cdc6 and Cdt1 in breast cancer. *Sci Rep, 7*(1), 985. doi:10.1038/s41598-017-00998-9

Maki, M., Bagci, H., Hamaguchi, Ueda, M., Murachi, T., & Hatanaka, M. (1989). Inhibition of calpain by a synthetic oligopeptide corresponding to an exon of the human calpastatin gene. *J Biol Chem, 264*(32), 18866-18869.

Maki, M., Takano, E., Osawa, T., Ooi, T., Murachi, T., & Hatanaka, M. (1988). Analysis of structure-function relationship of pig calpastatin by expression of mutated cDNAs in Escherichia coli. *J Biol Chem, 263*(21), 10254-10261.

Makki, J. (2015). Diversity of Breast Carcinoma: Histological Subtypes and Clinical Relevance. *Clin Med Insights Pathol, 8*, 23-31. doi:10.4137/CPath.S31563

Malhotra, G., Zhao, X., Band, H., & Band, V. (2010). Histological, molecular and functional subtypes of breast cancers. *Cancer Biol Ther, 10*(10), 955-960. doi:10.4161/cbt.10.10.13879

Mandic, A., Viktorsson, K., Strandberg, L., Heiden, T., Hansson, J., Linder, S., & Shoshan, M. (2002). Calpain-mediated Bid cleavage and calpain-independent Bak modulation: two separate pathways in cisplatin-induced apoptosis. *Mol Cell Biol, 22*(9), 3003-3013. doi:10.1128/mcb.22.9.3003-3013.2002

Martinez, J., Zhang, Z., Svetlov, S., Hayes, R., Wang, K., & Larner, S. (2010). Calpain and caspase processing of caspase-12 contribute to the ER stress-induced cell death pathway in differentiated PC12 cells. *Apoptosis, 15*(12), 1480-1493. doi:10.1007/s10495-010-0526-4

Martoni, A., Tomasi, L., Farabegoli, G., Giovannini, M., Monetti, N., Ganzina, F., & Pannuti, F. (1984). A phase II study of 4'-epi-doxorubicin plus cis-platinum in advanced solid tumors. *Eur J Cancer Clin Oncol, 20*(1), 11-17. doi:10.1016/0277-5379(84)90028-2

Mashino, K., Sadanaga, N., Tanaka, F., Yamaguchi, H., Nagashima, H., Inoue, H., . . . Mori, M. (2001). Expression of multiple cancer-testis antigen genes in gastrointestinal and breast carcinomas. *Br J Cancer, 85*(5), 713-720. doi:10.1054/bjoc.2001.1974

Maughan, K., Lutterbie, M., & Ham, P. (2010). Treatment of breast cancer. *Am Fam Physician, 81*(11), 1339-1346.

McCartney, C., MacLeod, J., Greer, P., & Davies, P. (2018). An easy-to-use FRET protein substrate to detect calpain cleavage in vitro and in vivo. *Biochim Biophys Acta Mol Cell Res, 1865*(2), 221-230. doi:10.1016/j.bbamcr.2017.10.013

Mellgren , R. (1997). Evidence for participation of a calpain-like cysteine protease in cell cycle progression through late G1 phase. *Biochem Biophys Res Commun, 236*(3), 555-558. doi:10.1006/bbrc.1997.7003

Mellgren, R., Lu, Q., Zhang, W., Lakkis, M., Shaw, E., & Mericle, M. (1996). Isolation of a Chinese hamster ovary cell clone possessing decreased mu-calpain content and a reduced proliferative growth rate. *J Biol Chem, 271*(26), 15568-15574. doi:10.1074/jbc.271.26.15568

Miao, X., Sun, T., Barletta, H., Mager, J., & Cui, W. (2020). Loss of RBBP4 results in defective inner cell mass, severe apoptosis, hyperacetylated histones and preimplantation lethality in mice†. *Biol Reprod, 103*(1), 13-23. doi:10.1093/biolre/ioaa046

Mikosik, A., Henc, I., Ruckemann-Dziurdzińska, K., Frąckowiak, J., Płoszyńska, A., Balcerska, A., . . . Witkowski, J. (2015). Increased μ-Calpain Activity in Blasts of Common B-Precursor Childhood Acute Lymphoblastic Leukemia Correlates with Their Lower Susceptibility to Apoptosis. *PLoS One, 10*(8), e0136615. doi:10.1371/journal.pone.0136615

Minami, Y., Emori, Y., Kawasaki, H., & Suzuki, K. (1987). E-F hand structure-domain of calcium-activated neutral protease (CANP) can bind Ca2+ ions. *J Biochem, 101*(4), 889-895. doi:10.1093/oxfordjournals.jbchem.a121956

Minotti, G., Menna, P., Salvatorelli, E., Cairo, G., & Gianni, L. (2004). Anthracyclines: molecular advances and pharmacologic developments in antitumor activity and cardiotoxicity. *Pharmacol Rev, 56*(2), 185-229. doi:10.1124/pr.56.2.6

Miyawaki, A. (2011). Development of probes for cellular functions using fluorescent proteins and fluorescence resonance energy transfer. *Annu Rev Biochem, 80*, 357-373. doi:10.1146/annurev-biochem-072909-094736

Mo, X., Chen, Q., Li, X., Zheng, M., Ke, D., Deng, W., . . . Cao, G. (2011). Suppression of NHE1 by small interfering RNA inhibits HIF-1α-induced angiogenesis in vitro via modulation of calpain activity. *Microvasc Res, 81*(2), 160-168. doi:10.1016/j.mvr.2010.12.004

Mogushkova, K., Vodolazhsky, D., Kutilin, D., & Kit, O. (2017). Comparative characteristics of the genes expression of cancer-testis antigens in tumor and non-tumor breast tissues. *Journal of Clinical Oncology, 35*(15_suppl), e23085-e23085. doi:10.1200/JCO.2017.35.15_suppl.e23085

Mohamed, A., Krajewski, K., Cakar, B., & Ma, C. (2013). Targeted therapy for breast cancer. *Am J Pathol, 183*(4), 1096-1112. doi:10.1016/j.ajpath.2013.07.005

Mohammed, R., Martin, S., Mahmmod, A., Macmillan, R., Green, A., Paish, E., & Ellis, I. (2011). Objective assessment of lymphatic and blood vascular invasion in lymph node-negative breast carcinoma: findings from a large case series with long-term follow-up. *J Pathol, 223*(3), 358-365. doi:10.1002/path.2810

Moldoveanu, T., Hosfield, C., Lim, D., Elce, J., Jia, Z., & Davies, P. (2002). A Ca(2+) switch aligns the active site of calpain. *Cell, 108*(5), 649-660. doi:10.1016/s0092-8674(02)00659-1

Moldoveanu, T., Jia, Z., & Davies, P. (2004). Calpain activation by cooperative Ca2+ binding at two non-EF-hand sites. *Journal of Biological Chemistry, 279*(7), 6106-6114.

Moleirinho, S., Guerrant, W., & Kissil, J. (2014). The Angiomotins--from discovery to function. *FEBS Lett, 588*(16), 2693-2703. doi:10.1016/j.febslet.2014.02.006

Morrow, M., White, J., Moughan, J., Owen, J., Pajack, T., Sylvester, J., . . . Winchester, D. (2001). Factors predicting the use of breast-conserving therapy in stage I and II breast carcinoma. *J Clin Oncol, 19*(8), 2254-2262. doi:10.1200/jco.2001.19.8.2254

Mukherjee, A., Huber, K., Evans, H., Lakhani, N., & Martin, S. (2007). A cellular and molecular investigation of the action of PMX464, a putative thioredoxin

inhibitor, in normal and colorectal cancer cell lines. *Br J Pharmacol, 151*(8), 1167-1175. doi:10.1038/sj.bjp.0707342

Murachi, T. (1989). Intracellular regulatory system involving calpain and calpastatin. *Biochem Int, 18*(2), 263-294.

Murray Brunt, A., Haviland, J., Wheatley, D., Sydenham, M., Alhasso, A., Bloomfield, D., . . . Yarnold, J. (2020). Hypofractionated breast radiotherapy for 1 week versus 3 weeks (FAST-Forward): 5-year efficacy and late normal tissue effects results from a multicentre, non-inferiority, randomised, phase 3 trial. *Lancet, 395*(10237), 1613-1626. doi:10.1016/s0140-6736(20)30932-6

Nabholtz, J., Falkson, C., Campos, D., Szanto, J., Martin, M., Chan, S., . . . Pouillart, P. (2003). Docetaxel and doxorubicin compared with doxorubicin and cyclophosphamide as first-line chemotherapy for metastatic breast cancer: results of a randomized, multicenter, phase III trial. *J Clin Oncol, 21*(6), 968-975. doi:10.1200/jco.2003.04.040

Nakagawa, K., Masumoto, H., Sorimachi, H., & Suzuki, K. (2001). Dissociation of m-calpain subunits occurs after autolysis of the N-terminus of the catalytic subunit, and is not required for activation. *J Biochem, 130*(5), 605-611. doi:10.1093/oxfordjournals.jbchem.a003025

Nakajima, E., Hammond, K., Rosales, J., Shearer, T., & Azuma, M. (2011). Calpain, not caspase, is the causative protease for hypoxic damage in cultured monkey retinal cells. *Invest Ophthalmol Vis Sci, 52*(10), 7059-7067. doi:10.1167/iovs.11-7497

Nanduri, J., Wang, N., Yuan, G., Khan, S., Souvannakitti, D., Peng, Y., . . . Prabhakar, N. (2009). Intermittent hypoxia degrades HIF-2alpha via calpains resulting in oxidative stress: implications for recurrent apnea-induced morbidities. *Proc Natl Acad Sci U S A, 106*(4), 1199-1204. doi:10.1073/pnas.0811018106

Neefjes, J., & Dantuma, N. (2004). Fluorescent probes for proteolysis: tools for drug discovery. *Nature Reviews Drug Discovery, 3*(1), 58-69.

Nemoto, T., Natarajan, N., Bedwani, R., Vana, J., & Murphy, G. (1983). Breast cancer in the medial half. Results of 1978 National Survey of the American College of Surgeons. *Cancer, 51*(8), 1333-1338. doi:10.1002/1097-0142(19830415)51:8<1333::aid-cncr2820510802>3.0.co;2-t

Nettersheim, J., Janel-Bintz, R., Kuhn, L., & Cordonnier, A. (2021). DNA polymerase η is a substrate for calpain: a possible mechanism for pol η retention in UV-induced replication foci. *J Cell Sci, 134*(13). doi:10.1242/jcs.258637

Neville, A., Bettelheim, R., Gelber, R., Säve-Söderbergh, J., Davis, B., Reed, R., . . . et al. (1992). Factors predicting treatment responsiveness and prognosis in node-negative breast cancer. The International (Ludwig) Breast Cancer Study Group. *J Clin Oncol, 10*(5), 696-705. doi:10.1200/jco.1992.10.5.696

Ng, J., & Shuryak, I. (2015). Minimizing second cancer risk following radiotherapy: current perspectives. *Cancer Manag Res, 7*, 1-11. doi:10.2147/cmar.s47220

Niapour, M., Farr, C., Minden, M., & Berger, S. (2012). Elevated calpain activity in acute myelogenous leukemia correlates with decreased calpastatin expression. *Blood Cancer J, 2*(1), e51. doi:10.1038/bcj.2011.50

NICE. (2018). Early and locally advanced breast cancer: diagnosis and management. Retrieved from https://www.nice.org.uk/guidance/ng101/chapter/Recommendations#radiotherapy

Nikjoo, H., Uehara, S., Wilson, W., Hoshi, M., & Goodhead, D. (1998). Track structure in radiation biology: theory and applications. *Int J Radiat Biol, 73*(4), 355-364. doi:10.1080/095530098142176

Nixon, A., Neuberg, D., Hayes, D., Gelman, R., Connolly, J., Schnitt, S., . . . Harris, J. (1994). Relationship of patient age to pathologic features of the tumor

and prognosis for patients with stage I or II breast cancer. *J Clin Oncol, 12*(5), 888-894. doi:10.1200/jco.1994.12.5.888

Nowak, A., Alfieri, C., Stirnimann, C., Rybin, V., Baudin, F., Ly-Hartig, N., . . . Müller, C. (2011). Chromatin-modifying complex component Nurf55/p55 associates with histones H3 and H4 and polycomb repressive complex 2 subunit Su(z)12 through partially overlapping binding sites. *J Biol Chem, 286*(26), 23388-23396. doi:10.1074/jbc.M110.207407

O'Sullivan, C., & Smith, K. (2014). Therapeutic Considerations in Treating HER2-Positive Metastatic Breast Cancer. *Curr Breast Cancer Rep, 6*(3), 169-182. doi:10.1007/s12609-014-0155-y

Ohno, S., Emori, Y., Imajoh, S., Kawasaki, H., Kisaragi, M., & Suzuki, K. (1984). Evolutionary origin of a calcium-dependent protease by fusion of genes for a thiol protease and a calcium-binding protein? *Nature, 312*(5994), 566-570. doi:10.1038/312566a0

Olivotto, I., Bajdik, C., Ravdin, P., Speers, C., Coldman, A., Norris, B., . . . Gelmon, K. (2005). Population-based validation of the prognostic model ADJUVANT! for early breast cancer. *J Clin Oncol, 23*(12), 2716-2725. doi:10.1200/jco.2005.06.178

Ono, Y., Ojima, K., Shinkai-Ouchi, F., Hata, S., & Sorimachi, H. (2016). An eccentric calpain, CAPN3/p94/calpain-3. *Biochimie, 122*, 169-187. doi:10.1016/j.biochi.2015.09.010

Orgéas, C., Hall, P., Rosenberg, L., & Czene, K. (2008). The influence of menstrual risk factors on tumor characteristics and survival in postmenopausal breast cancer. *Breast Cancer Res, 10*(6), R107. doi:10.1186/bcr2212

Oronsky, B., Knox, S., & Scicinski, J. (2011). Six degrees of separation: the oxygen effect in the development of radiosensitizers. *Transl Oncol, 4*(4), 189-198. doi:10.1593/tlo.11166

Ortmann, B., Druker, J., & Rocha, S. (2014). Cell cycle progression in response to oxygen levels. *Cell Mol Life Sci, 71*(18), 3569-3582. doi:10.1007/s00018-014-1645-9

Otake, S., & Goto, T. (2019). Stereotactic Radiotherapy for Oligometastasis. *Cancers (Basel), 11*(2). doi:10.3390/cancers11020133

Paik, S., Shak, S., Tang, G., Kim, C., Baker, J., Cronin, M., . . . Wolmark, N. (2004). A multigene assay to predict recurrence of tamoxifen-treated, node-negative breast cancer. *N Engl J Med, 351*(27), 2817-2826. doi:10.1056/NEJMoa041588

Pardoll, D. (2012). The blockade of immune checkpoints in cancer immunotherapy. *Nat Rev Cancer, 12*(4), 252-264. doi:10.1038/nrc3239

Pariat, M., Carillo, S., Molinari, M., Salvat, C., Debüssche, L., Bracco, L., . . . Piechaczyk, M. (1997). Proteolysis by calpains: a possible contribution to degradation of p53. *Mol Cell Biol, 17*(5), 2806-2815. doi:10.1128/mcb.17.5.2806

Parr, T., Sensky, P., Bardsley, R., & Buttery, P. (2001). Calpastatin expression in porcine cardiac and skeletal muscle and partial gene structure. *Arch Biochem Biophys, 395*(1), 1-13. doi:10.1006/abbi.2001.2546

Pawlik, T., & Keyomarsi, K. (2004). Role of cell cycle in mediating sensitivity to radiotherapy. *Int J Radiat Oncol Biol Phys, 59*(4), 928-942. doi:10.1016/j.ijrobp.2004.03.005

PCA. (2022). The PanCancer Atlas. Retrieved from https://www.cell.com/pb-assets/consortium/pancanceratlas/pancani3/index.html

Pearlman, A., Rahman, M., Upadhyay, K., Loke, J., & Ostrer, H. (2019). Ectopic Otoconin 90 expression in triple negative breast cancer cell lines is associated with metastasis functions. *PLoS One, 14*(2), e0211737. doi:10.1371/journal.pone.0211737

Pereira, B., Chin, S., Rueda, O., Vollan, H., Provenzano, E., Bardwell, H., . . . Caldas, C. (2016). The somatic mutation profiles of 2,433 breast cancers

refines their genomic and transcriptomic landscapes. *Nat Commun, 7*, 11479. doi:10.1038/ncomms11479

Perou, C., Sørlie, T., Eisen, M., van de Rijn, M., Jeffrey, S., Rees, C., . . . Botstein, D. (2000a). Molecular portraits of human breast tumours. *Nature, 406*(6797), 747-752. doi:10.1038/35021093

Perou, C., Sørlie, T., Eisen, M., van de Rijn, M., Jeffrey, S., Rees, C., . . . Botstein, D. (2000b). Molecular portraits of human breast tumours. *Nature, 406*(6797), 747-752. doi:10.1038/35021093

Peto, R., Davies, C., Godwin, J., Gray, R., Pan, H., Clarke, M., . . . Pritchard, K. (2012). Comparisons between different polychemotherapy regimens for early breast cancer: meta-analyses of long-term outcome among 100,000 women in 123 randomised trials. *Lancet, 379*(9814), 432-444. doi:10.1016/s0140-6736(11)61625-5

Pianetti, S., Arsura, M., Romieu-Mourez, R., Coffey, R., & Sonenshein, G. (2001). Her-2/neu overexpression induces NF-kappaB via a PI3-kinase/Akt pathway involving calpain-mediated degradation of IkappaB-alpha that can be inhibited by the tumor suppressor PTEN. *Oncogene, 20*(11), 1287-1299. doi:10.1038/sj.onc.1204257

Piccart-Gebhart, M., Procter, M., Leyland-Jones, B., Goldhirsch, A., Untch, M., Smith, I., . . . Gelber, R. (2005). Trastuzumab after adjuvant chemotherapy in HER2-positive breast cancer. *N Engl J Med, 353*(16), 1659-1672. doi:10.1056/NEJMoa052306

Pichot, C., Hartig, S., Xia, L., Arvanitis, C., Monisvais, D., Lee, F., . . . Corey, S. (2009). Dasatinib synergizes with doxorubicin to block growth, migration, and invasion of breast cancer cells. *Br J Cancer, 101*(1), 38-47. doi:10.1038/sj.bjc.6605101

Pierce, L., Fowble, B., Solin, L., Schultz, D., Rosser, C., & Goodman, R. (1992). Conservative surgery and radiation therapy in black women with early stage breast cancer. Patterns of failure and analysis of outcome. *Cancer, 69*(11), 2831-2841. doi:10.1002/1097-0142(19920601)69:11<2831::aid-cncr2820691132>3.0.co;2-j

Pilco-Ferreto, N., & Calaf, G. (2016). Influence of doxorubicin on apoptosis and oxidative stress in breast cancer cell lines. *Int J Oncol, 49*(2), 753-762. doi:10.3892/ijo.2016.3558

Pinto, Ades, F., de Azambuja, E., & Piccart-Gebhart, M. (2013). Trastuzumab for patients with HER2 positive breast cancer: delivery, duration and combination therapies. *Breast, 22 Suppl 2*, S152-155. doi:10.1016/j.breast.2013.07.029

Pinto , M., Prise, K., & Michael, B. (2005). Evidence for complexity at the nanometer scale of radiation-induced DNA DSBs as a determinant of rejoining kinetics. *Radiat Res, 164*(1), 73-85. doi:10.1667/rr3394

Plasilova, M., Hayse, B., Killelea, B., Horowitz, N., Chagpar, A., & Lannin, D. (2016). Features of triple-negative breast cancer: Analysis of 38,813 cases from the national cancer database. *Medicine (Baltimore), 95*(35), e4614. doi:10.1097/md.0000000000004614

Pomp, J., Wike, J., Ouwerkerk, I., Hoogstraten, C., Davelaar, J., Schrier, P., . . . Brock, W. (1996). Cell density dependent plating efficiency affects outcome and interpretation of colony forming assays. *Radiother Oncol, 40*(2), 121-125. doi:10.1016/0167-8140(96)01767-7

Pongor, L., Kormos, M., Hatzis, C., Pusztai, L., Szabó, A., & Győrffy, B. (2015). A genome-wide approach to link genotype to clinical outcome by utilizing next generation sequencing and gene chip data of 6,697 breast cancer patients. *Genome Med, 7*, 104. doi:10.1186/s13073-015-0228-1

Potter, C., & Harris, A. (2004). Hypoxia inducible carbonic anhydrase IX, marker of tumour hypoxia, survival pathway and therapy target. *Cell Cycle, 3*(2), 164-167.

Prat, A., Cheang, M., Martín, M., Parker, J., Carrasco, E., Caballero, R., . . . Perou, C. (2013). Prognostic significance of progesterone receptor-positive tumor cells within immunohistochemically defined luminal A breast cancer. *J Clin Oncol, 31*(2), 203-209. doi:10.1200/jco.2012.43.4134

Prentice, R., Chlebowski, R., Stefanick, M., Manson, J., Pettinger, M., Hendrix, S., . . . Anderson, G. (2008). Estrogen plus progestin therapy and breast cancer in recently postmenopausal women. *Am J Epidemiol, 167*(10), 1207-1216. doi:10.1093/aje/kwn044

Pu, X. (2016a). *Role of calpain in breast cancer and regulation of therapeutic response to targeted treatment.* (Doctoral thesis).

Pu , X., Storr, S., Ahmad, N., Chan, S., Moseley, P., Televantou, D., . . . Martin, S. (2016b). Calpain-1 is associated with adverse relapse free survival in breast cancer: a confirmatory study. *Histopathology, 68*(7), 1021-1029. doi:10.1111/his.12896

Puhalla, S., Bhattacharya, S., & Davidson, N. (2012). Hormonal therapy in breast cancer: a model disease for the personalization of cancer care. *Mol Oncol, 6*(2), 222-236. doi:10.1016/j.molonc.2012.02.003

Qian, Y., Wang, Y., Hollingsworth, R., Jones, D., Ling, N., & Lee, E. (1993). A retinoblastoma-binding protein related to a negative regulator of Ras in yeast. *Nature, 364*(6438), 648-652. doi:10.1038/364648a0

Rakha, E., Reis-Filho, J., Baehner, F., Dabbs, D., Decker, T., Eusebi, V., . . . Ellis, I. (2010). Breast cancer prognostic classification in the molecular era: the role of histological grade. *Breast Cancer Res, 12*(4), 207. doi:10.1186/bcr2607

Ran, F., Zhang, Y., Shi, Y., Liu, J., Li, H., Ding, L., & Ye, Q. (2021). miR-1224-3p Promotes Breast Cancer Cell Proliferation and Migration through PGM5-Mediated Aerobic Glycolysis. *Journal of Oncology, 2021*, 5529770. doi:10.1155/2021/5529770

Reis-Filho, J., Milanezi, F., Steele, D., Savage, K., Simpson, P., Nesland, J., . . . Schmitt, F. (2006). Metaplastic breast carcinomas are basal-like tumours. *Histopathology, 49*(1), 10-21. doi:10.1111/j.1365-2559.2006.02467.x

Reverter, D., Strobl, S., Fernandez-Catalan, C., Sorimachi, H., Suzuki, K., & Bode, W. (2001). Structural basis for possible calcium-induced activation mechanisms of calpains. *Biol Chem, 382*(5), 753-766. doi:10.1515/bc.2001.091

Ridolfi, R., Rosen, P., Port, A., Kinne, D., & Miké, V. (1977). Medullary carcinoma of the breast: a clinicopathologic study with 10 year follow-up. *Cancer, 40*(4), 1365-1385. doi:10.1002/1097-0142(197710)40:4<1365::aid-cncr2820400402>3.0.co;2-n

Rimawi, M., Schiff, R., & Osborne, C. (2015). Targeting HER2 for the treatment of breast cancer. *Annu Rev Med, 66*, 111-128. doi:10.1146/annurev-med-042513-015127

Rios-Doria, J., Day, K., Kuefer, R., Rashid, M., Chinnaiyan, A., Rubin, M., & Day, M. (2003). The role of calpain in the proteolytic cleavage of E-cadherin in prostate and mammary epithelial cells. *J Biol Chem, 278*(2), 1372-1379. doi:10.1074/jbc.M208772200

Rios-Doria, J., Kuefer, R., Ethier, S., & Day, M. (2004). Cleavage of beta-catenin by calpain in prostate and mammary tumor cells. *Cancer Res, 64*(20), 7237-7240. doi:10.1158/0008-5472.can-04-1048

Robertson, F., Bondy, M., Yang, W., Yamauchi, H., Wiggins, S., Kamrudin, S., . . . Cristofanilli, M. (2010). Inflammatory breast cancer: the disease, the biology, the treatment. *CA Cancer J Clin, 60*(6), 351-375. doi:10.3322/caac.20082

Robson, Im, S., Senkus, E., Xu, B., Domchek, S., Masuda, N., . . . Conte, P. (2017). Olaparib for Metastatic Breast Cancer in Patients with a Germline BRCA Mutation. *N Engl J Med, 377*(6), 523-533. doi:10.1056/NEJMoa1706450

Robson, Tung, N., Conte, P., Im, S., Senkus, E., Xu, B., . . . Domchek, S. (2019). OlympiAD final overall survival and tolerability results: Olaparib versus chemotherapy treatment of physician's choice in patients with a germline BRCA mutation and HER2-negative metastatic breast cancer. *Ann Oncol, 30*(4), 558-566. doi:10.1093/annonc/mdz012

Rockwell, S., Dobrucki, I., Kim, E., Marrison, S., & Vu, V. (2009). Hypoxia and radiation therapy: past history, ongoing research, and future promise. *Curr Mol Med, 9*(4), 442-458. doi:10.2174/156652409788167087

Rofstad, E. (2000). Microenvironment-induced cancer metastasis. *Int J Radiat Biol, 76*(5), 589-605. doi:10.1080/095530000138259

Romond, E., Perez, E., Bryant, J., Suman, V., Geyer, C., Davidson, N., . . . Wolmark, N. (2005). Trastuzumab plus adjuvant chemotherapy for operable HER2-positive breast cancer. *N Engl J Med, 353*(16), 1673-1684. doi:10.1056/NEJMoa052122

Rong, D., Dong, Q., Qu, H., Deng, X., Gao, F., Li, Q., & Sun, P. (2021). m6A-induced LINC00958 promotes breast cancer tumorigenesis via the miR-378a-3p/YY1 axis. *Cell Death Discovery, 7*(1), 27. doi:10.1038/s41420-020-00382-z

Roots, R., & Smith, K. (1974). On the nature of the oxygen effect on x-ray-induced DNA single-strand breaks in mammalian cells. *Int J Radiat Biol Relat Stud Phys Chem Med, 26*(5), 467-480. doi:10.1080/09553007414551491

Roperto, S., De Tullio, R., Raso, C., Stifanese, R., Russo, V., Gaspari, M., . . . Roperto, F. (2010). Calpain3 is expressed in a proteolitically active form in papillomavirus-associated urothelial tumors of the urinary bladder in cattle. *PLoS One, 5*(4), e10299. doi:10.1371/journal.pone.0010299

Rosen, P., Groshen, S., Kinne, D., & Norton, L. (1993). Factors influencing prognosis in node-negative breast carcinoma: analysis of 767 T1N0M0/T2N0M0 patients with long-term follow-up. *J Clin Oncol, 11*(11), 2090-2100. doi:10.1200/jco.1993.11.11.2090

Rosen, P., Groshen, S., Saigo, P., Kinne, D., & Hellman, S. (1989). Pathological prognostic factors in stage I (T1N0M0) and stage II (T1N1M0) breast carcinoma: a study of 644 patients with median follow-up of 18 years. *J Clin Oncol, 7*(9), 1239-1251. doi:10.1200/jco.1989.7.9.1239

Ross, J., & Fletcher, J. (1998). The HER-2/neu oncogene in breast cancer: prognostic factor, predictive factor, and target for therapy. *Stem Cells, 16*(6), 413-428. doi:10.1002/stem.160413

Rosser, B., Powers, S., & Gores, G. (1993). Calpain activity increases in hepatocytes following addition of ATP. Demonstration by a novel fluorescent approach. *J Biol Chem, 268*(31), 23593-23600.

Sadeghi, H., Golalipour, M., Yamchi, A., Farazmandfar, T., & Shahbazi, M. (2019). CDC25A pathway toward tumorigenesis: Molecular targets of CDC25A in cell-cycle regulation. *J Cell Biochem, 120*(3), 2919-2928. doi:10.1002/jcb.26838

Saez, R., McGuire, W., & Clark, G. (1989). Prognostic factors in breast cancer. *Semin Surg Oncol, 5*(2), 102-110. doi:10.1002/ssu.2980050206

Saidy, B., Kotecha, S., Butler, A., Rakha, E., Ellis, I., Green, A., . . . Storr, S. (2021). PP1, PKA and DARPP-32 in breast cancer: A retrospective assessment of protein and mRNA expression. *J Cell Mol Med, 25*(11), 5015-5024. doi:10.1111/jcmm.16447

Saidy, B., Rakha, E., Green, A., Ellis, I., Martin, S., & Storr, S. (2020). Retrospective assessment of cyclin-dependent kinase 5 mRNA and protein expression and its association with patient survival in breast cancer. *J Cell Mol Med, 24*(11), 6263-6271. doi:10.1111/jcmm.15268

Salehin, D., Fromberg, I., Haugk, C., Dohmen, B., Georg, T., Bohle, R., . . . Friedrich, M. (2010). Immunhistochemical analysis for expression of calpain 1, calpain 2 and calpastatin in endometrial cancer. *Anticancer Res, 30*(7), 2837-2843.

Salehin, D., Fromberg, I., Haugk, C., Dohmen, B., Georg, T., Bohle, R., . . . Friedrich, M. (2011). Immunhistochemical analysis for expression of calpain 1, calpain 2 and calpastatin in ovarian cancer. *Eur J Gynaecol Oncol, 32*(6), 628-635.

Sammut, S., Crispin-Ortuzar, M., Chin, S., Provenzano, E., Bardwell, H., Ma, W., . . . Caldas, C. (2022). Multi-omic machine learning predictor of breast cancer therapy response. *Nature, 601*(7894), 623-629. doi:10.1038/s41586-021-04278-5

Sang, T., Yang, J., Liu, J., Han, Y., Li, Y., Zhou, X., & Wang, X. (2021). AMOT suppresses tumor progression via regulating DNA damage response signaling in diffuse large B-cell lymphoma. *Cancer Gene Ther, 28*(10-11), 1125-1135. doi:10.1038/s41417-020-00258-5

Sankaranarayanan, R., Swaminathan, R., Brenner, H., Chen, K., Chia, K., Chen, J., . . . Al-Hamdan, N. (2010). Cancer survival in Africa, Asia, and Central America: a population-based study. *Lancet Oncol, 11*(2), 165-173. doi:10.1016/s1470-2045(09)70335-3

Santonja, A., Sánchez-Muñoz, A., Lluch, A., Chica-Parrado, M. R., Albanell, J., Chacón, J. I., . . . Alba, E. (2018). Triple negative breast cancer subtypes and pathologic complete response rate to neoadjuvant chemotherapy. *Oncotarget, 9*(41), 26406-26416. doi:10.18632/oncotarget.25413

Saphner, T., Tormey, D., & Albertini, M. (1991). Continuous infusion 5-fluorouracil with escalating doses of intermittent cisplatin and etoposide. A phase I study. *Cancer, 68*(11), 2359-2362. doi:10.1002/1097-0142(19911201)68:11<2359::aid-cncr2820681105>3.0.co;2-a

Saraiva, N., Prole, D., Carrara, G., Johnson, B., Taylor, C., Parsons, M., & Smith, G. (2013). hGAAP promotes cell adhesion and migration via the stimulation of store-operated Ca2+ entry and calpain 2. *J Cell Biol, 202*(4), 699-713. doi:10.1083/jcb.201301016

Sato, K., Minegishi, S., Takano, J., Plattner, F., Saito, T., Asada, A., . . . Hisanaga, S. (2011). Calpastatin, an endogenous calpain-inhibitor protein, regulates the cleavage of the Cdk5 activator p35 to p25. *J Neurochem, 117*(3), 504-515. doi:10.1111/j.1471-4159.2011.07222.x

Schmid, P., Cortes, J., Pusztai, L., McArthur, H., Kümmel, S., Bergh, J., . . . O'Shaughnessy, J. (2020a). Pembrolizumab for Early Triple-Negative Breast Cancer. *N Engl J Med, 382*(9), 810-821. doi:10.1056/NEJMoa1910549

Schmid, P., Rugo, H., Adams, S., Schneeweiss, A., Barrios, C., Iwata, H., . . . Emens, L. (2020b). Atezolizumab plus nab-paclitaxel as first-line treatment for unresectable, locally advanced or metastatic triple-negative breast cancer (IMpassion130): updated efficacy results from a randomised, double-blind, placebo-controlled, phase 3 trial. *Lancet Oncol, 21*(1), 44-59. doi:10.1016/s1470-2045(19)30689-8

Schütz, F., Stefanovic, S., Mayer, L., von Au, A., Domschke, C., & Sohn, C. (2017). PD-1/PD-L1 Pathway in Breast Cancer. *Oncol Res Treat, 40*(5), 294-297. doi:10.1159/000464353

Semenza, G. (2012). Hypoxia-inducible factors in physiology and medicine. *Cell, 148*(3), 399-408. doi:10.1016/j.cell.2012.01.021

Sensky, P., Jewell, K., Ryan, K., Parr, T., Bardsley, R., & Buttery, P. (2006). Effect of anabolic agents on calpastatin promoters in porcine skeletal muscle and their responsiveness to cyclic adenosine monophosphate- and calcium-related stimuli. *J Anim Sci, 84*(11), 2973-2982. doi:10.2527/jas.2006-073

Sergeev, I. (2004). Genistein induces Ca2+ -mediated, calpain/caspase-12-dependent apoptosis in breast cancer cells. *Biochem Biophys Res Commun, 321*(2), 462-467. doi:10.1016/j.bbrc.2004.06.173

Shao, H., Chou, J., Baty, C., Burke, N., Watkins, S., Stolz, D., & Wells, A. (2006). Spatial localization of m-calpain to the plasma membrane by phosphoinositide biphosphate binding during epidermal growth factor

receptor-mediated activation. *Mol Cell Biol, 26*(14), 5481-5496. doi:10.1128/mcb.02243-05

Shapovalov, I., Harper, D., & Greer, P. (2022). Calpain as a therapeutic target in cancer. *Expert Opin Ther Targets, 26*(3), 217-231.

Sharma, R. (2021). Global, regional, national burden of breast cancer in 185 countries: evidence from GLOBOCAN 2018. *Breast Cancer Res Treat, 187*(2), 557-567. doi:10.1007/s10549-020-06083-6

Shiovitz, S., & Korde, L. (2015). Genetics of breast cancer: a topic in evolution. *Ann Oncol, 26*(7), 1291-1299. doi:10.1093/annonc/mdv022

Shumway, S., Maki, M., & Miyamoto, S. (1999). The PEST domain of IkappaBalpha is necessary and sufficient for in vitro degradation by mu-calpain. *J Biol Chem, 274*(43), 30874-30881. doi:10.1074/jbc.274.43.30874

Siegel, R., Miller, K., Fuchs, H., & Jemal, A. (2021). Cancer Statistics, 2021. *CA Cancer J Clin, 71*(1), 7-33. doi:10.3322/caac.21654

Siklos, M., BenAissa, M., & Thatcher, G. (2015). Cysteine proteases as therapeutic targets: does selectivity matter? A systematic review of calpain and cathepsin inhibitors. *Acta Pharm Sin B, 5*(6), 506-519. doi:10.1016/j.apsb.2015.08.001

Skowronek, J., & Chicheł, A. (2014). Brachytherapy in breast cancer: an effective alternative. *Prz Menopauzalny, 13*(1), 48-55. doi:10.5114/pm.2014.41090

Skowronek, J., Wawrzyniak-Hojczyk, M., & Ambrochowicz, K. (2012). Brachytherapy in accelerated partial breast irradiation (APBI) - review of treatment methods. *J Contemp Brachytherapy, 4*(3), 152-164. doi:10.5114/jcb.2012.30682

Slamon, D., Eiermann, W., Robert, N., Pienkowski, T., Martin, M., Press, M., . . . Crown, J. (2011). Adjuvant trastuzumab in HER2-positive breast cancer. *N Engl J Med, 365*(14), 1273-1283. doi:10.1056/NEJMoa0910383

Small, G., Chou, T., Dang, C., & Orlowski, R. (2002). Evidence for involvement of calpain in c-Myc proteolysis in vivo. *Arch Biochem Biophys, 400*(2), 151-161. doi:10.1016/s0003-9861(02)00005-x

Smith , I., Dowsett, M., Ebbs, S., Dixon, J., Skene, A., Blohmer, J., . . . Walsh, G. (2005). Neoadjuvant treatment of postmenopausal breast cancer with anastrozole, tamoxifen, or both in combination: the Immediate Preoperative Anastrozole, Tamoxifen, or Combined with Tamoxifen (IMPACT) multicenter double-blind randomized trial. *J Clin Oncol, 23*(22), 5108-5116. doi:10.1200/jco.2005.04.005

Smith, I., Procter, M., Gelber, R., Guillaume, S., Feyereislova, A., Dowsett, M., . . . Piccart-Gebhart, M. (2007). 2-year follow-up of trastuzumab after adjuvant chemotherapy in HER2-positive breast cancer: a randomised controlled trial. *Lancet, 369*(9555), 29-36. doi:10.1016/s0140-6736(07)60028-2

Smith , I., & Talbot, D. (1992). Cisplatin and its analogues in the treatment of advanced breast cancer: a review. *Br J Cancer, 65*(6), 787-793. doi:10.1038/bjc.1992.169

Song, J., Miermont, A., Lim, C., & Kamm, R. (2018). A 3D microvascular network model to study the impact of hypoxia on the extravasation potential of breast cell lines. *Sci Rep, 8*(1), 17949. doi:10.1038/s41598-018-36381-5

Soong, G., Chun, J., Parker, D., & Prince, A. (2012). Staphylococcus aureus activation of caspase 1/calpain signaling mediates invasion through human keratinocytes. *J Infect Dis, 205*(10), 1571-1579. doi:10.1093/infdis/jis244

Sorimachi, H., Hata, S., & Ono, Y. (2010). Expanding members and roles of the calpain superfamily and their genetically modified animals. *Exp Anim, 59*(5), 549-566. doi:10.1538/expanim.59.549

Sørlie, T., Perou, C., Tibshirani, R., Aas, T., Geisler, S., Johnsen, H., . . . Børresen-Dale, A. (2001). Gene expression patterns of breast carcinomas distinguish tumor subclasses with clinical implications. *Proc Natl Acad Sci U S A, 98*(19), 10869-10874. doi:10.1073/pnas.191367098

Squìer, M., Miller, A., Malkinson, A., & Cohen, J. (1994). Calpain activation in apoptosis. *J Cell Physiol, 159*(2), 229-237. doi:10.1002/jcp.1041590206

Stein, R., Dunn, J., Bartlett, J., Campbell, A., Marshall, A., Hall, P., . . . Makris, A. (2016). OPTIMA prelim: a randomised feasibility study of personalised care in the treatment of women with early breast cancer. *Health Technol Assess, 20*(10), xxiii-xxix, 1-201. doi:10.3310/hta20100

Stifanese, R., Averna, M., De Tullio, R., Pedrazzi, M., Beccaria, F., Salamino, F., . . . Melloni, E. (2010). Adaptive modifications in the calpain/calpastatin system in brain cells after persistent alteration in Ca2+ homeostasis. *J Biol Chem, 285*(1), 631-643. doi:10.1074/jbc.M109.031674

Storr, S., Carragher, N., Frame, M., Parr, T., & Martin, S. (2011). The calpain system and cancer. *Nat Rev Cancer, 11*(5), 364-374. doi:10.1038/nrc3050

Storr, S., Carragher, N., Frame, M., Parr, T., & Martin, S. (2011a). The calpain system and cancer. *Nat Rev Cancer, 11*(5), 364-374. doi:10.1038/nrc3050

Storr, S., Lee, K., Woolston, C., Safuan, S., Green, A., Macmillan, R., . . . Martin, S. (2012a). Calpain system protein expression in basal-like and triple-negative invasive breast cancer. *Ann Oncol, 23*(9), 2289-2296. doi:10.1093/annonc/mds176

Storr, S., Mohammed, R., Woolston, C., Green, A., Parr, T., Spiteri, I., . . . Martin, S. (2011b). Calpastatin is associated with lymphovascular invasion in breast cancer. *Breast, 20*(5), 413-418. doi:10.1016/j.breast.2011.04.002

Storr, S., Pu, X., Davis, J., Lobo, D., Reece-Smith, A., Parsons, S., . . . Martin, S. (2013). Expression of the calpain system is associated with poor clinical outcome in gastro-oesophageal adenocarcinomas. *J Gastroenterol, 48*(11), 1213-1221. doi:10.1007/s00535-012-0743-4

Storr, S., Safuan, S., Woolston, C., Abdel-Fatah, T., Deen, S., Chan, S., & Martin, S. (2012). Calpain-2 expression is associated with response to platinum based chemotherapy, progression-free and overall survival in ovarian cancer. *J Cell Mol Med, 16*(10), 2422-2428. doi:10.1111/j.1582-4934.2012.01559.x

Storr, S., Safuan, S., Woolston, C., Abdel-Fatah, T., Deen, S., Chan, S., & Martin, S. (2012b). Calpain-2 expression is associated with response to platinum based chemotherapy, progression-free and overall survival in ovarian cancer. *J Cell Mol Med, 16*(10), 2422-2428. doi:10.1111/j.1582-4934.2012.01559.x

Storr, S., Thompson, N., Pu, X., Zhang, Y., & Martin, S. (2015). Calpain in Breast Cancer: Role in Disease Progression and Treatment Response. *Pathobiology, 82*(3-4), 133-141. doi:10.1159/000430464

Storr, S., Woolston, C., Barros, F., Green, A., Shehata, M., Chan, S., . . . Martin, S. (2011c). Calpain-1 expression is associated with relapse-free survival in breast cancer patients treated with trastuzumab following adjuvant chemotherapy. *Int J Cancer, 129*(7), 1773-1780. doi:10.1002/ijc.25832

Storr, S., Zaitoun, A., Arora, A., Durrant, L., Lobo, D., Madhusudan, S., & Martin, S. (2012c). Calpain system protein expression in carcinomas of the pancreas, bile duct and ampulla. *BMC Cancer, 12*, 511. doi:10.1186/1471-2407-12-511

Storr, S., Zhang, S., Perren, T., Lansdown, M., Fatayer, H., Sharma, N., . . . Martin, S. (2016). The calpain system is associated with survival of breast cancer patients with large but operable inflammatory and non-inflammatory tumours treated with neoadjuvant chemotherapy. *Oncotarget, 7*(30), 47927-47937. doi:10.18632/oncotarget.10066

Stricker, T., Brown, C., Bandlamudi, C., McNerney, M., Kittler, R., Montoya, V., . . . White, K. (2017). Robust stratification of breast cancer subtypes using differential patterns of transcript isoform expression. *PLoS Genet, 13*(3), e1006589. doi:10.1371/journal.pgen.1006589

Sukkarn, B. (2020). *Role of calpastatin isoforms in breast cancer lymphovascular invasion.* (Doctoral thesis).

Sun, L., Zhu, Y., Qian, Q., & Tang, L. (2018). Body mass index and prognosis of breast cancer: An analysis by menstruation status when breast cancer diagnosis. *Medicine (Baltimore), 97*(26), e11220. doi:10.1097/md.0000000000011220

Sung, H., Ferlay, J., Siegel, R., Laversanne, M., Soerjomataram, I., Jemal, A., & Bray, F. (2021). Global Cancer Statistics 2020: GLOBOCAN Estimates of Incidence and Mortality Worldwide for 36 Cancers in 185 Countries. *CA Cancer J Clin, 71*(3), 209-249. doi:10.3322/caac.21660

Suzuki, K., Hata, S., Kawabata, Y., & Sorimachi, H. (2004). Structure, Activation, and Biology of Calpain. *Diabetes, 53*(suppl_1), S12-S18. doi:10.2337/diabetes.53.2007.S12

Suzuki, K., Sorimachi, H., Yoshizawa, T., Kinbara, K., & Ishiura, S. (1995). Calpain: novel family members, activation, and physiologic function. *Biol Chem Hoppe Seyler, 376*(9), 523-529. doi:10.1515/bchm3.1995.376.9.523

Swain, S., Baselga, J., Kim, S., Ro, J., Semiglazov, V., Campone, M., . . . Cortés, J. (2015). Pertuzumab, trastuzumab, and docetaxel in HER2-positive metastatic breast cancer. *N Engl J Med, 372*(8), 724-734. doi:10.1056/NEJMoa1413513

Swinson, D., Jones, J., Richardson, D., Wykoff, C., Turley, H., Pastorek, J., . . . O'Byrne, K. (2003). Carbonic anhydrase IX expression, a novel surrogate marker of tumor hypoxia, is associated with a poor prognosis in non-small-cell lung cancer. *J Clin Oncol, 21*(3), 473-482. doi:10.1200/jco.2003.11.132

Tacar, O., Sriamornsak, P., & Dass, C. (2013). Doxorubicin: an update on anticancer molecular action, toxicity and novel drug delivery systems. *J Pharm Pharmacol, 65*(2), 157-170. doi:10.1111/j.2042-7158.2012.01567.x

Takano , E., & Murachi, T. (1982). Purification and Some Properties of Human Erythrocyte Calpastatin1. *The Journal of Biochemistry, 92*(6), 2021-2028. doi:10.1093/oxfordjournals.jbchem.a134134

Takano, J., Kawamura, T., Murase, M., Hitomi, K., & Maki, M. (1999). Structure of mouse calpastatin isoforms: implications of species-common and species-specific alternative splicing. *Biochem Biophys Res Commun, 260*(2), 339-345. doi:10.1006/bbrc.1999.0903

Takano, J., Watanabe, M., Hitomi, K., & Maki, M. (2000). Four types of calpastatin isoforms with distinct amino-terminal sequences are specified by alternative first exons and differentially expressed in mouse tissues. *J Biochem, 128*(1), 83-92. doi:10.1093/oxfordjournals.jbchem.a022733

Tan , S., & Wolff, A. (2007a). Luteinizing hormone-releasing hormone agonists in premenopausal hormone receptor-positive breast cancer. *Clin Breast Cancer, 7*(6), 455-464. doi:10.3816/CBC.2007.n.002

Tan, Y., Dourdin, N., Wu, C., De Veyra, T., Elce, J., & Greer, P. (2006). Ubiquitous calpains promote caspase-12 and JNK activation during endoplasmic reticulum stress-induced apoptosis. *J Biol Chem, 281*(23), 16016-16024. doi:10.1074/jbc.M601299200

TCGA, G. (2022). The Cancer Genome Atlas. Retrieved from https://portal.gdc.cancer.gov/

Te Boekhorst, V., Jiang, L., Mähler, M., Meerlo, M., Dunkel, G., Durst, F., . . . Friedl, P. (2022). Calpain-2 regulates hypoxia/HIF-induced plasticity toward amoeboid cancer cell migration and metastasis. *Curr Biol, 32*(2), 412-427.e418. doi:10.1016/j.cub.2021.11.040

Telli, M., Jensen, K., Vinayak, S., Kurian, A., Lipson, J., Flaherty, P., . . . Wapnir, I. (2015). Phase II study of gemcitabine, carboplatin, and iniparib as neoadjuvant therapy for triple-negative and BRCA1/2 mutation–associated breast cancer with assessment of a tumor-based measure of genomic instability: PrECOG 0105. *Journal of Clinical Oncology, 33*(17), 1895.

Terry, P., & Rohan, T. (2002). Cigarette smoking and the risk of breast cancer in women: a review of the literature. *Cancer Epidemiol Biomarkers Prev, 11*(10 Pt 1), 953-971.

Thompson, V., Goll, D., & Kleese, W. (1990). Effects of autolysis on the catalytic properties of the calpains. *Biol Chem Hoppe Seyler, 371 Suppl*, 177-185.

Thor, A., Liu, S., Moore, D. n., & Edgerton, S. (1999). Comparison of mitotic index, in vitro bromodeoxyuridine labeling, and MIB-1 assays to quantitate proliferation in breast cancer. *J Clin Oncol, 17*(2), 470-477. doi:10.1200/jco.1999.17.2.470

Titus-Ernstoff, L., Longnecker, M., Newcomb, P., Dain, B., Greenberg, E., Mittendorf, R., . . . Willett, W. (1998). Menstrual factors in relation to breast cancer risk. *Cancer Epidemiol Biomarkers Prev, 7*(9), 783-789.

Todd, B., Moore, D., Deivanayagam, C., Lin, G., Chattopadhyay, D., Maki, M., . . . Narayana, S. (2003). A structural model for the inhibition of calpain by calpastatin: crystal structures of the native domain VI of calpain and its complexes with calpastatin peptide and a small molecule inhibitor. *J Mol Biol, 328*(1), 131-146. doi:10.1016/s0022-2836(03)00274-2

Tolaney, S., Wardley, A., Zambelli, S., Hilton, J., Troso-Sandoval, T., Ricci, F., . . . André, F. (2020). Abemaciclib plus trastuzumab with or without fulvestrant versus trastuzumab plus standard-of-care chemotherapy in women with hormone receptor-positive, HER2-positive advanced breast cancer (monarcHER): a randomised, open-label, phase 2 trial. *Lancet Oncol, 21*(6), 763-775. doi:10.1016/s1470-2045(20)30112-1

Tompa, P., Buzder-Lantos, P., Tantos, A., Farkas, A., Szilágyi, A., Banoczi, Z., . . . Friedrich, P. (2004). On the sequential determinants of calpain cleavage. *Journal of Biological Chemistry, 279*(20), 20775-20785.

Tompa, P., Emori, Y., Sorimachi, H., Suzuki, K., & Friedrich, P. (2001). Domain III of calpain is a ca2+-regulated phospholipid-binding domain. *Biochem Biophys Res Commun, 280*(5), 1333-1339. doi:10.1006/bbrc.2001.4279

Trudeau, M., Chapman, J., Guo, B., Clemons, M., Dent, R., Jong, R., . . . Parissenti, A. (2015). A phase I/II trial of epirubicin and docetaxel in locally advanced breast cancer (LABC) on 2-weekly or 3-weekly schedules: NCIC CTG MA.22. *Springerplus, 4*, 631. doi:10.1186/s40064-015-1392-x

Trump, D., Ettinger, D., & Abeloff, M. (1981). Doxorubicin, vincristine, and cis-diamminedichloroplatinum (II) therapy in patients with advanced breast cancer. *Med Pediatr Oncol, 9*(1), 1-3. doi:10.1002/mpo.2950090102

Tsujinaka, T., Kajiwara, Y., Kambayashi, J., Sakon, M., Higuchi, N., Tanaka, T., & Mori, T. (1988). Synthesis of a new cell penetrating calpain inhibitor (calpeptin). *Biochem Biophys Res Commun, 153*(3), 1201-1208. doi:10.1016/s0006-291x(88)81355-x

Turk, B., Huang, L., Piro, E., & Cantley, L. (2001). Determination of protease cleavage site motifs using mixture-based oriented peptide libraries. *Nature biotechnology, 19*(7), 661-667.

Tyas, L., Brophy, V., Pope, A., Rivett, J., & Tavaré, J. (2000). Rapid caspase-3 activation during apoptosis revealed using fluorescence-resonance energy transfer. *EMBO reports, 1*(3), 266-270.

Uemori, T., Shimojo, T., Asada, K., Asano, T., Kimizuka, F., Kato, I., . . . et al. (1990). Characterization of a functional domain of human calpastatin. *Biochem Biophys Res Commun, 166*(3), 1485-1493. doi:10.1016/0006-291x(90)91035-q

Ursin, G., Bernstein, L., Lord, S., Karim, R., Deapen, D., Press, M., . . . Spirtas, R. (2005). Reproductive factors and subtypes of breast cancer defined by hormone receptor and histology. *Br J Cancer, 93*(3), 364-371. doi:10.1038/sj.bjc.6602712

Vaidya, J., Bulsara, M., Baum, M., Wenz, F., Massarut, S., Pigorsch, S., . . . Tobias, J. (2020). Long term survival and local control outcomes from single dose targeted intraoperative radiotherapy during lumpectomy (TARGIT-IORT) for

early breast cancer: TARGIT-A randomised clinical trial. *Bmj, 370*, m2836. doi:10.1136/bmj.m2836

Vaidya, J., Joseph, D., Tobias, J., Bulsara, M., Wenz, F., Saunders, C., . . . Baum, M. (2010). Targeted intraoperative radiotherapy versus whole breast radiotherapy for breast cancer (TARGIT-A trial): an international, prospective, randomised, non-inferiority phase 3 trial. *Lancet, 376*(9735), 91-102. doi:10.1016/s0140-6736(10)60837-9

Van Ba, H., & Inho, H. (2013). Significant role of μ-calpain (CANP1) in proliferation/survival of bovine skeletal muscle satellite cells. *In Vitro Cell Dev Biol Anim, 49*(10), 785-797. doi:10.1007/s11626-013-9666-5

Van den Eynden, G., Van der Auwera, I., Van Laere, S., Colpaert, C., Turley, H., Harris, A., . . . Van Marck, E. (2005). Angiogenesis and hypoxia in lymph node metastases is predicted by the angiogenesis and hypoxia in the primary tumour in patients with breast cancer. *Br J Cancer, 93*(10), 1128-1136. doi:10.1038/sj.bjc.6602828

van der Leij, F., Bosma, S., van de Vijver, M., Wesseling, J., Vreeswijk, S., Rivera, S., . . . Elkhuizen, P. (2015). First results of the preoperative accelerated partial breast irradiation (PAPBI) trial. *Radiother Oncol, 114*(3), 322-327. doi:10.1016/j.radonc.2015.02.002

Vaupel, P., & Mayer, A. (2007). Hypoxia in cancer: significance and impact on clinical outcome. *Cancer Metastasis Rev, 26*(2), 225-239. doi:10.1007/s10555-007-9055-1

Vaupel, P., Mayer, A., Briest, S., & Höckel, M. (2005). Hypoxia in breast cancer: role of blood flow, oxygen diffusion distances, and anemia in the development of oxygen depletion. *Adv Exp Med Biol, 566*, 333-342. doi:10.1007/0-387-26206-7_44

Vaupel, P., Schlenger, K., Knoop, C., & Höckel, M. (1991). Oxygenation of human tumors: evaluation of tissue oxygen distribution in breast cancers by computerized O2 tension measurements. *Cancer Res, 51*(12), 3316-3322.

Verma, S., Miles, D., Gianni, L., Krop, I., Welslau, M., Baselga, J., . . . Blackwell, K. (2012). Trastuzumab emtansine for HER2-positive advanced breast cancer. *N Engl J Med, 367*(19), 1783-1791. doi:10.1056/NEJMoa1209124

Vermaak, D., Wade, P., Jones, P., Shi, Y., & Wolffe, A. (1999). Functional analysis of the SIN3-histone deacetylase RPD3-RbAp48-histone H4 connection in the Xenopus oocyte. *Mol Cell Biol, 19*(9), 5847-5860. doi:10.1128/mcb.19.9.5847

Vinh-Hung, V., & Verschraegen, C. (2004). Breast-conserving surgery with or without radiotherapy: pooled-analysis for risks of ipsilateral breast tumor recurrence and mortality. *J Natl Cancer Inst, 96*(2), 115-121. doi:10.1093/jnci/djh013

Vo, T., Burchett, R., Brun, M., Monckton, E., Poon, H., & Godbout, R. (2019). Effects of nuclear factor I phosphorylation on calpastatin (CAST) gene variant expression and subcellular distribution in malignant glioma cells. *J Biol Chem, 294*(4), 1173-1188. doi:10.1074/jbc.RA118.004787

Vosler, P., Brennan, C., & Chen, J. (2008). Calpain-mediated signaling mechanisms in neuronal injury and neurodegeneration. *Mol Neurobiol, 38*(1), 78-100. doi:10.1007/s12035-008-8036-x

Waks, A., & Winer, E. (2019). Breast Cancer Treatment: A Review. *Jama, 321*(3), 288-300. doi:10.1001/jama.2018.19323

Wang, Hui, T., Wang, M., Liu, H., Li, R., & Song, Z. (2019c). Body Mass Index at Diagnosis as a Prognostic Factor for Early-Stage Invasive Breast Cancer after Surgical Resection. *Oncol Res Treat, 42*(4), 195-201. doi:10.1159/000496548

Wang , Nath, R., Posner, A., Raser, K., Buroker-Kilgore, M., Hajimohammadreza, I., . . . Yuen, P. (1996). An alpha-mercaptoacrylic acid derivative is a selective nonpeptide cell-permeable calpain inhibitor and is neuroprotective. *Proc Natl Acad Sci U S A, 93*(13), 6687-6692. doi:10.1073/pnas.93.13.6687

Wang , Rosales, J., Magliocco, A., Gnanakumar, R., & Lee, K. (2003). Cyclin E in breast tumors is cleaved into its low molecular weight forms by calpain. *Oncogene, 22*(5), 769-774. doi:10.1038/sj.onc.1206166

Wang, Wang, W., Mao, W., Kuerbantayi, N., Jia, N., Chen, Y., . . . Wang, Y. (2021). RBBP4 Enhances Platinum Chemo Resistance in Lung Adenocarcinoma. *Biomed Res Int, 2021*, 6905985. doi:10.1155/2021/6905985

Wang, Xu, H., Chen, W., Cheng, M., Zou, L., Yang, Q., . . . Jiao, B. (2022). Rab13 sustains breast cancer stem cells by supporting tumor-stroma crosstalk. *Cancer Res*. doi:10.1158/0008-5472.can-21-4097

Wang , B., Zheng, J., Li, R., Tian, Y., Lin, J., Liang, Y., . . . Yuan, Y. (2019a). Long noncoding RNA LINC02582 acts downstream of miR-200c to promote radioresistance through CHK1 in breast cancer cells. *Cell Death & Disease, 10*(10), 764. doi:10.1038/s41419-019-1996-0

Wang, D., Jiang, Z., Ben-David, Y., Woodgett, J., & Zacksenhaus, E. (2019b). Molecular stratification within triple-negative breast cancer subtypes. *Sci Rep, 9*(1), 19107. doi:10.1038/s41598-019-55710-w

Watanabe, N., Okochi, E., Mochizuki, M., Sugimura, T., & Ushijima, T. (2001). The presence of single nucleotide instability in human breast cancer cell lines. *Cancer Res, 61*(21), 7739-7742.

Wei, W., Zou, Y., Jiang, Q., Zhou, Z., Ding, H., Yan, L., & Yang, S. (2018). PSMB5 is associated with proliferation and drug resistance in triple-negative breast cancer. *Int J Biol Markers, 33*(1), 102-108. doi:10.5301/ijbm.5000283

Weigelt, B., Baehner, F., & Reis-Filho, J. (2010a). The contribution of gene expression profiling to breast cancer classification, prognostication and prediction: a retrospective of the last decade. *J Pathol, 220*(2), 263-280. doi:10.1002/path.2648

Weigelt, B., Geyer, F., & Reis-Filho, J. (2010b). Histological types of breast cancer: how special are they? *Mol Oncol, 4*(3), 192-208. doi:10.1016/j.molonc.2010.04.004

Weigelt, B., & Reis-Filho, J. (2009). Histological and molecular types of breast cancer: is there a unifying taxonomy? *Nat Rev Clin Oncol, 6*(12), 718-730. doi:10.1038/nrclinonc.2009.166

Wells, A., Grahovac, J., Wheeler, S., Ma, B., & Lauffenburger, D. (2013). Targeting tumor cell motility as a strategy against invasion and metastasis. *Trends Pharmacol Sci, 34*(5), 283-289. doi:10.1016/j.tips.2013.03.001

Wendt, A., Thompson, V., & Goll, D. (2004). Interaction of calpastatin with calpain: a review. *Biol Chem, 385*(6), 465-472. doi:10.1515/bc.2004.054

Wenger, C., & Clark, G. (1998). S-phase fraction and breast cancer--a decade of experience. *Breast Cancer Res Treat, 51*(3), 255-265. doi:10.1023/a:1006188512927

Williams, A., Sarkar, S., Cuddon, P., Ttofi, E., Saiki, S., Siddiqi, F., . . . Goldsmith, P. (2008). Novel targets for Huntington's disease in an mTOR-independent autophagy pathway. *Nature chemical biology, 4*(5), 295-305.

Wishart, G., Azzato, E., Greenberg, D., Rashbass, J., Kearins, O., Lawrence, G., . . . Pharoah, P. (2010). PREDICT: a new UK prognostic model that predicts survival following surgery for invasive breast cancer. *Breast Cancer Res, 12*(1), R1. doi:10.1186/bcr2464

Witherby, S., Rizack, T., Sakr, B., Legare, R., & Sikov, W. (2016). Advances in Medical Management of Early Stage and Advanced Breast Cancer: 2015. *Semin Radiat Oncol, 26*(1), 59-70. doi:10.1016/j.semradonc.2015.09.005

Wood, D., Thomas, A., Devi, L., Berman, Y., Beavis, R., Reed, J., & Newcomb, E. (1998). Bax cleavage is mediated by calpain during drug-induced apoptosis. *Oncogene, 17*(9), 1069-1078. doi:10.1038/sj.onc.1202034

Woolston, C., & Martin, S. (2011). Analysis of tumor and endothelial cell viability and survival using sulforhodamine B and clonogenic assays. *Methods Mol Biol, 740*, 45-56. doi:10.1007/978-1-61779-108-6_7

Wu, A., Loutherback, K., Lambert, G., Estévez-Salmerón, L., Tlsty, T., Austin, R., & Sturm, J. (2013). Cell motility and drug gradients in the emergence of resistance to chemotherapy. *Proc Natl Acad Sci U S A, 110*(40), 16103-16108. doi:10.1073/pnas.1314385110

Xie, W., Sun, Y., Zeng, Y., Hu, L., Zhi, J., Ling, H., . . . Gao, M. (2022). Comprehensive analysis of PPPCs family reveals the clinical significance of PPP1CA and PPP4C in breast cancer. *Bioengineered, 13*(1), 190-205. doi:10.1080/21655979.2021.2012316

Xu , & Deng, X. (2006a). Protein kinase Ciota promotes nicotine-induced migration and invasion of cancer cells via phosphorylation of micro- and m-calpains. *J Biol Chem, 281*(7), 4457-4466. doi:10.1074/jbc.M510721200

Xu, Gu, J., Lu, C., Mao, W., Wang, L., Zhu, Q., . . . Ge, D. (2019). Calpain-2 Enhances Non-Small Cell Lung Cancer Progression and Chemoresistance to Paclitaxel via EGFR-pAKT Pathway. *Int J Biol Sci, 15*(1), 127-137. doi:10.7150/ijbs.28834

Xu , Wei, Q., Guo, J., Zhou, J., Mei, J., Jiang, Z., . . . Wang, L. (2015a). FOXA1 Expression Significantly Predict Response to Chemotherapy in Estrogen Receptor-Positive Breast Cancer Patients. *Ann Surg Oncol, 22*(6), 2034-2039. doi:10.1245/s10434-014-4313-2

Xu , L., & Deng, X. (2006b). Suppression of cancer cell migration and invasion by protein phosphatase 2A through dephosphorylation of mu- and m-calpains. *J Biol Chem, 281*(46), 35567-35575. doi:10.1074/jbc.M607702200

Ye, X., Liu, Z., Wang, J., Dai, J., Qiao, P., Gao, P., & Liao, W. (2021). YWHAG Mutations Cause Childhood Myoclonic Epilepsy and Febrile Seizures: Molecular Sub-regional Effect and Mechanism. *Front Genet, 12*, 632466. doi:10.3389/fgene.2021.632466

Yersal, O., & Barutca, S. (2014). Biological subtypes of breast cancer: Prognostic and therapeutic implications. *World J Clin Oncol, 5*(3), 412-424. doi:10.5306/wjco.v5.i3.412

Yildirim, E., Dalgiç, T., & Berberoğlu, U. (2000). Prognostic significance of young age in breast cancer. *J Surg Oncol, 74*(4), 267-272.

Youlden, D., Cramb, S., Dunn, N., Muller, J., Pyke, C., & Baade, P. (2012). The descriptive epidemiology of female breast cancer: an international comparison of screening, incidence, survival and mortality. *Cancer Epidemiol, 36*(3), 237-248. doi:10.1016/j.canep.2012.02.007

Yousefi, S., Perozzo, R., Schmid, I., Ziemiecki, A., Schaffner, T., Scapozza, L., . . . Simon, H. (2006). Calpain-mediated cleavage of Atg5 switches autophagy to apoptosis. *Nat Cell Biol, 8*(10), 1124-1132. doi:10.1038/ncb1482

Yue, H., Meng, F., Qian, J., Xu, B., Li, G., & Wu, J. (2019). Calpastatin participates in the regulation of cell migration in BAP1-deficient uveal melanoma cells. *Int J Ophthalmol, 12*(11), 1680-1687. doi:10.18240/ijo.2019.11.03

Zhang, Gu, J., Li, L., Liu, J., Luo, B., Cheung, H., . . . Bommi-Reddy, A. (2009). Control of cyclin D1 and breast tumorigenesis by the EglN2 prolyl hydroxylase. *Cancer Cell, 16*(5), 413-424. doi:10.1016/j.ccr.2009.09.029

Zhang, Lane, R., & Mellgren, R. (1996). The major calpain isozymes are long-lived proteins. Design of an antisense strategy for calpain depletion in cultured cells. *J Biol Chem, 271*(31), 18825-18830. doi:10.1074/jbc.271.31.18825

Zhang, Liu, N., Wang, Y., Youn, J., & Cai, H. (2017). Endothelial cell calpain as a critical modulator of angiogenesis. *Biochim Biophys Acta Mol Basis Dis, 1863*(6), 1326-1335. doi:10.1016/j.bbadis.2017.03.021

Zhang, Lu, Q., Xie, Z., & Mellgren, R. (1997). Inhibition of the growth of WI-38 fibroblasts by benzyloxycarbonyl-Leu-Leu-Tyr diazomethyl ketone: evidence that cleavage of p53 by a calpain-like protease is necessary for G1 to S-phase transition. *Oncogene, 14*(3), 255-263. doi:10.1038/sj.onc.1200841

Zhang , Ng, H., Erdjument-Bromage, H., Tempst, P., Bird, A., & Reinberg, D. (1999). Analysis of the NuRD subunits reveals a histone deacetylase core

complex and a connection with DNA methylation. *Genes Dev, 13*(15), 1924-1935. doi:10.1101/gad.13.15.1924

Zhang , Patel, J., & Block, E. (1998). Hypoxia-specific upregulation of calpain activity and gene expression in pulmonary artery endothelial cells. *Am J Physiol, 275*(3), L461-468. doi:10.1152/ajplung.1998.275.3.L461

Zhang, Storr, S., Johnson, K., Green, A., Rakha, E., Ellis, I., . . . Martin, S. (2014). Involvement of metformin and AMPK in the radioresponse and prognosis of luminal versus basal-like breast cancer treated with radiotherapy. *Oncotarget, 5*(24), 12936-12949. doi:10.18632/oncotarget.2683

Zhang, S. (2018). *Calpain in ovarian cancer progression and chemotherapeutic response.* (PhD), University of Nottingham.

Zhang , S., Liu, X., Abdulmomen Ali Mohammed, S., Li, H., Cai, W., Guan, W., . . . Wang, H. (2021). Adaptor SH3BGRL drives autophagy-mediated chemoresistance through promoting PIK3C3 translation and ATG12 stability in breast cancers. *Autophagy*, 1-19. doi:10.1080/15548627.2021.2002108

Zheng, Zhou, A., Rouhi, P., Uramoto, H., Borén, J., Cao, Y., . . . Poellinger, L. (2014). Hypoxia-induced and calpain-dependent cleavage of filamin A regulates the hypoxic response. *Proc Natl Acad Sci U S A, 111*(7), 2560-2565. doi:10.1073/pnas.1320815111

Zheng , L., Tang, W., Wei, F., Wang, H., Liu, J., Lu, Y., . . . Zhao, W. (2013). Radiation-inducible protein RbAp48 contributes to radiosensitivity of cervical cancer cells. *Gynecol Oncol, 130*(3), 601-608. doi:10.1016/j.ygyno.2013.06.002

Zhou, Y., Li, Z., Wu, X., Tou, L., Zheng, J., & Zhou, D. (2020). MAGOH/MAGOHB Inhibits the Tumorigenesis of Gastric Cancer via Inactivation of b-RAF/MEK/ERK Signaling. *Onco Targets Ther, 13*, 12723-12735. doi:10.2147/ott.s263913

Zhu , L., Li, X., Zeng, R., & Gorodeski, G. (2006). Changes in tight junctional resistance of the cervical epithelium are associated with modulation of content and phosphorylation of occludin 65-kilodalton and 50-kilodalton forms. *Endocrinology, 147*(2), 977-989. doi:10.1210/en.2005-0916

Zhu, Y., Chen, G., Song, Y., Chen, Z., & Chen, X. (2020). POLE2 knockdown reduce tumorigenesis in esophageal squamous cells. *Cancer Cell Int, 20*, 388. doi:10.1186/s12935-020-01477-4

Zubair, M., Wang, S., & Ali, N. (2020). Advanced Approaches to Breast Cancer Classification and Diagnosis. *Front Pharmacol, 11*, 632079. doi:10.3389/fphar.2020.632079

Appendix A: Supplementary information for Chapter 2

A1.1 MDA-MB-231 and T47D DT and PE

Growth curves were constructed by plotting total cell number against time (Figure A1.1a). The doubling times were 23.4±1.6 hours and 39.3±0.36 hours for MDA-MB-231 and T47D cells respectively. To perform clonogenic assay, MDA-MB-231 and T47D cells were seeded in low densities and allowed to grow colonies. The plating efficiencies were 50±4.0% and 18.3±1.6% for MDA-MB-231 and T47D cell lines, respectively (Figure A1.1b). The DTs and PEs obtained are similar to the data previously generated in the lab, (Aiyappa, 2020) as well as previously published in the literature (Lagadec *et al.*, 2012; Watanabe *et al.*, 2001)

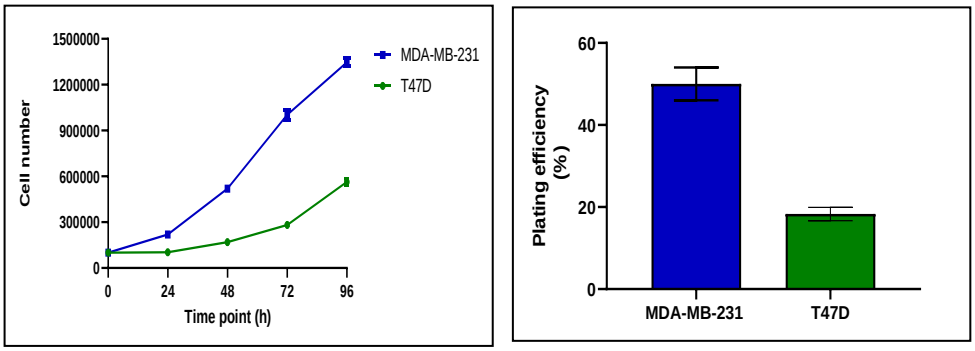

A **B**

Figure A1.1 Growth curves and plating efficiencies of breast cancer cell lines. (A) Growth curves for T47D and MDA-MB-231 cell lines. Cells were allowed to grow and counted over 96 hours. The graphs were used to calculate the cell doubling times. (B) Plating efficiencies for T47D and MDA-MB-231 cell lines. Analyses for each cell lines were performed independently. Data represents mean values ± SD of three independent experiments conducted in triplicates.

Table A1.1 doubling times for T47D and MDA-MB-231 cell lines.

Cell line	Doubling time (hours)
T47D	39.3±0.36
MDA-MB-231	23.4±1.6

A1.2 HA-tagged calpastatin isoform sequence and plasmid map

The calpastatin type I, type II and type III DNA constructs were designed by Dr. K. Jewell form Professor T. Parr's group, University of Nottingham. Calpastatin types I, II and III cDNA genes were cloned on to the HA-tagged, GFP removed, pZsGreen1-N1 plasmids in the high efficiency JM109 *E.coli* cells by Dr. K. Jewell. Calpastatin type I, calpastatin type II and calpastatin type III sequences and the plasmid maps are presented in sections B2.2.1, B2.2.2, B2.2.3 and B2.2.4

A1.2.1 Sequence for calpastatin type I

ATGTCCCAGCCCGGCCAGAAGCCCGCCGCCTCCCCGCGGCCCCGGCGA
GCAGCCGCCGCCCGCCGCACCCATGAGCATGTCAGTGAAAAAACCAGT
GAATCGCCTTCCAAACCAGGAGAAAAGAAAGGATCAGATGAGAAAAAAG
CAGCAAGCCTCGGCAGCAGTCAATCCTCCAGAACCTATGCTGGTGGAAC
AGCCTCGGCCACCAAGGTGTCAGCTTCCTCTGGTGCAACCAGCAAGTCT
TCCAGTATGAATCCCACAGAAACCAAGGCCATTCCAGTCAGCCAACAGA
TGGAAGGACCACATCTTCCTAACAAGAAAAAACACAAAAAACAGGCTGTA
AAAACAGAACCTGAGAAGAAGTCACAGTCAACCAAGCTGTCTGTGGTTC
ATGAGAAAAAATCCCAAGAAGGAAAGCCAAAAGAACACACAGAGCCAAA
AAGCCTACCCAAGCAGGCATCAGATACAGGAAGTAACGATGCTCACAAT
AAAAAAGCAGTTTCCAGATCAGCTGAACAGCAGCCATCAGAGAAATCAA
CAGAACCAAAGACTAAACCACAAGACATGATTTCTGCTGGTGGAGAGAG
TGTTGCTGGTATCACTGCAATATCTGGCAAGCCGGGTGACAAGAAAAAA
GAAAAGAAATCATTAACCCCAGCTGTGCCAGTTGAATCTAAACCGGATAA
ACCATCGGGAAAGTCAGGCATGGATGCTGCTTTGGATGACTTAATAGAT
ACTTTAGGAGGACCTGAAGAAACTGAAGAAGAAAATACAACGTATACTG
GACCAGAAGTTTCAGATCCAATGAGTTCCACCTACATAGAGGAATTGGG
TAAAAGAGAAGTCACAATTCCTCCAAAATATAGGGAACTATTGGCTAAAA
AGGAAGGGATCACAGGGCCTCCTGCAGACTCTTCGAAACCCATAGGGCC
AGATGATGCTATAGACGCCTTGTCATCTGACTTCACCTGTGGGTCGCCTA
CAGCTGCTGGAAAGAAAACTGAAAAAGAGGAATCTACAGAAGTTTTAAA
AGCTCAGTCAGCAGGGACAGTCAGAAGTGCTGCTCCACCCCAAGAGAAG
AAAAGAAAGGTGGAGAAGGATACAATGAGTGATCAAGCACTCGAGGCTC
TGTCGGCTTCACTGGGCACCCGGCAAGCAGAACCTGAGCTCGACCTCCG
CTCAATTAAGGAAGTCGATGAGGCAAAAGCTAAAGAAGAAAAACTAGAG
AAGTGTGGTGAGGATGATGAAACAATCCCATCTGAGTACAGATTAAAAC
CAGCCACGGATAAAGATGGAAAACCACTATTGCCAGAGCCTGAAGAAAA
ACCCAAGCCTCGGAGTGAATCAGAACTCATTGATGAACTTTCAGAAGATT
TTGACCGGTCTGAATGTAAAGAGAAACCATCTAAGCCAACTGAAAAGAC
AGAAGAATCTAAGGCCGCTGCTCCAGCTCCTGTGTCGGAGGCTGTGTGT
CGGACCTCCATGTGTAGTATACAGTCAGCACCCCCTGAGCCGGCTACCT
TGAAGGGCACAGTGCCAGATGATGCTGTAGAAGCCTTGGCTGATAGCCT

GGGGAAAAAGGAAGCAGATCCAGAAGATGGAAAACCTGTGATGGATAA
AGTCAAGGAGAAGGCCAAAGAAGAAGACCGTGAAAAGCTTGGTGAAAA
AGAAGAAACAATTCCTCCTGATTATAGATTAGAAGAGGTCAAGGATAAAG
ATGGAAAGCCACTCCTGCCAAAAGAGTCTAAGGAACAGCTTCCACCCAT
GAGTGAAGACTTCCTTCTGGATGCTTTGTCTGAGGACTTCTCTGGTCCAC
AAAATGCTTCATCTCTTAAATTTGAAGATGCTAAACTTGCTGCTGCCATCT
CTGAAGTGGTTTCCCAAACCCCAGCTTCAACGACCCAAGCTGGAGCCCC
ACCCCGTGATACCTCGCAGAGTGACAAAGACCTCGATGATGCCTTGGAT
AAACTCTCTGACAGTCTAGGACAAAGGCAGCCTGACCCAGATGAGAACA
AACCAATGGAAGATAAAGTAAAGGAAAAAGCTAAAGCTGAACATAGAGA
CAAGCTTGGAGAAAGAGATGACACTATCCCACCTGAATACAGACATCTCC
TGGATGATAATGGACAGGACAAACCAGTGAAGCCACCTACAAAGAAATC
AGAGGATTCAAAGAAACCTGCAGATGACCAAGACCCCATTGATGCTCTC
TCAGGAGATCTGGACAGCTGTCCCTCCACTACAGAAACCTCACAGAACA
CAGCAAAGGATAAGTGCAAGAAGGCTGCTTCCAGCTCCAAAGCACCTAA
GAATGGAGGTAAAGCGAAGGATTCAGCAAAGACAACAGAGGAAACTTCC
AAGCCAAAAGATGACGGTGGTGGTGGTGGTGGTTACCCATACGATGTTC
CAGATTACGCT

Note: Glycine linker, HA tag

A1.2.2 Sequence for calpastatin type II

ATGGCATTCGCCAGCTGGTGGTACAAGACGCATGTCAGTGAAAAAACCA
GTGAATCGCCTTCCAAACCAGGAGAAAAGAAAGGATCAGATGAGAAAAA
AGCAGCAAGCCTCGGCAGCAGTCAATCCTCCAGAACCTATGCTGGTGGA
ACAGCCTCGGCCACCAAGGTGTCAGCTTCCTCTGGTGCAACCAGCAAGT
CTTCCAGTATGAATCCCACAGAAACCAAGGCCATTCCAGTCAGCCAACA
GATGGAAGGACCACATCTTCCTAACAAGAAAAAACACAAAAAACAGGCT
GTAAAAACAGAACCTGAGAAGAAGTCACAGTCAACCAAGCTGTCTGTGG
TTCATGAGAAAAAATCCCAAGAAGGAAAGCCAAAAGAACACACAGAGCC
AAAAAGCCTACCCAAGCAGGCATCAGATACAGGAAGTAACGATGCTCAC
AATAAAAAAGCAGTTTCCAGATCAGCTGAACAGCAGCCATCAGAGAAAT
CAACAGAACCAAAGACTAAACCACAAGACATGATTTCTGCTGGTGGAGA
GAGTGTTGCTGGTATCACTGCAATATCTGGCAAGCCGGGTGACAAGAAA
AAAGAAAAGAAATCATTAACCCCAGCTGTGCCAGTTGAATCTAAACCGGA
TAAACCATCGGGAAAGTCAGGCATGGATGCTGCTTTGGATGACTTAATA
GATACTTTAGGAGGACCTGAAGAAACTGAAGAAGAAAATACAACGTATA
CTGGACCAGAAGTTTCAGATCCAATGAGTTCCACCTACATAGAGGAATTG
GGTAAAAGAGAAGTCACAATTCCTCCAAAATATAGGGAACTATTGGCTAA
AAAGGAAGGGATCACAGGGCCTCCTGCAGACTCTTCGAAACCCATAGGG
CCAGATGATGCTATAGACGCCTTGTCATCTGACTTCACCTGTGGGTCGCC
TACAGCTGCTGGAAAGAAAACTGAAAAAGAGGAATCTACAGAAGTTTTAA
AAGCTCAGTCAGCAGGGACAGTCAGAAGTGCTGCTCCACCCCAAGAGAA
GAAAAGAAAGGTGGAGAAGGATACAATGAGTGATCAAGCACTCGAGGCT
CTGTCGGCTTCACTGGGCACCCGGCAAGCAGAACCTGAGCTCGACCTCC
GCTCAATTAAGGAAGTCGATGAGGCAAAAGCTAAAGAAGAAAAACTAGA
GAAGTGTGGTGAGGATGATGAAACAATCCCATCTGAGTACAGATTAAAA

CCAGCCACGGATAAAGATGGAAAACCACTATTGCCAGAGCCTGAAGAAA
AACCCAAGCCTCGGAGTGAATCAGAACTCATTGATGAACTTTCAGAAGAT
TTTGACCGGTCTGAATGTAAAGAGAAACCATCTAAGCCAACTGAAAAGAC
AGAAGAATCTAAGGCCGCTGCTCCAGCTCCTGTGTCGGAGGCTGTGTGT
CGGACCTCCATGTGTAGTATACAGTCAGCACCCCCTGAGCCGGCTACCT
TGAAGGGCACAGTGCCAGATGATGCTGTAGAAGCCTTGGCTGATAGCCT
GGGGAAAAAGGAAGCAGATCCAGAAGATGGAAAACCTGTGATGGATAA
AGTCAAGGAGAAGGCCAAAGAAGAAGACCGTGAAAAGCTTGGTGAAAA
AGAAGAAACAATTCCTCCTGATTATAGATTAGAAGAGGTCAAGGATAAAG
ATGGAAAGCCACTCCTGCCAAAAGAGTCTAAGGAACAGCTTCCACCCAT
GAGTGAAGACTTCCTTCTGGATGCTTTGTCTGAGGACTTCTCTGGTCCAC
AAAATGCTTCATCTCTTAAATTTGAAGATGCTAAACTTGCTGCTGCCATCT
CTGAAGTGGTTTCCCAAACCCCAGCTTCAACGACCCAAGCTGGAGCCCC
ACCCCGTGATACCTCGCAGAGTGACAAAGACCTCGATGATGCCTTGGAT
AAACTCTCTGACAGTCTAGGACAAAGGCAGCCTGACCCAGATGAGAACA
AACCAATGGAAGATAAAGTAAAGGAAAAAGCTAAAGCTGAACATAGAGA
CAAGCTTGGAGAAAGAGATGACACTATCCCACCTGAATACAGACATCTCC
TGGATGATAATGGACAGGACAAACCAGTGAAGCCACCTACAAAGAAATC
AGAGGATTCAAAGAAACCTGCAGATGACCAAGACCCCATTGATGCTCTC
TCAGGAGATCTGGACAGCTGTCCCTCCACTACAGAAACCTCACAGAACA
CAGCAAAGGATAAGTGCAAGAAGGCTGCTTCCAGCTCCAAAGCACCTAA
GAATGGAGGTAAAGCGAAGGATTCAGCAAAGACAACAGAGGAAACTTCC
AAGCCAAAAGATGAC**GGTGGTGGTGGTGGTGGT**TACCCATACGATGTTC
CAGATTACGCT

Note: Glycine linker, HA tag

A1.2.3 Sequence for calpastatin type III

ATGAATCCCACAGAAACCAAGGCCATTCCAGTCAGCCAACAGATGGAAG
GACCACATCTTCCTAACAAGAAAAAACACAAAAAACAGGCTGTAAAAACA
GAACCTGAGAAGAAGTCACAGTCAACCAAGCTGTCTGTGGTTCATGAGA
AAAAATCCCAAGAAGGAAAGCCAAAAGAACACACAGAGCCAAAAAGCCT
ACCCAAGCAGGCATCAGATACAGGAAGTAACGATGCTCACAATAAAAAA
GCAGTTTCCAGATCAGCTGAACAGCAGCCATCAGAGAAATCAACAGAAC
CAAAGACTAAACCACAAGACATGATTTCTGCTGGTGGAGAGAGTGTTGC
TGGTATCACTGCAATATCTGGCAAGCCGGGTGACAAGAAAAAAGAAAAG
AAATCATTAACCCCAGCTGTGCCAGTTGAATCTAAACCGGATAAACCATC
GGGAAAGTCAGGCATGGATGCTGCTTTGGATGACTTAATAGATACTTTA
GGAGGACCTGAAGAAACTGAAGAAGAAAATACAACGTATACTGGACCAG
AAGTTTCAGATCCAATGAGTTCCACCTACATAGAGGAATTGGGTAAAAGA
GAAGTCACAATTCCTCCAAAATATAGGGAACTATTGGCTAAAAAGGAAG
GGATCACAGGGCCTCCTGCAGACTCTTCGAAACCCATAGGGCCAGATGA
TGCTATAGACGCCTTGTCATCTGACTTCACCTGTGGGTCGCCTACAGCTG
CTGGAAAGAAAACTGAAAAAGAGGAATCTACAGAAGTTTTAAAAGCTCA
GTCAGCAGGGACAGTCAGAAGTGCTGCTCCACCCCAAGAGAAGAAAAG
AAAGGTGGAGAAGGATACAATGAGTGATCAAGCACTCGAGGCTCTGTCG
GCTTCACTGGGCACCCGGCAAGCAGAACCTGAGCTCGACCTCCGCTCAA
TTAAGGAAGTCGATGAGGCAAAAGCTAAAGAAGAAAAACTAGAGAAGTG

TGGTGAGGATGATGAAACAATCCCATCTGAGTACAGATTAAAACCAGCC
ACGGATAAAGATGGAAAACCACTATTGCCAGAGCCTGAAGAAAAACCCA
AGCCTCGGAGTGAATCAGAACTCATTGATGAACTTTCAGAAGATTTTGAC
CGGTCTGAATGTAAAGAGAAACCATCTAAGCCAACTGAAAAGACAGAAG
AATCTAAGGCCGCTGCTCCAGCTCCTGTGTCGGAGGCTGTGTGTCGGAC
CTCCATGTGTAGTATACAGTCAGCACCCCCTGAGCCGGCTACCTTGAAG
GGCACAGTGCCAGATGATGCTGTAGAAGCCTTGGCTGATAGCCTGGGG
AAAAAGGAAGCAGATCCAGAAGATGGAAAACCTGTGATGGATAAAGTCA
AGGAGAAGGCCAAAGAAGAAGACCGTGAAAAGCTTGGTGAAAAAGAAG
AAACAATTCCTCCTGATTATAGATTAGAAGAGGTCAAGGATAAAGATGGA
AAGCCACTCCTGCCAAAAGAGTCTAAGGAACAGCTTCCACCCATGAGTG
AAGACTTCCTTCTGGATGCTTTGTCTGAGGACTTCTCTGGTCCACAAAAT
GCTTCATCTCTTAAATTTGAAGATGCTAAACTTGCTGCTGCCATCTCTGAA
GTGGTTTCCCAAACCCCAGCTTCAACGACCCAAGCTGGAGCCCCACCCC
GTGATACCTCGCAGAGTGACAAAGACCTCGATGATGCCTTGGATAAACT
CTCTGACAGTCTAGGACAAAGGCAGCCTGACCCAGATGAGAACAAACCA
ATGGAAGATAAAGTAAAGGAAAAAGCTAAAGCTGAACATAGAGACAAGC
TTGGAGAAAGAGATGACACTATCCCACCTGAATACAGACATCTCCTGGAT
GATAATGGACAGGACAAACCAGTGAAGCCACCTACAAAGAAATCAGAGG
ATTCAAAGAAACCTGCAGATGACCAAGACCCCATTGATGCTCTCTCAGGA
GATCTGGACAGCTGTCCCTCCACTACAGAAACCTCACAGAACACAGCAA
AGGATAAGTGCAAGAAGGCTGCTTCCAGCTCCAAAGCACCTAAGAATGG
AGGTAAAGCGAAGGATTCAGCAAAGACAACAGAGGAAACTTCCAAGCCA
AAAGATGACGGTGGTGGTGGTGGTGGTTACCCATACGATGTTCCAGATT
ACGCT

Note: Glycine linker, HA tag

A1.2.4 Plasmid map

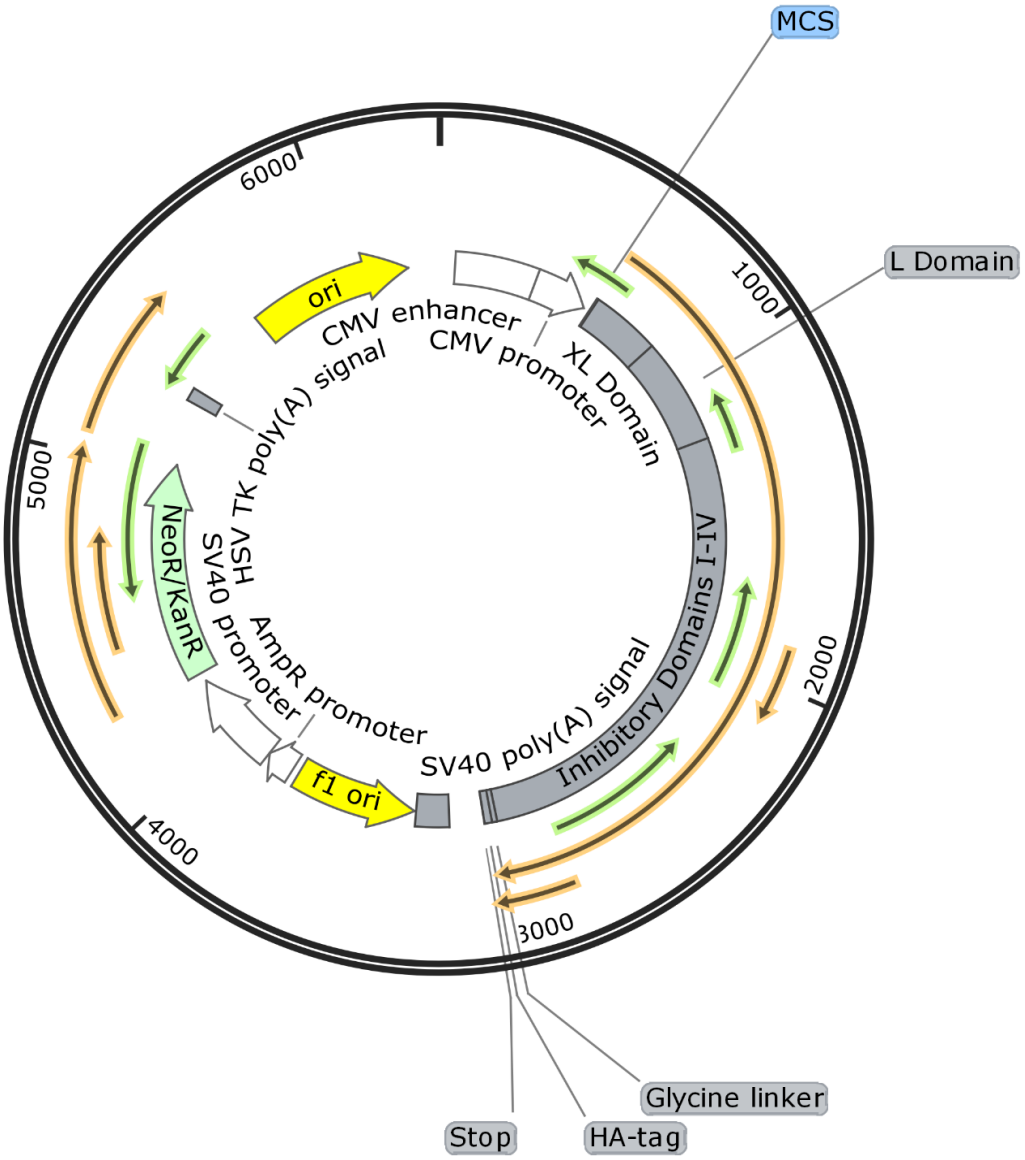

A1.3 HA-tagged calpastatin type II expression in T47D clones

Table A1.2 Table showing the number of T47D clones taken through single cell cloning.

Cells seeded in	Number of clones in Plate 1	Number of clones in Plate 2	Number of clones in Plate 3
96-well plate	22	16	21
48-well plate	18	10	15
24-well plate	10	7	12
12-well plate	9	7	8
6-well plate	9	7	6
T-25 cm^2 flask	5	4	3
T-75 cm^2 flask	3	2	3
T-175 cm^2 flask	3	2	3

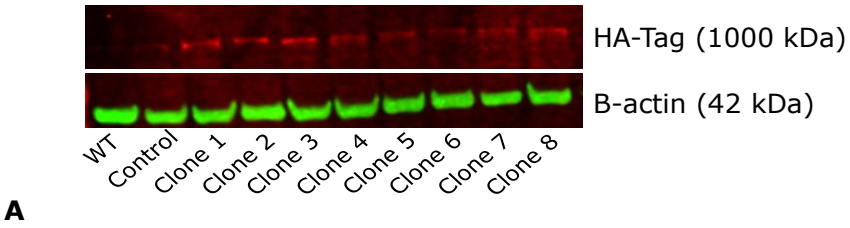

A

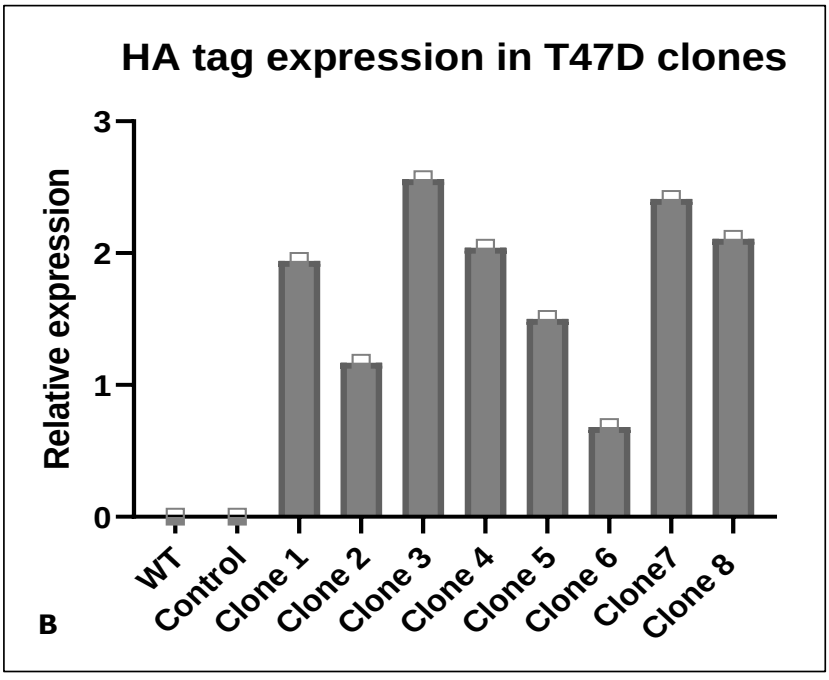

B

Figure A1.2 Expression of HA-tagged CAST II in T47D clones. (A) Representative blot showing expression of HA-tagged CAST II (red bands, ~100 kDa) expression in T47D clones. B-actin was used as a loading control (green bands, 42 kDa). (B) Quantitative analysis of HA-tagged CAST II expression relative to B-actin expression.

A1.4 HA-tagged calpastatin type III expression in MDA-MB-231 clones

Table A1.3 Table showing the number of MDA-MB-231 clones taken through single cell cloning.

Cells seeded in	No. of clones	
	1:1.5 dilution	1:3 dilution
96-well plate	50	50
48-well plate	22	24
24-well plate	18	20
12-well plate	15	12
6-well plate	12	12
T-25 cm^2 flask	10	12
T-75 cm^2 flask	5	5
T-175 cm^2 flask	5	5

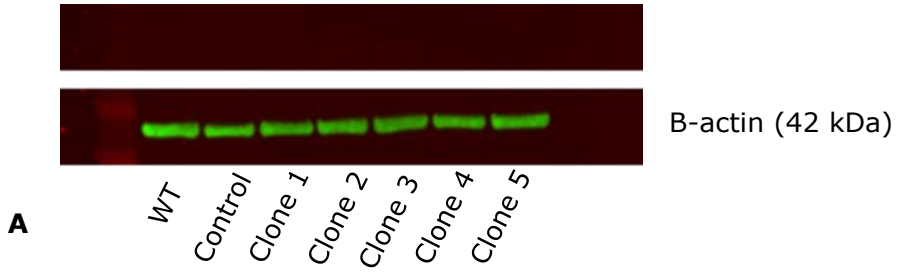

A

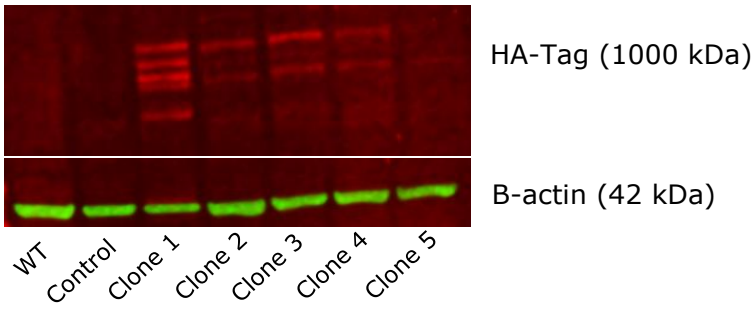

B



C

Figure A1.3 Expression of HA-tagged CAST III in MDA-MB-231 clones. (A) Representative blot from lysates prepared from clones transfected with 1:1.5 DNA: transfection reagent. No HA-tagged bands were observed. B-actin was used as a loading control (green bands, 42 kDa). (B) Representative blot showing expression of HA-tagged CAST III (1:3 DNA: transfection reagen) (red bands, ~100 kDa) expression in MDA-MB-231 clones. B-actin was used as a loading control (green bands, 42 kDa). (C) Quantitative analysis of HA-tagged CAST III expression relative to B-actin expression.

A1.5 Top 10 affected pathways

A1.5.1 Top 10 inhibited and activated pathways by calpastatin type I DEGs in T47D cells

Top 10 inhibited signalling pathways	Pathway enrichment p-value	z-score
RHOGDI signalling	2.13E-02	-2.03
Estrogen mediated S-phase entry	3.72E-02	-1.508
Complement system	4.24E-03	-1.387
Cyclins and cell cycle regulation	4.52E-02	-1.147
Eicosanoid signalling	4.69E-03	-1.069
Melanoma signalling	3.2E-02	-1.069
Calcium signalling	4E-02	-1.061
Estrogen dependent breast cancer signalling	2.84E-02	-1
Ovarian cancer signalling	7.2E-02	-0.943
UVA-induced MAPK signalling	3.77E-02	-0.728

Top 10 activated signalling pathways	Pathway enrichment p-value	z-score
Osteoarthritis pathway	2.63E-04	2.832
Cholecystokinin/Gastrin-mediated signalling	4E-02	2.828
Inhibition of angiogenesis by TSP1	1.01E-02	2.714
Wound healing signalling pathway	2.02E-05	2.712
PI3K/AKT signalling	9.28E-05	2.667
Pulmonary fibrosis idiopathic signalling pathway	2.34E-09	2.518
Senescence pathway	4.69E-03	2.458
Tumour microenvironment pathway	1.111E-04	2.433
Cardiac hypertrophy signalling (Enhanced)	7.51E-06	2.324
Hepatic fibrosis signalling pathway	1.76E-08	2.292

A1.5.2 Top 10 inhibited and activated pathways by calpastatin type II DEGs in T47D cells

Top 10 inhibited signalling pathways	Pathway enrichment p-value	z-score
Neuropathic pain signalling in dorsal horn neurons	1.4E-02	-2.874
GPCR-mediated nutrient sensing in enteroendocrine cells	2.71E-03	-2.343
Synaptogenesis signalling pathway	7.13E-05	-2.178
CDK5 signalling	7.52E-05	-2.137
G beta gamma signalling	1.28E-02	-2.082
Mouse embryonic stem cell pluripotency	1.32E-02	-1.915
PPARα/RXRα activation	1.19E-02	-1.896
Netrin signalling	2.08E-02	-1.877
PI3K signalling in B lymphocytes	1.19E-02	-1.852
Synaptic long term depression	3.61-03	-1.838

Top 10 activated signalling pathways	Pathway enrichment p-value	z-score
PD-1, PD-L1 cancer immunotherapy pathway	2.69E-02	3.024
Apelin adipocyte signalling pathway	2.51E-02	2.646
Inhibition of angiogenesis by TSP1	1.13E-03	2.496
PI3K/AKT signalling	4.16E-05	2.287
ILK signalling	3.6E-05	2.255
LPS/IL-1 mediated inhibition of RXR function	2.57E-02	1.964
Pancreatic adenocarcinoma signalling	1.94E-04	1.826
Paxillin signalling	2.81E-03	1.732
Endoplasmic reticulum stress pathway	3.8E-03	1.732
Apelin endothelial signalling pathway	2.12E-02	1.622

A1.5.3 Top 10 inhibited and activated pathways by CAST type III DEGs in T47D cells

Top 10 inhibited signalling pathways	Pathway enrichment p-value	z-score
Cyclins and cell cycle regulation	2.41E-04	-2.502
CDK5 signalling	2.61E-02	-1.633
Apelin cardiac fibroblast signalling pathway	2.01E-02	-1.265
Cell cycle regulation by BTG family proteins	6.55E-03	-1.265
Estrogen-mediated S-phase entry	1.7E-03	-1.155
Aryl hydrocarbon receptor signalling	1.3E-02	-0.756
Sermaphorin neuronal repulsive signalling pathway	5.23E-04	-0.745
Sperm motility	2.6E-02	-0.728
WNT/β-catenin signalling	3.56E-06	-0.603
PTEN signalling	2.89E-03	-0.507

Top 10 activated signalling pathways	Pathway enrichment p-value	z-score
Role of hypercytokinemia /hyperchemokinemia in the pathogenesis of influenza	3.56E-03	4.914
Wound healing signalling pathway	6.74E-05	4.565
Tumour microenvironment pathway	7.99E-05	3.742
Neuroinflammation signalling pathway	1.81E-02	3.654
Interferon signalling	1.24E-02	3.606
Pulmonary fibrosis idiopathic signalling pathway	4.96E-08	3.435
Neuroprotective role of THOP1 in Alzheimer's disease	4.62E-02	3.273
PAK signalling	8.61E-03	3.138
ILK signalling	3.56E-03	3
PI3K/AKT signalling	2.81E-04	3

A1.5.4 Top 10 inhibited and activated pathways by CAST type I DEGs in MDA-MB-231 cells

Top 10 inhibited signalling pathways	Pathway enrichment p-value	z-score
Netrin signaling	4.65E-02	-1.941
Wound healing signalling pathway	1.66E-06	-1.571
Senescence pathway	5.64E-03	-1.333
Tumour microenvironment pathway	7.68E-03	-1.3
Cell cycle: G2/M DNA damage checkpoint regulation	4.99E-02	-1.265
IL-17 signalling	4.66E-02	-1.177
MYC mediated apoptosis signalling	1.07E-02	-1.155
Osteoarthiritis pathway	2.53E-04	-1.061
VDR/RXR Activation	7.5E-04	-0.905
Sirtuin signalling pathway	4.66E-02	-0.898

Top 10 activated signalling pathways	Pathway enrichment p-value	z-score
Integrin signalling	1.77E-02	2.117
Cell cycle control of chromosomal replication	4.65E-02	2.111
HMG1 signalling	1.66E-02	1.698
Macropinocytosis signalling	3.8E-03	1.508
Fcy receptor-mediated phagocytosis in macrophages and monocytes	5.62E-03	1.414
Paxillin signalling	3.31E-02	1.387
Apoptosis signalling	4.54E-02	1.291
G-protein coupled receptor signalling	4.76E-02	1.254
PAK signalling	1.84E-02	1.069
Role of PKR in inteferon induction and antiviral response	3.75E-02	1

A1.5.5 Top 10 inhibited and activated pathways by CAST type II DEGs in MDA-MB-231 cells

Top 10 inhibited signalling pathways	Pathway enrichment p-value	z-score
STAT3 pathway	1.47E-04	-1.89
Factors promoting cardiogenesis in vertebrates	9.61E-03	-1.715
Sumoylation pathway	3.2E-02	-1.606
Role of pattern receptors in recognition of bacteria and virusses	9.5E-03	-1.606
Reelin signalling in neurons	4.69E-02	-1.569
Role of PKR in interferon induction and antiviral response	4.02E-02	-1.225
Inhibition of matrix metalloproteases	1.45E-02	-1.155
Breast cancer regulation by Stathmin 1	1.87E-02	-1.106
Cell cycle: G1/S checkpoint regulation	2.76E-02	-1.069
Erythropoetin signalling pathway	3.79E-02	-1.029

Top 10 activated signalling pathways	Pathway enrichment p-value	z-score
Endoplasmic reticulum stress pathway	1.27E-02	2.121
Leukocyte extravasaion signalling	3.2E-02	1.859
Unfolded protein response	1.45E-02	1.604
Necroptosis signalling pathway	4.77E-02	1.414
RHOGDI signalling	9.5E-03	1.372
HMGB1 signalling	1.25E-02	1.225
Cholecystokinin/Gastrin-mediated signalling	4.22E-02	1.091
Autophagy	1.41E-03	1.021
Role of NFAT in cardiac hypertrophy	4.88E-02	0.667
Osteoarthritis pathway	1.02E-05	0.59

A1.5.6 Top 10 inhibited and activated pathways by CAST type III DEGs in MDA-MB-231 cells

Top 10 inhibited signalling pathways	Pathway enrichment p-value	z-score
CREB signalling in Neurons	1.27E-03	-5.051
Pulmonary Fibrosis Idiopathic Signalling pathway	1.25E-04	-4.417
Coronavirus pathogenesis pathway	1.03E-07	-4.318
Wound healing signalling pathway	6.56E-03	-4.276
Neuroinflammation signalling pathway	1.25E-04	-3.713
TREM1 signalling	2.59E-03	-3.545
Phagosome formation	1.33E-02	-3.536
Pyroptosis signalling pathway	1.37E-04	-3.413
Hepatic fibrosis signalling pathway	4.89E-04	-3.362
Acute phase response signalling	1.3E-03	-3.212

Top 10 activated signalling pathways	Pathway enrichment p-value	z-score
EIF2 signalling	1.82E-13	4.907
RHOA signalling	6.88E-03	1.976
LXR/RXR activation	3.56E-03	1.347
Regulation of Actin based motility by Rho	5.43E-03	1.347
PD-1, PD-L1 cancer immunotherapy pathway	5.43E-03	1.279
Gα12/13 signalling	6.45E-03	1.257
RHOGDI signalling	1.8E-03	0.632
Cyclins and cell cycle regulation	4.75E-02	0.5000
Bladder cancer signalling	2.88E-02	0.447
VEGF signalling	4.37E-02	0.426

A1.6 List of Reagents

Company	Reagent	Catalogue No.
Sigma	Dulbecco's Modified Eagle's Medium - high glucose	D5796
Sigma	Minimum essential medium	M2279
Sigma	MEM non-essential amino acids	M7145
Sigma	L-Glutamine solution	G7513
Sigma	Penicillin/Streptomycin	P0781
Sigma	Trypsin-EDTA solution 10x	T4174
Sigma	Dulbecco's PBS Ca^{2+} and Mg^{2+} free	D8537
Invitrogen	Lipofectamine 3000	L3000015
Thermo Fisher	OPTI-MEM reduced serum media	31985062
Thermo Fisher	Geneticin selective antibiotic (50mg/ml)	10131027
Sigma	RIPA Buffer	R0278
Themo Scientific	Halt™ Protease and Phosphatase Inhibitor Cocktail (100X)	78440
Thermo Fisher Scientific	Bolt 4-12% Bis-Tris Plus Gels	NW04122BOX
Thermo Fisher Scientific	20X Bolt MES SDS Running Buffer	B0002
Thermo Fisher Scientific	Bolt Transfer Buffer (20x)	BT0006
Sigma-Aldrich	Ponceau S solution	P7170
Invitrogen	SeeBlue Plus2 Pre-Stained Protein Standard	LC5925
Thermo Fisher Scientific	NuPAGE LDS Sample Buffer (4X)	NP0007
Thermo Fisher Scientific	NuPAGE Sample Reducing Agent (10X)	NP0009
Abcam	Anti-HA tag antibody	ab18181
Abcam	Anti-beta Actin antibody	ab8227
LI-COR	IRDye® 800 CW Donkey anti-rabbit	926-32213
LI-COR	IRDye® 680RD Donkey anti-mouse	926-68072
Sigma	RNase ZAP	R2020
Qiagen	RNAprotect Cell Reagent	76526
Qiagen	RNeasy Plus Mini Kit	74134
Qiagen	RT^2 First Strand Kit	330404
Qiagen	SYBR Green ROX qPCR Mastermix (2x)	330253
Invitrogen	RNase-free water	AM9935
Cell signalling technologies	HA Tag (HA tag (6E2) Ms mAb (Alexa 488 conjugated)	2350S
Thermo Fisher Scientific	Alexa Flour 635 Phalloidin	A34054
Sigma	TWEEN 20	P2287
Sigma-Aldrich	Bovine Serum Albumin	A9418
Sigma-Aldrich	Goat serum	G9023
Fisher Scientific	Vector Laboratories VECTASHIELD Antifade Mounting Medium with DAPI	NC9524612

Appendix B: Supplementary information for Chapter 3

B2.1 Inhibition of calpain activity by calpeptin using t-BOC assay.

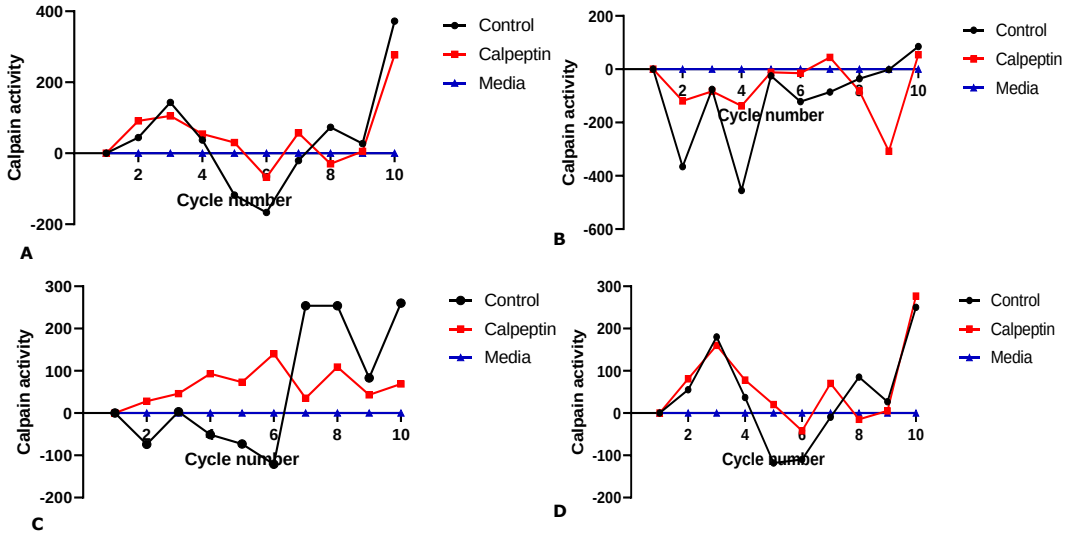

Figure B2.1. Inhibition of calpain activity by tBOC assay. MDA-MB-231 cells treated with 100 µM of calpeptin for 30 minutes were assessed for inhibition of calpain activity using the tBOC assay. A total of 7 experiments were conducted, Figure 3.5 represents the average of three independent experiments. (A-D) examples of inconclusive and unreliable results.

B2.2 Development of the FRET bio assay

B2.2.1 Sequence of the FRET plasmid

The nucleotide sequence of the FRET vector. The nucleotides in the red font is the sequence for the CFP-16PLFAAR-YFP construct

ttggaagggctaattcactcccaaagaagacaagatatccttgatctgtggatctaccacacac
aaggctacttccctgattagcagaactacacaccagggccaggggtcagatatccactgacctt
tggatggtgctacaagctagtaccagttgagccagataaggtagaagaggccaataaagga
gagaacaccagcttgttacaccctgtgagcctgcatgggatggatgacccggagagagaagt
gttagagtggaggtttgacagccgcctagcatttcatcacgtggcccgagagctgcatcccga
gtacttcaagaactgctgatatcgagcttgctacaagggactttccgctggggactttccaggg
aggcgtggcctgggcgggactggggagtggcgagccctcagatcctgcatataagcagctgc
tttttgcctgtactgggtctctctggttagaccagatctgagcctgggagctctctggctaactag
ggaacccactgcttaagcctcaataaagcttgccttgagtgcttcaagtagtgtgtgcccgtctg
ttgtgtgactctggtaactagagatccctcagacccttttagtcagtgtggaaaatctctagcagt
ggcgcccgaacagggacttgaaagcgaaagggaaaccagaggagctctctcgacgcagga
ctcggcttgctgaagcgcgcacggcaagaggcgaggggcggcgactggtgagtacgccaaa
aattttgactagcggaggctagaaggagagagatgggtgcgagagcgtcagtattaagcgg
gggagaattagatcgcgatgggaaaaaattcggttaaggccaggggaaagaaaaaatat
aaattaaaacatatagtatgggcaagcagggagctagaacgattcgcagttaatcctggcctg

ttagaaacatcagaaggctgtagacaaatactgggacagctacaaccatcccttcagacagg
atcagaagaacttagatcattatataatacagtagcaaccctctattgtgtgcatcaaaggata
gagataaaagacaccaaggaagctttagacaagatagaggaagagcaaaacaaaagtaag
accaccgcacagcaagcggccgctgatcttcagacctggaggaggagatatgagggacaatt
ggagaagtgaattatataaatataaagtagtaaaaattgaaccattaggagtagcacccacca
aggcaaagagaagagtggtgcagagagaaaaaagagcagtgggaataggagctttgttcct
tgggttcttgggagcagcaggaagcactatgggcgcagcgtcaatgacgctgacggtacagg
ccagacaattattgtctggtatagtgcagcagcagaacaatttgctgagggctattgaggcgca
acagcatctgttgcaactcacagtctggggcatcaagcagctccaggcaagaatcctggctgt
ggaaagatacctaaaggatcaacagctcctggggatttggggttgctctggaaaactcatttgc
accactgctgtgccttggaatgctagttggagtaataaatctctggaacagatttggaatcaca
cgacctggatggagtgggacagagaaattaacaattacacaagcttaatacactccttaattg
aagaatcgcaaaaccagcaagaaaagaatgaacaagaattattggaattagataaatgggc
aagtttgtggaattggtttaacataacaaattggctgtggtatataaaattattcataatgatagt
aggaggcttggtaggtttaagaatagtttttgctgtactttctatagtgaatagagttaggcagg
gatattcaccattatcgtttcagacccacctcccaaccccgaggggacccgacaggcccgaag
gaatagaagaagaaggtggagagagagacagagacagatccattcgattagtgaacggat
ctcgacggtatcgatgtcgacgataagctttgcaaagatggataaagttttaaacagagagga
atctttgcagctaatggaccttctaggtcttgaaaggagtgggaattggctccggtgcccgtca
gtgggcagagcgcacatcgcccacagtccccgagaagttgggggggaggggtcggcaattga
accggtgcctagagaaggtggcgcggggtaaactgggaaagtgatgtcgtgtactggctccg
cctttttcccgagggtgggggagaaccgtatataagtgcagtagtcgccgtgaacgttcttttc
gcaacgggtttgccgccagaacacaggtaagtgccgtgtgtggttcccgcgggcctggcctctt
tacgggttatggcccttgcgtgccttgaattacttccactggctgcagtacgtgattcttgatccc
gagcttcgggttggaagtgggtgggagagttcgaggccttgcgcttaaggagccccttcgcct
cgtgcttgagttgaggcctggcctgggcgctggggccgccgcgtgcgaatctggtggcacctt
cgcgcctgtctcgctgctttcgataagtctctagccatttaaaatttttgatgacctgctgcgacgc
ttttttttctggcaagatagtcttgtaaatgcgggccaagatctgcacactggtatttcggttttgg
ggccgcgggcggcgacggggcccgtgcgtcccagcgcacatgttcggcgaggcggggcctg
cgagcgcggccaccgagaatcggacgggggtagtctcaagctggccggcctgctctggtgcc
tggcctcgcgccgccgtgtatcgccccgccctgggcggcaaggctggcccggtcggcaccagt
tgcgtgagcggaaagatggccgcttcccggccctgctgcagggagctcaaaatggaggacgc
ggcgctcgggagagcgggcgggtgagtcacccacacaaaggaaaagggcctttccgtcctc
agccgtcgcttcatgtgactccacggagtaccgggcgccgtccaggcacctcgattagttctcg
agcttttggagtacgtcgtctttaggttgggggaggggttttatgcgatggagtttccccacac
tgagtgggtggagactgaagttaggccagcttggcacttgatgtaattctccttggaatttgccc
tttttgagtttggatcttggttcattctcaagcctcagacagtggttcaaagttttttttcttccatttc
aggtgtcgtgaggaatttcgacatttaaatttaattaatctcgacggtatcggttaacttttaaaa
gaaaaggggggattgggggtacagtgcaggggaaagaatagtagacataatagcaacag
acatacaaactaaagaattacaaaaacaaattacaaaaattcaaaattttccgatcacgagac
taGCTCGAGGCCACCATGGTTTCCAAGGGCGAAGAACTGTTCACCGGCG
TGGTGCCCATTCTGGTGGAACTGGATGGGGATGTGAACGGCCACAAGTT
CAGCGTCAGCGGAGAAGGCGAAGGCGACGCCACATACGGAAAGCTGAC
CCTGAAGTTCATCTGCACCACCGGCAAGCTGCCTGTGCCTTGGCCTACA
CTGGTCACCACACTGACATGGGGCGTGCAGTGCTTCAGCAGATACCCCG

ACCACATGAAGCAGCACGATTTCTTCAAGAGCGCCATGCCTGAGGGCTA
CGTGCAAGAGAGAACCATCTTCTTCAAGGACGACGGCAACTACAAGACC
AGAGCCGAAGTGAAGTTCGAGGGCGACACCCTGGTCAACAGAATCGAG
CTGAAGGGCATCGACTTCAAAGAGGATGGCAACATCCTGGGCCACAAGC
TTGAGTACAACTACATCAGCCACAACGTGTACATCACCGCCGACAAGCA
GAAGAACGGCATCAAGGCCAACTTCAAGATCCGGCACAACATCGAGGAC
GGCTCTGTGCAGCTGGCCGATCACTACCAGCAGAACACACCTATCGGCG
ACGGACCTGTGCTGCTGCCTGATAACCACTACCTGAGCACACAGAGCGC
CCTGAGCAAGGACCCTAACGAGAAGAGGGACCACATGGTGCTGCTGGA
ATTTGTGACCGCCGCTGGCATCACACTCGGCATGGATGAGCTGTACAAG
TCCGGCGCCGGCTTGCCTTTATTCGCCGCGCGTCCGGGCGCGAATTCTA
TCGTGTCCAAAGGCGAGGAACTCTTTACAGGGGTCGTGCCTATCCTGGT
CGAACTCGACGGCGACGTGAACGGACATAAGTTTTCCGTGTCCGGCGAA
GGCGAAGGGGATGCTACTTACGGCAAACTCACACTCAAGTTTATCTGTA
CGACAGGGAAACTGCCCGTGCCATGGCCAACTCTCGTGACCACATTTGG
CTACGGCCTGCAGTGTTTCGCCCGGTATCCTGATCACATGAAGCAACAT
GACTTTTTTAAGTCCGCTATGCCCGAGGGATATGTCCAAGAGCGGACGA
TTTTCTTTAAGGATGATGGGAATTATAAGACACGGGCTGAAGTCAAGTTT
GAAGGGGATACACTGGTTAACCGGATCGAACTCAAGGGGATTGATTTCA
AAGAGGACGGGAATATTCTCGGACATAAGTTGGAGTACAATTACAACTC
CCACAATGTCTATATCATGGCTGATAAGCAGAAAAATGGGATCAAAGTGA
ACTTTAAGATCAGACATAATATTGAGGACGGCAGCGTCCAGCTGGCTGA
CCATTATCAGCAAAACACCCCAATCGGAGATGGCCCCGTCCTGCTGCCA
GACAATCACTATCTGTCCTACCAGTCCGCTCTGTCTAAGGACCCCAATGA
GAAACGCGATCACATGGTCTTGTTGGAGTTCGTGACAGCTGCCGGAATC
ACCCTCGGAATGGACGAACTCTATAAGGGATCCACCGGATCTAGATAAC
TGATCATAATCAGCCATACCACATATGataatcaacctctggattacaaaatttgtga
aagattgactggtattcttaactatgttgctcctttacgctatgtggatacgctgctttaatgcctt
tgtatcatgctattgcttcccgtatggctttcattttctcctccttgtataaatcctggttgctgtctct
ttatgaggagttgtggcccgttgtcaggcaacgtggcgtggtgtgcactgtgtttgctgacgca
acccccactggttggggcattgccaccacctgtcagctcctttccgggactttcgctttcccctcc
ctattgccacggcggaactcatcgccgcctgccttgcccgctgctggacaggggctcggctgtt
gggcactgacaattccgtggtgttgtcggggaagctgacgtcctttccatggctgctcgcctgtg
ttgccacctggattctgcgcgggacgtccttctgctacgtcccttcggccctcaatccagcggac
cttccttcccgcggcctgctgccggctctgcggcctcttccgcgtcttcgccttcgccctcagacg
agtcggatctccctttgggccgcctccccgcatcggtacgtatggccaggtacctttaagaccaa
tgacttacaaggcagctgtagatcttagccacttttaaaagaaaaggggggactggaagggc
taattcactcccaacgaagacaagatgggatcaattcaccatgggaataacttcgtatagcata
cattatacgaagttatgctgcttttgcttgtactgggtctctctggttagaccagatctgagcctg
ggagctctctggctaactagggaacccactgcttaagcctcaataaagcttgccttgagtgcttc
aagtagtgtgtgcccgtctgttgtgtgactctggtaactagagatccctcagacccttttagtcag
tgtggaaaatctctagcagcatctagaattaattccgtgtattctatagtgtcacctaaatcgtat
gtgtatgatacataaggttatgtattaattgtagccgcgttctaacgacaatatgtacaagccta
attgtgtagcatctggcttactgaagcagaccctatcatctctctcgtaaactgccgtcagagtcg
gtttggttggacgaaccttctgagtttctggtaacgccgtcccgcacccggaaatggtcagcga

accaatcagcagggtcatcgctagccagatcctctacgccggacgcatcgtggccggcatcac
cggcgccacaggtgcggttgctggcgcctatatcgccgacatcaccgatggggaagatcggg
ctcgccacttcgggctcatgagcgcttgtttcggcgtgggtatggtggcaggccccgtggccgg
gggactgttgggcgccatctccttgcatgcaccattccttgcggcggcggtgctcaacggcctc
aacctactactgggctgcttcctaatgcaggagtcgcataagggagagcgtcgaatggtgcac
tctcagtacaatctgctctgatgccgcatagttaagccagccccgacacccgccaacacccgct
gacgcgccctgacgggcttgtctgctcccggcatccgcttacagacaagctgtgaccgtctccg
ggagctgcatgtgtcagaggttttcaccgtcatcaccgaaacgcgcgagacgaaagggcctc
gtgatacgcctatttttataggttaatgtcatgataataatggtttcttagacgtcaggtggcactt
ttcggggaaatgtgcgcggaacccctatttgtttatttttctaaatacattcaaatatgtatccgct
catgagacaataaccctgataaatgcttcaataatattgaaaaaggaagagtatgagtattca
acatttccgtgtcgcccttattccctttttgcggcattttgccttcctgtttttgctcacccagaaac
gctggtgaaagtaaaagatgctgaagatcagttgggtgcacgagtgggttacatcgaactgg
atctcaacagcggtaagatccttgagagttttcgccccgaagaacgttttccaatgatgagcact
tttaaagttctgctatgtggcgcggtattatcccgtattgacgccgggcaagagcaactcggtcg
ccgcatacactattctcagaatgacttggttgagtactcaccagtcacagaaaagcatcttacg
gatggcatgacagtaagagaattatgcagtgctgccataaccatgagtgataacactgcggcc
aacttacttctgacaacgatcggaggaccgaaggagctaaccgcttttttgcacaacatgggg
gatcatgtaactcgccttgatcgttgggaaccggagctgaatgaagccataccaaacgacgag
cgtgacaccacgatgcctgtagcaatggcaacaacgttgcgcaaactattaactggcgaacta
cttactctagcttcccggcaacaattaatagactggatggaggcggataaagttgcaggacca
cttctgcgctcggcccttccggctggctggtttattgctgataaatctggagccggtgagcgtgg
gtctcgcggtatcattgcagcactggggccagatggtaagccctcccgtatcgtagttatctaca
cgacggggagtcaggcaactatggatgaacgaaatagacagatcgctgagataggtgcctc
actgattaagcattggtaactgtcagaccaagtttactcatatatactttagattgatttaaaactt
cattttaatttaaaaggatctaggtgaagatccttttgataatctcatgaccaaaatcccttaac
gtgagttttcgttccactgagcgtcagaccccgtagaaaagatcaaaggatcttcttgagatcct
ttttttctgcgcgtaatctgctgcttgcaaacaaaaaaaccaccgctaccagcggtggtttgtttg
ccggatcaagagctaccaactctttttccgaaggtaactggcttcagcagagcgcagatacca
aatactgtccttctagtgtagccgtagttaggccaccacttcaagaactctgtagcaccgcctac
atacctcgctctgctaatcctgttaccagtggctgctgccagtggcgataagtcgtgtcttaccgg
gttggactcaagacgatagttaccggataaggcgcagcggtcgggctgaacgggggttcgt
gcacacagcccagcttggagcgaacgacctacaccgaactgagatacctacagcgtgagcat
tgagaaagcgccacgcttcccgaagggagaaaggcggacaggtatccggtaagcggcagg
gtcggaacaggagagcgcacgagggagcttccagggggaaacgcctggtatctttatagtcc
tgtcgggtttcgccacctctgacttgagcgtcgatttttgtgatgctcgtcaggggggcggagcc
tatggaaaaacgccagcaacgcggccttttacggttcctggccttttgctggccttttgctcaca
tgttctttcctgcgttatcccctgattctgtggataaccgtattaccgcctttgagtgagctgatacc
gctcgccgcagccgaacgaccgagcgcagcgagtcagtgagcgaggaagcggaagagcgc
ccaatacgcaaaccgcctctccccgcgcgttggccgattcattaatgcagctgtggaatgtgtgt
cagttagggtgtggaaagtccccaggctccccagcaggcagaagtatgcaaagcatgcatct
caattagtcagcaaccaggtgtggaaagtccccaggctccccagcaggcagaagtatgcaaa
gcatgcatctcaattagtcagcaaccatagtcccgcccctaactccgcccatcccgcccctaact
ccgcccagttccgcccattctccgccccatggctgactaatttttttatttatgcagaggccgag
gccgcctcggcctctgagctattccagaagtagtgaggaggctttttggaggcctaggcttttg

caaaaagcttggacacaagacaggcttgcgagatatgtttgagaataccactttatcccgcgtc
agggagaggcagtgcgtaaaaagacgcggactcatgtgaaatactggtttttagtgcgccag
atctctataatctcgcgcaacctattttcccctcgaacacttttaagccgtagataaacaggctg
ggacacttcacatgagcgaaaaatacatcgtcacctgggacatgttgcagatccatgcacgta
aactcgcaagccgactgatgccttctgaacaatggaaaggcattattgccgtaagccgtggcg
gtctgtaccgggtgcgttactggcgcgtgaactgggtattcgtcatgtcgataccgtttgtatttc
cagctacgatcacgacaaccagcgcgagcttaaagtgctgaaacgcgcagaaggcgatggc
gaaggcttcatcgttattgatgacctggtggataccggtggtactgcggttgcgattcgtgaaat
gtatccaaaagcgcactttgtcaccatcttcgcaaaaccggctggtcgtccgctggttgatgact
atgttgttgatatcccgcaagatacctggattgaacagccgtgggatatgggcgtcgtattcgtc
ccgccaatctccggtcgctaatcttttcaacgcctggcactgccgggcgttgttctttttaacttca
ggcgggttacaatagtttccagtaagtattctggaggctgcatccatgacacaggcaaacctga
gcgaaaccctgttcaaaccccgctttaaacatcctgaaacctcgacgctagtccgccgctttaat
cacggcgcacaaccgcctgtgcagtcggcccttgatggtaaaaccatccctcactggtatcgca
tgattaaccgtctgatgtggatctggcgcggcattgacccacgcgaaatcctcgacgtccaggc
acgtattgtgatgagcgatgccgaacgtaccgacgatgatttatacgatacggtgattggctac
cgtggcggcaactggatttatgagtgggccccggatctttgtgaaggaaccttacttctgtggtg
tgacataattggacaaactacctacagagatttaaagctctaaggtaaatataaaatttttaagt
gtataatgtgttaaactactgattctaattgtttgtgtattttagattccaacctatggaactgatg
aatgggagcagtggtggaatgcctttaatgaggaaaacctgttttgctcagaagaaatgccat
ctagtgatgatgaggctactgctgactctcaacattctactcctccaaaaaagaagagaaaggt
agaagaccccaaggactttccttcagaattgctaagtttttgagtcatgctgtgtttagtaatag
aactcttgcttgctttgctatttacaccacaaaggaaaaagctgcactgctatacaagaaaatta
tggaaaaatattctgtaacctttataagtaggcataacagttataatcataacatactgttttttct
tactccacacaggcatagagtgtctgctattaataactatgctcaaaaattgtgtacctttagcttt
ttaatttgtaaaggggttaataaggaatatttgatgtatagtgccttgactagagatcataatca
gccataccacatttgtagaggttttacttgctttaaaaaacctcccacacctccccctgaacctga
aacataaaatgaatgcaattgttgttgttaacttgtttattgcagcttataatggttacaaataaa
gcaatagcatcacaaatttcacaaataaagcatttttttcactgcattctagttgtggtttgtccaa
actcatcaatgtatcttatcatgtctggatcaactggataactcaagctaaccaaaatcatccca
aacttcccacccctataccctattaccactgccaattacctagtggtttcatttactctaaacctgtg
attcctctgaattattttcattttaaagaaattgtatttgttaaatatgtactacaaacttagtag

B2.2.2 FRET plasmid map and transfection efficiency

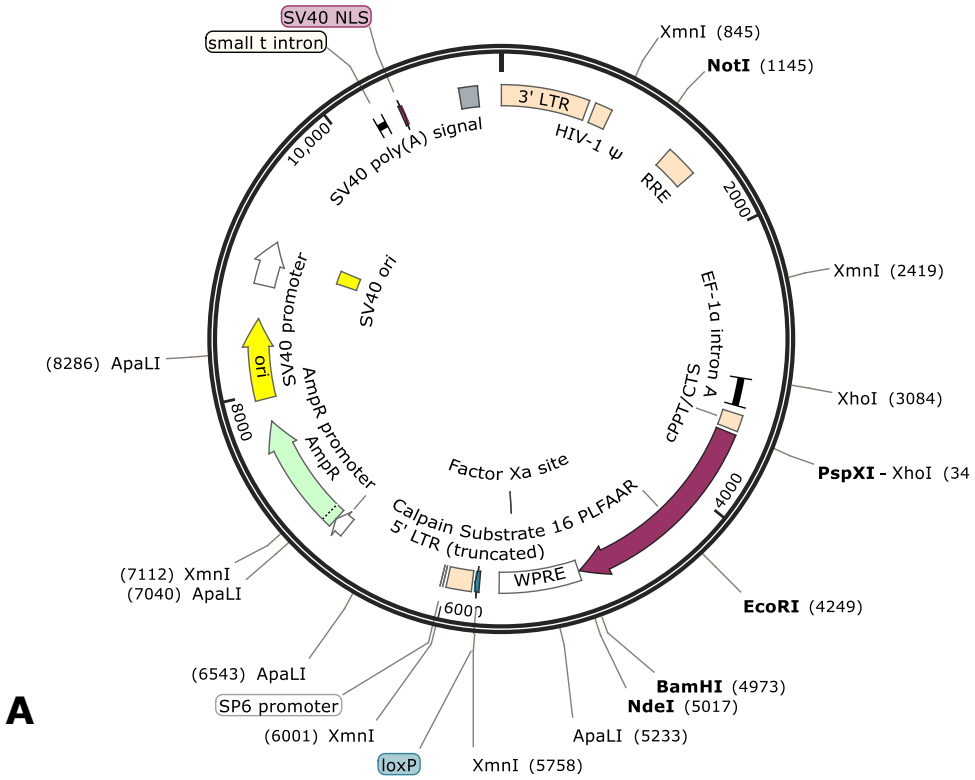

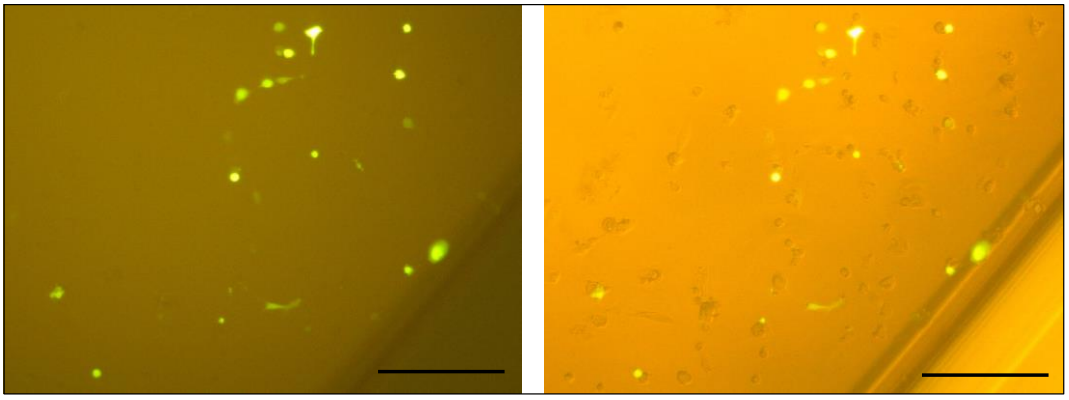

B

Figure B2.2 Development of the FRET bio-assay. (A) Plasmid map of the FRET vector containing the CFP-PLFAAR-YFP sequences. Obtained from Professor P. Davies, Queen's University, Canada. **(B)** Transfection efficiency was optimised to DNA: transfection reagent ratio of 1:3 and at 48 hour time point at x10 magnification. Transfected cells were seen to be fluorescent in the dark field (left panel) and light field (right panel).

B2.3 List of Reagents

Company	Reagent	Catalogue No.
Sigma	Minimum essential medium	M2279
Sigma	MEM non-essential amino acids	M7145
Sigma	L-Glutamine solution	G7513
Sigma	Penicillin/Streptomycin	P0781
Sigma	Trypsin-EDTA solution 10x	T4174
Sigma	Dulbecco's PBS Ca^{2+} and Mg^{2+} free	D8537
Invitrogen	Lipofectamine 3000	L3000015
Thermo Fisher	OPTI-MEM reduced serum media	31985062
Merck	Calpeptin	03-34-0051
Invitrogen	t-BOC-Leu-Met CMAC	A6520
Sigma-Aldrich	LB broth	L3022
Thermo Fisher	Ampicillin	69-53-4
Sigma-Aldrich	Bacteriological agar	A5306
Thermo Fisher Scientific	One Shot TOP TEN Competent cells	C404003
Qiagen	Plasmid mini kit	12123
Qiagen	Endofree Plasmid Maxi Kit	12362
Sigma-Aldrich	A23187 Calcium ionophore	C7522
Sigma-Aldrich	PD150606 calpain inhibitor	D5946
Sigma-Aldrich	Doxorubicin	D1515
Sigma-Aldrich	Crystal Violet	C3886

Appendix C: Supplementary information for Chapter 4

C3.1 Mycoplasma negative vs positive cells- cell proliferation

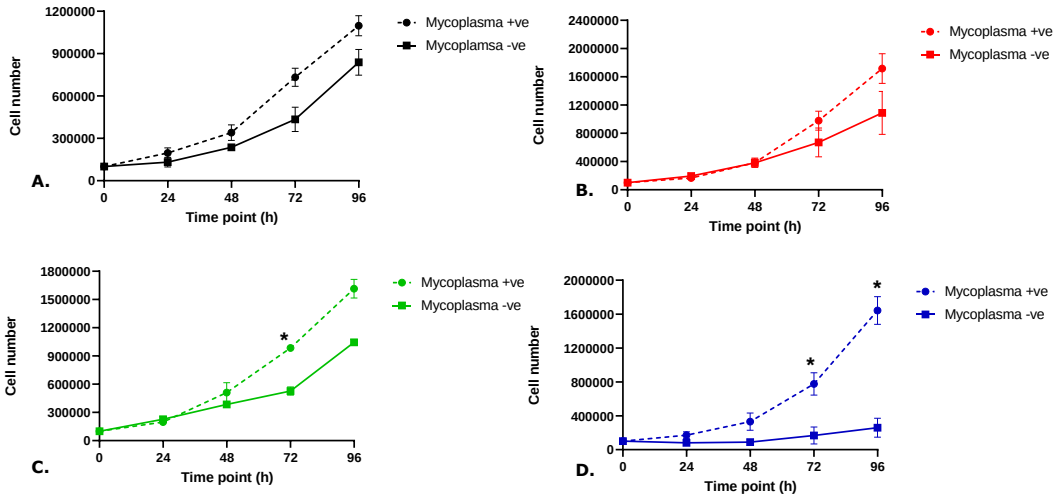

Figure C3.1 Mycoplasma positive vs mycoplasma negative growth curves. Cell growth curves for **(A)** MDA-MB-231 WT, **(B)** Capn1 KO, **(C)** Capn2 KO and **(D)** Capns1 KO cells before and after mycoplasma removal. Data represent the average number of cells/well ± SD of three independent experiments each conducted in triplicate. Statistical analysis was carried out using the Student's *t*-test *(*P*<0.05), **(*P*<0.01), ***(*P*<0.001).

C3.2 Mycoplasma negative vs positive cells- PE

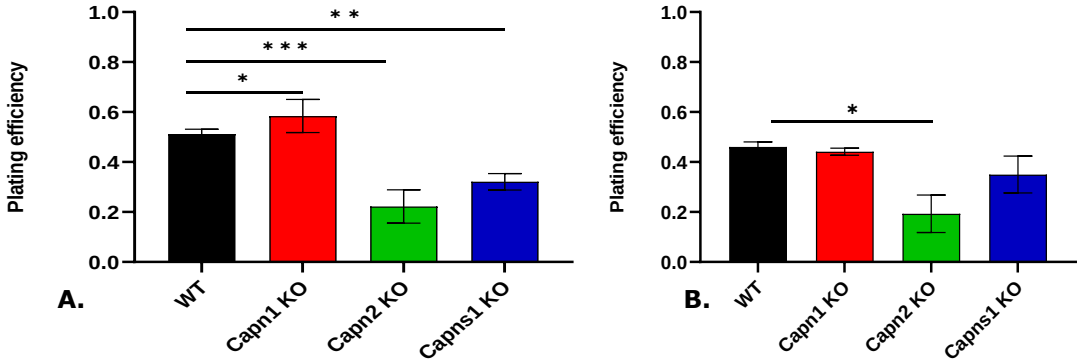

Figure C3.2 Plating efficiencies. Plating efficiency for **(A)** Mycoplasma negative and **(B)** Mycoplasma positive MDA-MB-231 WT, Capn1 KO, Capn2 KO and Capns1 KO cells. Data represents the average plating efficiencies ± SD of three independent experiments, each conducted in triplicate. Statistical analysis was carried out using the Student's *t*-test *(*P*<0.05), **(*P*<0.01), ***(*P*<0.001).

C3.3 Mycoplasma negative vs positive cells- DT and PE

Table C3.1 Doubling time and plating efficiencies for Mycoplasma negative cells

Cell lines	Doubling time	Plating efficiency
MDA-MB-231 WT	27±2.45 hours	51.2±1.2%
MDA-MB-231 Capn1 KO	29±8.04 hours	58.4±1.3%
MDA-MB-231 Capn2 KO	30.5±0.5 hours	22.2±6.5%
MDA-MB-231 Capns1 KO	82.6±5.4 hours	32.1±5.2%

Table C3.2 Doubling time and plating efficiencies for Mycoplasma positive cells

Cell lines	Doubling time	Plating efficiency
MDA-MB-231 WT	20.67±1.5 hours	46±2.3% (n=3)
MDA-MB-231 Capn1 KO	21.34±2.5 hours	44.10±1.4% (n=3)
MDA-MB-231 Capn2 KO	21±3.4 hours	19.31±7.5% (n=3)
MDA-MB-231 Capns1 KO	22.34±3.2 hours	35±7.4% (n=3)

C3.4 Mycoplasma negative vs positive cells- doxorubicin cell proliferation response

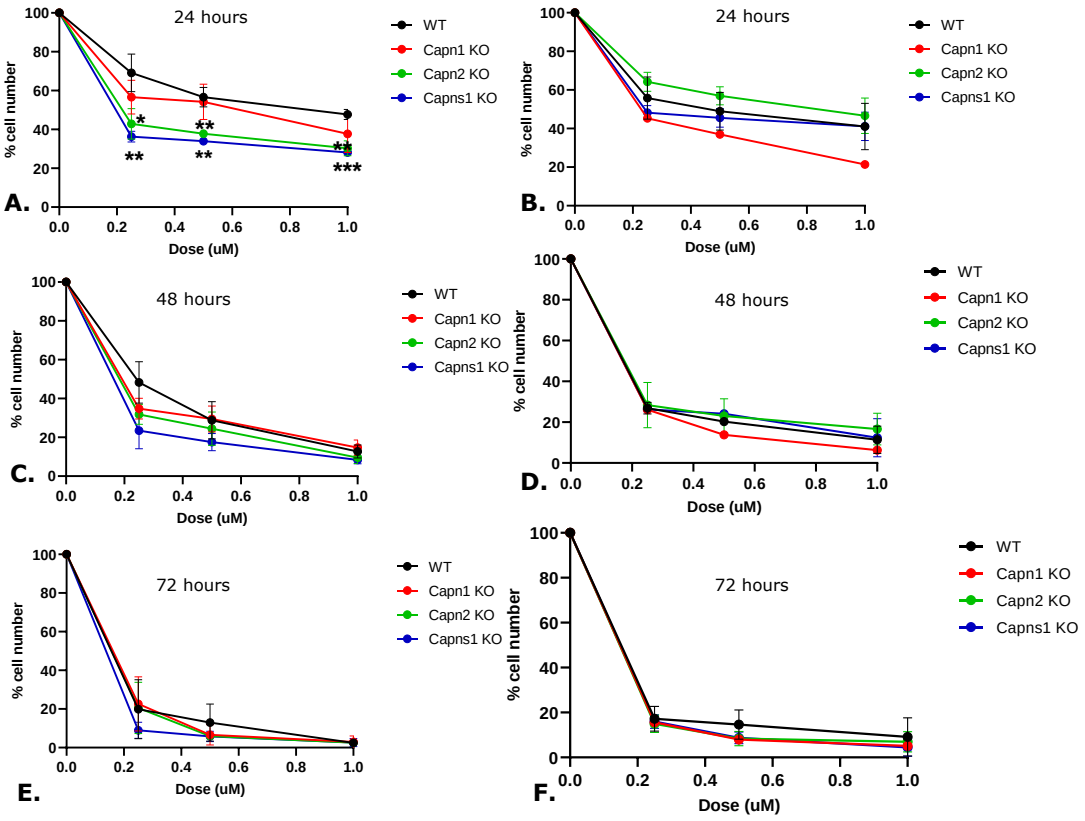

Figure C3.3 Doxorubicin proliferation response. MDA-MB-231 WT and calpain KO cells were treated with doxorubicin for 24 hours, 48 hours and 72 hours. The left panel shows the dose response curves for Mycoplasma negative cells. The right panel shows the dose response curves for Mycoplasma positive cells. The graphs represent the average data ± SD from two or three independent experiments, each conducted in triplicate. Statistical analysis was carried out using the Student's *t*-test *(*P*<0.05), **(*P*<0.01), ***(*P*<0.001).

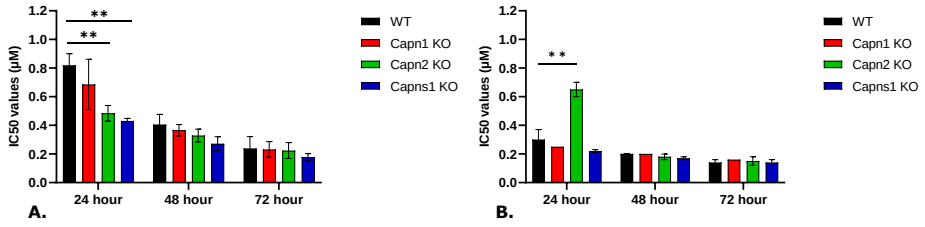

Figure C3.4 Doxorubicin proliferation IC50. IC50 values were calculated from dose response curves for **(A)** mycoplasma negative and **(B)** mycoplasma positive MDA-MB-231 WT, Capn1 KO, Capn2 KO and Capns1 KO cells treated with doxorubicin for 24 hours, 48 hours and 72 hours. The graphs represent the average data ± SD from two or three independent experiments, each conducted in triplicate. Statistical analysis was carried out using the Student's *t*-test *(*P*<0.05), **(*P*<0.01), ***(*P*<0.001).

C3.5 Mycoplasma negative vs positive cells- doxorubicin clonogenic survival response

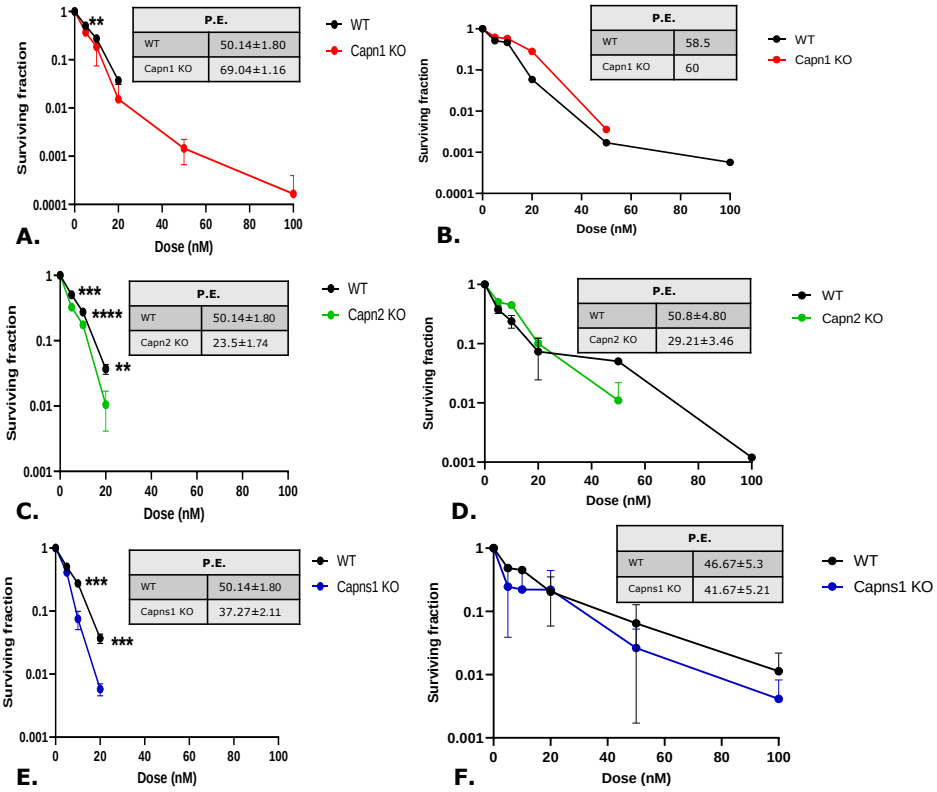

Figure C3.5 Doxorubicin clonogenic survival response. MDA-MB-231 WT and calpain KO cells were treated with doxorubicin for 24 hours. The left panel shows the dose response curves for Mycoplasma negative cells. The right panel shows the dose response curves for Mycoplasma positive cells. The graphs represent the average data ± SD from two or three independent experiments, each conducted in triplicate. Statistical analysis was carried out using the Student's *t*-test *(*P*<0.05), **(*P*<0.01), ***(*P*<0.001).

C3.6 Mycoplasma negative vs positive cells- radiation response

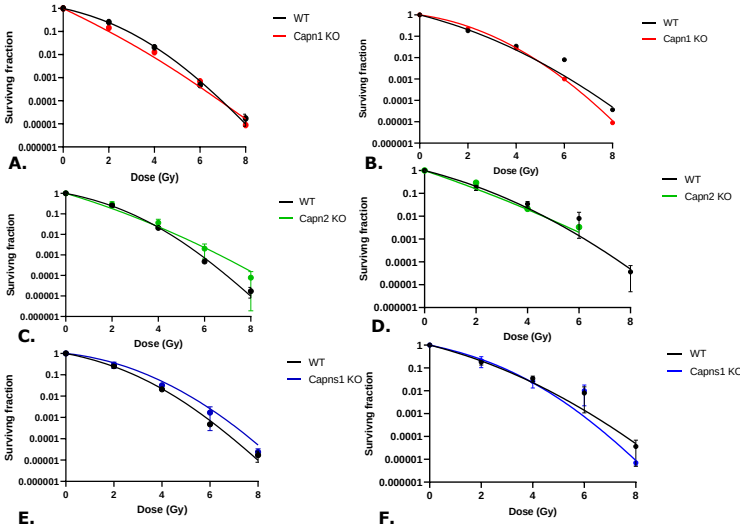

Mycoplasma	Cell line	PE	SF2
Positive	WT Capn1 KO	54.2 48.3	0.22 0.29
Negative	WT Capn1KO	50.67±3.8 57.67±4.2	0.24±0.08 0.14±0.02

Mycoplasma	Cell line	PE	SF2
Positive	WT Capn2 KO	56.5±0.03 29±0.07	0.18±0.07 0.16±0.05
Negative	WT Capn2 KO	50.67±3.8 26±2.9	0.24±0.08 0.20±0.10

Mycoplasma	Cell line	PE	SF2
Positive	WT Capns1 KO	59.4±0.5 39.11±0.02	0.20±0.02 0.24±0.13
Negative	WT Capns1 KO	50.67±3.8 37.67±4.5	0.24±0.08 0.19±0.10

Figure C3.6 Radiation response. MDA-MB-231 WT and calpain KO cells were treated with radiation and the survival curves for each cell lines were fitted according to the Linear Quadratic Model. The left panel shows the dose response curves for Mycoplasma negative cells. The right panel shows the dose response curves for Mycoplasma positive cells. The graphs represent the average data ± SD from two or three independent experiments, each conducted in triplicate. Statistical analysis was carried out using the Student's *t*-test *($P<0.05$), **($P<0.01$), ***($P<0.001$).

C3.7 Breast cancer cell line radiation response in normoxia and hypoxia

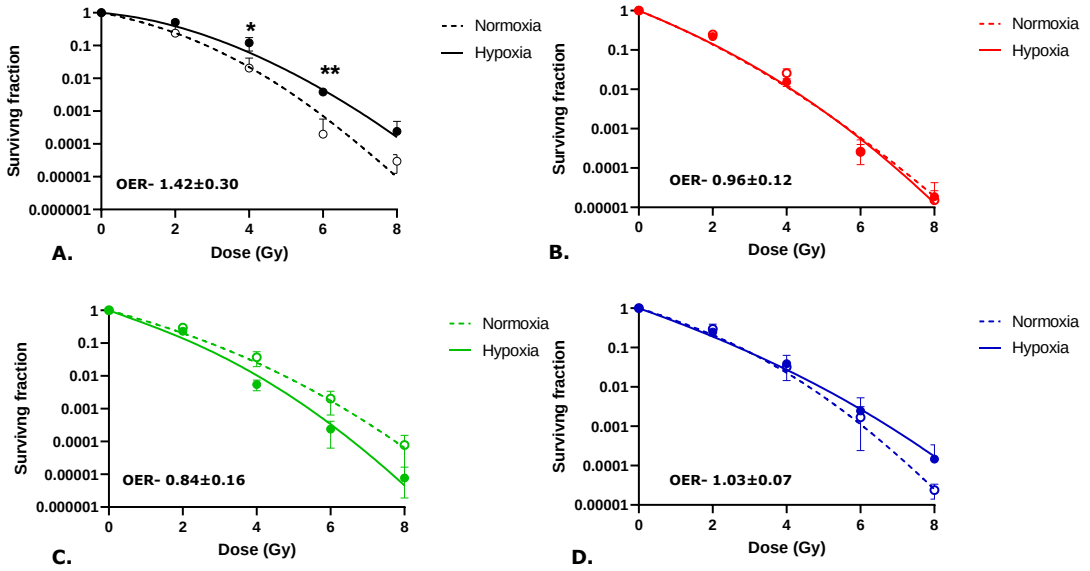

Figure C3.7 Radiation response in normoxia (21% O2) and hypoxia (1% O2). MDA-MB-231 WT and calpain KO cells were treated with radiation in the presence of normoxia (21% O2) and hypoxia (1%O2) and the survival curves for each cell lines were fitted according to the Linear Quadratic Model. The OER was calculated at 1% survival. The graphs represent the average data ± SD from three independent experiments, each conducted in triplicate. Statistical analysis was carried out using the Student's *t*-test *(*P*<0.05), **(*P*<0.01), ***(*P*<0.001).

C3.8 List of Reagents

Company	Reagent	Catalogue No.
Sigma	Dulbecco's Modified Eagle's Medium - high glucose	D5796
Sigma	L-Glutamine solution	G7513
Sigma	Penicillin/Streptomycin	P0781
Sigma	Trypsin-EDTA solution 10x	T4174
Sigma	Dulbecco's PBS Ca^{2+} and Mg^{2+} free	D8537
Invivogen	Plasmocin treatment	ant-mpt
Millipore	Anti-calpain 1	MAB3104
Novus Biologicals	Anti-calpain 2	NBP246063
Millipore	Anti-calpain small subunit	MAB3083
2BScientific	Anti-CA9	ab00414-1.1
Abcam	Anti-β-actin	ab8227
LI-COR	IRDye® 800 CW Donkey anti-rabbit	926-32213
LI-COR	IRDye® 680RD Donkey anti-mouse	926-68072
DAKO	Rabbit anti-mouse HRP	P0260
DAKO	Goat anti-rabbit HRP	P0448
Scientific Laboratory Supplies	Amersham ECL select Western blotting detection reagent	RPN2235
Sigma-Aldrich	Doxorubicin	D1515

Appendix D: Supplementary information for chapter 5

D4.1 Gene probe details

Table D4.1 Gene probe numbers and sequences

Gene name	Probe Number	Probe ID	Probe sequence
CAPN1	-	ILMN_1705261	AAAGGGGACTCTTCAGGGACTTGTGTACTGGTTATGGGGGTGCCAGAGGC
PPP1CA	Probe 1	ILMN_1695827	TGGCCAAGTTCCTCCACAAGCACGACTTGGACCTCATCTGCCGAGCACAC
	Probe 2	ILMN_2377980	GCCAAGAAATAGCCCCCGCACACCACCCTGTGCCCCAGATGATGGATTGA
CAPN2	-	ILMN_1716057	TGGAGGGCAGCCCCACAGGACGGTTTATGAGCACACAATTATAGCTTGTT
AMOT	-	ILMN_1792409	GGAAGGTATCAGCTGTGGGCTAATTGCCACCAATTTCAGCCTGCCACGAT
PRKAB2	-	ILMN_1786021	TACACGGCAGCATTTCGAATGAGTGCAGCTCTGTGTCTGTCAGAAAGGAG
AMOTL1	-	ILMN_1748141	GGTTTGTATGACCCTTCCGAGTTGTCACCTTCCCACGCTGATCCCACATG
RAB13	-	ILMN_1788180	GAGCAGGGGAGAAATAGCAGAGGGGCTTGGAGGGTCACATAGGTAGATGG
CAPNS1	Probe 1	ILMN_2393254	TCCCCTGTACCTGTGCCAAGCCTAGCACTTGTGATGCCTCCATGCCCCGA
	Probe 2	ILMN_1655418	AGGAGTGGCTGCAGCTGACTATGTATTCCTGAACTGGAGCCCCAGACCCG
MAGOH		ILMN_2215656	TCCTGACCGAGTGGGCCGGCAGGAGCTTGAAATCGTCATTGGAGATGAAC
POLE2		ILMN_1774336	CCCAAGGACATCTGACTCCCCTACCTCTTTATGTCTGCCCAGTGTATTGG
CAST	Probe 1	ILMN_1717234	GCTGTCCCTCCACTACAGAAACCTCACAGAACACAGCAAAGGATAAGTGC
	Probe 2	ILMN_1783627	CATTCCAGTCAGCCAACAGATGGAAGGACCACATCTTCCTAACAAGAAAA
	Probe 3	ILMN_1774674	GAACATAGGGTACTCCGAGTGAAGAATTCAGCAGCTAAGTGGAAGTTGTC
	Probe 4	ILMN_2322806	CTGGAGTAAGCTACAGGATCTAAAGCAGCCCTTTTTACAGTCTAGTTAGG
	Probe 5	ILMN_1694943	GATGGGCCAGTTTCTATCTTCGACTTTCTTGGAGGGCTCACCGGCCACAG
	Probe 6	ILMN_1672947	GGGCTTTTCCAAAAGCAAACAAAGATAGGTTCCTCAGGTGACCAAAACTG
YWHAG	Probe 1	ILMN_1750145	CCTGAGGGCTGAAAACGGAGAGGGAATGGGAGACTTGATATTTAAGCAGC
	Probe 2	ILMN_2228809	CCAGCTCCGTGTTTCTCTAAGGAATTATTTCACACACGGACCATCTTTAG
HDAC1	-	ILMN_1727458	TTTCGTACCTTCCCACTGGCCTCAAGTGAGCCAAGAAACACTGCCTGCCC
RBBP4	Probe 1	ILMN_1653514	AGGGGGGCTTGATTCAACAAAGCCACAGACTTAACGTTGAAATTTTCTTC
	Probe 2	ILMN_2062524	CCTGACAGTTATACCACAGGTAGACTGTCAAGTTGAGAAGAGTGAATCAA
PSMB5	-	ILMN_1744649	ACAGAGATGCCTACTCAGGAGGTGCAGTCAACCTCTACCACGTGCGGGAG

D4.2 Probe binding to the genes

Table D4.2 Gene probes and their respective binding gene transcripts

Probe number	Gene transcript on Ensemble database
CAST probe 1	CAST-229, 258, 251, 254, 202, 210, 244, 222, 232, 205, 233, 248, 245, 213, 236, 228, 201, 234, 207, 256, 252, 204, 253, 223, 257, 247, 250, 246, 206, 224, 203.
CAST probe 2	CAST- 224, 203, 204, 207, 230, 250, 240, 220, 217, 215, 208, 255, 236, 234, 256, 252, 218.
CAST probe 3	CAST 205
CAST probe 4	CAST- 251, 202, 209, 248, 245, 201, 207, 252, 253, 257, 247, 250, 246, 206.
CAST probe 5	CAST- 210,244,202.
CAST probe 6	CAST-209, 250, 206, 201, 251, 202, 248, 245, 207, 252, 247.
RBBP4 probe 1	RBBP4- 202, 204, 206.
RBBP4 probe 2	RBBP4- 202.

The above mentioned CAST gene probes were aligned against different CAST transcripts. The probe sequences were then aligned against the different CAST domain sequences provided previously by our collaborator Dr. Parr, University of Nottingham. Figure E5.12 represents the binding domain for each CAST probe. CAST probe 1 was seen to bind to a non-coding region of the gene. CAST probe 2 was seen to bind between exon 3 and 4 of the gene sequence which encodes the L-domain region. CAST probe 3 was seen to bind to the exon 28 which encodes the inhibitory domains I-IV. CAST probe 4 binds to exon 3 which encodes the L-domain. CAST probe 5 binds between the exons 22 and 23, and CAST probe 6 binds to the exon 27, both of which encode the inhibitory domains I-IV. RBBP4 probes 1 and 2 were seen to be located in untranslated regions.

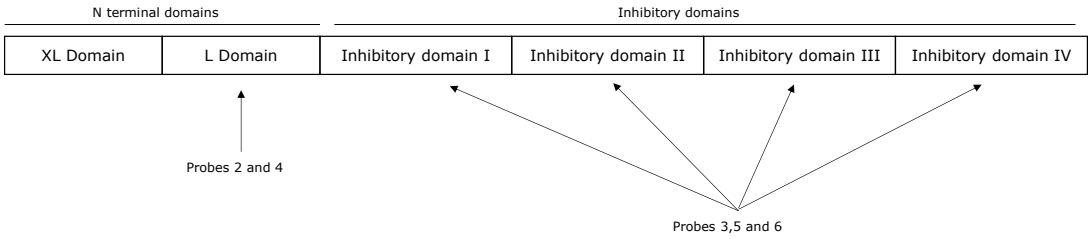

Figure D4.1 Schematic representation calpastatin highlighting binding of probes.

D4.3 List of Reagents

Company	Reagent	Catalogue No.
Leica	Novolink Polymer Detection System (500 tests)	RE7150-CE
Abcam	Anti-DARPP32	ab40801
Abcam	Anti-RBBP4	epr3411
Abcam	Anti-β-actin	ab8227
LI-COR	IRDye® 800 CW Donkey anti-rabbit	926-32213
LI-COR	IRDye® 680RD Donkey anti-mouse	926-68072

Appendix E: Permission for republish or display content

Copyright for Figures 1.1, 1.2, 1.3, 1.4 and 2.1

SPRINGER NATURE LICENSE
TERMS AND CONDITIONS

Jun 29, 2022

This Agreement between University of Nottingham -- Richa Vasan ("You") and Springer Nature ("Springer Nature") consists of your license details and the terms and conditions provided by Springer Nature and Copyright Clearance Center.

License Number	5302480772931
License date	May 05, 2022
Licensed Content Publisher	Springer Nature
Licensed Content Publication	Nature Reviews Cancer
Licensed Content Title	The calpain system and cancer
Licensed Content Author	Sarah J. Storr et al
Licensed Content Date	Apr 21, 2011
Type of Use	Thesis/Dissertation
Requestor type	academic/university or research institute
Format	print and electronic
Portion	figures/tables/illustrations
Number of figures/tables/illustrations	4
High-res required	no
Will you be translating?	no
Circulation/distribution	1 - 29
Author of this Springer Nature content	no
Title	The role of the calpain system in breast cancer progression and treatment response
Institution name	University of Nottingham
Expected presentation date	Jun 2022
Order reference number	RIN01
Portions	Figure 1.1 Figure 1.2 Figure 1.3 Figure 1.4 Figure 2.1
Requestor Location	University of Nottingham Biodiscovery Institute 3 University of Nottingham Nottingham, NG7 2RD United Kingdom Attn: University of Nottingham
Billing Type	Invoice
Billing Address	University of Nottingham Biodiscovery Institute 3 University of Nottingham Nottingham, United Kingdom NG7 2RD Attn: University of Nottingham
Total	**0.00 GBP**

Copyright for Figure 3.1

AMERICAN DIABETES ASSOCIATION LICENSE TERMS AND CONDITIONS

Jun 29, 2022

This Agreement between University of Nottingham -- Richa Vasan ("You") and American Diabetes Association ("American Diabetes Association") consists of your license details and the terms and conditions provided by American Diabetes Association and Copyright Clearance Center.

License Number	5318450294823
License date	May 29, 2022
Licensed Content Publisher	American Diabetes Association
Licensed Content Publication	Diabetes
Licensed Content Title	Structure, Activation, and Biology of Calpain
Licensed Content Author	Suzuki, Koichi; Hata, Shoji
Licensed Content Date	Feb 1, 2004
Licensed Content Volume	53
Licensed Content Issue	suppl_1
I would like to...	Thesis/Dissertation
Requestor type	Student
Format	Print, Electronic
Portion	image/photo
Number of images/photos requested	1
Rights for	Main product
Duration of use	Life of current edition
Creation of copies for the disabled	yes
With minor editing privileges	yes
For distribution to	Worldwide
In the following language(s)	Original language of publication
With incidental promotional use	no
The lifetime unit quantity of new product	0 to 499
Title	The role of the calpain system in breast cancer progression and treatment response
Institution name	University of Nottingham
Expected presentation date	Jun 2022
Order reference number	RIN04
Portions	Figure 3.1
Requestor Location	University of Nottingham Biodiscovery Institute 3 University of Nottingham Nottingham, NG7 2RD United Kingdom Attn: University of Nottingham
Total	0.00 GBP

Copyright for Figure 3.4

SPRINGER NATURE LICENSE
TERMS AND CONDITIONS

Jun 29, 2022

This Agreement between University of Nottingham -- Richa Vasan ("You") and Springer Nature ("Springer Nature") consists of your license details and the terms and conditions provided by Springer Nature and Copyright Clearance Center.

License Number	5318440350359
License date	May 29, 2022
Licensed Content Publisher	Springer Nature
Licensed Content Publication	Springer eBook
Licensed Content Title	Assaying Calpain Activity
Licensed Content Author	Neil O. Carragher
Licensed Content Date	Jan 1, 2007
Type of Use	Thesis/Dissertation
Requestor type	academic/university or research institute
Format	print and electronic
Portion	figures/tables/illustrations
Number of figures/tables/illustrations	1
Will you be translating?	no
Circulation/distribution	50000 or greater
Author of this Springer Nature content	no
Title	The role of the calpain system in breast cancer progression and treatment response
Institution name	University of Nottingham
Expected presentation date	Jun 2022
Order reference number	RIN03
Portions	Figure 3.7
Requestor Location	University of Nottingham Biodiscovery Institute 3 University of Nottingham Nottingham, NG7 2RD United Kingdom Attn: University of Nottingham
Total	**0.00 GBP**